Synthesis and characterization of new flavin systems with biomimetic and photovoltaic applications

Nada Yilmaz Zainalabdeen

Submitted in the Fulfilment of the Requirements for the Degree of Doctor of Philosophy

April 2012

School of Chemistry

UNIVERSITY

of **GLASGOW**

IN THE NAME OF GOD MOST GRACIOUS

MOST MERCIFUL

Abstract

This thesis describes the incorporation of a flavin unit into a range of systems spanning photovoltaics and biomimetic self-assembly. The flavin unit is better known as a cofactor in a range of enzymes. However, the unique physical and self-assembly properties were exploited in this research programme to develop new systems with photovoltaic and biomimetic self-assembly applications.

In Chapter 1 a general introduction relating to flavins and photovoltaics is provided. In Chapter 2, the aim was to explore the effect of the addition of fullerene to a range of acceptors in the expectation of forming new acceptor materials with a wide range of LUMO energies. In Chapter 3, the aim was to investigate the effect of coupling a flavin unit to a naphthalenediimides (NDI) unit in the expectation of forming hybrid materials for solar energy conversion.Chapter 4 describes the formation of conjugated polymers featuring a flavin moiety, in the expectation that these materials will have photovoltaic properties. Chapter 5 describes the synthesis of push-pull flavin systems with pH dependent visisble light absorption characteristics. Finally Chapter 6 describes the synthesis of water soluble ammonium salts to furnish new micelle based systems with hydrogen bonding recognition properties.

Dedication

This thesis is especially dedicated as a tribute to

my beloved father

for his love and support over the years

Acknowledgments

First of all, my uncountable praise to Al-Mighty Allah who guided me and gave me the strength to continue this learning process as it is only by His grace and the prayers of my loved ones that this momentous journey has reached its end.

I would like to show my gratitude to my sponser the Iraqi Ministry of Higher Education and Scientific Research for providing me the necessary funding to carry out my reseach work.

I owe my deepest gratitude to Prof. Vincent Rotello from University of Massachusetts and Prof. Ifor Samuel and his research group at St-Andrews University. In particular, I would like to thank Mr Bernd Ebenhoch for fabricating photovoltaic devices.
I also wish to thank Dr Deliang Long for X-RAY and Jim Tweedie for mass spectroscopic analysis. Special thanks to Dr. Stuart Caldwell and Dr Brian Fitzpatrick for all their help.
My thanks also to my fellow PhD students, Catherine MacLean, Mohanad alhachamii, Manal Aleid, Abbas Attya, Alan Wiles and Helen Armstrong for making the lab an enjoyable place to work.

Never could I have done alone without those people around me who have provided considerable support, my family and friends, especially my parents for their encouraging me.
Finally, I would like to thank my husband Jihad and children (Maab, Mustafa and Manaf), for all their help in terms of their own time dedicated to my support throughout my research.

Contents

Abbreviations.

A.....Acceptor

MeCN.....Acetonitrile.

Ac.....Acetyl

acac.....Acetyl acetonate

bpy (or bipy).....2,2'-Bipyridine

CI…..... Chemical ionisation

δ…..... Chemical shift

cm.....Centimetre

CV.....Cyclic Voltammetry

CMC…….…… ...Critical Micelle Concentration

DTC…….. ...Defferential titration calorymetry

^{o}C..... Degrees Celsius

DNA..... Deoxyribonucleic acid

DAP..... Diamidopyridine

DMAP..... 4-(Dimethylamido) pyridine. D

.....Donor

DCC…….…… ....*N*,*N*'-Dicyclohexylcarbodiimide

η…… ..Efficiency

EI.....Electron ionization

eV .....Electron volt

E…… ..Energy

EtOH.....Ethanol.

EDCI..... 1-Ethyl 3-(3-dimethylaminopropyl) carbodiimide.

eq..... Equivalents

EQE……...External quantum efficiency

FAB.....Fast atom bombardment.

FAD.....Flavin adenine dineucleotide.

FMN.....Flavin mononucleotide

FF …… ..Fill Factor

C_{60}……..……. Fullerene

GPC.....Gel Permeation Chromatography

g .....Gram

ΔG…… ..Gipps free energy

$E_{1/2}$.....Half wave potential

HF.....Hartree-Fock (Molecular Mechanics)

HH.....Head to head

HT.....Head to tail

Δ.....Heat

HRMS.....High resolutions mass spectroscopy

HOMO.....Highest occupied molecular orbital.

h.....Hour

HOBt.....1-Hydroxybenzotriazole hydrate.

ITO.. .....Indium tin oxide

IR .....Infrared

Lit.....Literature

L….....Litre

LUMO.....Lowest unoccupied molecular orbital.

Me….....Methyl

ml.....Millilitre

min….....Minute

M….....Molar(Mol per litre)

NBS….....*N*-bromosuccinimide

DCC…… *N,N'*-Dicyclohexylcarbodiimide

nm.....Nanometer

NPs…….…….. Nanoparticles

NDI…….. 1,4,5,8-Naphthalenediimide

NADH…….. Nicotinamide adenine dinucleotide

NMR.....Nuclear magnetic resonance

V_{OC}……...…….. Open voltage Current

OM……..……. Optical Microscope

OPVs……..…….. Organic Photovoltaics

Pd(C).....Palladium(on carbon).

ppm.....Parts per million.

PTDCI.....3,4,9,10-Perylenetetracarboxylicdiimide

PCBA.....Phenyl-C_{61}-Butyric Acid

PCBCl.....Phenyl-C_{61}-Butyric Acid Chloride

PCBM.....Phenyl-C_{61}-Butyric Acid Methyl Ester

PLQY.....Photoluminescence quantum yield

PEDOT……..Poly(3,4-ethylenedioxythiophene)

P3HT.....Poly(3-hexylthiophene)

PSS…….…….. Poly(styrenesulfonate)

PCE……Power conversion efficiency

J_{SC}……..Short circuit current

SDS……Sodium dodecyl sulfate

TEM……...……Transmission electron microscope

TCB……...…..……..1,2,4-Trichlorobenzene

TEI…….…….... Triethylimine

TCNQ.....Tetracyano-*p*-quinodimethane

TCNAQ.....Tetracyano-*p*-anthraquinodimethane

OFETs…….. Thin Film Effective Transistors

TLC.....Thin layer chromatography

NEt_3.....Triethylamine.

PCBM…….……. .Phenyl-C_{61}-Butyric Acid Methyl Ester

PPV…….…… ..Poly Phenylene Vinylene

P3HT…….……Poly(3-phenyl thiophene-2,5-diyl)

PLQY……..…..……..Photoluminescence quantum yield

UV/Vis.....Ultraviolet/Visible light

Vs^{-1}.....Volts per second

Declaration:

I hereby declare that the substance of this thesis has not been submitted, nor is currently submitted in candidature for any other degree. Portions of the work described herein have been published elsewhere and are listed below.

I also declare that the work presented in this thesis is the result of my own investigations and where the work of other investigators has been used, this has been fully acknowledged within the text.

Nada Y. Zainalabdeen

Prof. Graeme Cooke.

CHAPTER 1

INTRODUCTION

1.1. Flavoenzymes.

Flavin is a general term for a group of compounds that have the heterocyclic isoalloxazine chromophore. It was discovered in the early 1930s in a number of biological systems. The structure of flavin chromophore was then determined and was observed that it functions as an active constituent in flavoenzyme [1] which is responsible of catalyzing a wide range of reactions. Researchers have been able to isolate and characterize flavoenzymes from great variety of biological sources. In spite of isoalloxazine which is the basic chemical unit in flavin, it cannot be synthesized in the human body, and as a consequence riboflavin (vitamin B_2) is essential to maintain human life. Figure 1 illustrates the structures of flavin species. The most common flavin cofactors found in the body are FMN (flavin mononucleotide) and FAD (flavin adenine dinucleotide) but the essential part of the flavoenzymes that are responsible for the catalytic activity of these enzymes is the isoalloxazine ring. Naturally the isoalloxazine unit bears a side chain at N10. The isoalloxazine centre contains a hydrophobic benzene ring capable of π-π stacking and a hydrophilic pyrimidine unit which is able to form hydrogen bonds to the peptide backbone. Both FAD and FMN contain a ribityl chain and a phosphate group; but FAD differs from FMN in that it has an adenine moiety joined to the phosphate group (Figure 1). These differences in side chain functional group are important because they help determine, along with hydrogen bonding and π-π stacking forces the position of the cofactor in the protein [2].

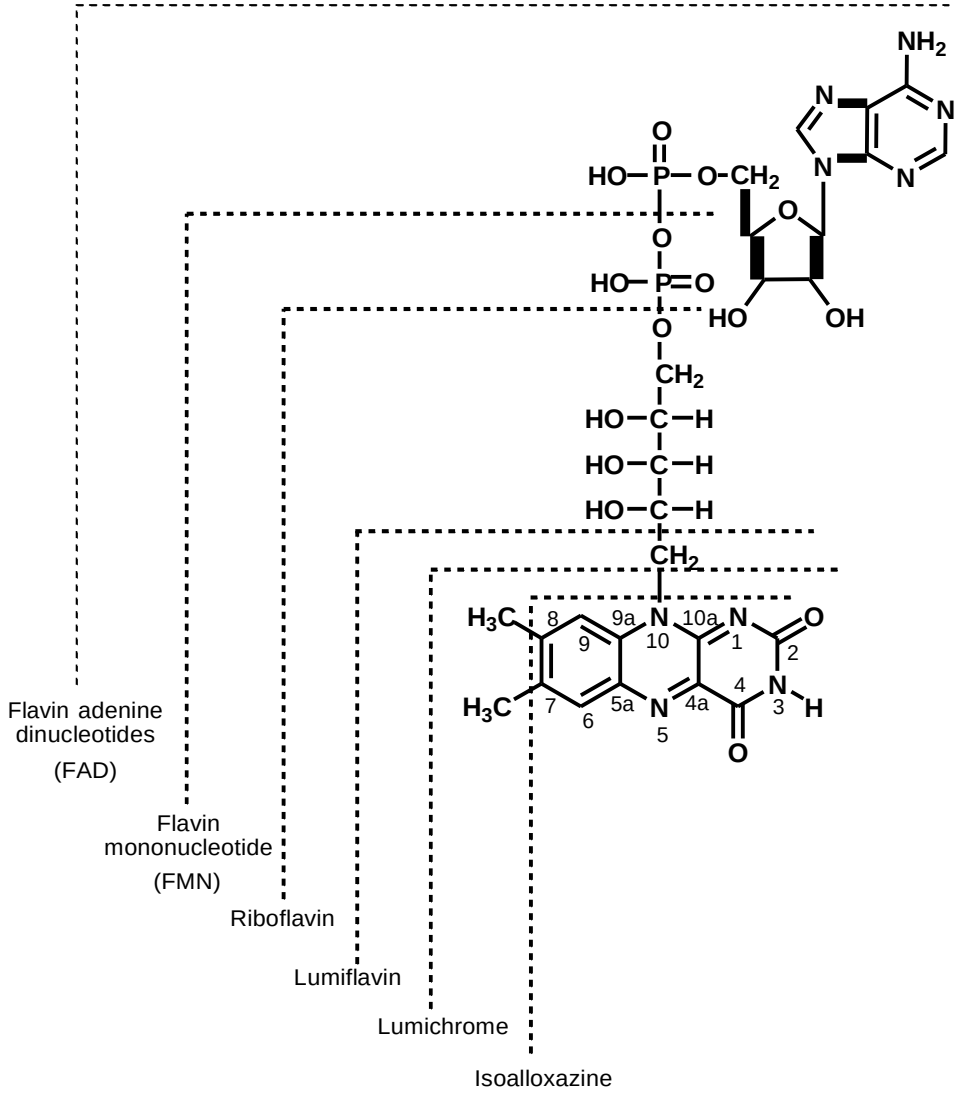

Figure 1. The structure of flavin species and the numbering system for isoalloxazine.[3]

1.1.1. Versatility of flavins.

Flavins are chemically versatile and as they are redox agents they can exist in different redox states.[4] They engage in aerobic metabolism through their ability to catalyse two-electron dehydrogenations and contribute in one-electron transfers into different metal centres through their free radical states. Thus, they often form part of multi redox-centre enzymes, such as the NADH dehydrogenases. Scheme 1 describes flavin's redox states. These are: oxidized, one electron-reduced (semiquinoid), and two electron-reduced (fully reduced) states, each can acquire different protonated, deprotonated or ionic states. In addition to these forms, there are other electronic states known as charge-transfer states. Charge-transfer states are novel electronic states in which partial charge is transferred to or from one of the three redox states. They can be described as the interaction between the

highest occupied molecular orbital (HOMO) of an electron donor and the lowest unoccupied molecular orbital (LUMO) of an electron acceptor.[3]

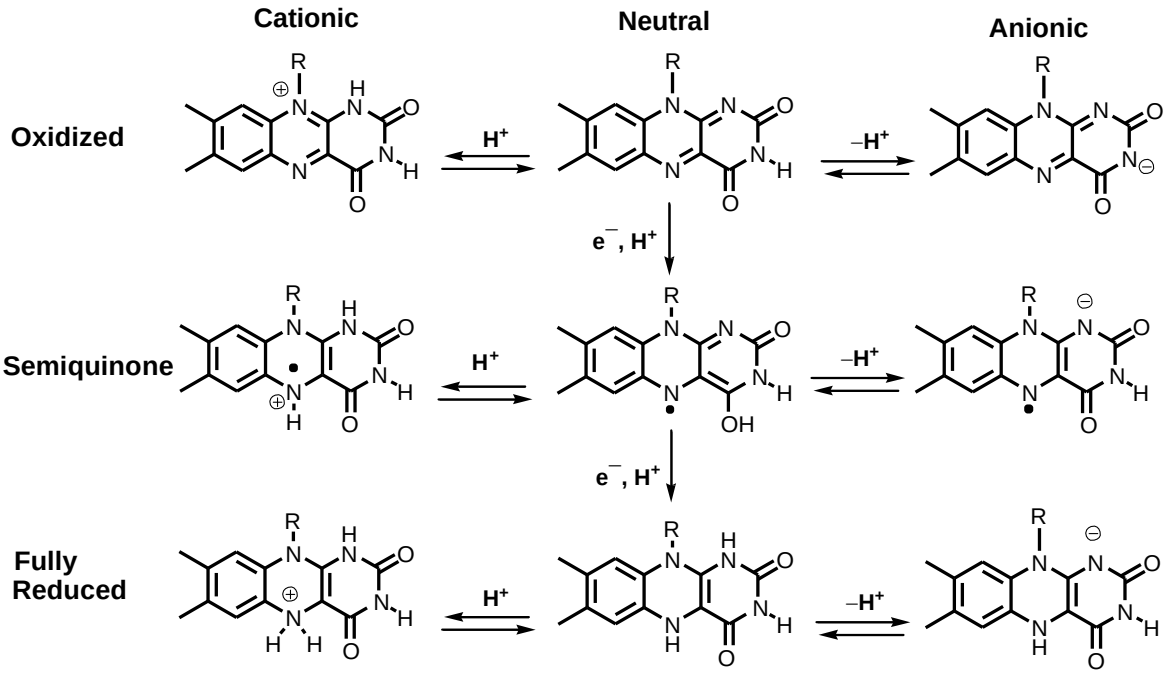

Scheme 1. Redox and acid-base equilibrium of flavin.[3]

The absorption spectra of flavin in different redox, ionic, and charge-transfer states in the visible region are presented in Figure 2. These states are the origins of the different colours of flavins and flavoproteins, and each state of flavin has a different chemical property and can be modulated by altering the environment of enzyme. In addition, modulation of each can control the redox potential of flavin to cope with a wide range of reactions.[3]

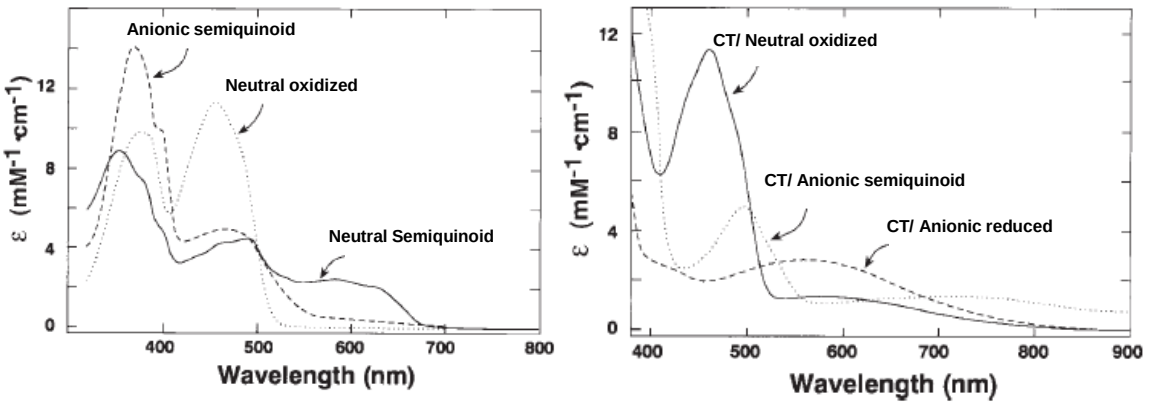

Figure 2. Absorption spectra of *d*-amino acid oxidase at different states of flavin. Left: neutral oxidized (dotted line), anionic semiquinoid (dashed line), and neutral semiquinoid (solid line) states of flavin. Right: charge-transfer states of neutral oxidized flavin (solid line), anionic semiquinoid flavin (dotted line), and anionic reduced flavin (dashed line).[3]

1.1.2. Hydrogen bonding system.

Flavins in oxidized and reduced states have both hydrogen-bond donating and accepting sites. The hydrogen-bond accepting sites of oxidized flavin are N(1), C(2), C(4), and N(5), and of reduced flavin C(2) and C(4), whereas N(3) of oxidized and reduced flavin, and N(1) and N(5) of reduced flavin can be either hydrogen-bond accepting or donating sites. Accordingly, flavin's hydrogen bonding may be contradictory. Because, in oxidized flavin at hydrogen-accepting site, N(1), N(5), C(2) or C(4), hydrogen bond decreases the electron density of flavin and hence increases the electron accepting nature of the oxidized flavin, while the same hydrogen bond of reduced flavin decreases the electron density and declines the electron-donating property. Thus, the hydrogen bond for the reductive half reaction is preferable but it is not preferable in the oxidative half reaction. For instance, the isoalloxazine moiety of flavin adenine dinucleotide (FAD) is hydrogen- bonded to the protein moiety at C(2)=O, N(3)-H, C(4)=O, and N(5). D-amino acid which is catalyzed by *d*-amino acid oxidase (DAO), undergo dehydrogenation to the corresponding imino acid by reducing the enzyme bound flavin in the reductive half reaction. Consequently, reduced flavin is reoxidized by molecular oxygen in the oxidative half reaction (Scheme 2).[5]

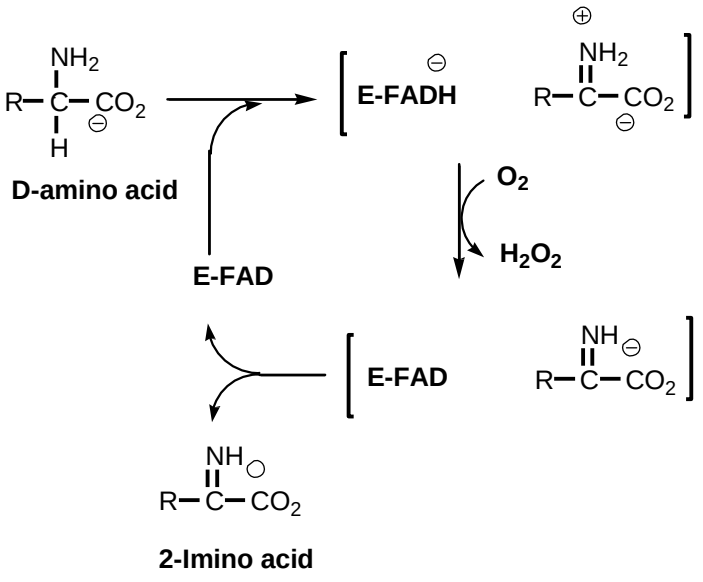

Scheme 2. Reaction catalyzed by *d*-amino acid oxidase (DAO).[3]

1.1.3. Flavin electrochemistry

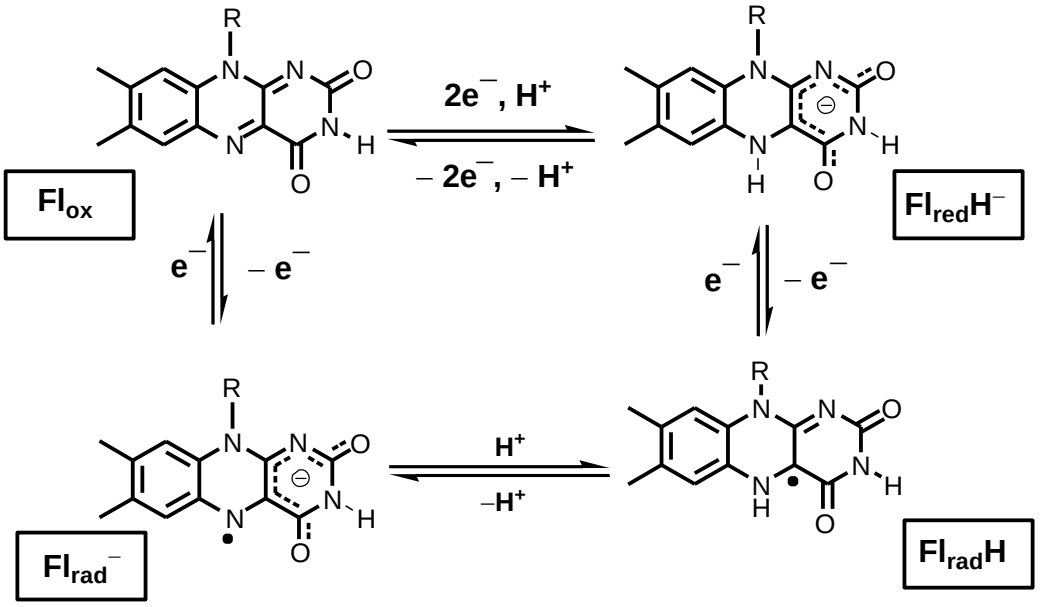

Scheme 3. Common redox and protonation states of the flavin cofactor.[2]

Specific enzyme-cofactor interactions such as hydrogen bonding, π-stacking, and other electrostatic interactions are used to stabilize particular oxidation and protonation states of the cofactor through redox-active organic molecules such as flavins. Therefore, redox enzymes can be considered as complicated and efficient molecular devices that use molecular recognition to control redox events. Flavoproteins involving the flavin cofactors FAD (flavin adenine dinucleotide) or FMN (flavin mononucleotide) enzymes display significant variation in flavin redox behaviour depending on the active site microenvironment. Within two-electron process, the oxidized flavin (Fl_{ox}) can be reduced directly to the flavohydroquinone anion ($Fl_{red}H^-$). Reduction can take place in sequence through two one-electron processes including the flavosemiquinone radical, in either the anionic (Fl_{rad}^-) or neutral ($Fl_{rad}H$) form (Scheme 3)[2].

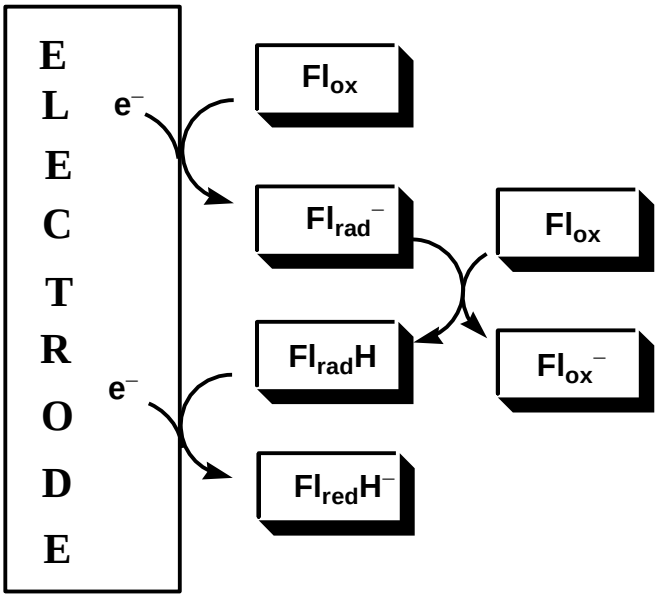

Figure 3. Mechanism of flavin reduction at an electrode surface. [2]

Aprotic solvents such as CH_2Cl_2 are the solvent of choice for the study of flavin electrochemistry because they mimic efficiently the hydrophobic protein interior in which the flavin cofactor is placed within. The mechanism for the reduction process of flavins in aprotic organic solvents has been investigated intensively. It has been found that the intermolecular proton transfer of the acidic imide from the oxidized flavin Fl_{ox} causes both electrochemical and chemical reactions. At the electrode, the oxidize flavin Fl_{ox} is reduced to the radical anion Fl_{rad}^- (Figure 3). The radical anion then obtains a proton from the imide of oxidised flavin Fl_{ox} in solution, producing the neutral radical $Fl_{rad}H$ and this is then reduced instantly at the electrode to give the fully reduced flavin $Fl_{red}H^-$ because $Fl_{rad}H$ has a less negative reduction potential than Fl_{ox}. This ece (electrochemical-chemical-electrochemical) process appears as only one reduction wave in the cyclic voltammogram (Figure 4). During the reoxidation process, two oxidation waves are observed because the radical anion Fl_{rad}^- is oxidized at more negative potentials than the fully reduced flavin $Fl_{rad}H^-$. The $Fl_{ox} \rightarrow Fl_{rad}^-$ couple is reversible and thus makes the calculation of the ΔG for this process possible from the half-wave potential $E_{1/2}$ between the reduction and the first oxidation wave by means of a derivative of the Nernst equation.[2]

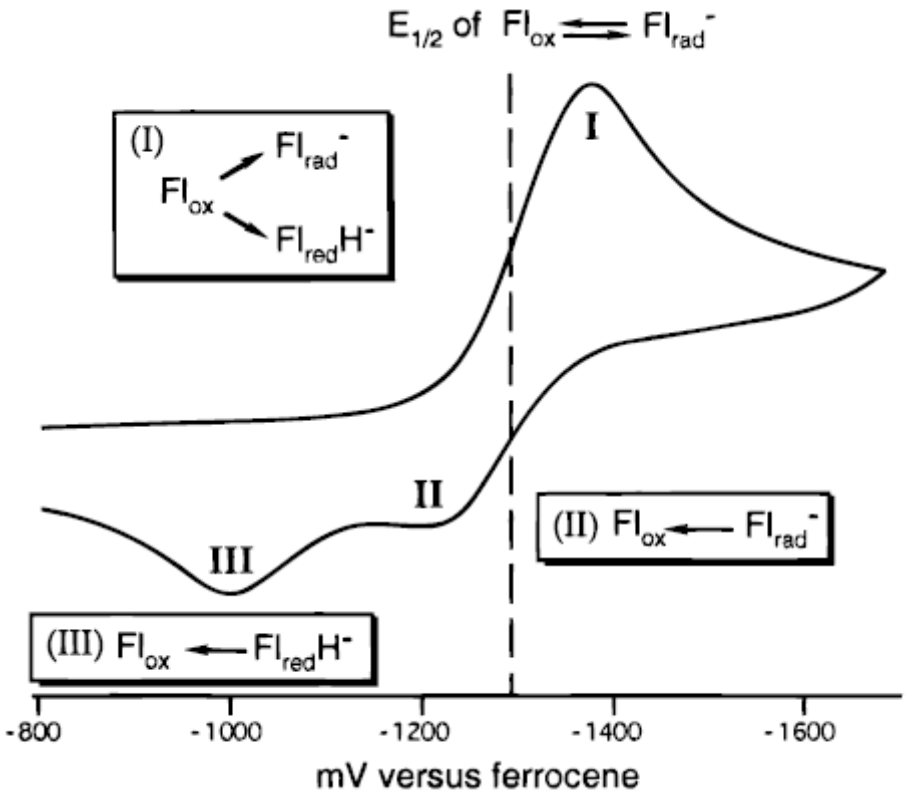

Figure 4. Cyclic Voltammogram of isobutyl flavin consisting of the reduction wave I and oxidation waves II and III caused by reoxidation of Fl_{rad}^- and $Fl_{red}H^-$ respectively.[2]

1.1.4. Redox modulation of flavin through hydrogen bonding.

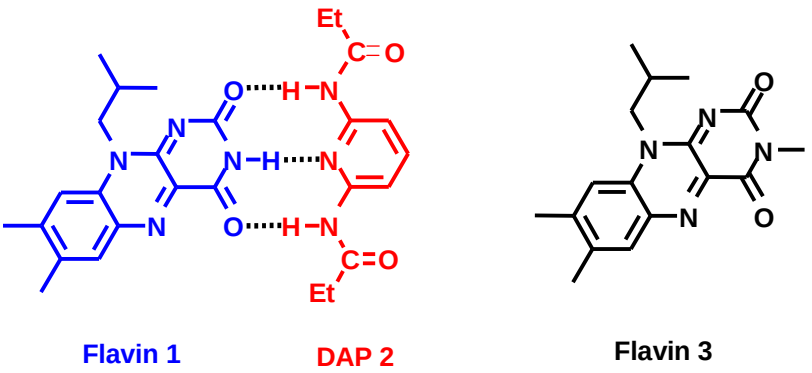

Figure 5. Flavin 1-receptor 2 complex, and N(3)-methyl flavin 3.

A common motif observed in the crystal structure of flavoproteins is the enzyme-cofactor hydrogen bonded and/or π-stacked to amino acid residues. These interactions have been thought to occupy a vital role in flavin redox modulation. The carbonyl oxygens O(2) and O(4), and imide proton N(3)H of the pyrimidone have been shown to participate in hydrogen bonding interactions with the apoenzyme. To study this issue, acylated diaminopyridine receptors (DAP) were examined to be capable of copying flavoprotein-cofactor interactions (Figure 5). Host-guest complexation has been shown to occur between DAP and the fully oxidised flavin Fl_{ox}, hence the effect of hydrogen bonding on the redox behaviour of flavin has been observed. Remarkably, the binding constant has increased upon reduction to radical anion Fl_{rad}^{-}. In addition, the reduction potentials of the flavin-DAP complex are shifted towards a lesser potential and the half wave potential ($E_{1/2}$) for the complex is found 155 mV less negative than that for the free flavin indicating a considerable stabilization of Fl_{rad}^{-}. Because of the inability to create hydrogen-bonded complexes, this shift in the reduction potential was not observed upon addition of DAP to N(3) methyl flavin. This confirms that specific hydrogen bond contacts are required for the stabilization of the flavin radical anion Fl_{rad}^{-} by DAP. These results indicate increasing binding to receptor upon reduction of Fl_{ox} to Fl_{rad}^{-}. This is due to increasing the electron density of the carbonyl oxygens O(2) and O(4) of flavin making them stronger hydrogen bond acceptors and suggests that the radical anion is more stable in the complexed rather than non-complexed form. The first oxidation wave relating to reoxidation of Fl_{rad}^{-} is considerably improved, signifying that the ece process leading to additional reduction of Fl_{rad}^{-} to $Fl_{red}H^{-}$ is efficiently suppressed in the flavin-receptor complex [2] (Figure 6).

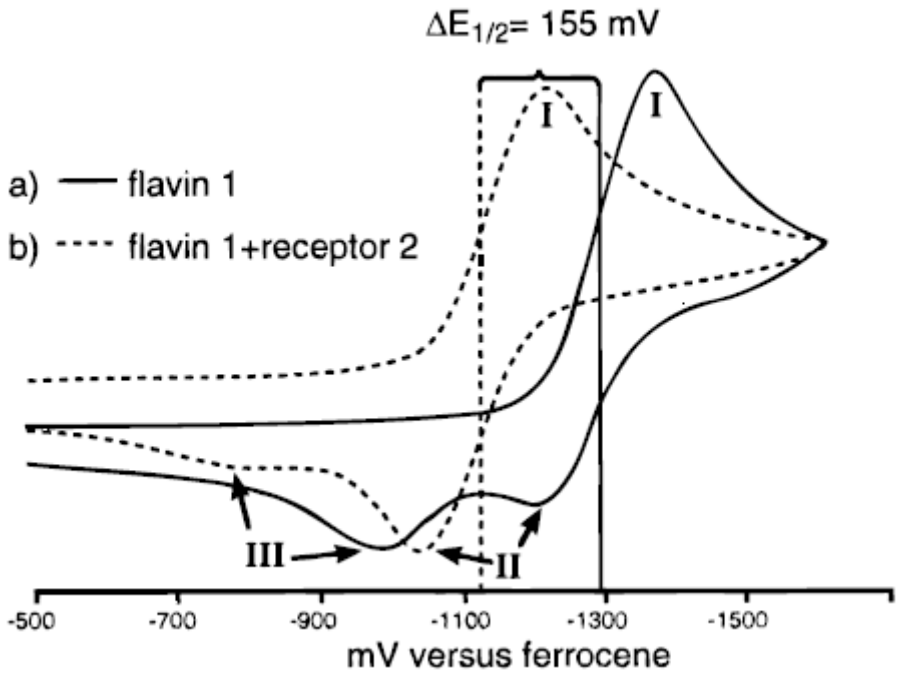

Figure 6. Cyclic voltammograms for (a) flavin 1 and (b) the flavin 1-receptor 2 complex showing the single reduction wave (I) and the two oxidation waves corresponding to reoxidation of Fl_{rad}^- (II) and $Fl_{red}H^-$ (III). [2]

1.2. Organic photovoltaics.

1.2.1. Operating principle of organic solar cells.

Photovoltaics (PVs) is a term that refers to the process of conversion of visible light into electrical energy. Although common materials used for photovoltaics are inorganic,[6] the applications of small organic molecules (pigments),[7,8] and of semiconducting polymers, incorporated into organic solar cells has resulted in remarkable developments within the past 20-30 years.[9] The ability of semiconducting organic materials to transport electric current and to absorb light in the UV-visible part of the solar spectrum combined with their flexibility makes them potentially interesting systems for photovoltaic applications. These can be improved by engineering the molecular structures or manipulating the functional groups of the semiconducting organic materials. The conjugation which is the common characteristic of the photovoltaic materials is formed when the electron in the pz-orbital of each sp^2-hybridized carbon atom will form π-bonds with adjacent pz electrons in a linear chain of sp^2-hybridized carbon atoms. This will lead to a chain of carbon atoms with alternating single and double bonds. A high electronic polarizability generates from the isomeric effect which lead to π-electrons delocalization. Unlike inorganic, organic semiconductors have poor charge carrier mobilities although they have comparatively strong absorption coefficients.[10]

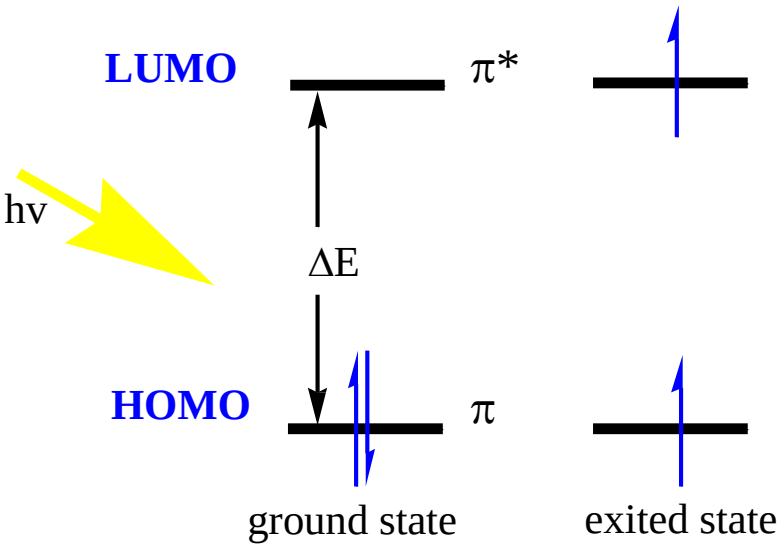

Figure 7 .π - molecular orbital configuration between the HOMO and the LUMO levels providing an energy gap ΔE in both ground and exited states.

The photovoltaic process occurs as photons of light excite electrons into higher energy levels, allowing them to act as charge carriers for an electric current. The delocalization of the electrons of pz orbitals generates a delocalized bonding π orbital (HOMO) and antibonding π* orbital (LUMO) (Figure 7). The distance between these two orbitals is considered as the band gap which is typically in the range of 1 – 4 eV. Once the organic semiconductors absorb a photon, an excited state is created. This is regarded as an electron-hole pair bound together by electrostatic interactions which can be called excitons. These excitons are the main intermediate in the solar energy conversion process. In photovoltaic cells, usually strong electric fields are required to dissociate these excitons into free electron-hole pairs, which are the required final products for photovoltaic conversion. In inorganic solar cells, the excited electrons are able to move independently from the holes and hence these charge carriers can be forced to the electrodes under the influence of an internal field created through a pn-junction. However, in organic solar cells, the exciton is first split at a donor/acceptor interface consisting of two different organic semiconductors of different energy levels. Then the charge carriers are forced to the electrodes by an internal field created by the difference of Fermi-levels of the used electrode materials. Remarkably, it was observed that the excitons of the organic semiconductors have relatively small diffusion length and higher binding energies usually exceeding those of inorganic semiconductors[11]. The effective field is set up by creating a heterojunction between two dissimilar materials. Effective fields break up excitons by causing the electron to fall from the conduction band of the absorber to the conduction band of the acceptor molecule. It is necessary that the acceptor material has a conduction band edge that is lower than that of the absorber material.

1.2.2. Types of junctions for OPVs.

1.2.2.1. Single layer organic photovoltaic cell.

The first generation and the simplest form of the organic photovoltaic solar cells were the single layer organic photovoltaic cells. These cells are made by sandwiching a layer of organic electronic materials between two metallic electrodes (Figure 8),[7,8] typically a layer of transparent indium tin oxide (ITO) as an anode, to allow light to be absorbed in the active layer, and a layer of low work function metal such as Al (4.28 eV) and Ca (2.87 eV). An internal electrical field is created in the organic layer due to the difference of work function between the two conductors. Light absorption by the organic layer leads to electrons to be exited to their LUMO and leaves holes in HOMO to form excitons. The

generated potential from the difference of work functions helps to separate the exciton pairs, drawing electrons to the positive electrode and holes to the negative electrode. The reported power conversion efficiencies were poor (in the range of 10^{-3} –10^{-2}%), but have achieved a recorded maximum of 0.7% for merocyanine dyes. [12,13]

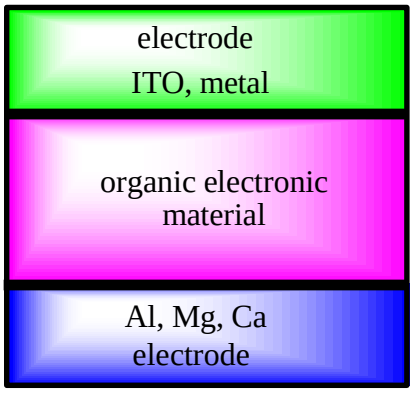

Figure 8. Single layer organic photovoltaic cell.

1.2.2.2. Bilayer organic photovoltaic cells.

The bilayer heterojunction concept was achieved later. The cell was constructed of two organic layers with specific electron or hole transporting properties sandwiched between the electrodes (Figure 9). Importantly, these two layers should have different electron affinity and ionization energy in order to create electrostatic forces at the interface between them. These differences must be large enough to create stronger electric fields, which may break up the excitons much more efficiently. The two organic layers are the electron acceptor, having higher electron affinity and ionization potential, and the electron donor.

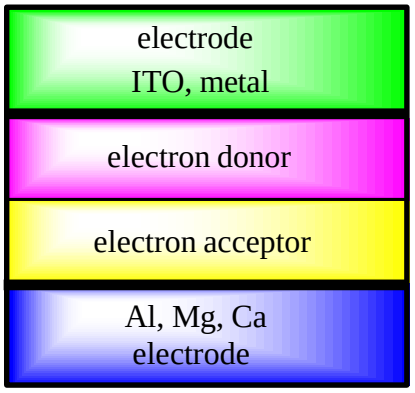

Figure 9. Bilayer organic photovoltaic cell.

This kind of cells recorded 1% conversion efficiency for phthalocyanine derivatives as p-type semiconductor and a perylene derivative as n-type semiconductor[14]. Subsequently, stacking two heterojunction devices were introduced[15] also a three layer p-i-n like structure with a co-deposited interlayer between the p-type (hole conducting) and n-type (electron conducting) layers was developed[16,17]. The power conversion efficiencies were less than 0.1% for polymer single layer devices.[18,19] Polymer–fullerene bilayer heterojunction and bulk heterojunction devices incorporating C_{60} and C_{60}-derivatives with conducting polymers were developed in the expectation that photoinduced electron transfer from optically excited conjugated polymers to the C_{60} molecule will result in high photoconductivity.[20,21] The photoinduced electron transfer arises as it is energetically favourable for the electron in the S1- excited state of the polymer to be transferred to the much more electronegative C_{60}, to present an effective quenching of the excitonic photoluminescence of the polymer (Figure 10).[22]

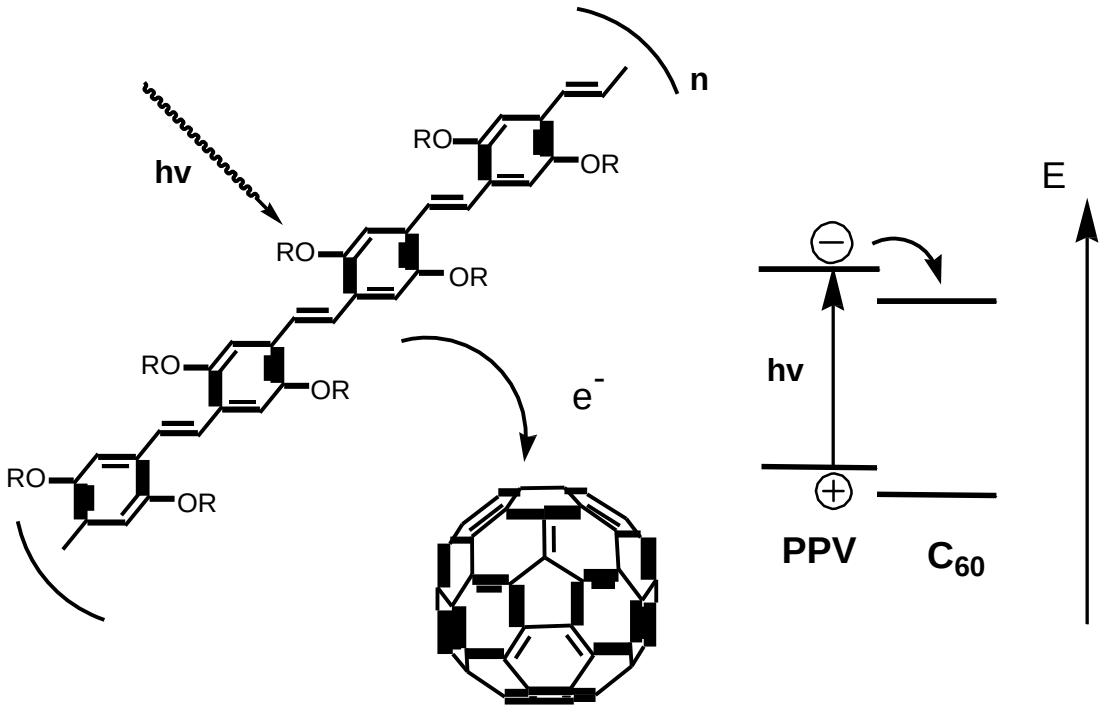

Figure 10. (Left) The photoinduced charge transfer, (right) the energy level. After excitation in the PPV polymer, the electron is transferred to the C_{60} due to its higher electron affinity.[23]

1.2.2.3. Bulk heterojunction photovoltaic cells

This type of photovoltaic cell was introduced by blending two polymers having donor (D) and acceptor (A) properties in solution (Figure 11).[24,25] Spin cast films then produce solid state mixtures of both materials. The length scale of the blend should be similar to the exciton diffusion length. The generated excitons may reach the interface and break efficiently to create electrons which move to the acceptor then collected by one electrode, and holes which pulled in the opposite direction and collected at the other side.

Subsequently, power conversion efficiencies were approached 2% upon fabricating devices by lamination of two polymer layers leading to a diffusive interface between D and A moieties.[26] More recently, evaporated bilayer devices,[27] bulk heterojunction polymer–fullerene devices,[28,29] co-evaporated molecular devices,[30,31] and organic–inorganic hybrid devices[32] have delivered conversion efficiencies to 1.5 – 4%. Furthermore, the dye sensitized electrochemical solar cells have received signifiant attention recently, and electrochemical and organic photovoltaic research have merged together by replacing organic hole conductors[33,34] with liquid electrolytes in electrochemical solar cells and by exchanging of the electron conducting acceptor materials in organic heterojunction devices with inorganic nanocrystals.[32,35]

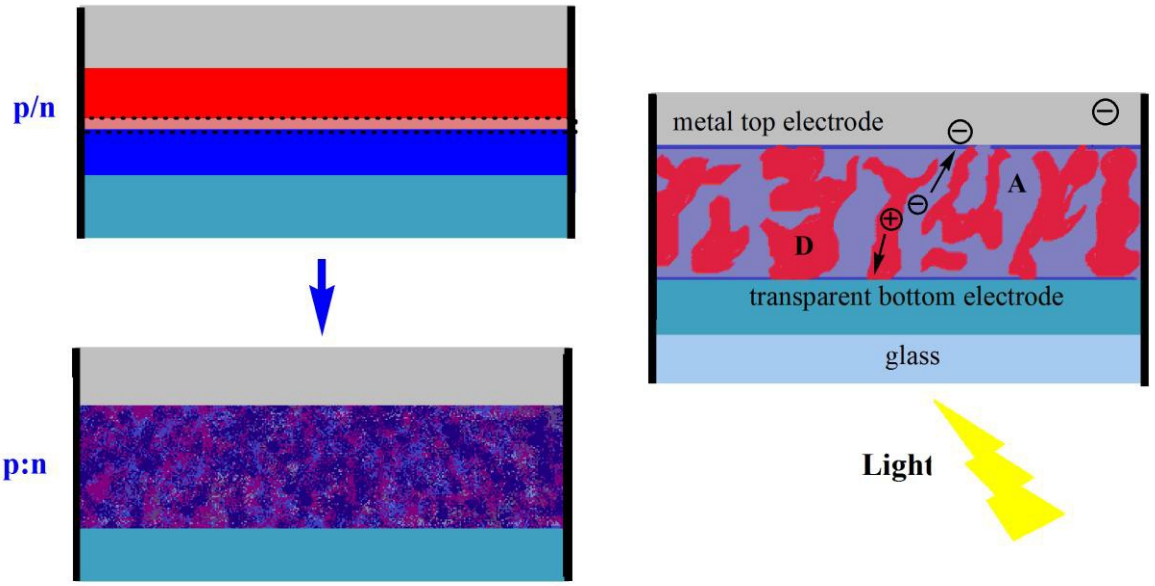

Figure 11. From bilayer to blend bulk heterojunction solar cells.

1.2.3. Some examples of photovoltaic materials.

Some of the first examples of *p*-type (hole-conducting) materials were based around phthalocyanine compounds whereas the *n*-type (electron-conducting) systems were based around perylene and its derivatives. Usually electrochemical doping processes were undertaken to increase the charge carrier concentration, because the charge carrier mobilities of these materials are relatively small. Doping for donor type materials is carried out by exposing to oxygen or other strong oxidizing agents such as iodine.[8,36] This can be obtained by transferring an electron from the ground state S_0 of the organic semiconductor to the oxidizing agent to increase the charge carrier concentrations in the hole conductor. Doping of acceptors such as perylene is carried out by exposing to hydrogen.[36] These doping processes cause the quite insulating materials to act as charge carriers and therefore the bilayer devices can work like classical *p-n* junctions.[37,38]

The co-evaporation of both materials and dopant can be regarded as a further controlled doping process. [39-42] Photodoping is a process of photoinduced charge transfer,[22] that has been obtained from blending the buckminster fullerene C_{60} (or derivatives) which is a strong electron acceptor[43] with hole-conducting materials. This does not improve charge transport in the dark, but leads to a large increase in photoconductivity under illumination. [44,45] The chemical structures of some organic molecular materials that commonly applied in evaporated organic solar cells are represented in Figure 12.

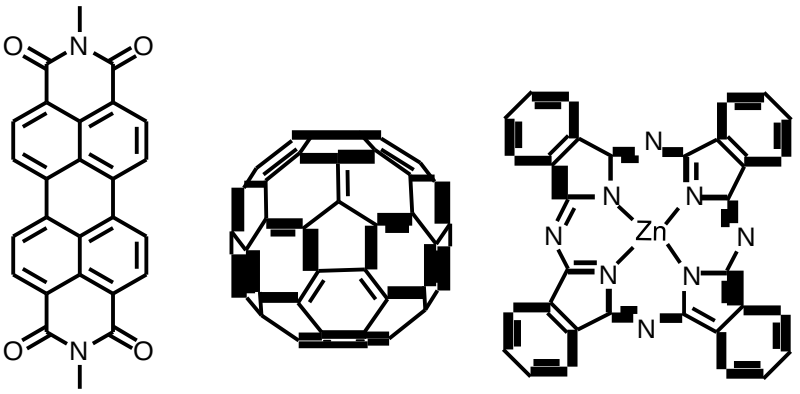

Me-Ptcdi **4** **C_{60}** **5** **ZnPc** **6**

Figure 12. Some organic molecules commonly applied in evaporated organic solar cells: ZnPc (zinc-phthalocyanine), Me-Ptcdi (*N,N'*-dimethylperylene-3,4,9,10-dicarboximide), and the buckminster fullerene C_{60}.[23]

The best examples for hole-conducting donor type polymers and electron-conducting acceptor polymers are represented in (Figure 13). They exhibit photo- and electroluminescence properties.[46,47] The side-chains confer solubility and provide the possibility of solution processing. In case of manufacturing donor–acceptor solar cells, the donor polymers are usually combined with an acceptor polymer or with fullerenes either in bilayer or in blend structures. Charge carrier mobilities in films of molecules and conjugated polymers can be manipulated by the preparation conditions [48-51] and the preferable orientation of polymer backbones is parallel to the substrate. [50-52] In addition, it has been found that the nanomorphology of the blend mixture is a sensitive function for the charge transport in bulk heterojunction solar cells.[53,54]

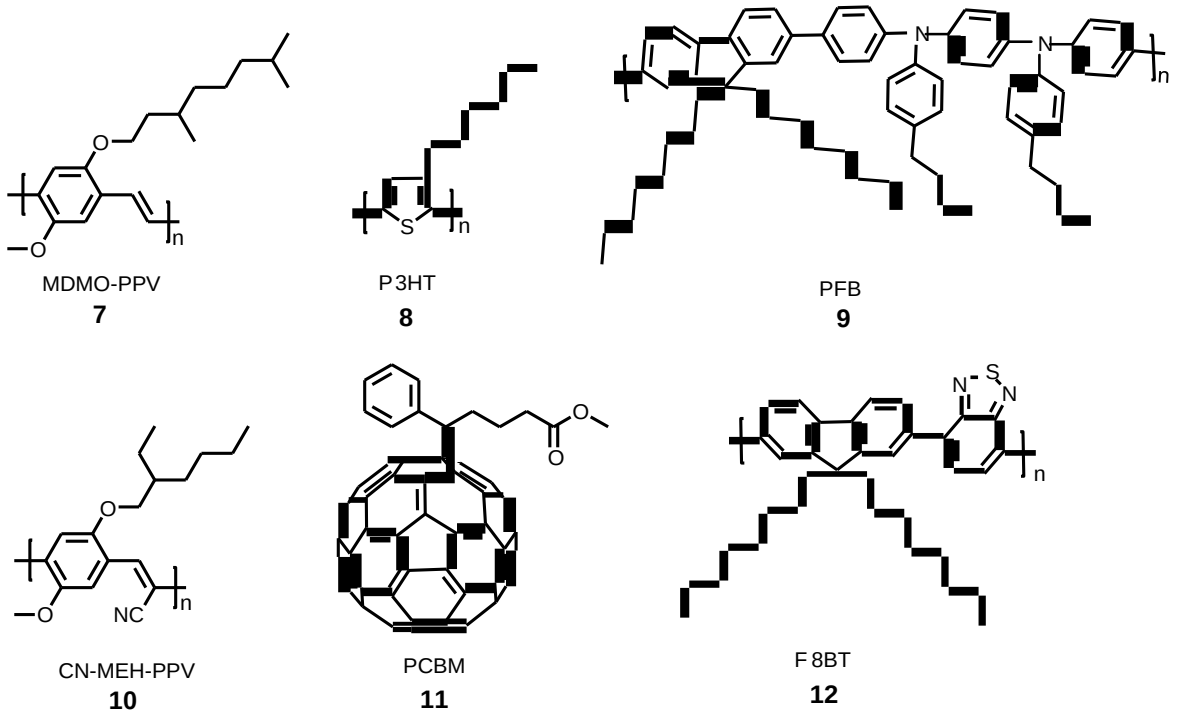

Figure 13. Several solution processible conjugated polymers and a fullerene derivative used in organic solar cells. Upper row: the p-type holeconducting donor polymers MDMO-PPV (poly[2-methoxy-5-(3,7-dimethyloctyloxy)]-1,4-phenylenevinylene), P3HT (poly(3-hexylthiophene-2,5-diyl) and PFB (poly(9,9'-dioctylfluorene-co-bis-*N,N'*-(4-butylphenyl)-bis-*N,N'*phenyl-1,4-phenylenediamine). Lower row: the electronconducting acceptor polymers CN-MEH-PPV (poly-[2-methoxy-5-(2-ethylhexyloxy)-1,4-(1-cyanovinylene)-phenylene), F8BT(poly(9,9'-dioctylfluorene-co-benzothiadiazole) and a soluble derivative of C_{60}, PCBM (1-(3-methoxycarbonyl)propyl-1-phenyl[6,6]C_{61}).[23]

1.2.4. Preparation techniques.

The two common techniques used for preparing materials are thin film production, which is mostly depended on the choice of materials, and evaporation which requires thermal stability. However, an important feature of both techniques is that the materials are required to be highly soluble in solvents. Most small molecules are thermally more stable but less soluble than polymers, therefore, evaporation is mostly used. Whereas, semiconducting polymers are mostly processed from solution due to the fact that excessive heat may decompose polymers. Furthermore, the large molecular weight of the polymer may make the evaporation difficult. However, solubility often is achieved by side-chain solubilization, therefore, less soluble molecules like C_{60} may become soluble when modified by attaching solubilizing groups (e.g., PCBM) and short polymers or oligomers may also be evaporated.[30,55]

1.2.4.1. Evaporation

Thermal evaporation is a techniques that is used to grow films under vacuum of ($<10^{-5}$ mbar) in order to offer a free path for the evaporated molecule longer than the distance between the evaporation source and the sample holder. The application of ultra high vacuum ($<10^{-9}$ mbar) or the evaporation inside of a glove box with inert atmosphere can be used to decrease or eliminate oxygen and water. On the other hand, co-evaporation techniques are applied to generate interpenetrating donor- acceptor system or to obtain molecular doping. [16,30,39,42,56]

1.2.4.2. Wet processing

The wet processing technique involves dissolving the organic materials in suitable solvents such as water or any other polar or nonpolar organic solvent. Some solution processing of soluble monomers are coupled with a polymerization reaction during (e.g., electrochemical polymerization) or after (e.g., via heat treatment, UV curing) the film forming process (precursor route) to yield insoluble polymers which in turn can be suitable for depositing another film from solutions on top of them. When the polymers or polymer/polymer or polymer/ molecule blends are directly processed from solution, several common techniques are applied like spin coating, doctor blading, screen-printing, and inkjet printing. For instance, screen-printing was applied to a MDMO-PPV:PCBM blend (Figure 14). [57] The use of existing printing techniques upgrades the production and presents low energy consumption during production of solar cells. This is important for the energy amortization (energy delivered by a solar cell throughout its lifetime as compared to the energy required to fabricate the solar cell itself).

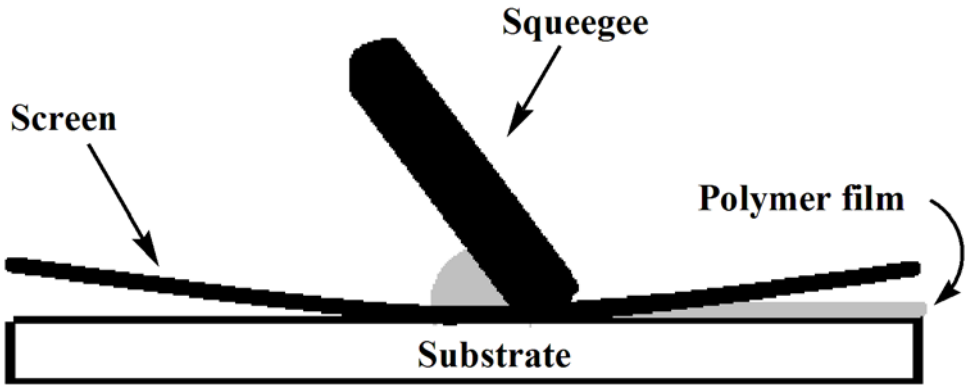

Figure 14. Schematic of the screen-printing of a polymer/fullerene–based organic solar cell.[23]

1.2.5. Basic working principles of a PV cell.

The main idea of organic photovoltaic cell is based on converting light into electric current. As shown in Figure 15, the four fundamentals of this process are:

(i) Absorption of a photon to create an excited state, the electron-hole pair (exciton).
(ii) Exciton diffusion to a region, where the charge separation takes place.
(iii) Charge separation.
(iv) Charge transport to the anode (holes) and cathode (electrons), to provide a direct current.

The number of generated charges that are collected on the electrodes determines the delivered electric current from the photovoltaic solar cell. This number is limited by three fractions to determine the overall photocurrent efficiency (η_j):

(i) The fraction of absorbed photons (η_{abs}).
(ii) The fraction of dissociated electron-hole pairs (η_{diss}).
(iii) The fraction of separated charges that reach the electrodes (η_{out}).

$$\boldsymbol{\eta_j = \eta_{abs} \times \eta_{diss} \times \eta_{out}}$$

The fraction of absorbed photons (η_{abs}) is a function of:

(i) The absorption spectrum.
(ii) The absorption coefficient.
(iii) The absorbing layer thickness.
(iv) The internal multiple reflections at, for instance, metallic electrodes.

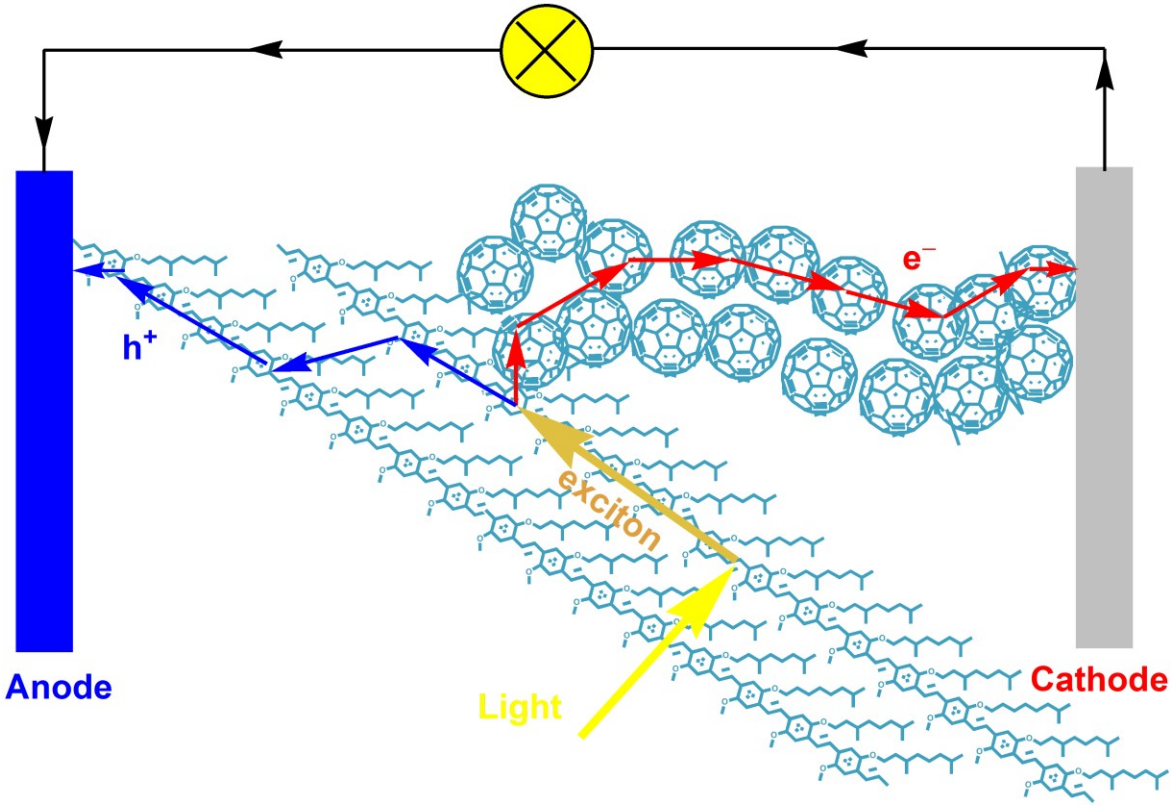

Figure 15. The four main steps of converting the light to electric current.

The fraction of dissociated electron-hole pairs (η_{diss}) is determined by the charge separation probability in the region where the excitons diffused into [58].

The charge carriers require a net driving force to reach the electrodes, which creates a gradient in the electrochemical potentials of electrons and holes. This driving force is supplied by two kinds of forces:

(i) Internal electric fields which lead to field induced drift. This is generally dominated with thin film devices (<100 nm).

(ii) Concentration gradients of the relevant charge carrier species that lead to a diffusion current. This is dominated with thick devices, having effective screening of the electrical fields inside the bulk

1.2.6. Device structures based upon P3HT:PCBM

P3HT and PCBM based devices have proved to be an important prototype system for explaining device function (Figure 16). P3HT is acting as the donor and has significant absorption in the visible range and therefore can absorb sunlight. To permit light to be absorbed in the active layer, the transparent electrode of ITO as the anode for hole extraction with a thin layer of the conducting polymer PEDOT should be present. Both ITO and PEDOT have a high work function of 4.8 eV[59] and 5.2 eV, respectively. On the other hand, the cathode, which is based on a metal, has a low work function like aluminium (4.28 eV) or calcium (2.87 eV). Once both electrodes are short circuited through an external connection, the Fermi levels arrange as electrons travel from the high Fermi level electrode to the low Fermi level electrode forming an internal electrical field (Figure 17). The binding energy of the exciton in P3HT is about 0.4 eV. As the LUMO level of PCBM is lower than that of P3HT, electron transfer from the LUMO of P3HT (-2.95 eV)[60] to the LUMO of PCBM (-3.75 eV)occurs. [59]

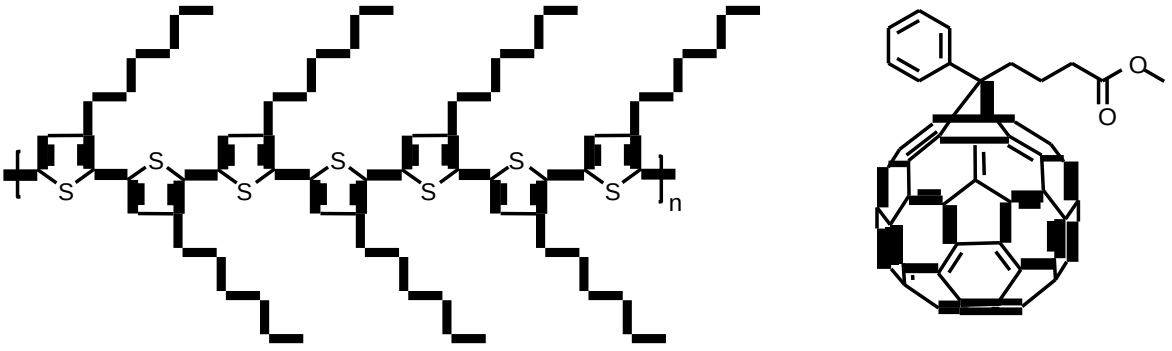

P3HT
8

PCBM
11

Figure 16. Molecular structures of P3HT (left) and PCBM (right).

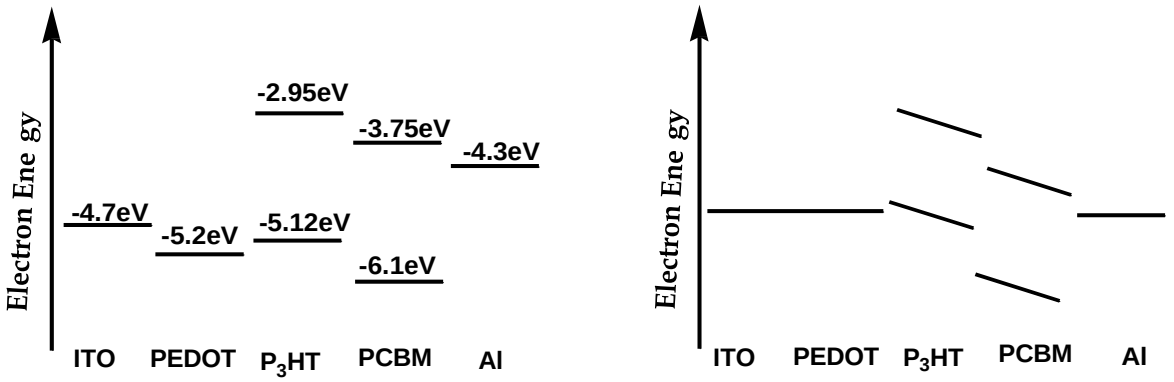

Figure 17. Energy levels of a planar donor/acceptor heterojunction based on ITO, PEDOT, P3HT, PCBM, Al at open circuit condition (left) and short circuit condition (right).[23]

In order to extend the interfacial area between the donor and the acceptor in the active layer and so minimise the exciton diffusing distance to nanometres, (because many excitons do not reach this interface during their life time and are lost due to recombination), blending the donor and the acceptor as a solution in the active layer is undertaken then dried through annealing. In this manner, both materials should be soluble in the same solvent. Interestingly, the solvent and the annealing conditions have a strong impact on the structure of the bulk-heterojunction.[61,62] Annealing has a strong effect on how the molecules are aligned in a phase. The donor which is often a conjugated polymer such as P3HT is able to align side by side in a semi-crystalline structure through van der Waals forces during annealing.[63] The acceptor such as PCBM is found to create crystalline structures. This crystallinity has a strong influence on the charge mobility.

1.2.7. Electrical behaviour.

A solar cell has a diode like behaviour having a nonlinear current/voltage source (Figure 18). The current of the externally short circuited solar cell (I_{SC}) is proportional to the power absorption by the cell and as a homogeneous light source is used, the short circuit current (I_{SC}) is proportional to the area (A) of the cell. The current density (J) is used to compare different solar cells since the current (I) is related to the area.

$$J = \frac{I}{A} \qquad (1.1)$$

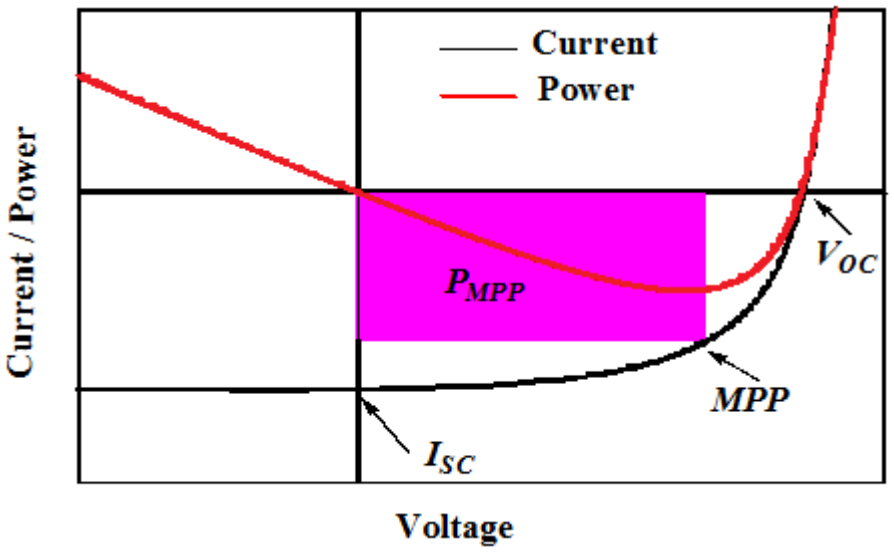

Figure 18 IV-curve characteristic of a solar cell with significant points

The open circuit voltage (V_{OC}) is the voltage generated by the solar cell in open circuit conditions. The V_{OC} of bulk-heterojunction solar cells depends on the energy levels of the materials used and is related to the difference of the LUMO of the acceptor and the HOMO of the donor[64] (Figure 19). The maximum power point (*MPP*) is found between V_{OC} and J_{SC} where the solar cell transfers the maximum power (P_{MPP}) to a load resistance.[23] At this point the power conversion efficiency (η) is defined as the produced electrical power per incident optical power (P_{Light}). The electrically modelled circuit of the optimized power conversion solar cell is illustrated in (Figure 20).

$$\eta = \frac{P_{MPP}}{A \times P_{Light}} \qquad (1.2)$$

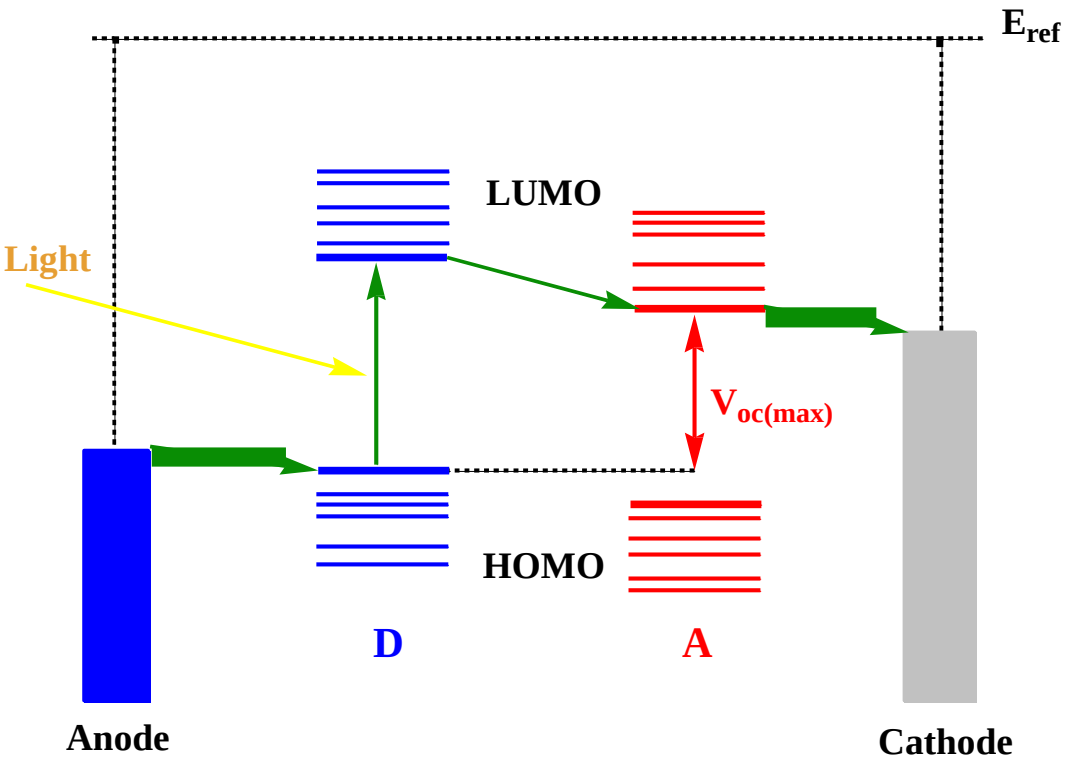

Figure 19. The photoinduced LUMO-LUMO electron transfer process.

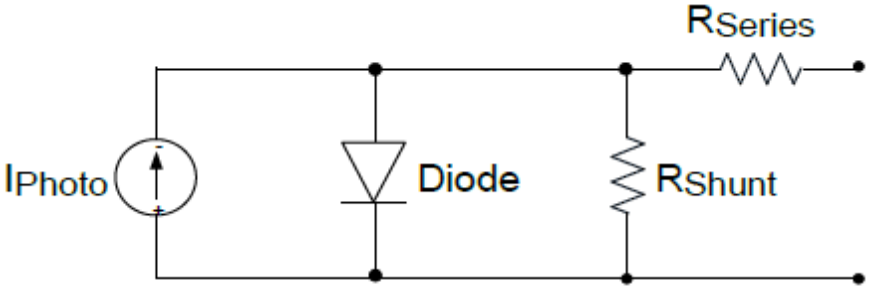

Figure 20. Equivalent circuit of a solar cell.

In this model, the current produced by the solar cell is flowing through a diode which generates the voltage at open circuit. Losses are applied with the shunt (R_p) and series resistance (R_s) which impact the IV-curve. In ideal solar cells, the shunt resistance is very large and the series resistance very small. A small shunt resistance points to short cuts between both electrodes or a high recombination rate in the active area. A large series resistance indicates poor conductivity of the materials or bad contacts of the device layers[23]. Both effects have a negative impact on the fill factor (*FF*) which is defined as the maximum power divided by V_{OC} and J_{SC}.

$$FF = \frac{P_{MPP}}{V_{OC}\, J_{SC}} \qquad (1.3)$$

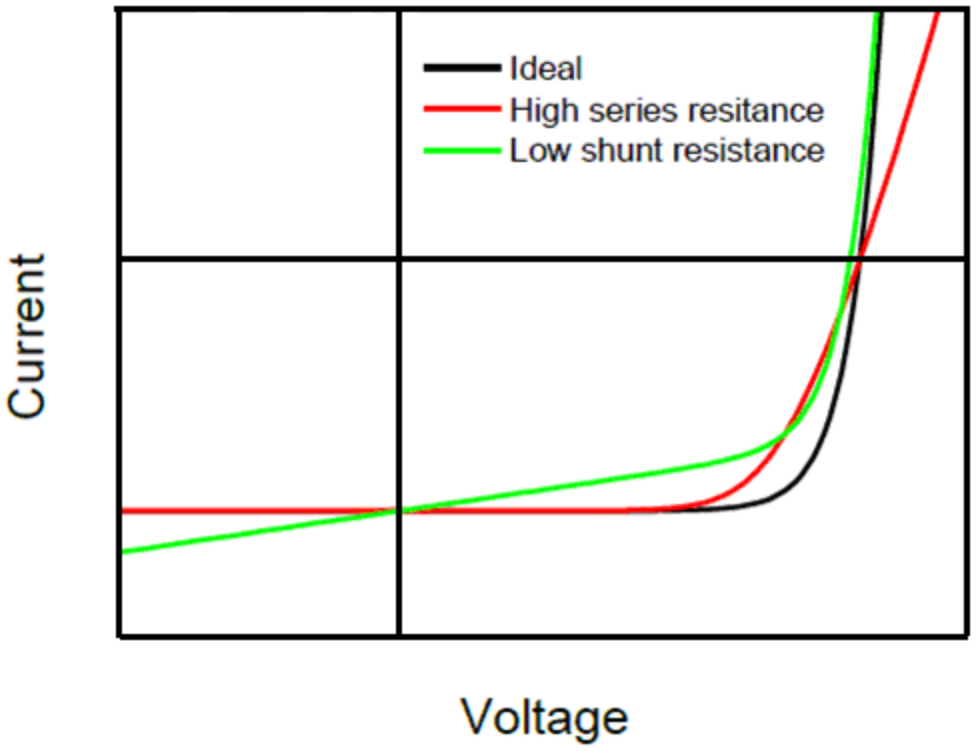

Figure 21. Graph showing the effect of series and shunt resistance.

CHAPTER 2

FULLERENE [C_{60}] BASED ELECTRON-ACCEPTORS FOR PHOTOVOLTAIC APPLICATIONS.

2.1. Introduction

2.1.1. [C_{60}] - Buckminsterfullerene

Buckminster fullerene C_{60} (**5**) is a molecule of 60 carbon atoms arranged in a spherical shape consisting of hexagonal and pentagonal rings (Figure 22). Although the geometrical structure of fullerene was first identified in 1980,[11] the synthetic fullerenes were only reported in 1985.[65] However, C_{60} is not the only fullerene as there are a whole set of stable, soluble, all-carbon molecules with C_{70}, C_{76}, C_{78}, C_{84} and even over 100 atoms per molecule. The unique chemical and physical properties of this three dimensional molecular allotrope of carbon has made it a subject of intensive research.[66] Thus an enormous number of chemical transformations of fullerene have been reported.

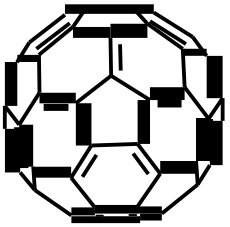

Figure 22. Buckministerfullerene [C_{60}].

Fullerenes have low reorganization energy following electron transfer and this makes them one of the most useful electron acceptor molecules in organic electronics.[67] Thus C_{60} compounds are considered as n-type semiconductors with a band gap = 2.3 eV. This property makes them a good complement to numerous p-type organic semiconductors. In addition, the spherical structure allows electron transfer to take place in any spatial direction without preference. This material also has an excellent electron mobility μ_e= 0.1cm^2/Vs for an organic material. C_{60} and C_{70} can be utilized in making transistors with exceptional performance in inert environments. Moreover, many C_{60} anion ("fulleride") salts are superconductors with desirable transition temperatures (~30 K). Furthermore, fullerenes have found significant application in the organic photovoltaic (OPV) field.

The route to production of macroscopic amounts of C_{60} is by evaporating graphite electrodes in an atmosphere of 100 torr of helium or by heating graphite soot to 400^{o}C in a vacuum or in an inert atmosphere.[68] The closed cage molecules are formed entirely of carbon in sp^2 hybridized state representing the third form of carbon after diamond and graphite. The C_{60} molecule would not be an extremely stable aromatic molecule due to the

stresses in the five membered rings adjacent to benzenoid rings and the tendency of the pentagonal rings to avoid having double bonds because the presence of double bonds shortens the bond in the already strained ring. Accordingly, the reactive sites C=C are localized at specific sites in C_{60} avoiding the pentagonal rings.[43] So the only proposed structure for C_{60} gives rise to two consequences: First, the poor delocalization of electrons, and secondly, C_{60} is not really an aromatic molecule (Figure 23).

13

Figure 23. Structure of stable fullerene.[69]

Unlike most aromatic molecules, unfunctionalised fullerenes have no hydrogen atoms. Thus they are unable to undertake substitution reactions. Substitution reactions can occur on derivatives which are produced by addition reactions.[69] In general, fullerenes are electron attracting molecules (electrophiles), hence reactions with electron donating species (nucleophiles) are preferable,[70] therefore the molecules undergo all the reactions associated with poorly- conjugated and electron deficient alkenes. However, fullerenes unique feature is the enormous number of products that may arise from addition of just one reagent.

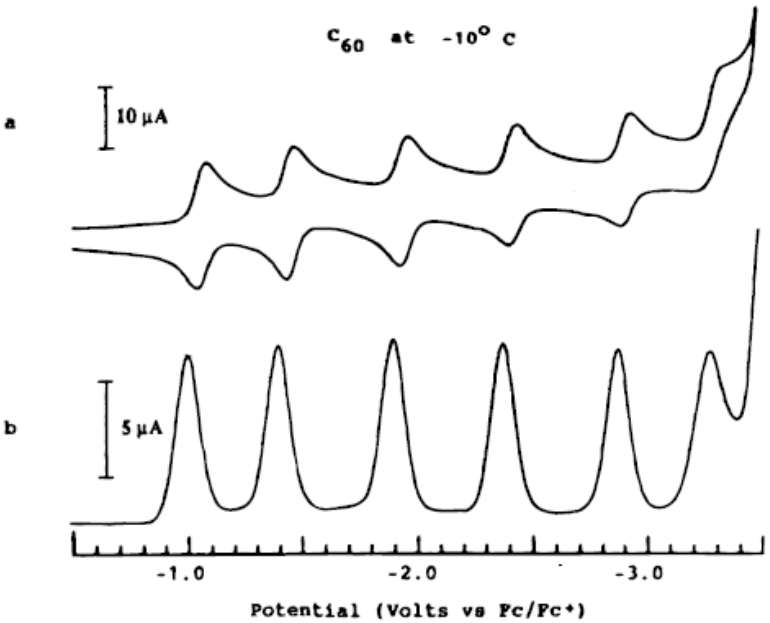

Figure 24. Reduction of C_{60} in CH_3CN / toluene at -10°C using cyclic voltammetry at 100 mV/s. [71]

The voltammetric response of C_{60} in solution is expressed by six redox transitions $C_{60}^{0/-1/-2/-3/-4/-5/-6}$ [71] (Figure 24). The presence of the hexaanionic molecule in the solid state is inferred from the formation of species such as K_6C_{60}[72]. The first three redox transitions of fullerene in solution are corresponding to the redox pairs $C_{60}^{0/-1}$, $C_{60}^{-1/-2}$ and $C_{60}^{-2/-3}$ [73,74] Subsequently, the fourth and the fifth reduction waves for C_{60} leading to C_{60}^{4-}, and C_{60}^{5-}, have been reported [73,75,76]. The first observation of the sixth electron reduction for C_{60}, leading to the formation of C_{60}^{6-} was under a wider expansion of the available potential window down to -3.3 V vs Fc/Fc^{+}. This was accomplished by the use of a mixed solvent system between 15 and 20% by volume of acetonitrile in toluene and low temperature up to 5 ^{o}C at very slow potential scan rates (100 mV/s)[71]. The high electron affinity and ionization potential of the fullerene C_{60} could be attributed to two factors.[73]

- The resultant negatively charged carbon atoms from electron attraction would have additional sp^3 character and would have longer bond lengths to their neighbours and so decrease the strain energy of the C_{60}. In contrast, positively charged C_{60} resulting from electron loss would have more sp^2 character and would have shorter bond lengths to their neighbours and thus increase the strain energy of the cage.
- In case of considering the C_{60} as "superbenzopyracylene", the cage would be expected to be electronegative because pyracylene **14** has a relatively high electron affinity (Figure 25).

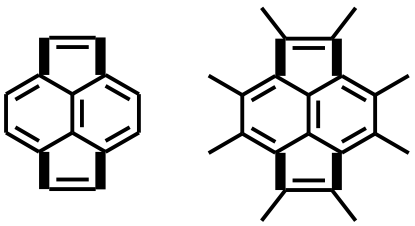

Pyracylene **14** C_{60} **5**

Figure 25. Pyracylene.[73]

2.1.2. Functionalized fullerene derivatives.

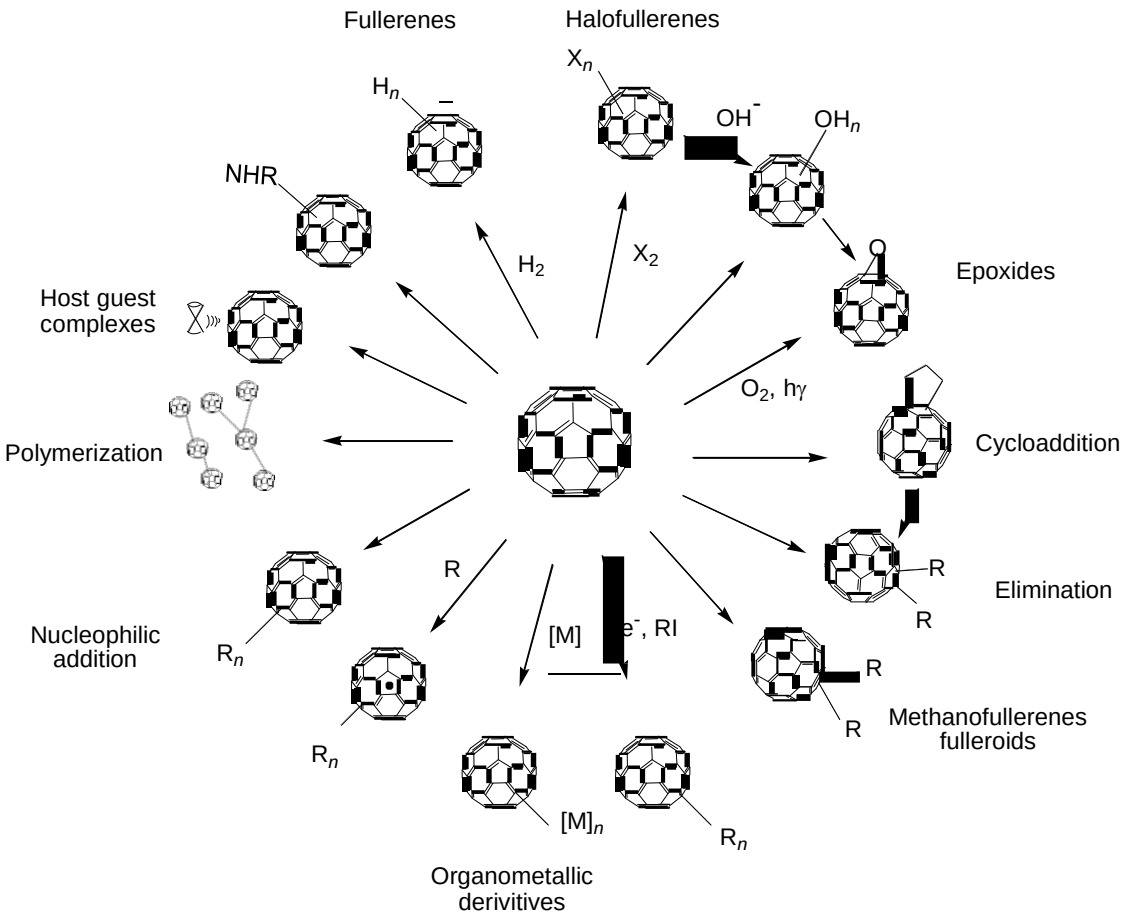

Figure 26. Some general fullerene reactions. [69]

C_{60} became a new building block in a family of molecules for novel architectures in biological,[77] supramolecular [78-80] and materials [81-83] chemistry (Figure 26).

Fullerenes can undergo (2+2) (B), and (2+4) (A) cycloaddition reactions with other organic molecules to form four, five and six membered rings fused outside the fullerene shell (Figure 27). A (2+4) addition involves a rearrangement of four π–electrons from a conjugated diene unit (C=C-C=C) on the organic reactant molecule and two π–electrons from a double bond in the fullerene. In the same way (2+2) involves a bond rearrangement in which two pairs of π–electrons, one pair from C_{60} and the other pair from the reactant organic molecule are redistributed to form new single bonds joining the molecules.[43]

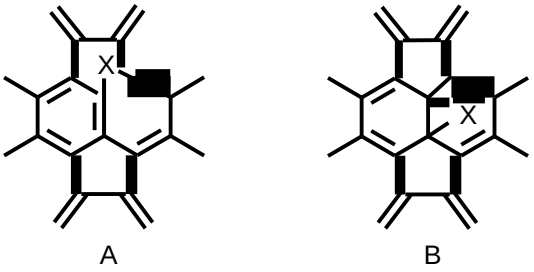

Figure 27. Two possible sites for bridge attachments.[43]

An example of a cycloaddition reaction is the reaction of C_{60} with azomethine ylides[84] (Scheme 4). Azomethine ylides can be represented as a reactive 1,3-dipole. It can be easily generated by decarboxylation of N-methylglycine (sarcosine) and paraformaldehyde when refluxing in toluene.

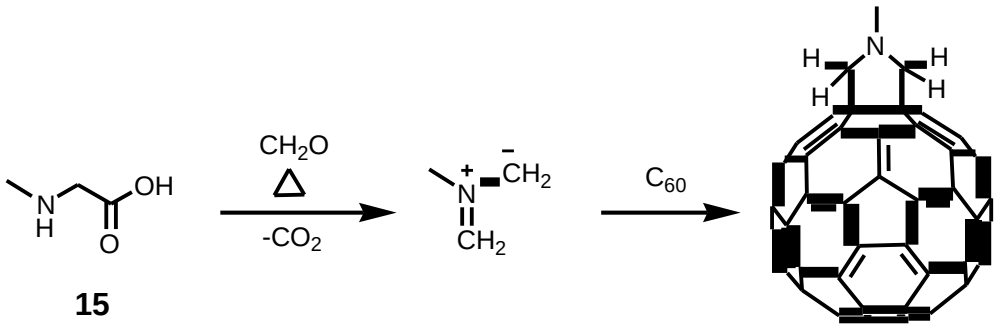

15 **16**

Scheme 4. Reaction of C_{60} with azomethine ylides.[84]

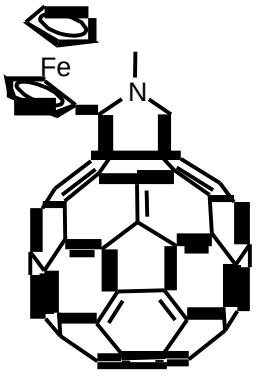

17

Figure 28. Reaction of C_{60} with ferrocene. [84]

However, it has been found that most of the C_{60} derivatives present poorer electron acceptor properties than the parent C_{60} as a consequence of the saturation of a double bond of the C_{60} structure that raises the LUMO energy.[85] But the reasonable electron affinity of the fullerene has persuaded researchers to connect the C_{60} with electro active molecules in

order to enhance the redox activity. The azomethine ylides methodology has been used to produce redox active species *via* the combination of C_{60} with an electroactive species like ferrocene **17** [84] (Figure 28).

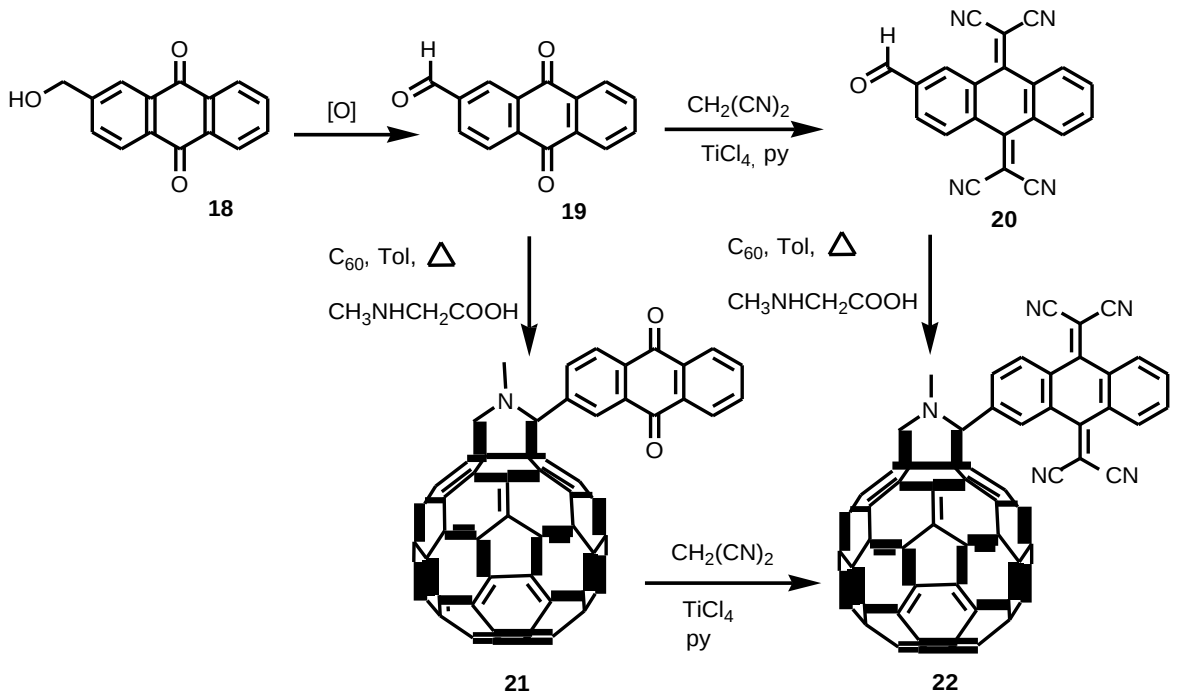

Scheme 5. Reaction of C_{60} with anthraquinone and TCNAQ.[86]

Donor molecules were added to C_{60} in order to form electrically conducting salts and charge transfer complexes[87]. But electrically insulated complexes were formed due to the weak electron acceptor behaviour of the fullerene[88]. Consequently, novel fullerene derivatives were synthesised to enhance the electron acceptor ability.[89] For example a strong electron acceptor moiety derived from tetracyano-*p*-quinodimethane (TCNQ) and dicyano-*p*-quinodiimine (DCNQI) have been used as precursors for novel C_{60} based electron acceptors[86]. These new systems have shown a remarkable electron acceptor behaviour that are able to accept up to six electrons in solution[90] (Scheme 5). In another example compound **23** was produced which upon reduction gave rise to a radical-anion located on the quinone moiety and the second electron located on the C_{60} cage[91] (Figure 29). In addition, C_{60} based triads from fulleropyrolidine moiety on C_{60} have been connected to an electron donor ferrocene and electron accepting anthraquinone **25** or (TCNAQ) (**24**).[92] On the other hand, charge – transfer complexes can be formed from host-guest complexes of fullerenes with [bis(ethylenedithio)tetrathiafulvene] and with ferrocene C_{60}(ferrocene)$_2$. (**26**) and (**27**). The extent of charge separation in these complexes is important for many aspects like molecular conductors.[92]

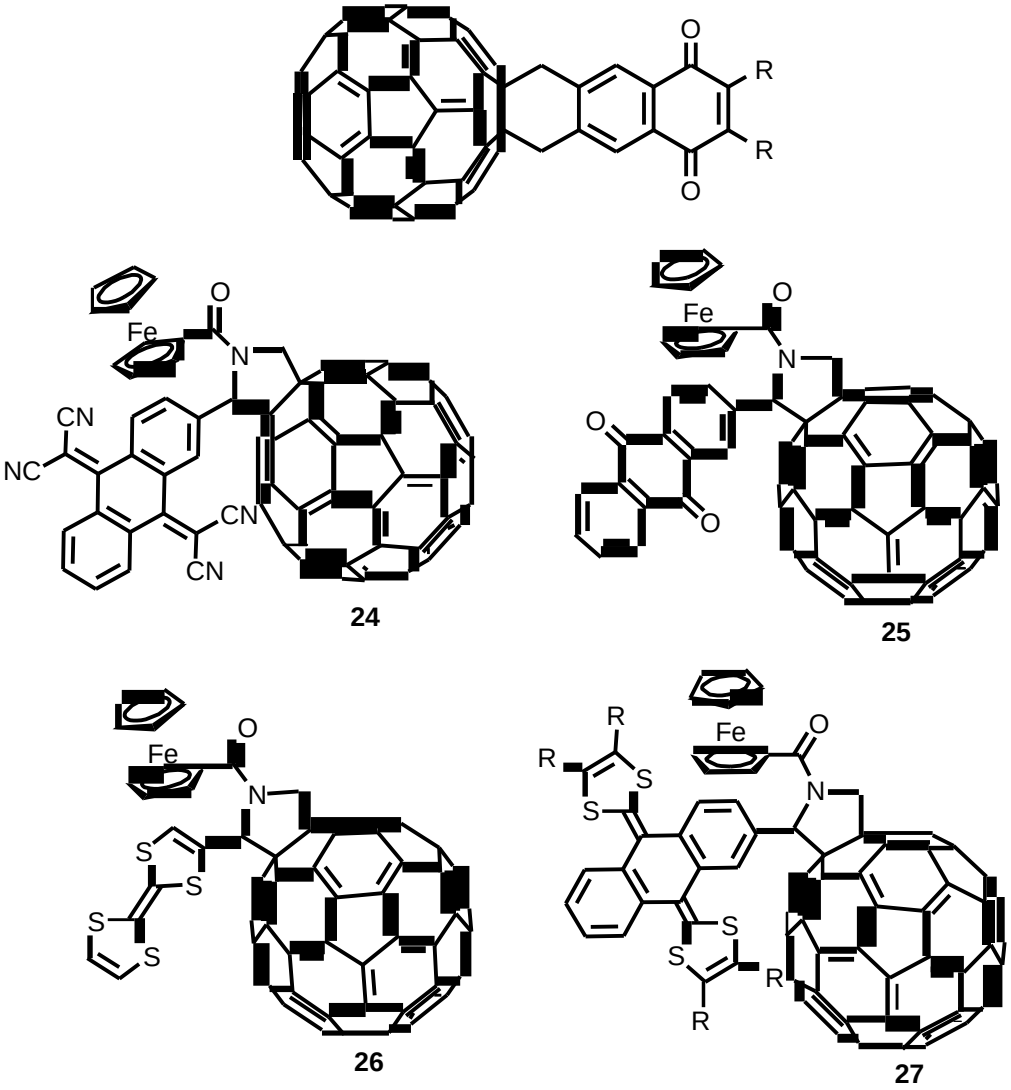

Figure 29. Functionalised C_{60} derivitives

It has been shown that the electrochemically-tuneable interactions occur between flavin-functionalised C_{60} derivatives and a diaminopyridine derivative. Nevertheless, the C_{60} unit does not considerably reduce the flavin's ability to undergo electrochemically-tuneable hydrogen bonding interactions with diamidopyridine derivative. In fact, the electrochemical reduction of the flavin moieties to their radical anion states has demonstrated a significant redox-enhanced binding between the flavin moieties and DAP (Figure 30).[79]

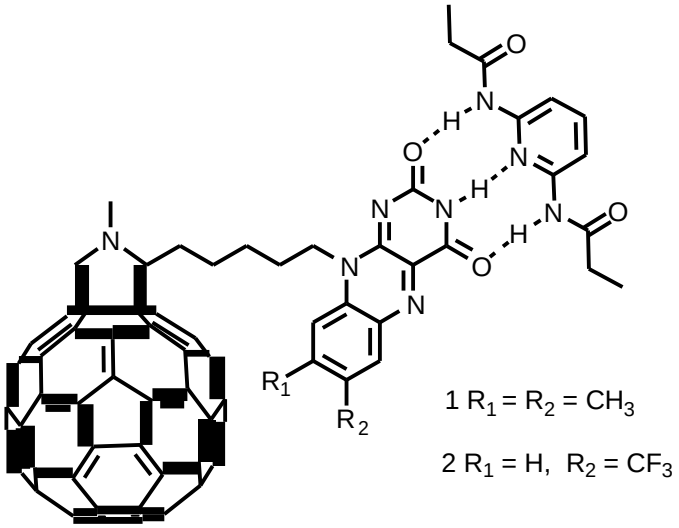

28

Figure 30. Flavin-functionalised C_{60} derivatives and diaminopyridene derivative.[79]

A dyad (C_{60}–PTCDI) and triad (C_{60}–PTCDI–C_{60}) were synthesised based on fullerene (C_{60}) and 3,4,9,10-perylene tetracarboxylic diimide (PTDCI). The dyad C_{60}–PTCDI was capable to reversibly accepting with up to four electrons whereas the triad C_{60}–PTCDI–C_{60} could accept up to six electrons [93] ((Figure 31) and (Figure 32)).

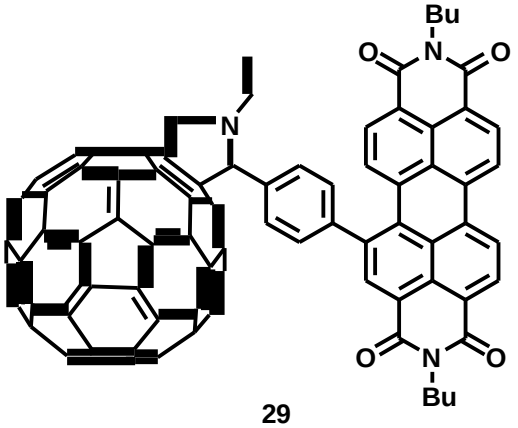

29

Figure 31. C_{60}–PTCDI. [93]

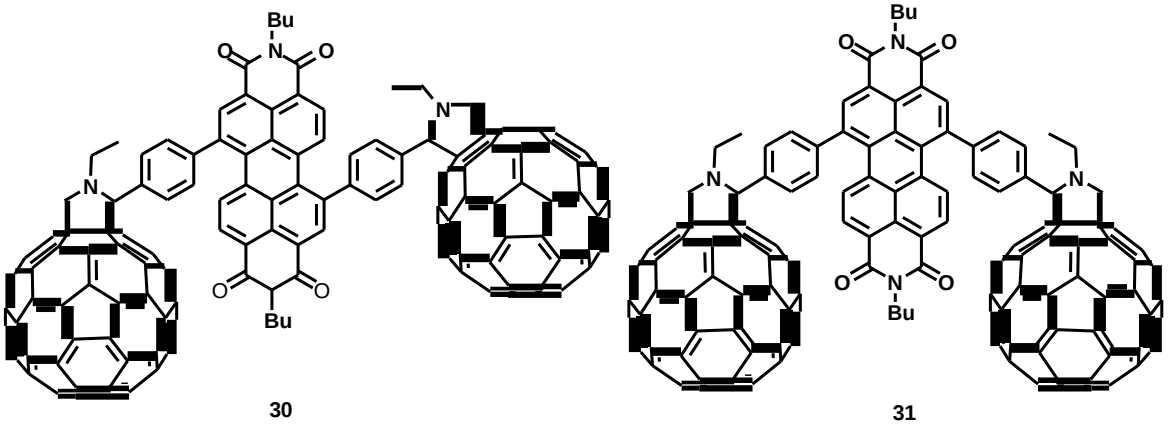

30 31

Figure 32. C_{60}–PTCDI–C_{60}.[93]

2.1.3. [PCBM] - Phenyl-C_{61}-Butyric Acid Methyl Ester.

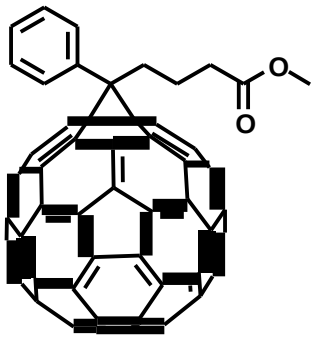

11

Figure 33. PCBM .

Fullerene has been modified to improve solubility in organic solvents. For example, phenyl -C_{61}-butyric acid methyl ester (PCBM) (Figure 33) is one of the most important fullerene derivatives, which is highly soluble in chlorobenzene. The methodology of synthesizing [6,6] methanofullerenes was by cyclopropanation of fullerenes based on the in situ formation of a reactive diazocompound from tosylhydrazone and sodium methoxide followed by carbene addition[21](Scheme 6).

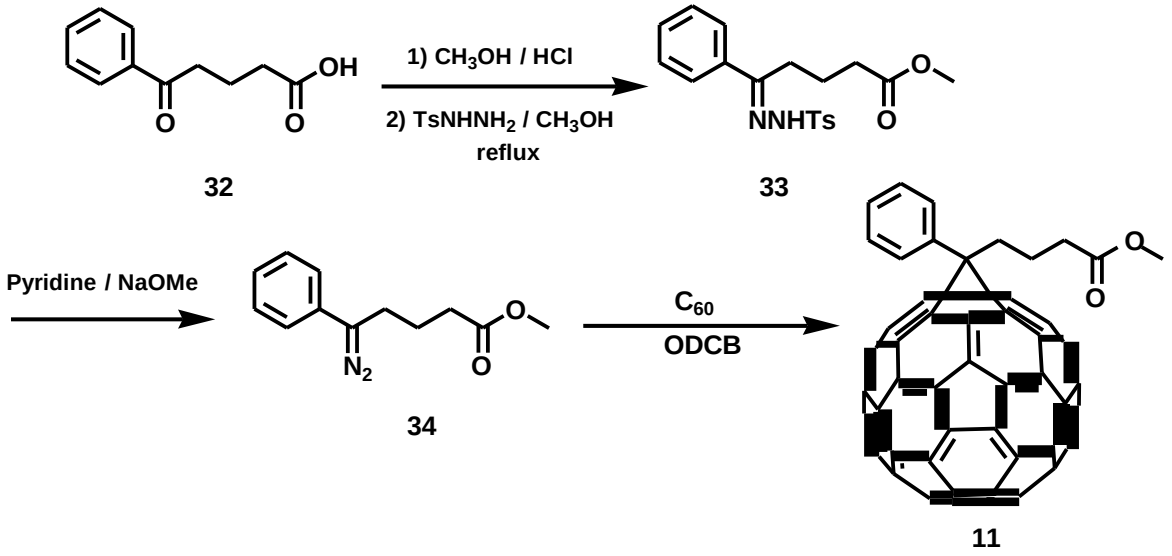

Scheme 6. Synthesis of PCBM.[21]

PCBM is an efficient solution processable electron acceptor. The high affinity of PCBM effects photo-induced electron transfer from electron donor molecules. Hence it has been incorporated in bulk heterojunction photodiodes.[94] Blending PCBM with electron donor molecules (like conjugated polymers) has been investigated in organic photovoltaic cells (PV),[95,96] thin-film organic field effect transistors (OFETs),[97] and photodetectors.[98] However, fabrication of bulk heterojunction organic photovoltaic cells OPVs requires soluble fullerene derivatives in order to form blends with p-type polymer semiconductors. Consequently, PCBM became a generally utilized material for solution processed organic solar cells. The power conversion efficiency (η) for OPVs is typically around 2.5% by devices incorporating PCBM.[99] The power conversion efficiency (η) has been raised to 6% through employing polythiophene/ PCBM system.[100,101]

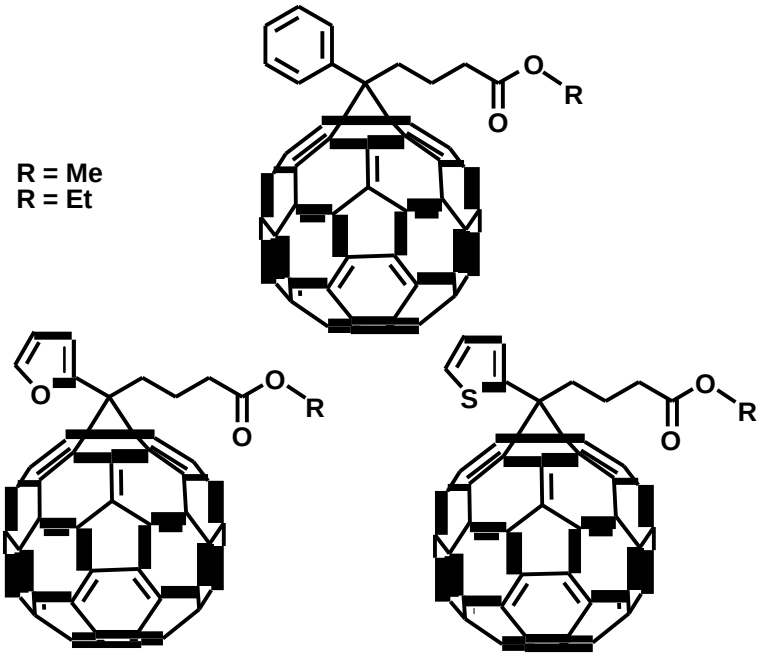

Figure 34. PCBM analogues.[61]

Various analogues of PCBM have been synthesized and tested as n-type semiconductors. PCBMs have shown significant electronic and optical properties compared to the parent fullerene, for instance, fast electron transfer, an adequate dielectric constant, electron accepting properties and good electron mobility. In addition to the improved solubility in common organic solvents, PCBMs provide robust formation of uniform nanoparticulate n-type domains in the final film. Modified PCBMs have been synthesised by replacing the phenyl ring with 2-thienyl and 2-furyl groups or replacing the methoxy group with different alkyl groups. These were blended with P3HT to be used as acceptors in bulk heterojunction polymer solar cells. However, the power conversion efficiencies for the solar cells were enhanced depending on the best material combinations between donor and acceptor components which should have sufficiently high solubility in the solvent used for the deposition of the active layer[61] (Figure 34).

2.2. The aim of the project

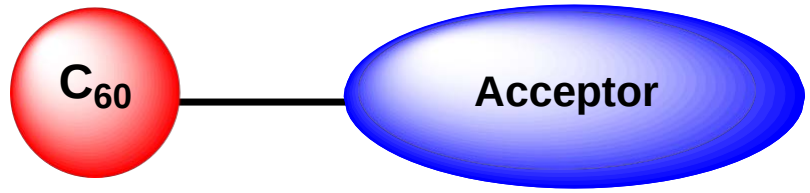

Acceptor - Flavin
NDI
TCNAQ
Anthraquinone
Phenyl
Benzyl

Figure 35 New PCBM analogues

This project describes the synthesis of a new series of electron acceptors based on PCBM with various electron poor moieties. Due to the extensive redox chemistry and photochemical properties of the associated species, these compounds can be an attractive target in fabricating of photovoltaic devices.[99] These acceptor–acceptor molecular systems could afford broader range of LUMO energies which may allow the investigation of a wider range of complementary donor polymers. In addition, by synthesising these kinds of compounds, we can modulate the absorption of light towards the near-IR region.

2.3. Synthesis of new C_{60} acceptor

Novel PCBM analogues were synthesised by connecting the PCBM to different electro active moieties like flavin, TCNAQ, NDI and anthraquinone. We also report the synthesis of phenyl and benzyl derivative to help improve solubility. Molecular structures of synthesised fullerene derivatives are shown in (Figure 36).

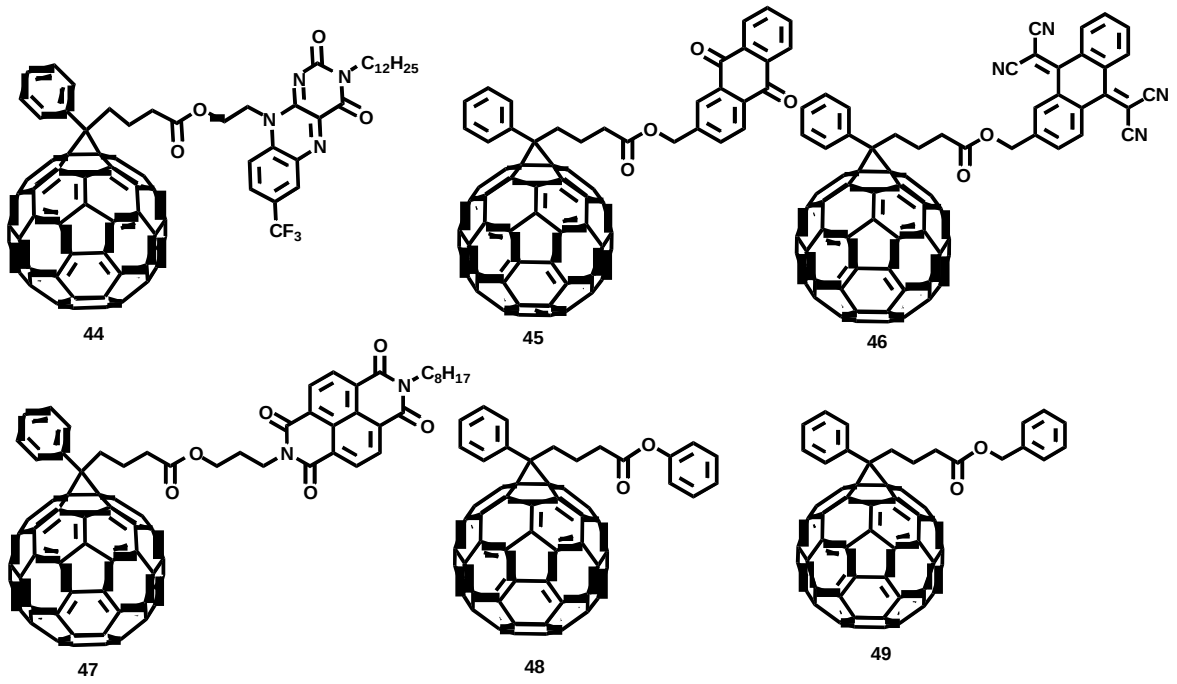

Figure 36. Synthesised PCBM-acceptors.

PCBM was used as the starting material for a range of new compounds. Firstly, the PCBM was hydrolysed under acid conditions.[21] The acid undergoes esterfication with corresponding alcohols in the presence of DCC as an activating coupling reagent and both DMAP and HOBT [102](Scheme 7).

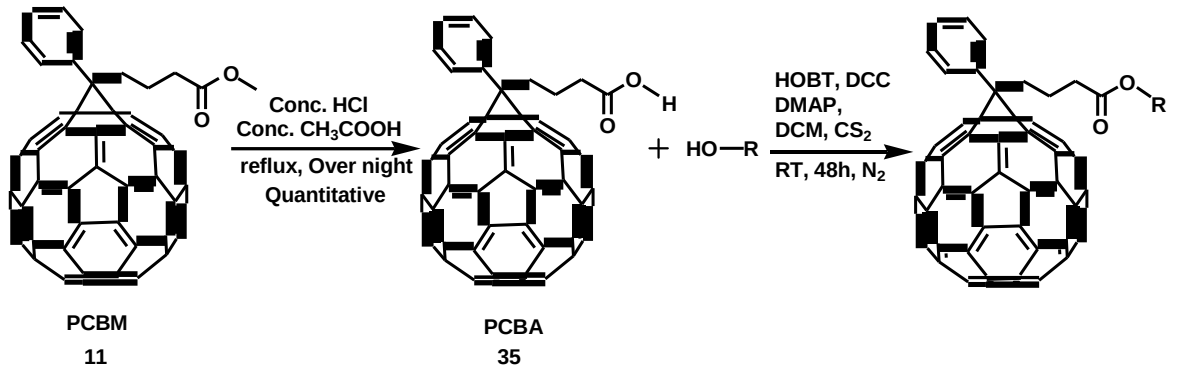

Scheme 7. Synthesis of PCBM analogues.

The novel esters were synthesized *via* a Steglich esterification. The reactions were undertaken in dichloromethane at ambient temperature, forming satisfactory yields of the required esters. Dicyclohexylcarbodiimide DCC was used as coupling reagent and 4-dimethylaminopyridine DMAP as a catalyst.[103,104] Hydroxybenzotriazole HOBT was added as coupling agent to produce the activated ester [105] (Scheme 8).

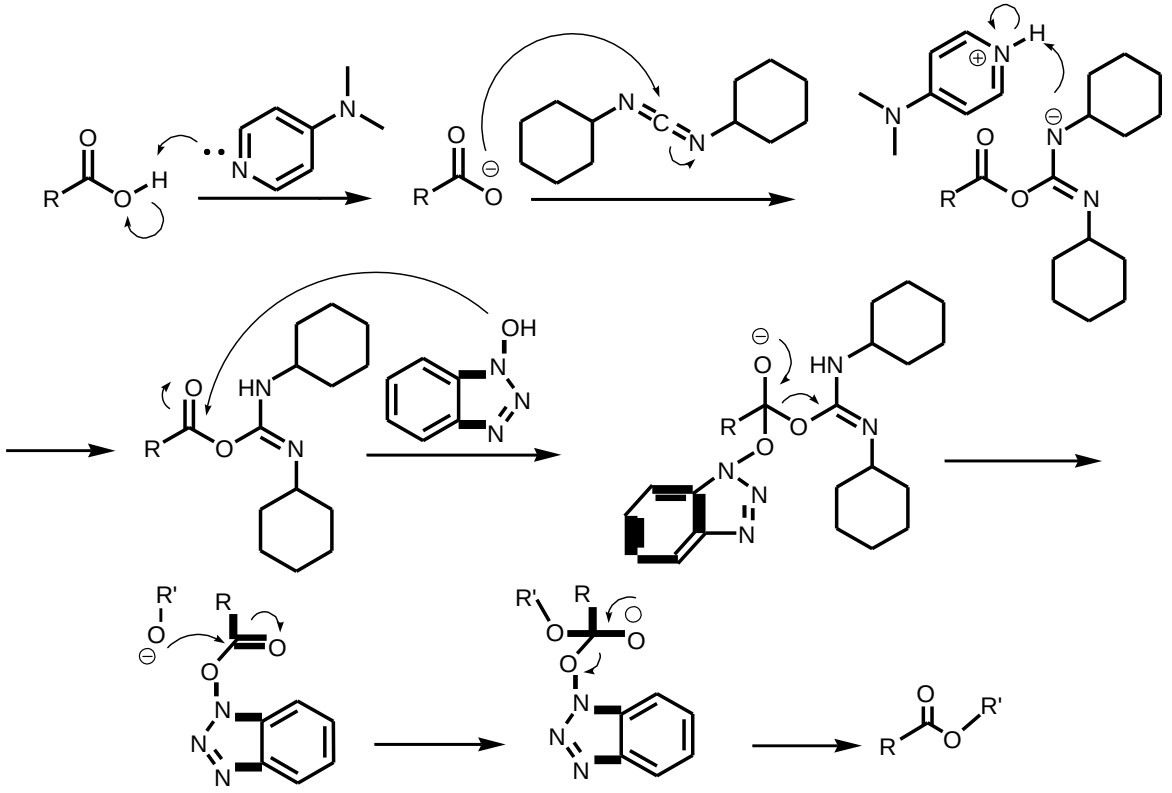

Scheme 8. Steglich esterification.

The synthesis of flavin-functionalised PCBM derivative **44** was carried out through preparation of compound **40** which was synthesised using the following synthetic pathway as illustrated in (Scheme 9).[102]

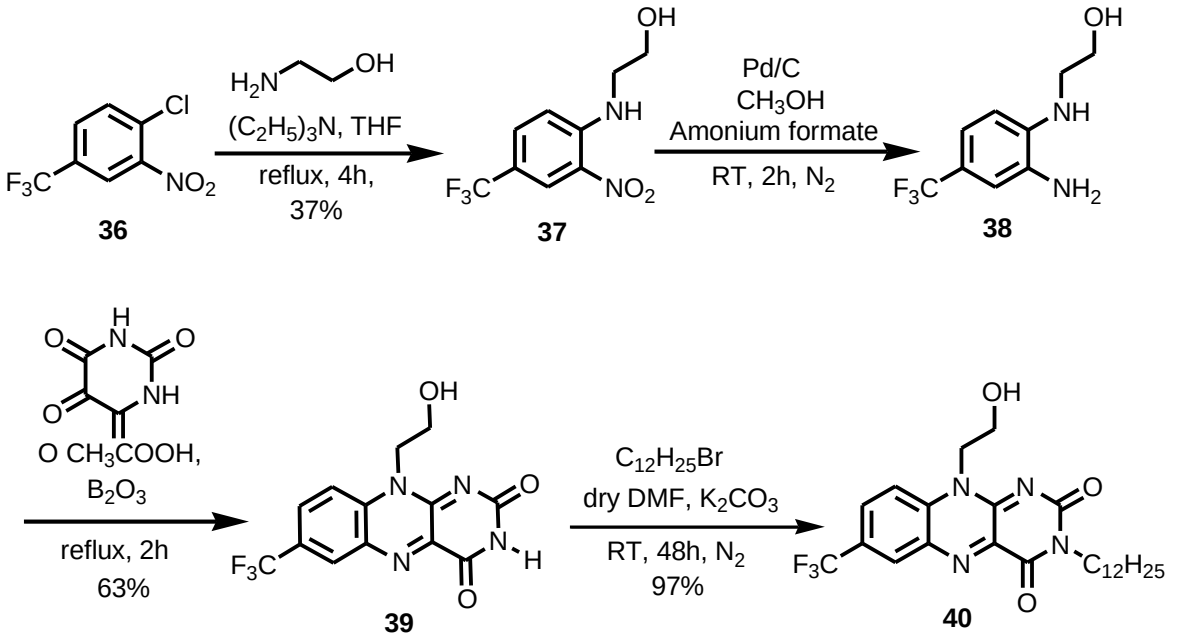

36 **37** **38** **39** **40**

Scheme 9. Synthesis of flavin 40.

2-(4-(Trifluoromethyl)-2-nitrophenylamino)ethanol (**37**) was synthesised in 37% yield by a nucleophilic aromatic substitution reaction between ethanol amine and 1-chloro-2-nitro-4-(trifluoromethyl)benzene in the presence of triethylamine. Since the carbon-halogen bond in aryl halide is stronger than the carbon-halogen bond in alkyl halide, aryl halide would be relatively unreactive towards nucleophilic substitution reactions. However, the presence of strong electron withdrawing groups in *para* and *ortho* positions to the -Cl in the aryl ring would facilitate the nucleophilic substitution reaction. The addition-elimination mechanism involves the addition of nitrogen's lone pair on the primary amine to the aromatic ring to produce the carbanion with delocalized electron pair which is stabilized by the presence of the electron withdrawing groups (-NO_2 and –CF_3) *ortho*- and *para*- to the –Cl. Chloride ion elimination occurs in order to recover the aromaticity of the ring. This mechanism is called the S_NAr mechanism. The presence of triethylamine is to neutralize the HCl that was being formed during the reaction.(Scheme 10, Scheme 11 and Scheme 12)

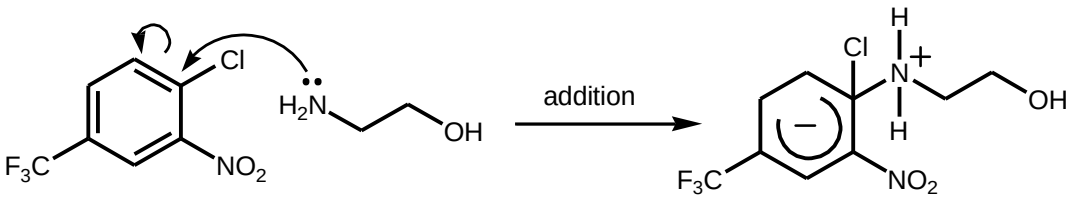

Scheme 10. Addition of ethanol amine to 1-chloro-2-nitro-4-(triflouromethyl)benzene.

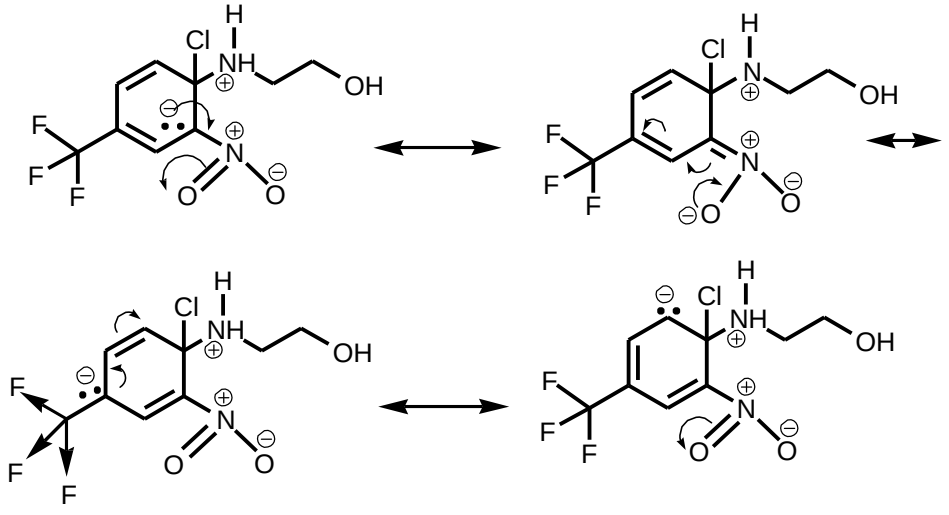

Scheme 11. Stabilization of the carbanion through resonance stucture.

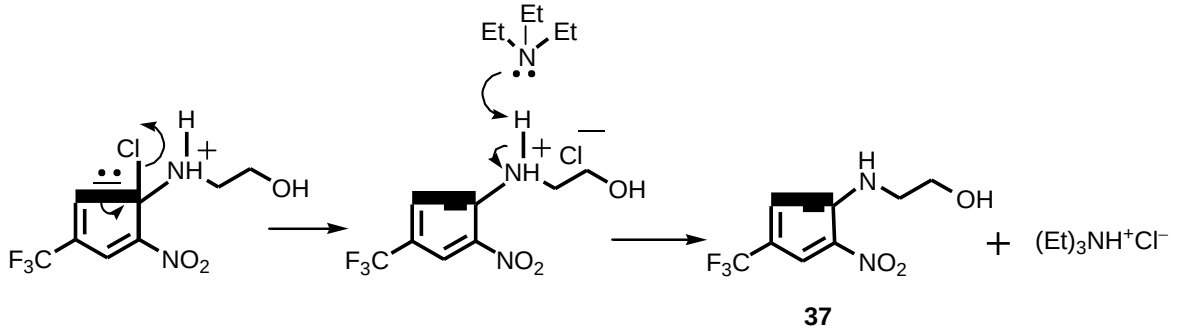

37

Scheme 12. Elimination of the chloride ion.

Reduction of the nitro group to amine was catalysed by using palladium on carbon in the presence of ammonium formate as the hydrogen donor to afford compound **38** which was converted directly to compound **39** due to instability of compound **38**. 7-(Trifluoromethyl)-10-(2-hydroxyethyl)-alloxazine **39** was synthesised by treating **38** with alloxan monohydrate and boric anhydride in glacial acetic acid.[106]. To enhance the solubility of the flavin an n-dodecyl group was added to the N3 of the flavin. The reaction took place in the polar solvent (DMF) in the presence of potassium carbonate.

The synthesis of TCNAQ analogue **41** was carried out by Knoevenagel condensation from commercially available 2-hydroxymethyl-9,10-anthraquinone by reaction with Lehnert reagent ($TiCl_4$, malononitrile, pyridine) and *β*-alanine. Thus, 2-hydroxymethyl substituted TCNAQ was obtained as a stable yellow solid in 43% yield[107] (Scheme 13).

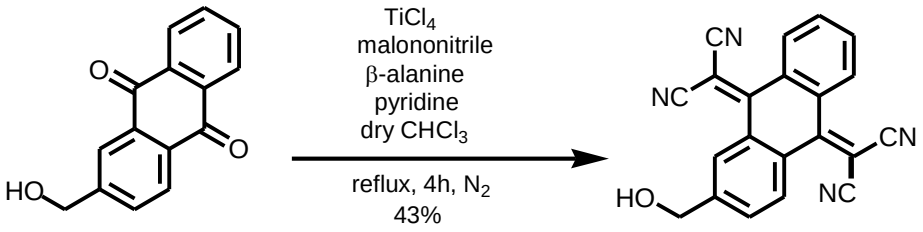

18 **41**

Scheme 13. Synthesis of TCNAQ 41.

A naphthalene diimide **43** bearing two different substituents on the diimide nitrogens was synthesized in a two step procedure in which commercially-available 1,4,5,8-naphthalenetetracarboxylic dianhydride was reacted with n-octyl amine and then with propanol amine in the high boiling solvent DMF (Scheme 14).

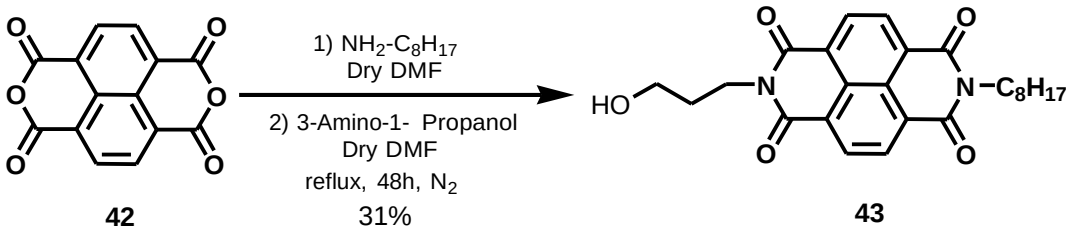

42 **43**

Scheme 14. Synthesis of unsymmetrical NDI 43.[108]

2.4. Characterisation.

2.4.1. NMR Spectroscopic studies.

The spectroscopic data of all derivatives are in agreement with the proposed structures.
The ^{1}H NMR spectra confirmed the expected signals for the PCBM and connected moieties. ^{13}C NMR spectra of all PCBM derivatives showed the relevant peak of methanofullerene in the 80 ppm region for the two cyclopropyl sp^3 carbon atoms of the fullerene cage. The infrared spectras have revealed ester's main absorptions between 1717 and 1751 cm^{-1}.

2.4.2. UV-Visible spectroscopy

UV-Vis spectroscopy in (1 x 10^{-5} M in CH_2Cl_2) provided the PCBM's main strong two peaks in the UV region at 260 nm and 328 nm and another two weak peaks in the visible region at 431 nm and 695 nm. Some of the synthesised compounds, akin to PCBM, have shown a long tail after 700 nm towards longer wave length. π-π^* transitions were clearly observed at 360 nm and 380 nm for PCBM –NDI **47** and at 412 nm and 460 nm for PCBM-Flavin **44** whereas the PCBM-TCNAQ **46** has shown a shoulder in the area 350-380 nm (Figure 37).

Table 1. UV-Vis spectroscopy data of the PCBM and PCBM derivatives.

Compounds	λ^1_{abs}	λ^1_{ons}	λ^2_{abs}	λ^2_{ons}	λ_{abs}	λ_{ons}	λ_{abs}	λ_{ons}	λ^3_{abs}	λ^3_{ons}	λ_{abs}	λ_{ons}	λ^4_{max}	λ^4_{ons}	E_{gap}
PCBM	259	300	328	347					431	440			695	T	
44	261	300	328	347			412	420	432	450	460	485	695	730	1.7
45	259	300	328	347					431	440			695	T	
46	260	300	330	347					431	440			695	T	
47	260	300	328	347	360	368	380	390	431	440			695	730	1.7
48	259	300	327	347					431	440			696	T	
49	262	314	330	425					432	450	508	648	696	730	1.7

λ_{abs}– maximum absorption wavelength of each peak (nm)

λ_{ons}– onset of each peak (nm)

λ_{max}– maximum wavelength (nm)

E_{gap}– gap energy (ev)

T – weak tail toward long wave lengths

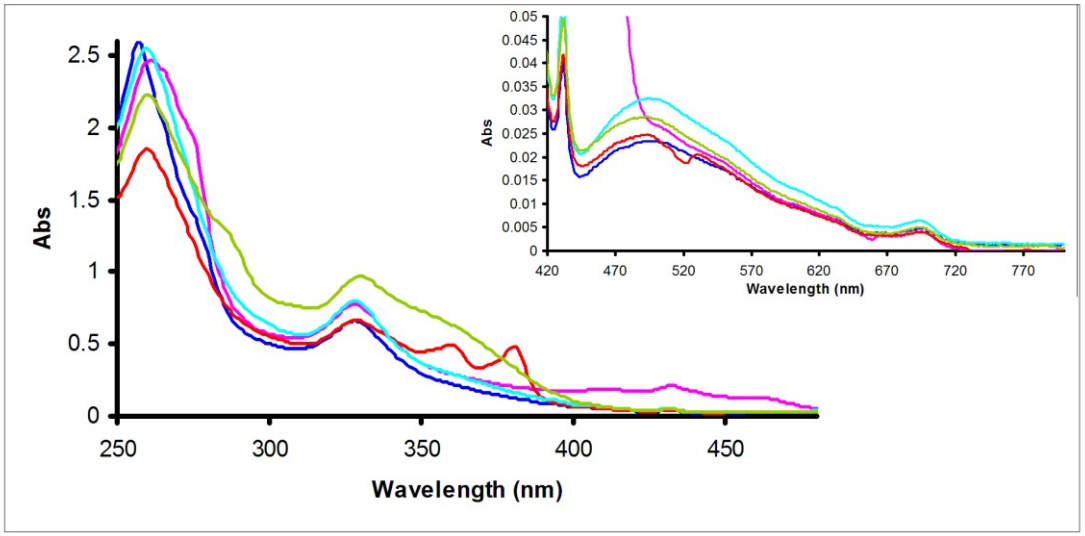

Figure 37. UV-Vis spectroscopy of PCBM analogues recorded in 1x 10^{-5} M DCM. PCBM 11 (blue line), PCBM-Flavin 44 (purple line), PCBM-NDI 47 (red line), PCBM-Anthraq 45 (turquoise line) and PCBM-TCNAQ 46 (green line).

2.4.3 Electrochemical Studies

Electrochemical properties of these acceptor-acceptor systems were investigated by cyclic voltammetry to determine the influence of substituents on the LUMO energy of PCBM.

The voltammetric behaviours of all compounds (1 x 10^{-4}M) were investigated at room temperature in CH_2Cl_2 containing tetra-n-butyl ammonium hexafluorophosphate (Bu_4NPF_6 0.1 M) as supporting electrolyte with a platinum wire as working and counter electrodes and a silver wire as a quasi-reference electrode. E_{LUMO} values for the compounds are referred to the potential of the Fc^+/ Fc redox couple utilized as an internal standard. The scan rate was 0.1 V/s. As summarised in Table 2, flavin **44**, anthraquinone **45** and TCNAQ **46** substituted PCBM derivatives have shown four reversible reduction waves, whereas the NDI derivative **47** has three reduction waves corresponding to the first reduction steps of the fullerene moiety. However, there was no significant difference between the first reduction potential of all PCBM derivatives and the first reduction potential of PCBM except for compound **46**. The reduction potential values are quite similar to those found for PCBM, however, another reversible reduction wave is observed corresponding to the reduction of the electroactive TCNAQ modified compound **46** (Figure 38) and (Figure 39).

Table 2. Cyclic Voltammetry Data of the PCBM and PCBM derivatives with the starting materials before connection.

Compounds	E^1_{red}	E^2_{red}	E^3_{red}	E^4_{red}	E^1_{rev}	E^2_{rev}	E^3_{rev}	E^4_{rev}	ΔE	$E_{1/2}$	E_{LUMO}
PCBM	-1.17	-1.55	-2.05	-2.20	-1.09	-1.47	-1.96		-0.08	-1.13	-3.67
40	-1.12	-1.95			-1.03	-1.76			-0.09	-1.08	-3.72
44	-1.15	-1.53	-1.94	-2.03	-1.05	-1.46	-1.84	-1.96	-0.10	-1.10	-3.70
18	-1.46	-1.96			-1.36	-1.83			-0.10	-1.41	-3.39
45	-1.16	-1.42	-1.52	-2.06	-1.09	-1.34	-1.46	-1.90	-0.07	-1.13	-3.68
41	-0.88	-1.61			-0.77				-0.11	-0.83	-3.98
46	-0.87	-1.14	-1.52	-2.03	-0.75	-1.07	-1.45	-1.95	-0.12	-0.81	-3.99
43	-1.10	-1.50			-1.02	-1.41			-0.08	-1.06	-3.74
47	-1.16	-1.55	-2.06		-1.06	-1.45	-1.95		-0.10	-1.11	-3.69
48	-1.14	-1.51			-1.07				-0.07	-1.11	-3.69
49	-1.19	-1.58	-2.07		-1.09	-1.48	-1.97		-0.10	-1.14	-3.66

ΔE – Energy difference between peaks potential (forward and backward sweep) in (V).

$E_{1/2}$ – Half wave potential $E^1_{red} + E^1_{rev}/2$ (V).

$$E_{LUMO} = - 4.8 – E_{1/2} (V)$$

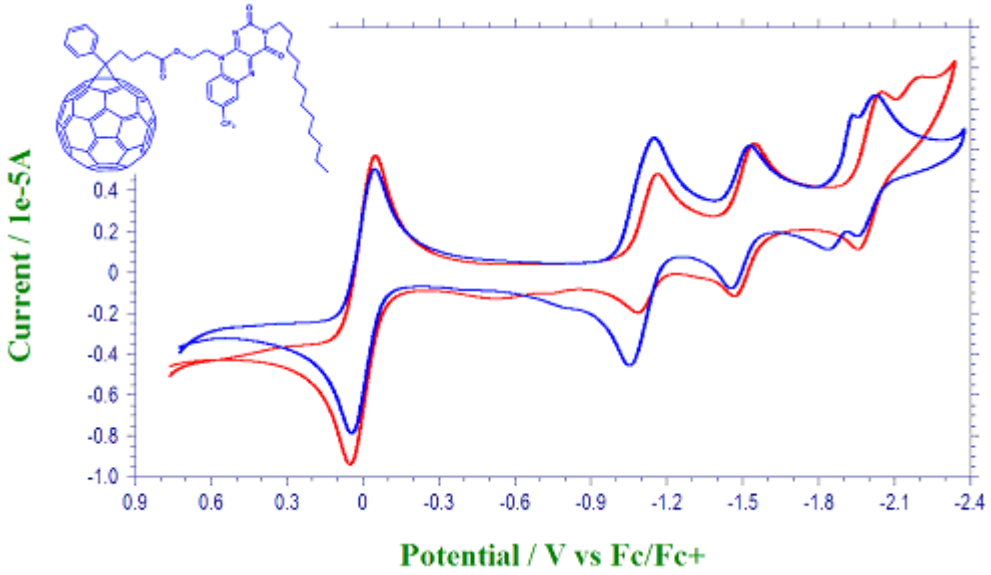

Figure 38. Cyclic Voltametry of compound (44) (blue line) and PCBM (red line).

The significant decrease of the first reduction potential is observed for TCNAQ functionalised PCBM derivative **46** (300 mV) (Figure 39), which indicates that it is stronger electron acceptor than PCBM. A possible reason for this anodic shift is the better accepting ability of the connected electron-acceptor unit. On the other hand, it is worth mentioning that the anthraquinone moiety in **45** which appear at -1.16 V gives rise to slightly better acceptor ability than the parent anthraquinone -1.46 V. This shift is probably due to the close proximity between the anthraquinone and the electron-withdrawing C_{60} core.

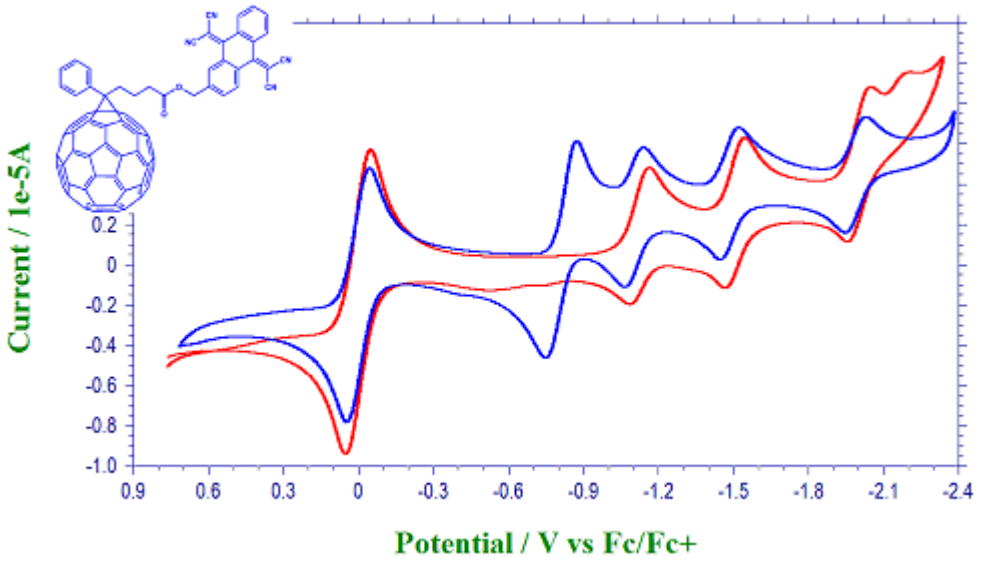

Figure 39. Cyclic Voltametry of compound 46 (blue line) and PCBM (red line).

PCBM was also functionalised with phenyl and benzyl groups to improve the solubility of this acceptor in chlorobenzene, which is the solvent of choice for device fabrication. Also it was anticipated that the aromatic substituent may interact with the fullerene thus influencing their reduction potentials.[109] Unfortunately, it was shown that PCBM functionalised with one phenyl moiety (**48**) had limited effect on the reduction potential of the PCBM unit.

It is worth mentioning that the LUMO levels for the most synthesised PCBM derivatives are negatively raised with respect to the LUMO level of parent PCBM. The higher LUMO level of the acceptor is important to decrease the lost energy that required splitting the exciton which cannot be gained as electrical energy in heterojunction solar cells.

On the other hand, all the compounds including the PCBM showed reduction waves shifted to more negative potentials than the parent C_{60} due to the saturation of a double bond in the C_{60} cage which raises the LUMO energy.[89]

2.5. Photovoltaic devices

The synthesised compounds have been forwarded to St-Andrews University to fabricate photovoltaic cells and to study their efficiencies. Photovoltaic cells were fabricated using P3HT as polymer component combined with three of the PCBM analogues and compared with the reference compound PCBM. Poly(3-hexylthiophene) (P3HT) is a conjugated polymer that is widely used in the ongoing researches in the field of organic photovoltaic. Therefore, compounds **44**, **46** and **47** were investigated as electron-acceptor materials in combination with P3HT which is used as the electron-donor component

2.5.1. Absorption measurements

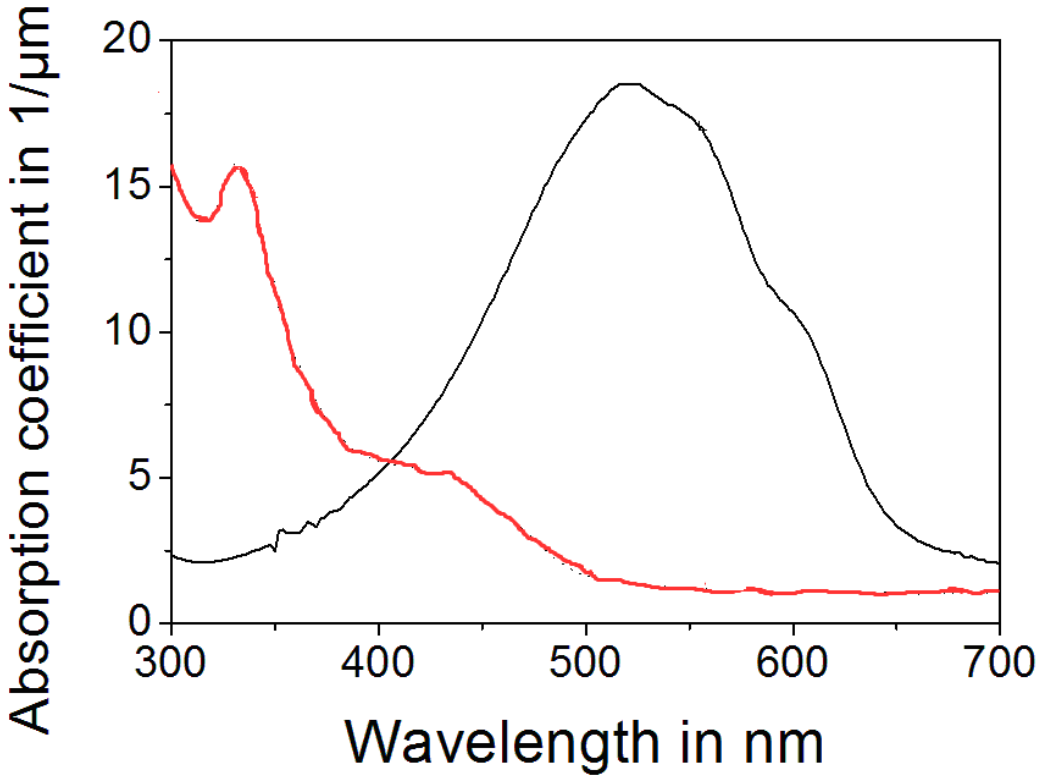

Figure 40. Absorption coefficients for P3HT (black line) and compound 44 (red line) for neat films not annealed.

UV-Vis spectroscopy was recorded for neat P3HT and neat PCBM-Flavin **44** films. Figure 40 shows a comparison of the two material combinations. Clearly, the absorption of the P3HT is higher within the visible region than that of **44**. Blending of both materials combine these absorption spectra. The absorption of (P3HT:**44**) was measured for blends of 1:1, 1:2, 1:3, 1:4 before and after annealing at 130°C for 20 minutes. Figure 41 shows the results of the measurements. All spectra are normalized at the maximum between 400 nm and 600 nm. The change of the absorption spectrum indicates that the morphology of the films changes through the annealing process. The morphology of the materials in the blend has a strong influence of the efficiency of the solar cells.

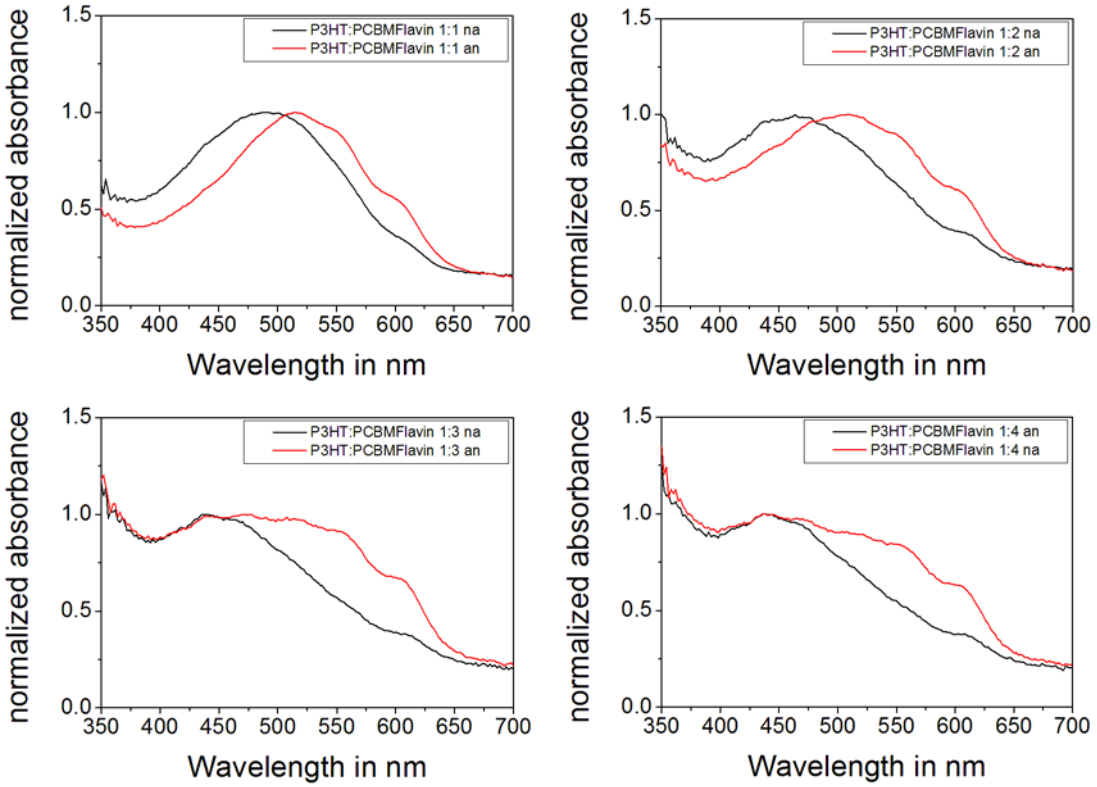

Figure 41. Absorption of different P3HT:PCBM-Flavin blends before (na) and after annealing (an) at 130 °C for 20 minutes.

The absorption was measured on PCBM-NDI **47** films fabricated with solutions made of 20 mg/ml of chlorobenzene, stirred over night at 70°C. The solutions are spin coated on quartz substrates with a spin speed of 1500 rotations per minute for 90 seconds and a ramp of 50. The resulting film thickness was about 73 nm. The absorption of PCBM-TCNAQ **46** was measured on a film based on a 4 mg/ml solution of chlorobenzene, as higher concentration leads to poor quality films. The film thickness was about 44 nm, where the solution was filtered before with 0.45 µm. The absorption spectra were similar for PCBM-NDI **47** and PCBM-TCNAQ **46** compared to PCBM and PCBM-Flavin **44** (Figure 42).

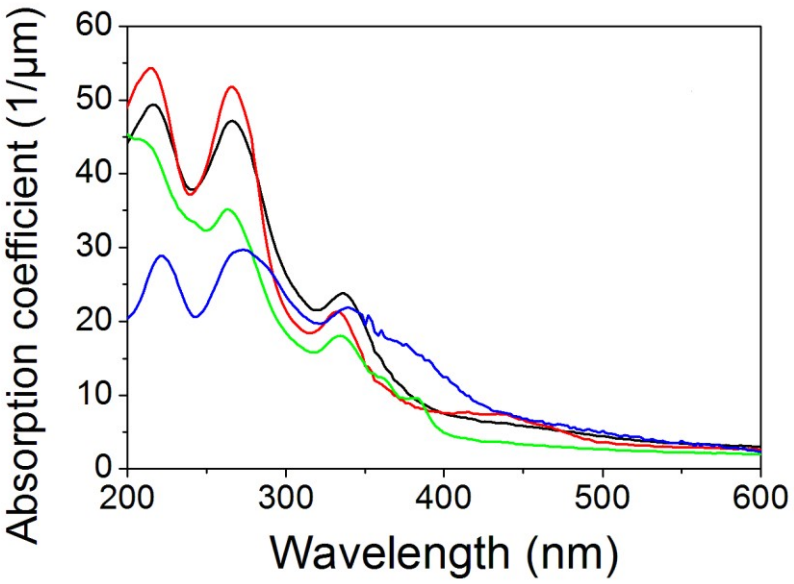

Figure 42. Absorption spectra for C_{60}-derivatives PCBM-Flavin 44 (red line), PCBM-NDI 47 (green line) and PCBM-TCNAQ 46 (blue line) compared to PCBM (black line). PCBM-TCNAQ 46 creates highly scattering films that causes lower transmission at longer wavelength.

2.5.2. Fluorescence quenching

Fluorescence of P3HT occurs when the exited singlet exciton recombines radiatively. Introducing an acceptor leads to charge separation of bounded charges and hence quenches the fluorescence of P3HT, so the quenching could be a good indication that the created charges from absorption of light are transferred to the acceptor. However, the decay of photoluminescence quantum yield (PLQY) over the concentration of the acceptor gives a good indication of charge separation. (PLQY) was measured with a Hamamatsu U6039-05 on P3HT:**44**, P3HT:**47** and P3HT:**46** blends of different ratios and were compared with a neat P3HT film. Films were prepared by mixing a solution of P3HT with solutions of 20 mg/ml for compound **44** and of 2 mg/ml for compounds **46** and **47** all dissolved in chlorobenzene. Solutions of P3HT and the acceptors were mixed by appropriate amounts to achieve a specific concentration of compounds **44**, **46** and **47** determined per total mass. The mixture was spin coated with 1500 rpm on quartz disks in a glove box. The films were not annealed. The excitation wavelength was 500 nm and the fluorescence was integrated over a range from 600 nm to 900 nm.

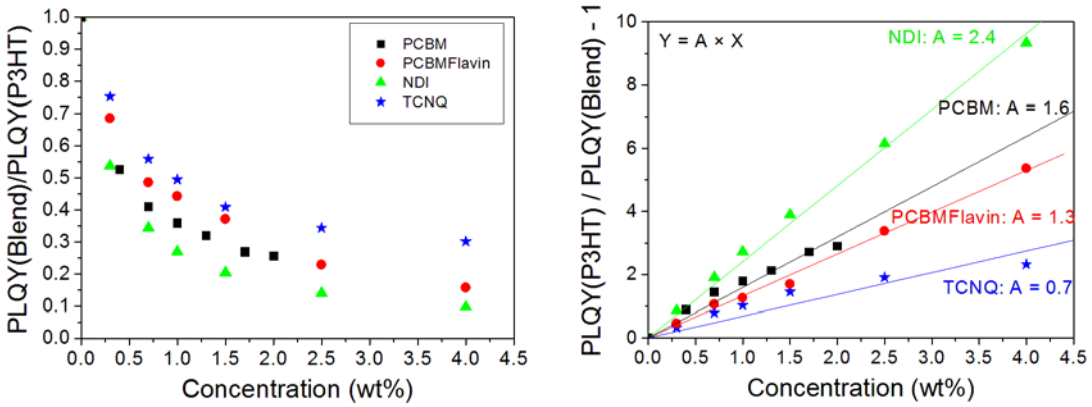

Figure 43 Left: Comparison of normalized fluorescence quantum yield of compounds 44, 46, 47 and PCBM. Right: Linear fits on the same data points assigned as PLQY(P3HT)/PLQY(Blend)-1.

The graph in Figure 43 (left) shows the normalized fluorescence quantum yield depending on the acceptor concentration. Compound **46** shows less quenching compared to the other curves. On the right plot the data points are assigned as PLQY(P3HT)/PLQY(Blend)-1 on the ordinate axis. The proportional regression matches well for compound **47**, PCBM, and compound **44**, but for compound **46** (blue line) a clear roll off with higher concentration is visible. This could be explained by clustering of PCBM-TCNAQ forming small crystals that decreases the active interface between P3HT and PCBM-**46**. PCBM-**47** shows the highest quenching of all tested C_{60} derivatives.

2.5.3. Phase aggregation.

Microscope images confirmed the microstructure of compound **46** films. The films compared in (Figure 44) are made of a P3HT:**47** and P3HT:**46** blend with a ratio of 1:1 and a concentration of 12 mg/ml in chlorobenzene. The films dried in a nitrogen atmosphere without annealing for three days. P3HT:**46** shows phase aggregation on the order of about 0.8 µm. P3HT:**47** has no particular structure.

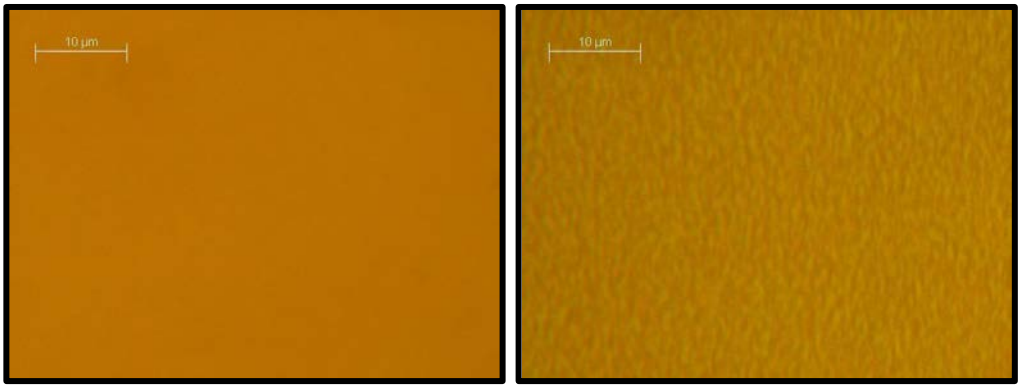

Figure 44. Left: Microscope image of P3HT:47. Right: Microscope image of P3HT:46. 46.

2.5.4. Device Fabrication.

Bulk heterojunction photovoltaic devices, consisting of a conjugated polymer P3HT/PCBMs blend were fabricated. The structure of the bulk-heterojunction solar cell is shown in Figure 45. The photovoltaic devices were prepared by etching the substrate with indium tin oxide (ITO) to 4 mm wide stripe followed by plasma ashing (100 w) in O_2 for 5 minutes. Then spin coating was undertaken for PEDOT:PSS (4000 rpm, Ramp 50, 60 s) onto ITO and was baked at 130^{o}C in a glove box (to prevent degradation of the device by water or oxygen, which is commonly observed for polymer devices) for 10 minutes. The photoactive layer, consisting of a blend of the conjugated polymer P3HT and the PCBM analogues were deposited by spin coating from the appropriate solvent (chlorobenzene) with ratios of weight of 1:1, 1:2, 1:3, 1:4 (1:1, 1:2 1500 rpm, 1:3, 1:4 1000 rpm) (Ramp 50, 60 s) these were baked at different temperatures in a glove box for 10 minutes. The counter electrode of (Al) aluminium was deposited by vacuum evaporation and annealed at temperatures of 130 °C and 140°C. To determine the power conversion efficiency, J–V measurements were carried out at 100 mW/cm² white light illumination from solar simulator from Steuernagel Lichttechnik GmbH. The current density *J* of the devices was measured by using a Keithley 2400 Sourcemeter for an applied voltage *V* from -1 to 1 V.

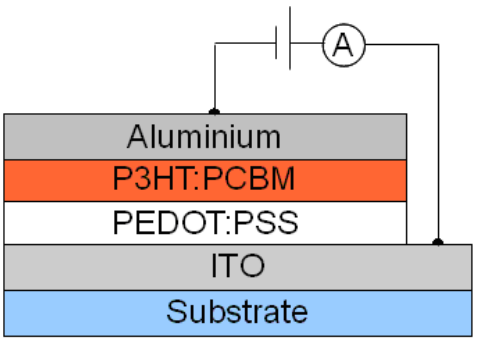

Figure 45. Schematic of the organic solar cells.

2.5.5. Testing of P3HT:PCBM-flavin solar cells.

Two batches of P3HT:**44** solar cells were produced by blending different ratios and two different annealing temperatures 130 °C and 140 °C. All devices show very low currents and clearly no photovoltaic effect was detectable for any of the four material blend ratios (Figure 46).

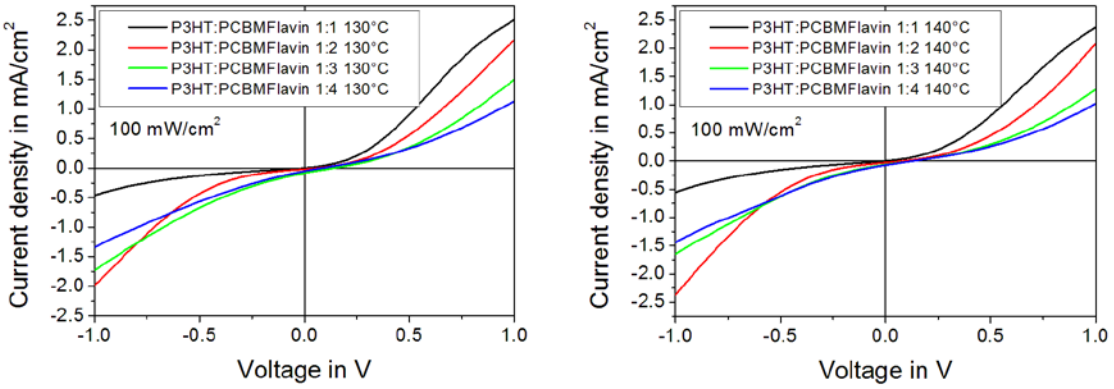

Figure 46. JV curves of P3HT:44 under illumination with 100 mW/cm². For four different blend ratios and annealing at 130 °C (left) and 140 °C (right). No photovoltaic effect could be observed.

J-V Characteristics for the P3HT:**44** solar cells were examined under dark and light conditions and compared to the standard device P3HT:PCBM (Figure 47). It can be clearly seen, that the current in positive bias of the standard device is much higher than the current for P3HT:**44** (90 mA/cm² at 1 V compared to 0.02 mA/cm²).

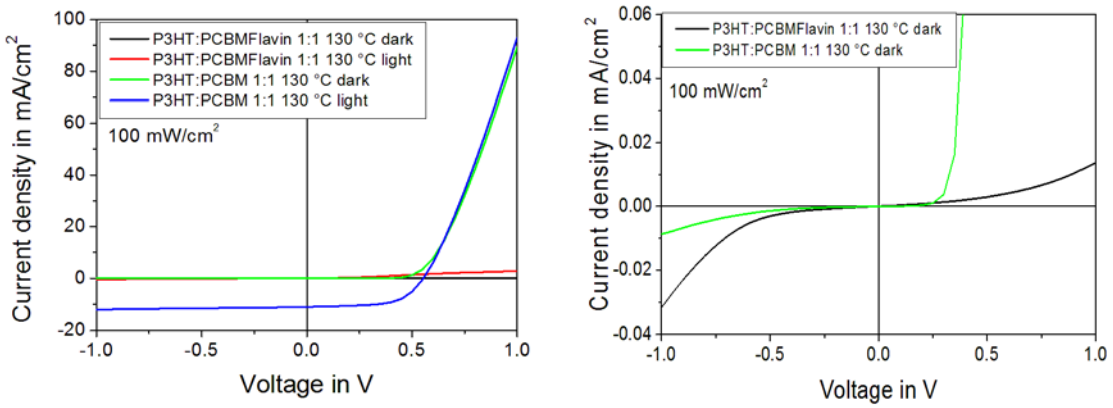

Figure 47 Curves of P3HT:PCBM and P3HT:44 under dark and light conditions. P3HT:PCBM. In positive bias the standard device shows a much higher current.

2.5.6. Test of chloroform as a different solvent

In order to examine the influence of solvents on the P3HT:**44** bulk heterojunction structure, chlorobenzene was substituted with chloroform. The change of the solvent shows an improvement in the dark current IV curve, which reveals a more diode like behaviour than the devices made of chlorobenzene as solvent but the current still is very low. Under illumination no change compared to solutions made of chlorobenzene could be observed (Figure 48).

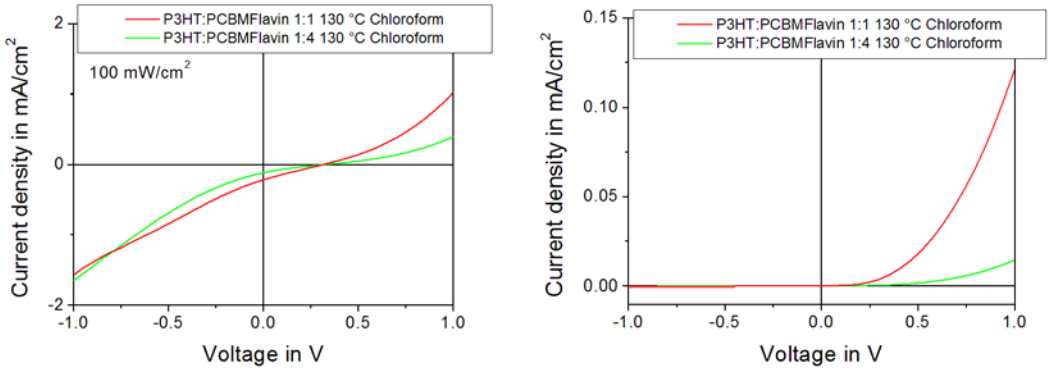

Figure 48 Left: Electrical measurement of P3HT:44 dissolved in chloroform under 100 mW/cm² illumination. Right: IV curve in dark

2.5.7. Influence of PEDOT:PSS on P3HT:44 solar cells

As flavins can be reduced in aqueous solutions and are capable to accepting two electrons, this may lead to trapping of electrons and reduce the electron mobility. Therefore this effect was investigated by making devices with and without PEDOT. The devices were fabricated according to standard procedure with solutions of P3HT:**44** 1:1 and 1:4 dissolved by 20 mg/ml in chlorobenzene. The devices were annealed at 130 °C. The results of the measurement are shown in (Figure 49) and Table 3. Clearly an improvement in the device performance is observable for the 1:1 blend as the power conversion efficiency raises by a factor of 40, but still remains poor with 0.08%.

Table 3. Results of JV curve analysis: The efficiency increases for the 1:1 blend by a factor of 40.

Device	V_{OC} (V)	J_{SC} (mA/cm²)	Efficiency η (%)
P3HT:44 1:1 no PEDOT	0.24	1.5	8×10^{-2}
P3HT:44 1:1 with PEDOT	0.18	0.04	2×10^{-3}
P3HT:44 1:4 no PEDOT	0.16	1.00	5×10^{-2}
P3HT:44 1:4 with PEDOT	0.14	0.09	2×10^{-3}

V_{OC} – Open circuit voltage (V)

J_{SC} – Short circuit current (mA/cm²)

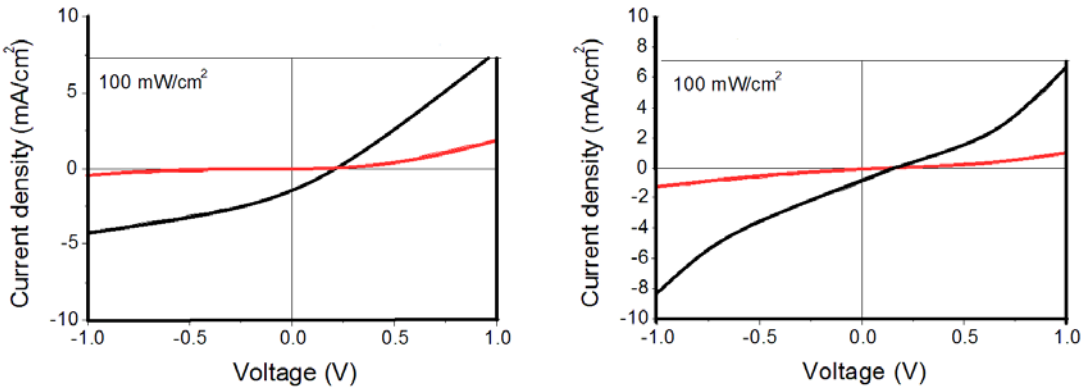

Figure 49 JV curves for solar cells with a 1:1 blend (left) and 1:4 blend (right) with (red) and without (black) PEDOT:PSS

2.5.8. Influence of PEDOT:PSS on P3HT:46 and P3HT:47 solar cells.

2.5.8.1. without PEDOT:PSS.

Four solar cells were fabricated according to the standard procedure but without PEDOT:PSS and with two different annealing temperatures 130 °C and 150 °C.

The P3HT and each of P3HT:**47** and P3HT:**46** were mixed in a ratio of 1:1 and dissolved in chlorobenzene then stirred over night at 70 °C yielding a concentration of 20 mg/ml. The active layers of photovoltaic devices were filtered with pore size 0.45 µm and spin cast on ITO substrate with 1500 rpm and 3000 rpm, ramp 50, 90 s respectively in a glove box then were annealed at 70 °C for 10 minutes. Devices were tested with a 100 mW/cm² solar simulator. Each device consists of four pixels with an area of 0.08 cm² each. The film thickness for the P3HT:**47** device was around 130 nm and for P3HT:**46** was around 150 nm. Films were created by filtering the solution before spin coating. Results for one selected pixel are shown in (Figure 50).

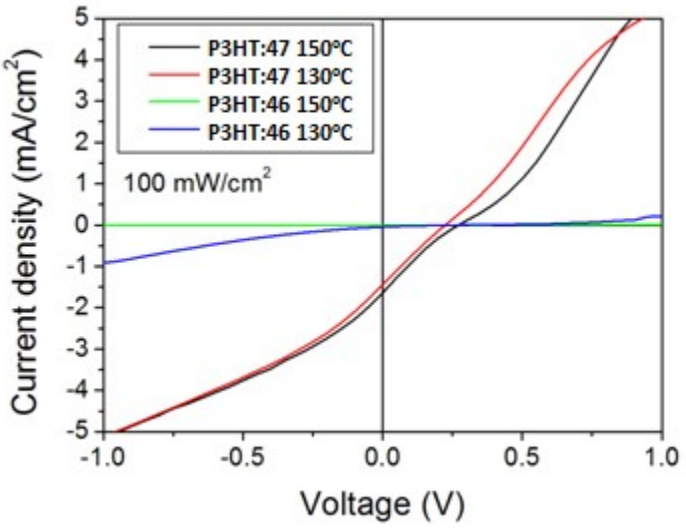

Figure 50. JV curves of solar cells fabricated from P3HT:46 and P3HT:47.

The fabricated solar cells have shown a power conversion efficiency of about 0.09 % for compound **47** (annealed at 150 °C) and 0.08 % (annealed at 130 °C) while compound **46** revealed instead no photovoltaic effect. For both devices, the short circuit current is 1.5 mA/cm² and the open circuit voltage reaches a value of 0.22 V.

2.5.8.2. with PEDOT:PSS.

According to the procedure above the fabrication of solar cells was repeated with PEDOT:PSS as buffer layer in between of ITO and the active layer. The concentration of compounds **47** and **46** was reduced to 12 mg/ml to achieve thinner films. The devices were prepared by spin coating at 900 rpm, where the solution was filtered with 0.45 µm pore size. Annealing temperature was 130 °C. The results of electrical characterisation are shown in (Figure 51). P3HT:**46** showed an inverted diode like behaviour (exponential raise for negative bias), but reveals a factor of ten lower currents compared to P3HT:**47**. PEDOT:PSS slightly improved the performance of P3HT:**47**, reaching 0.33 % power conversion efficiency (V_{OC} = 0.48 V, J_{SC} = 2.7 mA/cm², FF = 0.26).

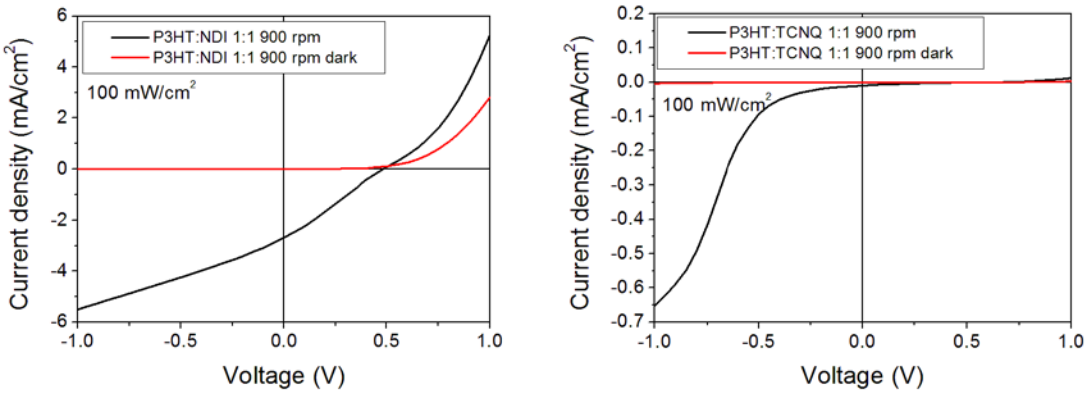

Figure 51 Left: JV-curves of P3HT:47 for 100 mW/cm² (black line) and in dark (red line). Right: JV curves for P3HT:46

2.6. Solubility measurement of the acceptors

The solubility of the acceptor in blends with P3HT in organic cells has a strong influence to the device characteristic and performance. From measuring the solubility of different C_{60}- derivatives in chlorobenzene and comparing the electrical performance, it appears that the highest efficiency of the photovoltaic device obtained when the solubility of the acceptor is equal to the solubility of the donor. To compare these results the solubility of the synthesized acceptors and the solubility of PCBM was measured, using a procedure similar to literature:[61]

Firstly dissolving the acceptors in chlorobenzene at a concentration of 50 mg/ml and stirring the solution for several days at 70 °C. More solvent was added when particle remain undissolved (appeared for compound **46**) and more powder was added when solvent becomes clear (appeared for compound **44**). The solution was filtered into an empty vial of known mass with 0.45 µm pore size syringe filters and the weight of solution was then measured. The solution was then left to dry out slowly in air atmosphere then the weight of residues was measured. Finally, the solubility was calculated by using the density of chlorobenzene (1.11 g/ml). The results of the measurement are shown in Table 4.

Table 4. Solubility of different acceptors.

Acceptor	PCBM	PCBM-Flavin 44	PCBM-NDI 47	PCBM-TCNAQ 46
Solubility	34 mg/ml	74 mg/ml	95 mg/ml	25 mg/ml

The value for PCBM with 34 mg/ml is lower compared to the recorded result of 50 mg/ml. Compounds **47** and **44** have shown high solubility in chlorobenzene with 95 mg/ml and 74 mg/ml respectively. Compound **46** has shown lower solubility which can be one reason for the low performance of solar cells made of these materials, but does not explain the poor performance of the other acceptors.

2.7. Conclusion

This study has described the synthesis of new series of electron acceptors based on PCBM with various electron accepting moieties attached. Cyclic voltammetry measuremnts have revealed that in most cases addition of the second acceptor group to the PCBM core only had a marginal effect on the electron affinity of the conjugate. However, the TCNAQ appended system had a higher electron affinity due the better accepting properties of this moiety. Photovoltaic cells have been synthesised from some of these materials, in all cases the efficiency was significantly less than the parent PCBM derivative. This may be due to lower solubility of the conjugates, compared to PCBM in chlorobenzene or alternatively the second acceptor group acts as a charge trap and thus reduces electron mobility. Further studies are underway to investigate the latter.

CHAPTER 3

SYNTHESIS OF FLAVIN-FUNCTIONALISED 1,4,5,8-NAPHTHALENEDIIMIDE (NDI) DERIVITIVES.

3.1. Introduction

3.1.1. 1,4,5,8-Naphthalenediimides (NDI).

1,4,5,8-Naphthalenediimides (NDIs) (Figure 52) (also known as naphthalene carbodiimides) are a compact, electron deficient class of aromatic compounds.[110] The initial report describing the synthesis and characterisation of NDIs occurred in 1937,[111] and was further developed synthetically in 1973.[112] However, it was not until the 1990s when researchers began to realize the potential of NDIs as useful precursors for the burgeoning field of supramolecular chemistry.[113,114] More recently, NDIs have attracted attention because of their application as n-type semiconductor materials.[115] These neutral, planar, chemically and thermally robust redox-active compounds[116] have found to be excellent building blocks for the creation of conducting materials.[117] Moreover, the convenient synthesis routes available has made NDI applicable to a range of diverse applications such as polymer chemistry,[118] and biological and medical application.[119,120]

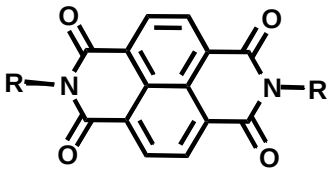

Figure 52. 1,4,5,8-Naphthalenediimides (NDIs).

The general synthesis of symmetrically functionalised NDI compounds is simple and efficient and usually involves the condensation of 1,4,5,8-naphthalenetetracarboxylic dianhydride with a primary amine in a high boiling solvent, usually DMF[116](Scheme 15). Utilising this procedure, different functional groups can be readily introduced to produce a range of imides. Recently, microwave irradiation was used to assist the synthetic methodology by reducing the reaction time to 5 min[121](Scheme 16).

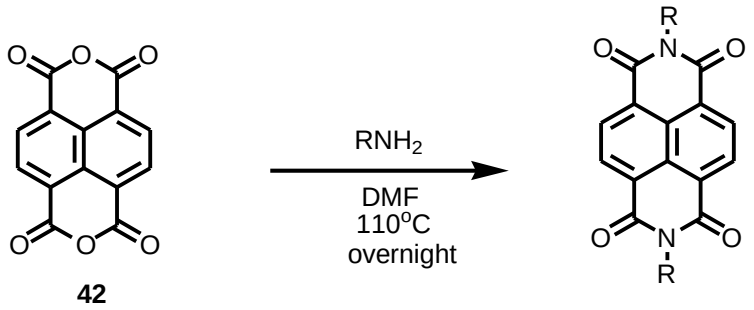

Scheme 15. General synthetic method for preparing symmetric di-substituted NDIs.[116]

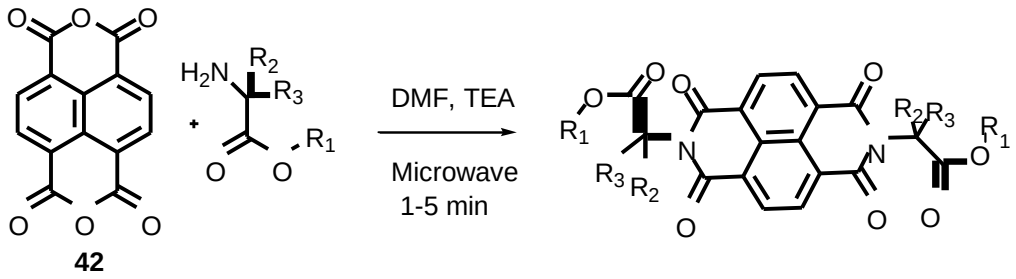

Scheme 16. Application of microwaves in the synthesis of symmetrical naphthalinediimine derivatives.[121]

Functionalization of NDI can also be achieved *via* reactions of the naphthalene core.[122] Scheme 17 shows the introduction of interesting fluorophore substituents like the electron-donating alkoxy and alkylamino groups at the 2,6-positions of naphthalene-1,4,5,8-tetracarboxylic acid bisimides. The highly coloured naphthalene bisimide dyes have been shown to emit green, orange, or red light depending on the respective substituents with fluorescence quantum yields of up to 76%.

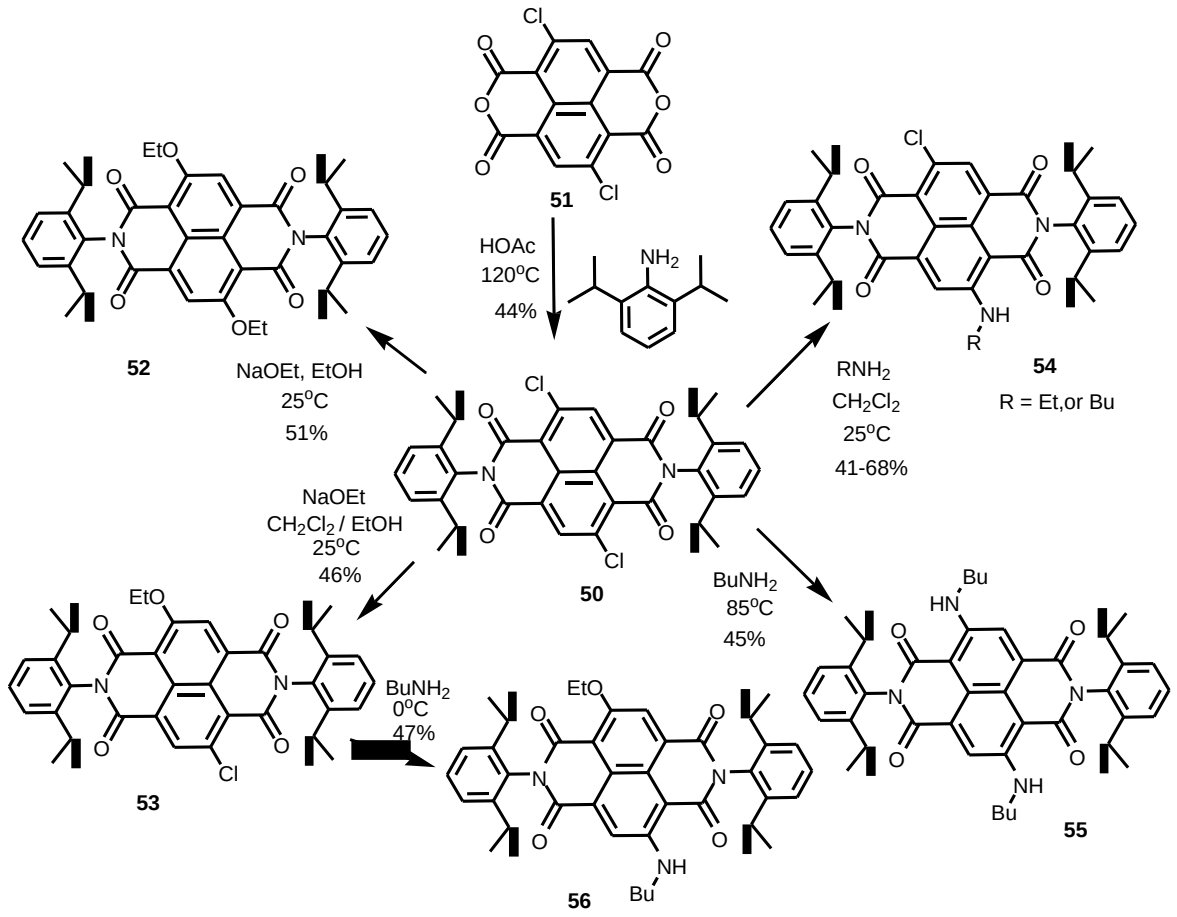

Scheme 17. Synthesis of core functionalized NDIs.[122]

The synthesis of core-tetrasubstituted NDI was carried out firstly by the bromination of naphthalene dianhydride with dibromoisocyanuric acid then followed by the condensation with 2,6-diisopropylaniline to yield the corresponding tetrabromo-substituted (NDI). This unit has proved to be a versatile precursor for the synthesis of symmetrical and unsymmetrical core-tetrafunctionalized NDIs by nucleophilic substitution with different nucleophiles. Interestingly, some of the substituents gave rise to markedly different physical properties (e.g strong bathochromic shift) compared to their precursor (Figure 53).[123] A method for synthesizing unsymmetrical NDIs bearing two different substituents on the diimide nitrogens has been found by careful controlling the pH (Scheme 18).[108,124]

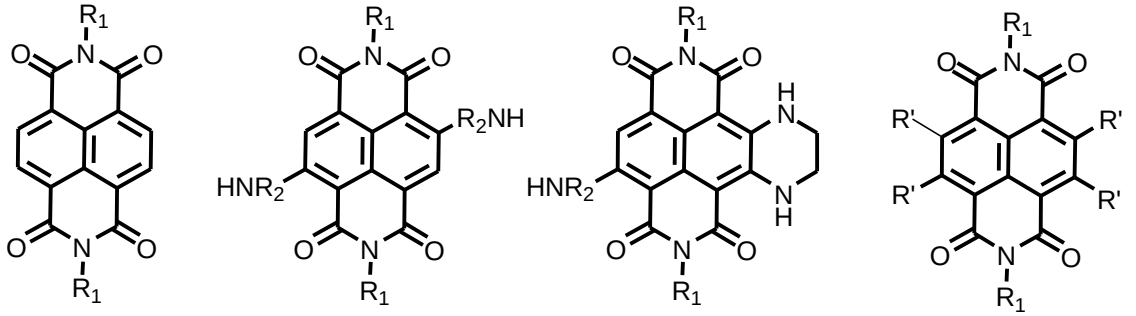

Figure 53. Structures of some core-substituted NDI derivatives.[123]

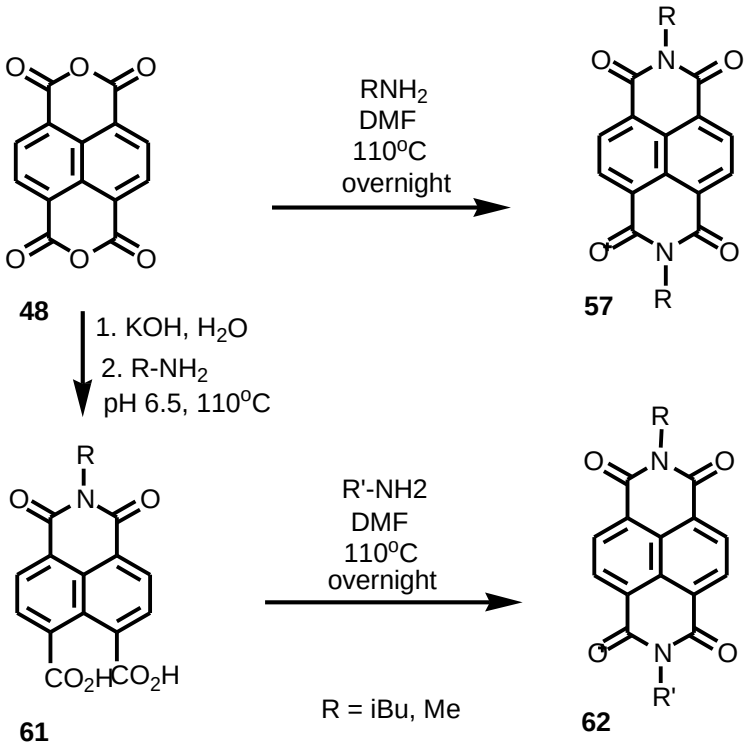

Scheme 18. Preparation of symmetrical and unsymmetrical NDI derivatives.[124]

The spectroscopic and electronic properties of N,N-dialkyl-substituted NDIs (in CH_2Cl_2), shows strong absorptions below 400 nm, and a weak mirror image emission with a 7 nm Stokes shift.[125] Excimer-like emissions have been observed in toluene. Functionalization of NDIs on diimide nitrogens with aromatic groups generates non-fluorescent or weakly fluorescent compounds while the alkyl functional groups produce the typical white–blue fluorescence compounds[122]. Stable radical anions of NDIs are generated from single reversible one-electron reduction at modest potentials (NDI: E^1_{red} = 21.10 V vs. Fc/Fc^+ in CH_2Cl_2). The radical anions are characterized by the visible and near-infrared (NIR) absorption bands at 450 nm and by strong and highly structured EPR signals [125,126]. In fact, EPR studies shows that the electronic coupling is not limited to the diimide core, but also extends to the methane (CH_2) carbons of aliphatic substituents on nitrogen[125] (Scheme 19).

Consequently, the NDIs are distinguished as attractive redox-active units because of their electronic complementarity to ubiquinones (E^1_{red} trimethylbenzoquinone = –1.20 V vs. Fc/Fc^+).[127]

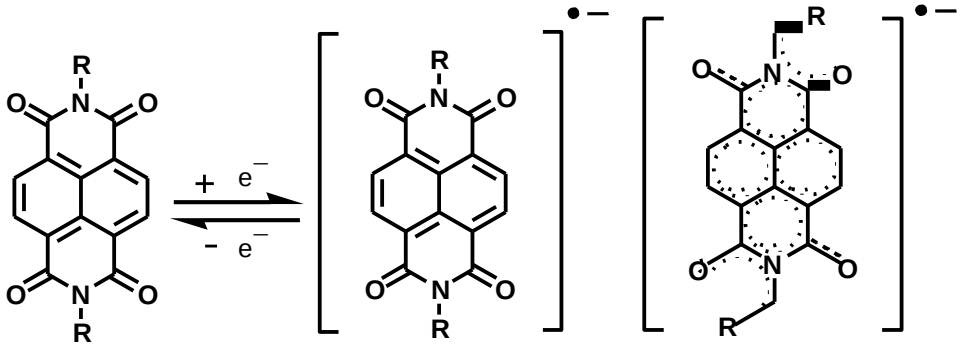

Scheme 19. Reduction of NDIs leading to a radical anion.[116]

The presence of a lipophilic naphthyl core and the four polar carbonyl groups in the naphthalene diimides make them soluble in low polarity lipophilic solvents (e.g. chloroform, toluene, DCM) and polar aprotic solvents (DMF, acetonitrile, DMSO) depending on the imide substituents. Naphthalene diimides are planar aromatic compounds, this leads to stacking in the solid-state with distances appropriate to π–π stabilisation and can develop to form continuous stacks (Figure 54). On the other hand, the solubility can be reduced when substituted with aryl side groups, whereas long and bulky aliphatic substituents on the imide nitrogens could increase the solubility[128]. Hence, the nature of the substituents can be used to control the solubility and self-assembly of NDI in both solution and the solid state.[129] The π -electrons have been shown to be delocalized along NDIs stacks to furnish so-called molecular wires.[116] NDIs bearing carboxylic acid groups display a self-assembly properties by forming hydrogen bonds between carboxylic acid groups and the hydrophobic contacts between the NDI cores (Figure 55).[130]

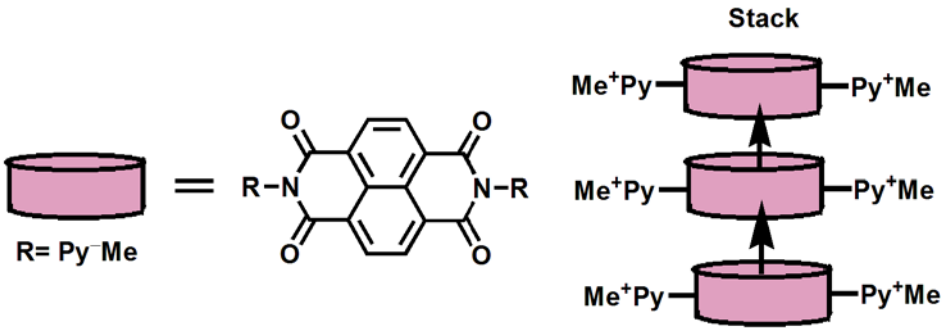

Figure 54. Self assembly of NDI units in aqueous NaCl solution.

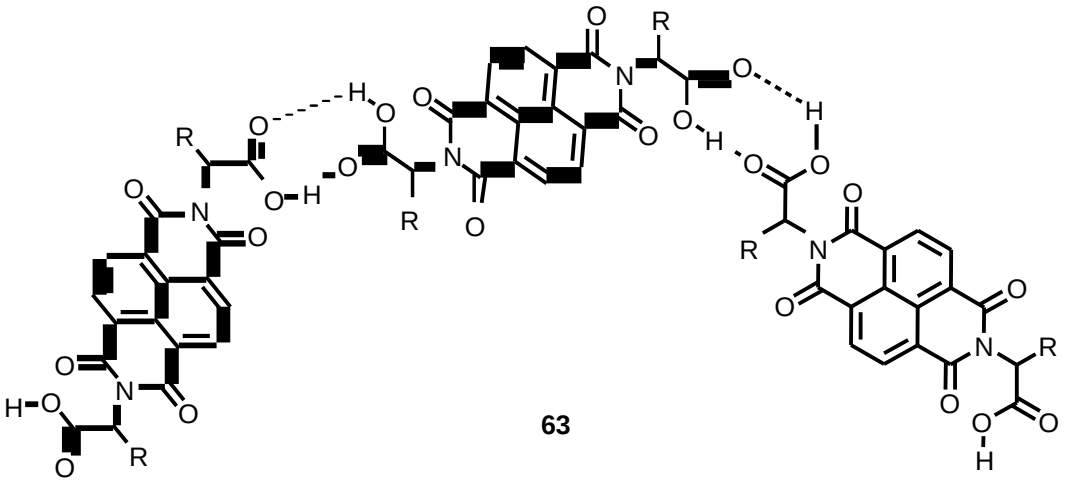

Figure 55. NDI dicarboxylic acid derivative forming hydrogen-bonded tapes in solution and the solid state.

Photoactive thin films have been fabricated from 1,4,5,8-naphthalenediimides with zirconium phosphonate on silica or quartz substrates. It has been shown that the NDIs stack efficiently within the layers. Furthermore, the fluorescence measurements indicated the large excimer-like emission was observed at (λ_{ex} = 355 nm). The irradiation of 16-layer films under steady-state or flash photolysis has improved NDI radical anion formation. Apparently, excitation of the NDI layer generates both triplet states and radical species in the presence of appropriate electron donors[131](Figure 56).

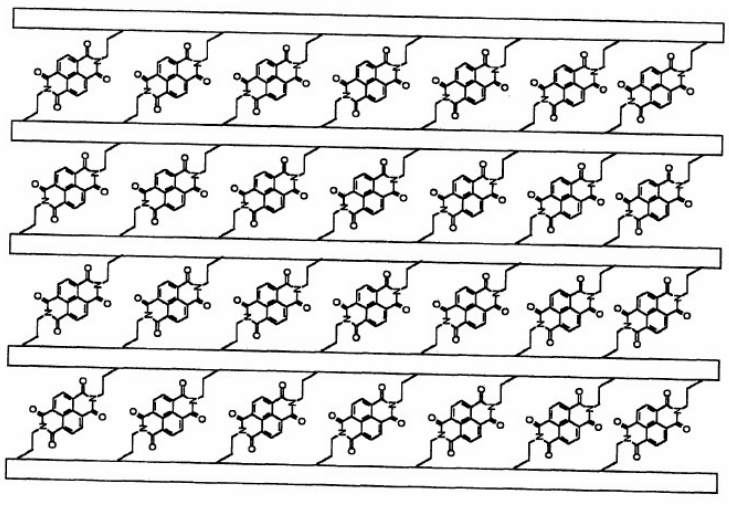

Figure 56. Proposed structure of NDI- BP/ZP crystalline materials.[131]

Photoinduced intramolecular processes were considered for a pentad composed of silicon phthalocyanine (SiPc) connected with two units of naphthalenediimide (NDI) and fullerene

C_{60} to form SiPc-$(NDI)_2$-$(C_{60})_2$ (Figure 57). The physical properties of this system were compared with a SiPc-$(NDI)_2$ triad and a NDI-C_{60} dyad. The photoexcitation of SiPc-$(NDI)_2$-$(C_{60})_2$ and SiPc-$(NDI)_2$ in polar solvents revealed charge-separated processes via NDI and SiPc forming the charge-separated state $SiPcC^{\bullet+}$-$(NDI)_2C^{\bullet-}$- $(C_{60})_2$. Significantly, the two naphthalenediimide/two fullerene electron acceptors were shown to stabilize the radical-ion pair state.[132]

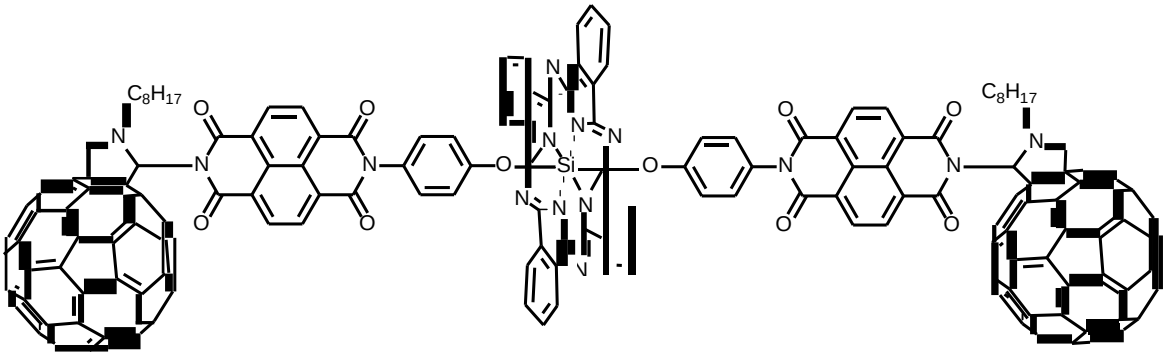

64

Figure 57. SiPc-$(NDI)_2$-$(C_{60})_2$.[132]

Naphthalene diimide has also been incorporated into interlocked supramolecular architectures (e.g. catenanes and rotaxanes) exhibiting interesting electronic and spectroscopic properties and better fabrication properties than the perylene diimide dyes (Figure 58).[133,134]

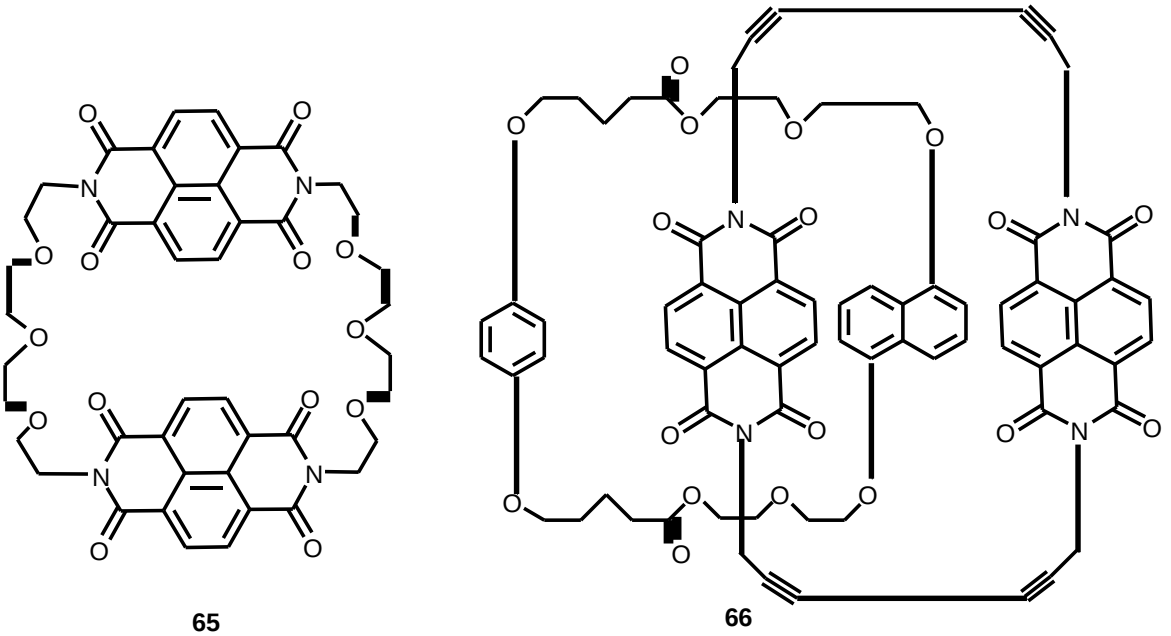

65 **66**

Figure 58. NDIs incorporated into supramolecular systems.[133,134]

NDI and C_{60} have been incorporated in perylene monoimide (PMI) based organic acceptor dyads for the fabrication of dye-sensitized solar cells (DSCs) with nanocrystalline NiO electrodes. Interestingly, it was found that the charge separation state lifetime of the three dyeds were extended for about five orders of magnitude compared to the relevant PMI dye, due to the effect of the secondary electron acceptor (NDI or C_{60}). The photovoltaic performance showed an efficiency of η = 0.14 % in the system in which the NDI is directly connected to the PMI (Figure 59).[135]

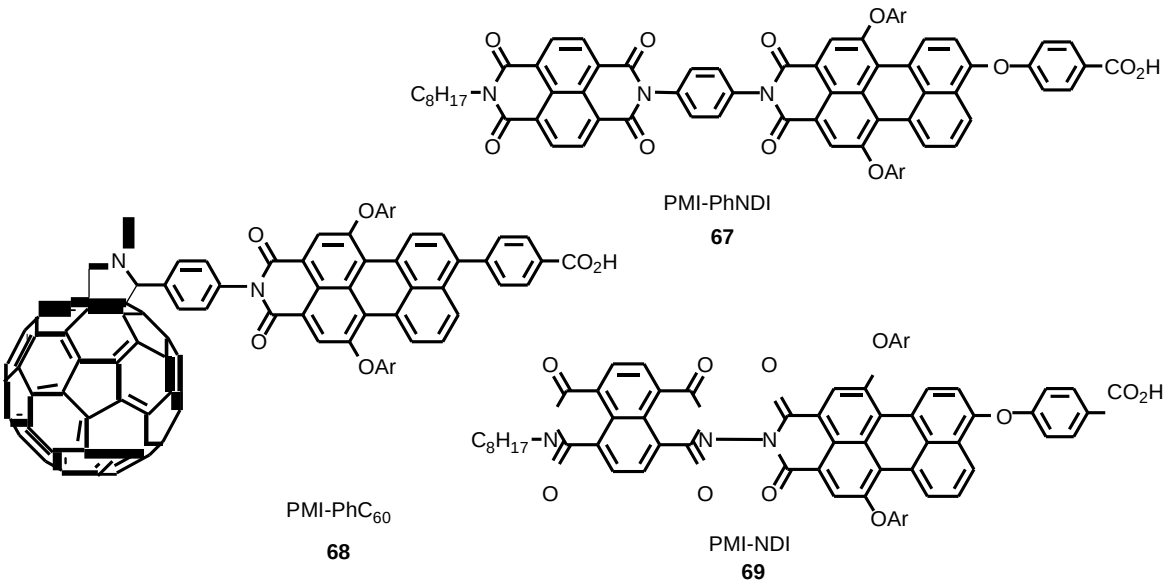

Figure 59. Structures of the PMI based acceptor dyads.[135]

Electron acceptors Py-NDI and Py-PDI possessing chelating 3-pyridylmethyl substituents have been incorporated into small molecular photovoltaic cells containing zinc phthalocyanine (ZnPc) as the electron donor component (Figure 60). The self-assembled coordination complexes that form between the electron acceptors (Py-NDI and Py-PDI) and the electron donor ZnPc improve photoinduced charge carrier generation and give advantages for the construction of organic solar cells and for the organic photodetectors with response times of less than 10 microseconds.[136]

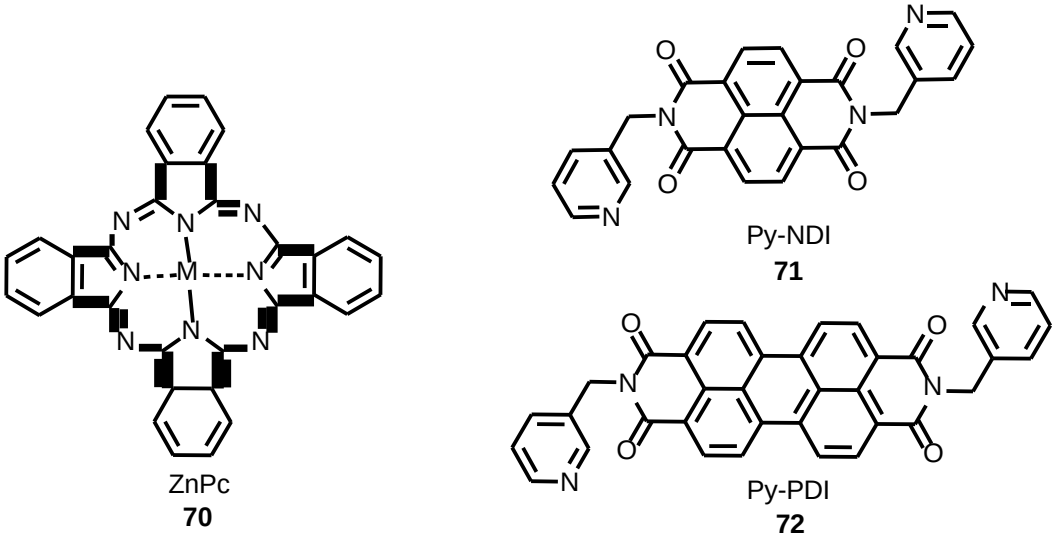

Figure 60. Molecular structures of zinc phthalocyanine (ZnPc), 3-pyridylmethyl substituted perylene diimide (PDI) and naphthalene diimide (NDI).[136]

NDI- thiophene copolymers have been synthesised as n-type compounds for use in organic electronic devices with high electron mobilities (0.076 cm^2 V^{-1} s^{-1}). Due to the high electron mobility, appropriate energy levels, and good absorption characteristics, the NDI-thiophene copolymers were utilised as high performance organic field effect transistors (OFET) (Figure 61).[137]

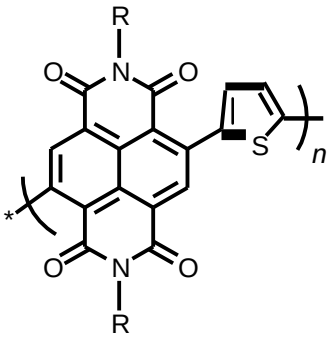

Figure 61. Molecular structure of the NDI-thiophene copolymer.[137]

3.1.2. Flavins.

Flavins are identified as electroactive compounds that have low redox potentials. They have been considered as attractive building blocks for incorporation into n-type semiconductors, due to their tuneable redox and interesting optical properties.[138] However, the adsorption of flavins on TiO_2 powder was examined and has shown strong adhesion at

the TiO_2 surface, in addition a photoinduced electron injection was observed from the adsorbed flavins into the conduction band of a TiO_2 electrode.[139]

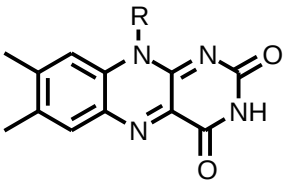

Figure 62. Structure of a simple flavin.

Ruthenium polypyridyl photosensitizers with substituted pteridine ligands (Figure 63) $[Ru(dcbpy)_2(ligands)]^{2+}$ attached to TiO_2 electrodes have been used to fabricate regenerative solar cells. The cells were illuminated with polychromic radiation in the presence of I_2 / I_3^- as redox electrolyte. The sensitizers were able to harvest large fractions of visible light. The incident photon to current conversion efficiency was found to be ~20–48%.[140]

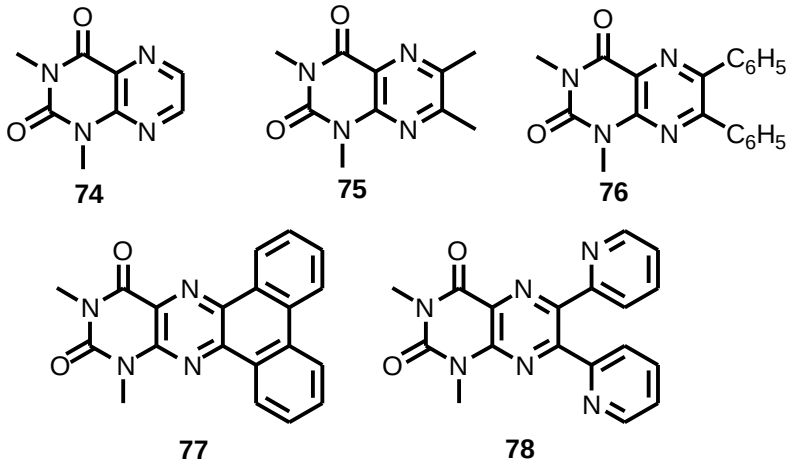

Figure 63. Substituted pteridines.[140]

Furthermore, flavin-based blue-light photosensors have shown to play an important role in light sensing protein modules. The study proved the occurrence of one- and two-electron transfer reactions preceding the formation of the final photoproduct, in agreement with the most characteristic trait of flavins—the ability to switch among different redox states that can provide the driving force for further reactions.[141]

3.2. The aim of the project

This project aims to prepare compounds of acceptor- acceptor system as a potential target in fabricating of photovoltaic devices. Naphthalenediimide (NDI) was connected with two different flavin moieties from two different sites, namely N10 in compound **83** and N3 in compound **89**. The project intends to enhance the acceptor ability and to extend the acceptor range of the parent NDI. In particular, the novel NDI-flavin system should offer a broad range of LUMO energies to provide a wider range of complementary HOMO donors. Furthermore conjugates of this type could adjust the absorption of light towards the near-IR region.

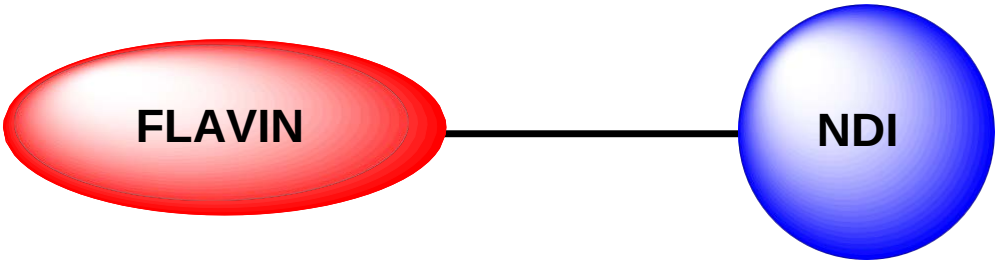

Figure 64. New NDI-Flavin acceptors.

3.3. Synthesis of new NDI-Flavin acceptors.

Two novel NDI analogues were synthesised by connecting the NDI to two different electro -active flavins. Molecular structures of synthesised NDI derivatives are shown in Figure 65.

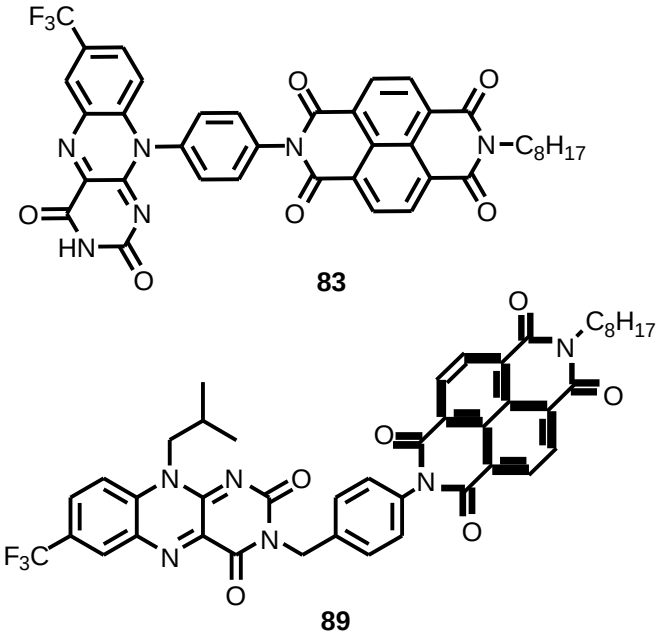

Figure 65. Novel NDI-Flavin acceptors.

The new NDI derivatives connected with two different flavin moieties was carried out using the nucleophilic substitution route. The first steps of both reactions were similar including a condensation of n-octyl amine with 1,4,5,8-naphthalene tetracarboxylicdianhydride. Whereas the second steps involve the addition of two different flavins bearing amino groups. The reactions were carried out under N_2 in the high boiling solvent DMF at 140^{o}C. The percentage yields of the NDI-Flavin products were poor about (10-11) % due to the multiple accompanying products and hence tricky purification by column chromatography.

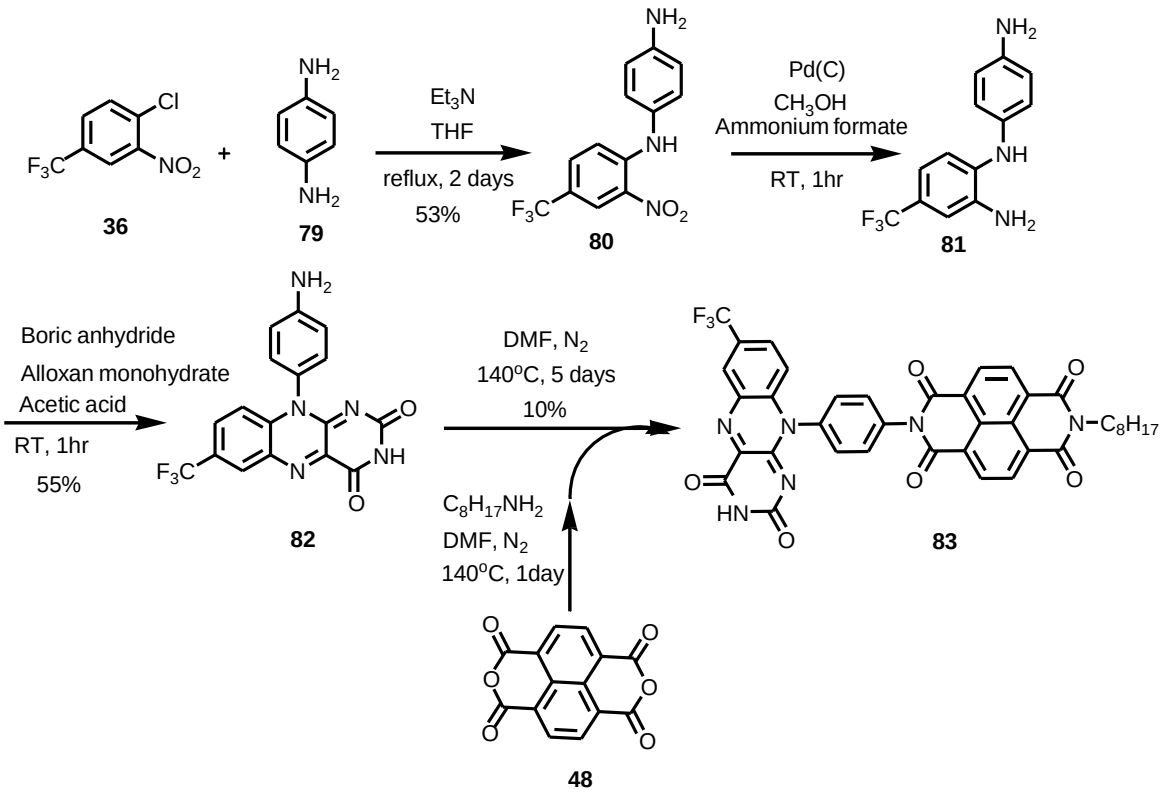

36 **79** **80** **81** **82** **83** **48**

Scheme 20. Synthesis of NDI-FLAVIN 83.

1-Chloro-2-nitro-4-(trifluoromethyl)benzene was the starting material for both of the flavin-NDI systems. Flavin **82** was synthesised following the synthetic pathway illustrated in Scheme 20. Firstly, *N*-(4-(trifluoromethyl)-2-nitrophenyl)benzene-1,4-diamine (**80**) was synthesised in 53% yield by a nucleophilic aromatic substitution reaction between *p*-phenylenediamine (**79)** and 1-chloro-2-nitro-4-(trifluoromethyl)benzene (**36**) in the presence of triethylamine. Secondly, the nitro group was reduced to an amine using palladium on carbon in the presence of ammonium formate in methanol to afford compound **81** which was treated directly with alloxan monohydrate and boric anhydride in glacial acetic acid to produce compound **82** in 55% yield.

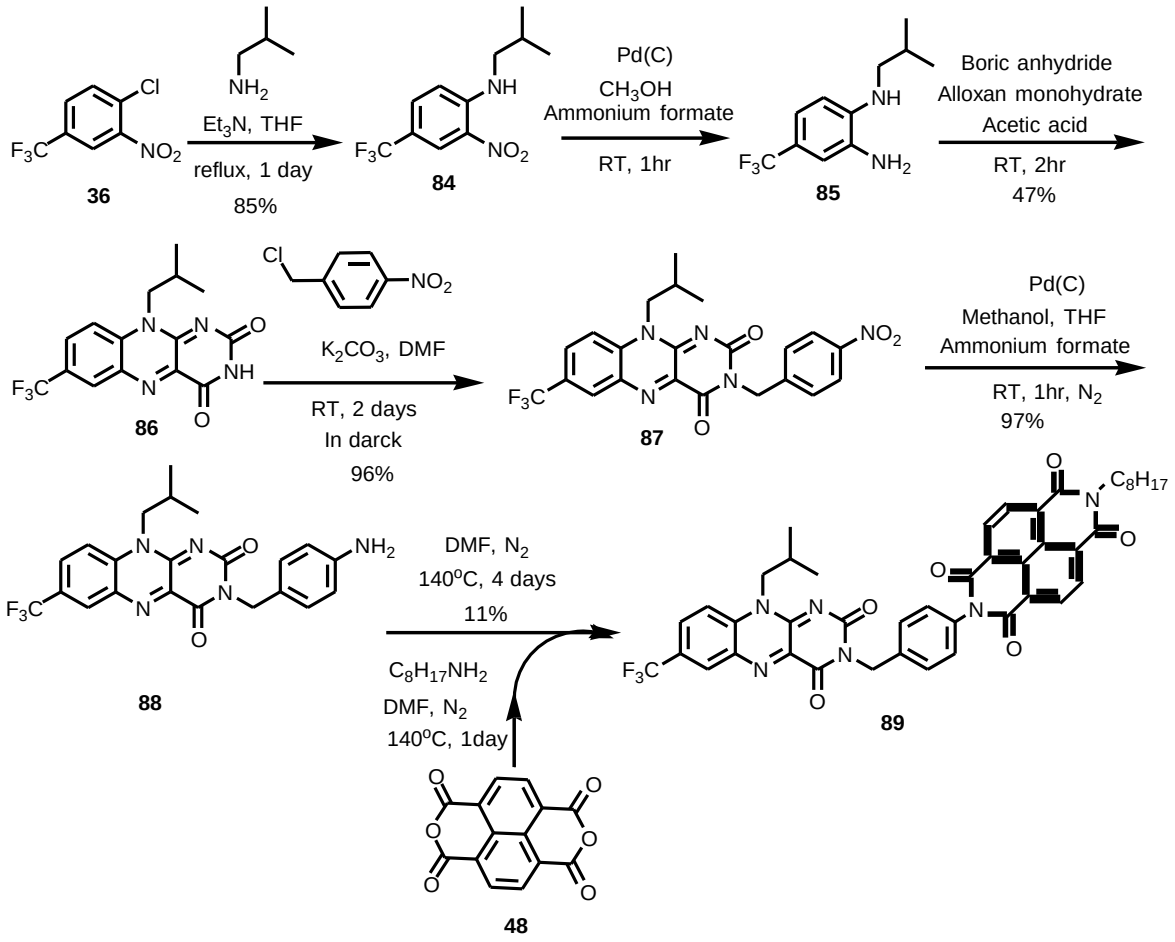

Scheme 21. Synthesis of compound 89.

Flavin **86** was synthesised following a similar synthetic route (Scheme 21). 4-(Trifluoromethyl)-*N*-isobutyl-2-nitrobenzenamine (**84**) was prepared in moderat yield and then further reacted to generate flavin **86** in 47%. Flavin's N3 was alkylated using 4-nitro benzyl chloride in the presence of potassium carbonate and DMF. The reaction proceded for 2 days at room temperature and was protected from light which resulted in the formation of **87** in 96% yield. Reduction of nitro group to amine catalysed by Pd(C) was undertaken in a 1:1 mixture of methanol/THF and in the presence of ammonium formate. The reduction was complete in 1 hour at room temperature to produce compound **88** in 97%.

3.4. Characterisation

The structures of the synthesised compounds were confirmed by spectroscopic data such as ^{1}H, ^{13}C NMR, mass spectra, UV–visible, IR, fluorescence spectroscopy and electrochemical studies.

3.4.1. NMR Spectroscopic studies

^{1}H NMR, ^{13}C NMR spectrums were found to be consistent with the expected structures. ^{1}HNMR spectrum in $CDCl_3$ recorded the presence of one singlet peak at 8.75 ppm and 8.78 ppm related to the four NDIs aromatic hydrogens. In addition the flavin's N10 methylene peaks 4.09 ppm and 4.26 ppm for compounds **83** and **89**, respectively, were clearly visible.

3.4.2. UV-Visible spectroscopy

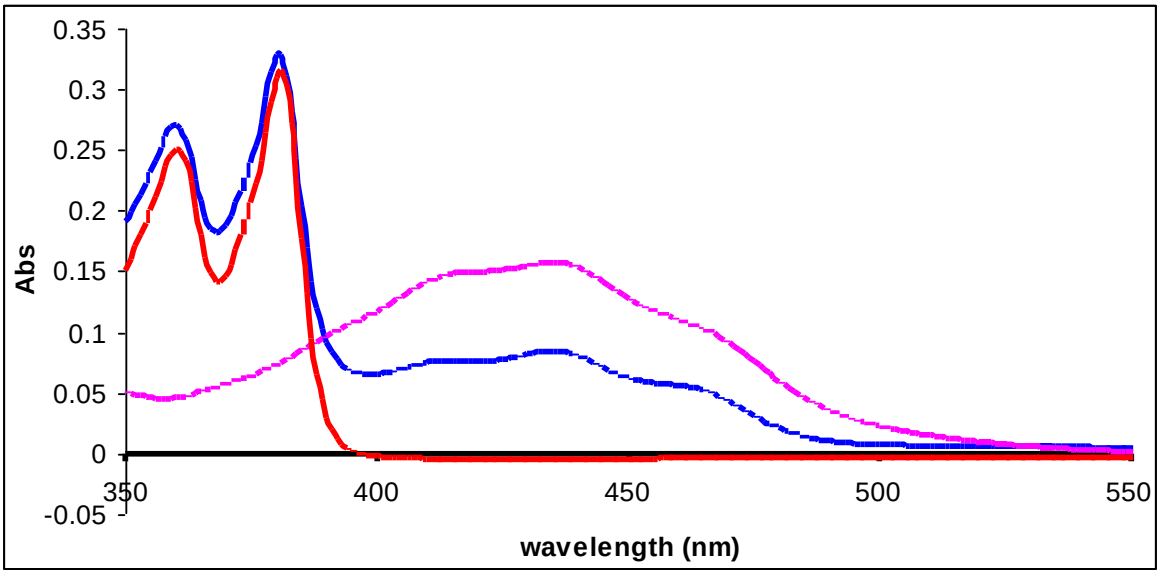

Figure 66. UV-Vis spectra of compound 83 (blue line) compared to parent NDI 48 (red line) and flavin 82 (purple line). Recorded in DCM at 1x 10^{-5} M.

UV-Vis absorptions and band gap energies of the novel compounds ($1x10^{-5}$ M in CH_2Cl_2) are provided in (Table 5). Flavin modified NDI compounds displayed the NDI's main two strong absorption peaks in the UV region at 360 nm and 380 nm. In addition to the flavin's main broad absorption peak at 435 nm in the visible region was observed. Furthermore, compound **83** has a long tail after 550 nm towards longer wave length (Figure 66). Remarkably, the gap energies were reduced from 3.15 eV for NDI to 2.48 eV and 2.54 eV for compounds **83** and compound **89**, respectively.

Table 5 UV-Vis spectroscopy data of modified NDI's and parent flavins and NDI

Compound	λ^1_{abs}	λ^1_{ons}	λ^2_{abs}	λ^2_{ons}	λ_{max}	λ_{ons}	E_{gap}
48	360	368	380	395			3.15
82					435	563	2.21
83	359	367	380	396	435	500	2.48
88					435	491	2.53
89	360	368	380	397	435	490	2.54

λ_{abs} – maximum absorption wavelength of each peak (nm)

λ_{ons} – onset of each peak (nm)

E_{gap} – gap energy (ev)

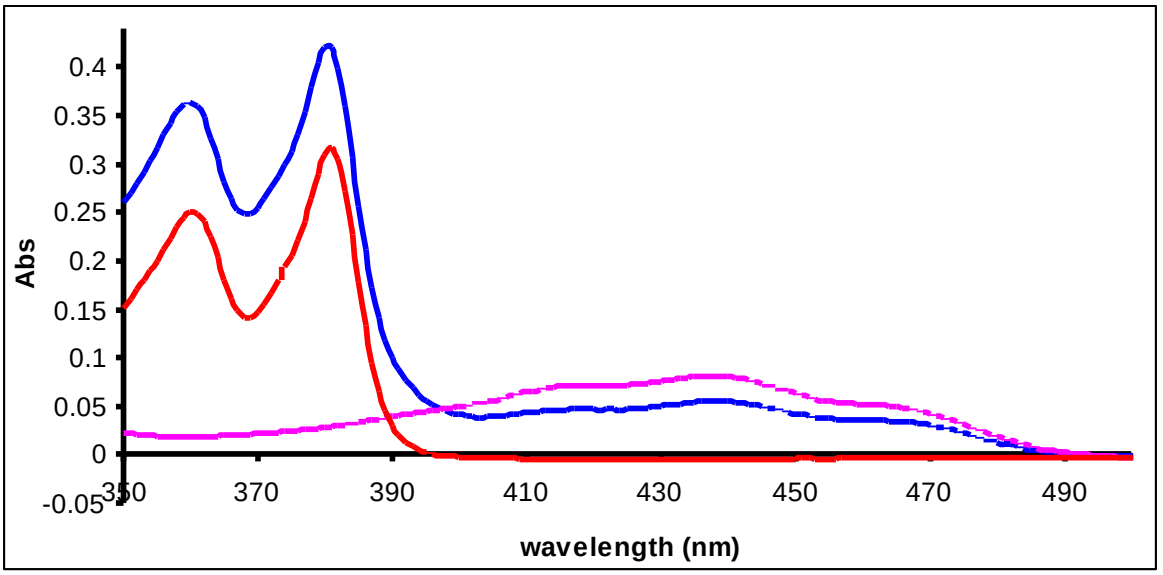

Figure 67. UV-Vis spectra of compound 89 (blue line) compared to the NDI 48 (red line) and flavin 88 (purple line). Recorded in DCM at 1x 10^{-5} M

3.4.3. Fluorescence

As shown in Figure 68 and Figure 69, the fluorescence emission band at 510 nm displayed by compound **83** is blue-shifted by about 45 nm relative to the corresponding bands of NDI under the same conditions. The intensities of the emission of compound **83** is raised relative to that of the other compounds. Compound **89** exhibited fluorescence emission band at 525 nm and is blue-shifted by about 30 nm relative to the corresponding band of NDI. The intensity has not risen as much as the compound **83**.

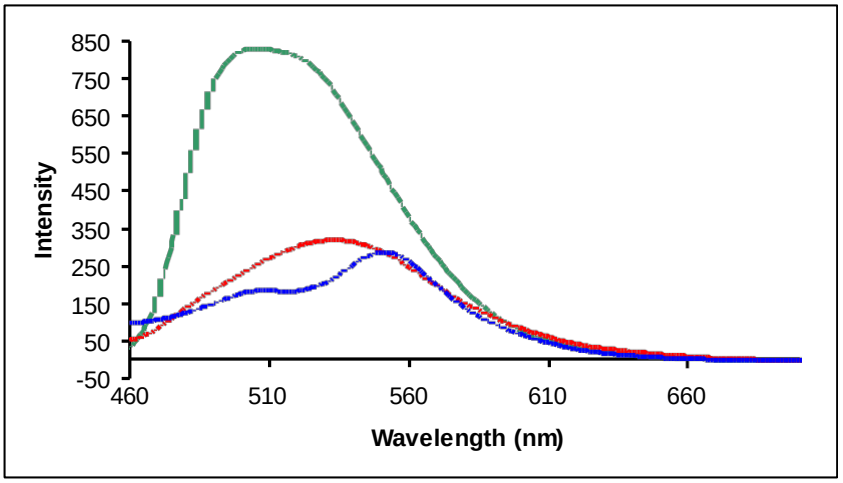

Figure 68. Fluorescence emission spectra (λ_{ex}= 435 nm) of compounds 83 (green line), 82 (red line) and 48 (blue line) recorded in CH_2Cl_2 ($1x10^{-5}$M).

As predicted, the ground-state electronic conduction between the flavin and the NDI is weak due to the presence of a nodal plane on the nitrogen of the imide group of the flavin and NDI in the HOMO and LUMO orbitals. In addition, it is likely that the bridging phenyl group in the NDI-flavin causes the NDI and the flavin to be out of plane.

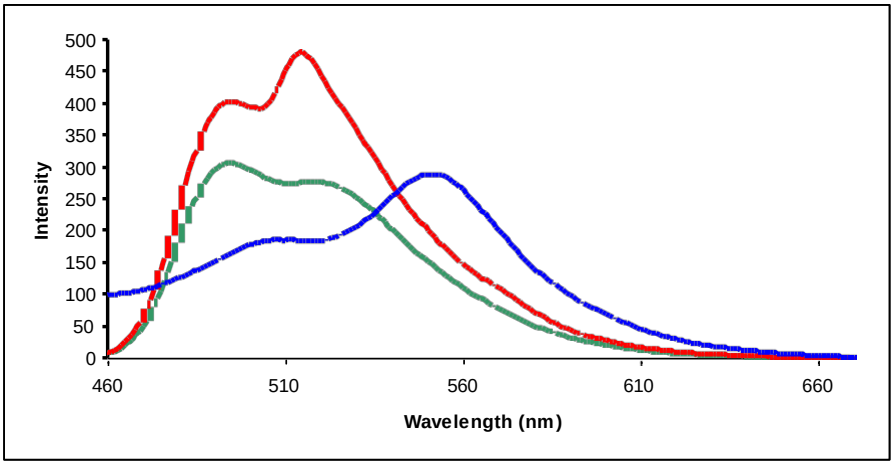

Figure 69. Fluorescence emission spectra (λ_{ex}= 435 nm) of compounds 89 (green line), 88 (red line) and 48 (blue line) recorded in CH_2Cl_2 ($1x10^{-5}$ M).

3.4.4. Electrochemical studies.

Electrochemical properties of the two NDI-flavin compounds were investigated by cyclic voltammetry to determine the influence of the flavin moieties on the LUMO energy of the NDI. The cyclic voltammetry of the two NDI-flavin compounds and their parent NDI and flavins were preformed at room temperature in a solution of (1×10^{-4}M) CH_2Cl_2 containing tetra-n-butyl ammonium hexafluorophosphate (Bu_4NPF_6 0.1 M) as supporting electrolyte with a platinum wire as working and counter electrodes and a silver wire as a quasi-reference electrode. E_{LUMO} values for the compounds are referred to the potential of the Fc^+/ Fc redox couple utilized as an internal standard. The scan rate was 0.1 V/s and the observed reduction potentials are collated in (Table 6).

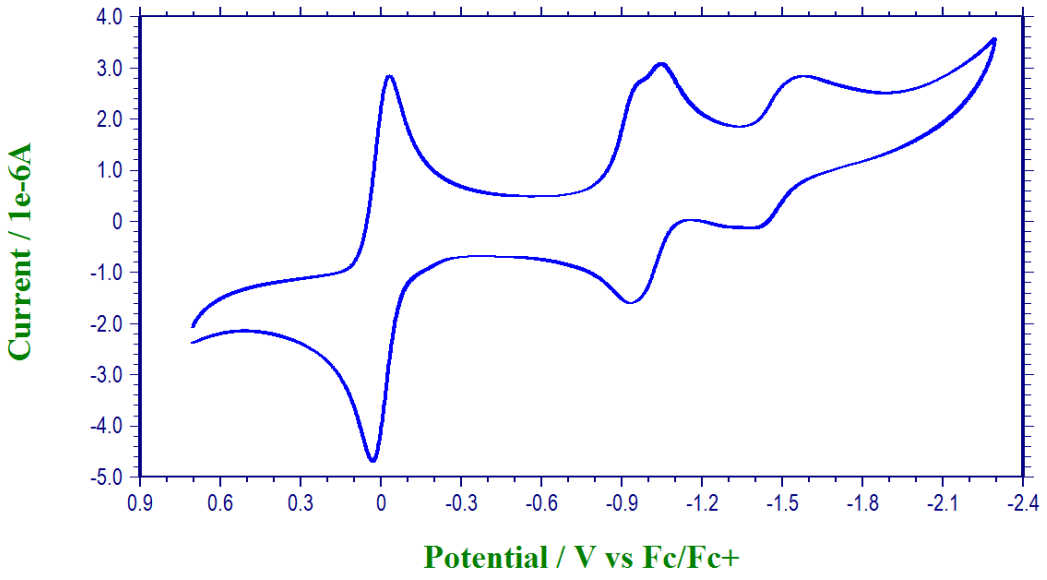

Figure 70. Cyclic voltammetry of compound (83).

The cyclic voltammogram of flavin modified NDIs showed two reversible reduction waves at -1.04 V and -1.94 V for compound **83** (Figure 70) and at –1.12 V and –1.02 V for compound **89** (Figure 71). However, for further examination of the influence of the flavins on the electrochemical properties of the NDIs, CV data of derivatives **83** and **89** were compared to the **48** and parent flavins **82** and **88**. Compound **48** displayed a single reversible one-electron reduction at modest potentials E^{1}_{red} = –1.10 V. Remarkably, there was no significant difference between the first reduction potential of the two flavin modified NDI's and the first reduction potential of NDI **48**, although, a slight decrease of the first reduction potentials is observed for compound **83** (60 mV) which indicates that it is better electron acceptor than NDI. On the other hand, it is worth mentioning that both the flavin modified NDI's give rise to a slightly better acceptor ability than the parent flavins.

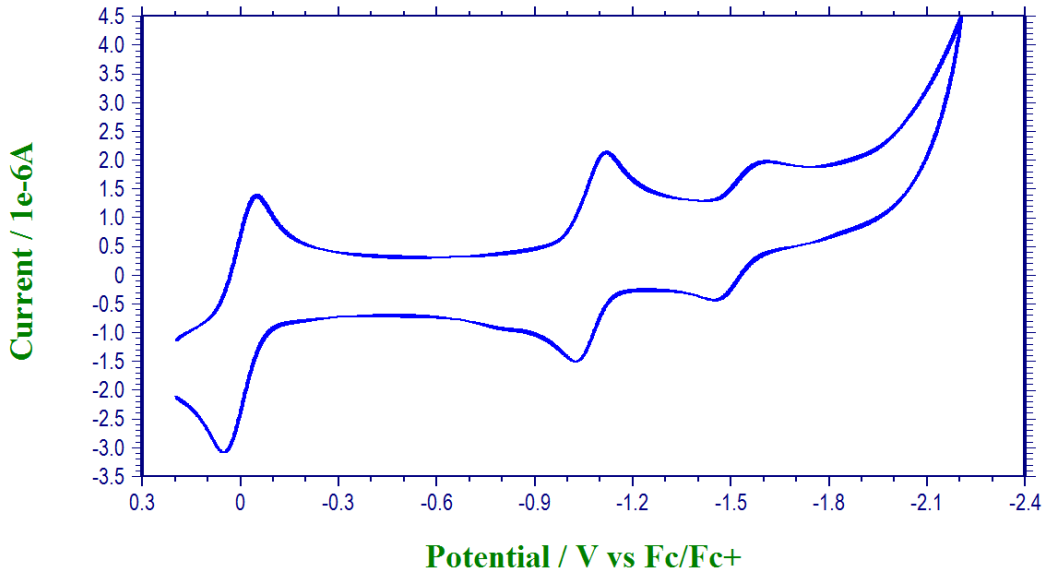

Figure 71. Cyclic voltammetry of compound 89 .

Table 6 Cyclic Voltammetry Data of modified NDI's and parent flavins

Compounds	E^1_{red}	E^2_{red}	E^1_{rev}	E^2_{rev}	ΔE	$E_{1/2}$	E_{LUMO}
48	-1.11	-1.52	-1.02	-1.41	-90	-1.06	-3.74
82	-1.06		-0.99		-70	-1.03	-3.78
83	-1.04	-1.51	-0.94	-1.43	-105	-0.99	-3.81
88	-1.16		-1.08		-80	-1.12	-3.68
89	-1.12	-1.61	-1.02	-1.45	-100	-1.07	-3.73

E^1_{red} - First reduction potential (V)

E^1_{rev} - First reversible potential (V)

ΔE - Energy difference between peak potential (forward and backward sweep) in (mV).

$E_{1/2}$ - Half wave potential $E^1_{red} + E^1_{rev}/2$ (V)

$E_{LUMO} = - 4.8 - E_{1/2}$ (V)

3.5. Conclusion

This chapter has described the synthesis of two electron acceptor-acceptor compounds based on the NDI and flavin moieties. The UV-vis study has displayed red shift for the novel compounds compared to the NDI and the parent flavins. The energy gaps for the NDI flavin derivatives (2.54 eV and 2.48 eV) were lower than that of NDI (3.15 eV). The electrochemical studies have shown two/three reversible reduction waves for the novel NDI-flavins; however, there were no significant differences in LUMO energies. These compounds are being investigated at St. Andrews University in order to test their efficiency in photovoltaic cells.

CHAPTER 4

THIOPHENE FUNCTIONALISED FLAVIN DERIVITIVES

4.1. Introduction

4.1.1. Conductive polymers

Conducting polymers (Figure 72) are polymers that have an extended system of conjugated bonds (extended π-orbital system) through which electrons can move from one end of the polymer to the other.[142] Due to the sp^2 hybridization and π-orbitals overlapping, electrons are delocalized along the conjugated backbones, leading to π-system extension with a filled valence band. A bipolaron is formed from removing electrons from the π-system (p-doping) (Figure 73), or adding electrons into the π-system (n-doping). It is the bipolaron's unit movement up and down the polymer chain that is responsible of the polymer's conductivity.[143]

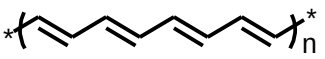

90

Figure 72. Conductive polymer (polyacetylene).

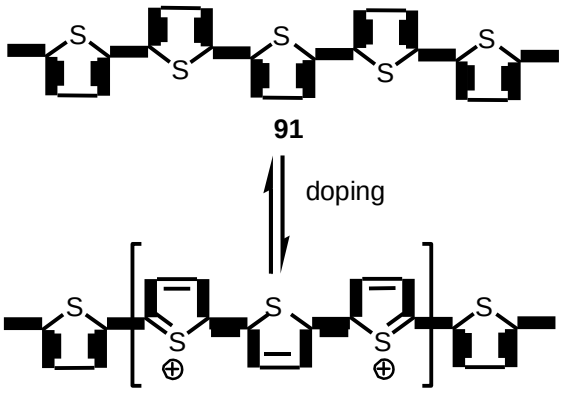

Figure 73. Removal of two electrons (p-doping) from a polythiophene chain produces a polaron.

4.1.2. Thiophene based conjugated polymers

Thiophene based polymers are promising components of organic electronic devices such as organic photovoltaic cells (OPV)[144] and light emitting diodes (LED).[145] They have been considered as electron-donor systems for their rich π-electron conjugated groups, which allow unusual electrical and optical properties.[146,147] Single molecules of thiophene can be considered as π–electron rich conjugated groups for their electron pairs on sulphur which

are significantly delocalized in the π–system.[146] Moreover, it has been found that oligothiophenes permit colour tuning by controlling the π–conjugation length.[147,148] They show red shift in the electronic spectra by increasing the repeat units in the molecules because of the planar molecular structure which causes an aggregation of the molecules[146]. Their conductive and optical properties combined with their ease of processing, ensure polythiophenes have potential applications as: field-effect transistors,[149] electroluminescent devices, solar cells, photochemical resists, nonlinear optic devices, batteries, diodes, and chemical sensors.[150]

4.1.2.1. Synthesis of polythiophene

Polythiophenes have been synthesised chemically and electrochemically. Chemical syntheses have been carried out using oxidant or cross-coupling catalysts and have two advantages: a perfect selectivity of monomers using suitable catalysts and the ability to synthesize regioregular substituted polythiophene. The initial chemical polymerization was reported by two groups in 1980 using metal-catalyzed polymerization of 2,5-dibromothiophene. The first example was by coupling of Grignard reagents to aryl halides using magnesium in THF and nickel(bipyridine) dichloride[151]. The second was also by using magnesium in THF, but with a series of acetylacetonate catalysts like $Pd(acac)_2$, $Ni(acac)_2$, $Co(acac)_2$ and $Fe(acac)_2$.[152] Polymers' molecular weights have been improved by using different methods like catalytic cross-coupling reactions to synthesize regioregular polythiophenes[153] and with oxidative polymerizations for polymers with different degrees of regioregularity.[154]

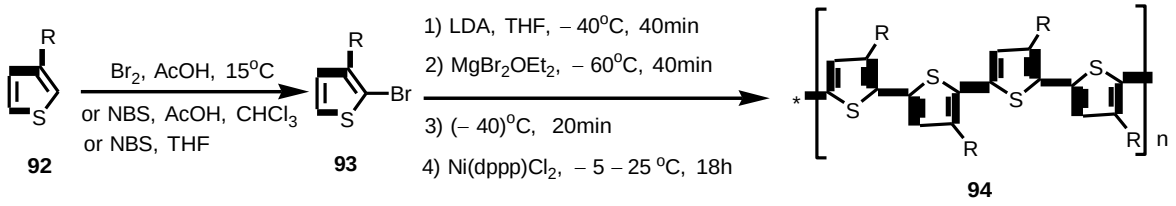

Scheme 22. Cross-coupling method for preparing regioregular polyalkylated thiophene.[153]

Polymers featuring regioregular polyalkylated thiophenes have been synthesised using brominated monomers under low temperatures and careful exclusion of water and oxygen using two different methods. The first method started with the bromination of 3-alkylated thiophene to produce 2-bromo-3-alkylthiophene then followed by lithiation, transmetallation and Kumada cross-coupling in the presence of a nickel catalyst (Scheme

22).[153] The second method was carried out by treating 2,5-dibromo-3-alkylthiophene with highly reactive zinc to form a mixture of organometallic isomers which in the presence of a catalytic amount of $Pd(PPh_3)_4$ produced a regiorandom polymer,[155] whereas, treatment with $Ni(dppe)Cl_2$ yields regioregular polyalkylated thiophenes in quantitative yield (Scheme 23).[156]

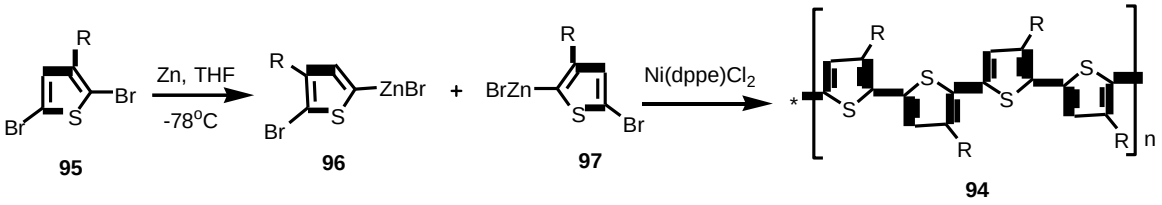

Scheme 23. Cross-coupling method for preparing regioregular polyalkylated thiophene.[156]

The oxidative polymerization of thiophenes has been carried out using ferric chloride at room temperature. The procedure required slow addition of ferric chloride[154] and in situ precipitation to maximize the surface area of the catalyst to higher monomer conversions.[157,158] Dry air bubbling through the reaction mixture during polymerization has been reported to produce higher molecular weight polymers.[159] Also, extraction *via* Soxhlet with polar solvents is beneficial to remove residual catalyst.[160] On the other hand, using a lower ratio of catalyst to monomer (2:1, rather than 4:1) may increase the regioregularity of the polymer.[161] Solvents, in turn, have their role to gain higher yields, like dissolving poly(dialkylterthiophene)s in carbon tetrachloride rather than chloroform, due to the stability of the radical species in carbon tetrachloride.[162] Thus, high molecular weight polyalkylated thiophenes with no insoluble polymer residues requires the use of high-quality catalyst, added at a slower rate and at reduced temperature[161]. Also, a longer polymerization time increases the yield of polymer.[163] The accepted mechanism of the oxidative polymerization *via* ferric chloride is illustrated in (Scheme 24).

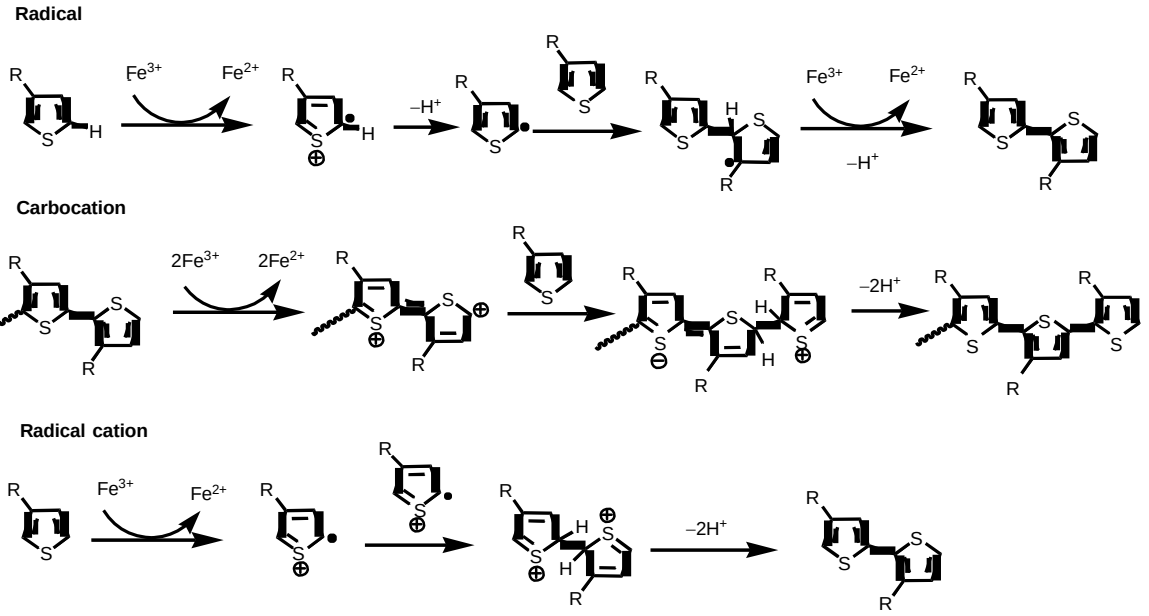

Scheme 24. Proposed mechanisms for iron-mediated oxidative polymerization of thiophenes.

As illustrated in Scheme 25, polythiophene can also undergo electrochemical polymerization *via* cyclic voltammetry[164]. This technique works by applying a potential across a solution containing thiophene and an electrolyte (tetrabutylammonium tetrafluoroborate) to produce polythiophene film on the anode. Interestingly, the synthesized polymer does not need to be isolated and purified. However, this technique produces undesirable alpha-beta linkages and varying degrees of regioregularity. The oxidation of a thiophene monomer produces a radical cation, which can then couple with a second radical cation to form a dication dimer, or with another monomer to produce a radical cation dimer.

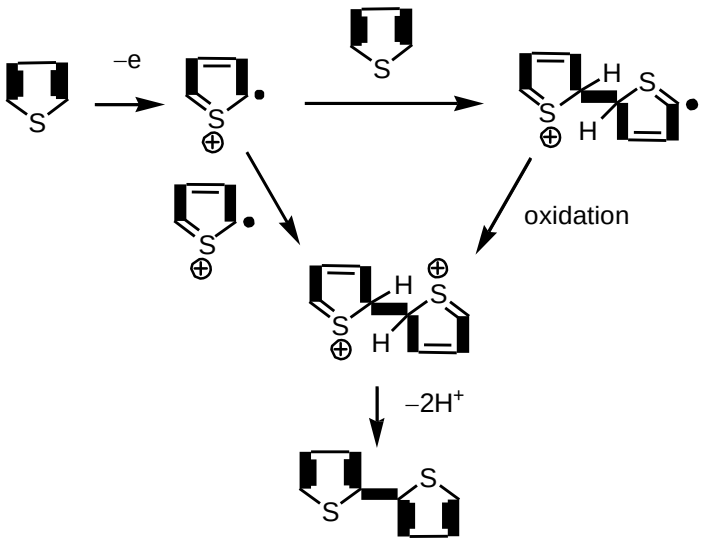

Scheme 25. Initial steps in the electropolymerization of thiophenes.

4.1.2.2. Modified polythiophene

To create a new generation of polymers to be exploited in practical applications, polymers with special properties should be prepared by combining the high conductivity and the high processability properties into a single material. This often requires a careful compromise between the two properties. Superior conductivity is often associated with highly planar and strongly interacting π-conjugated polymers, while good processability is usually associated with highly twisted and weakly interacting π-conjugated polymers, making it hard to achieve high conductivity and processability within one substance at the same time.[165] Connecting bulky side chains is a general technique to increase processability of the polythiophenes, although, it leads to reduced conductivity due to reduced intramolecular π-π interactions.[147]

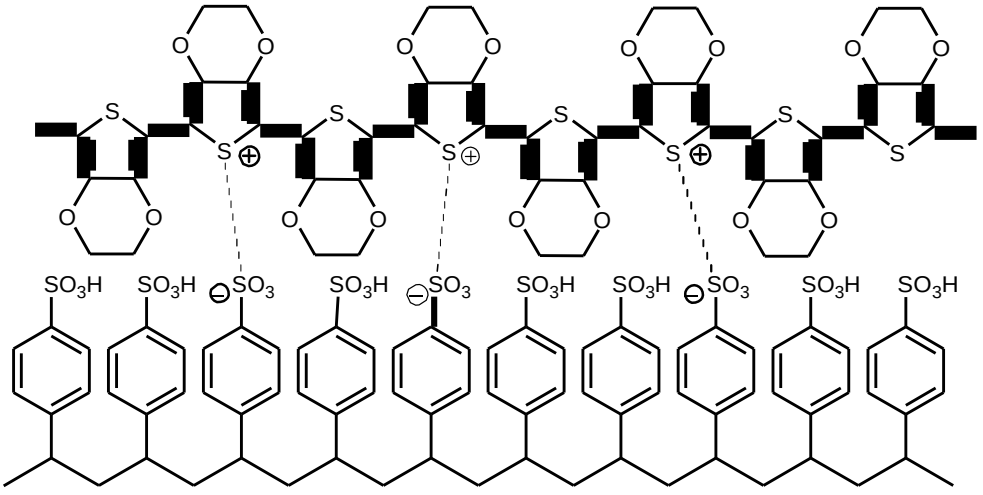

98

Figure 74. poly(3,4-ethylenedioxythiophene)-poly(styrenesulfonate) (PEDOT-PSS).

Polymerization of 3,4-ethylenedioxythiophene (EDOT) and polystyrenesulfonate (PSS) in aqueous solution resulting poly(3,4-ethylenedioxythiophene)-poly(styrenesulfonate) (PEDOT-PSS) (Figure 74)[166,167] is an alternative strategy to find polymers with improved qualities and extend applications. PEDOT-PSS is a water-soluble dispersion and it can be readily cast into conductive, transparent and stable films. It has various applications including polymer light emitting diodes (PLEDs),[168] photovoltaics,[169] antistatic coatings,[170] electrochromic displays,[171] supercapacitors,[172] solid state ion sensors,[173] biosensors,[174] and fuel cells.[175]

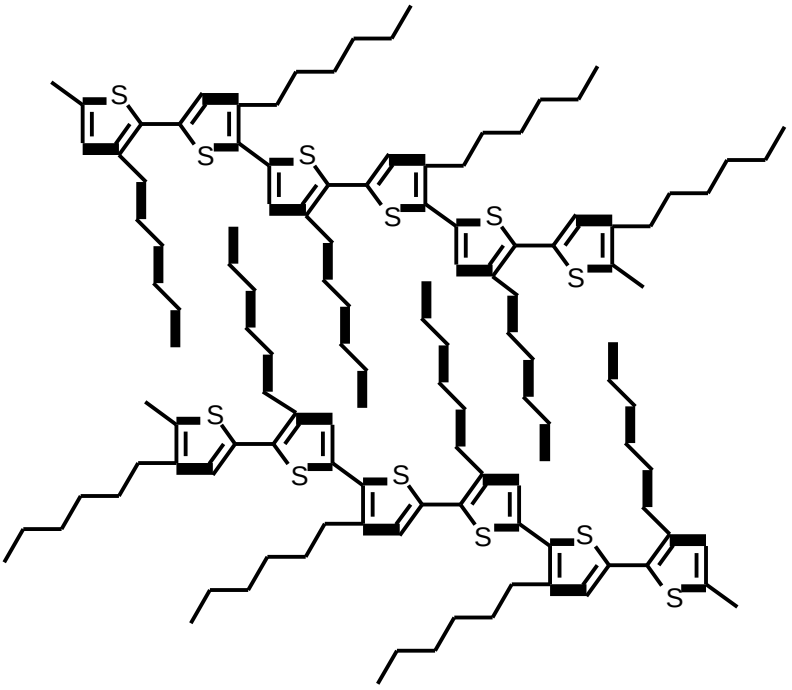

8

Figure 75. Poly(3-hexylthiophenes) (P3HT).

Poly(3-alkylthiophenes) (P3AT) (Figure 75) are another example for semiconducting thiophene polymer. Following the discovery of convenient and controllable methodology to produce high purity regioregular polymers [153,156,176] their electronic and charge transport properties have been investigated intensively. It has been found that controlling their self-organizing properties lead to materials with excellent charge carrier mobilities which allows their application in organic electronic devices.[50] Spin coated composite films of P3ATs as electron donor associated with fullerene derivatives as electron acceptor have been used as active layers in fabricating plastic photovoltaic devices having conversion efficiencies around 3.5%. [177,178]

4.1.2.3. Fluorene-Thiophene Copolymers.

Recently, polyfluorene derivatives have attracted attention for their high chemical and thermal stability, high photoluminescence and electroluminescence quantum efficiency and facile colour tunability (obtained by introducing low-band-gap co-monomers). They have potential applications in organic light-emitting diodes (OLEDs) because they can emit colours spanning the entire visible range with high efficiency and low operating voltage. Moreover, polyfluorenes have a high solubility in most solvents, which make them ideal for general applications.[179]

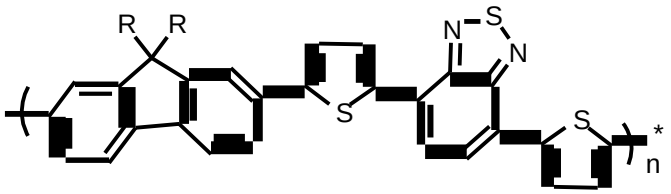

Figure 76. A low band gap polyfluorene-thiophene-benzothiadiazole derivative.[180]

Fluorenes have been incorporated in polythiophene copolymers (Figure 76) as they are effective moieties to alter the band-gap and the energy position of the valence and conductive levels. Fluorenes planar shape[181,182] and π-orbitals overlap at the linkage between the two benzene rings result in conjugation across the molecule which leads to delocalization in the excited state molecular orbital. The degree of delocalization and the spatial location of the orbitals on the molecule are influenced by the electron donating or withdrawing character of their substituents which in turn affect on the band gap energies. Furthermore, controlling the band gap influences the color of the molecule by limiting the energies of absorbing light.[183]

4.1.3. Donor-acceptor cooperation.

In order to fabricate high performance organic photovoltaic devices, electron donating polythiophenes have been co-polymerised with electron accepting moieties to optimize the absorption and electronic energy levels of the resulting polymer.[180,184] It has been shown that alternating donor-acceptor copolymers help to separate charge for higher power production, in other words, the addition of electron accepting moieties to conjugated polymers lowers the HOMO energy level and increases the voltage of the a solar cell.[184-186]

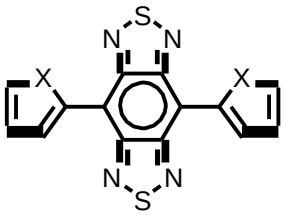

X = S or N-Me

99

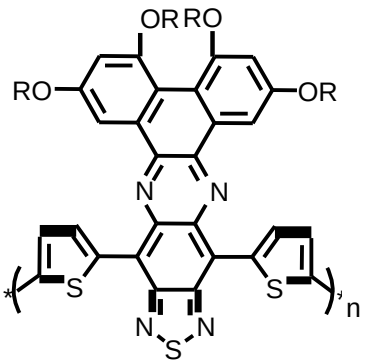

R= 2-ethylhexyl

100

Figure 77. A small band gap polymer. [187,188]

Donor-acceptor copolymers have afforded polymers with very narrow-band gaps. Since the initial discovery of polybenzene-thiophene with a band gap of 1.1 eV,[189] researchers have endeavoured to improve the values of the band gaps. Consequently, narrow-band gap (1.4 –0.5 eV) polymers and monomers have been synthesized containing aromatic-donor like thiophene rings with planar conformations and *o*-quinoid-acceptor units[188]. Moreover, a soluble conjugated polymer of alternating electron-rich bithiophene and electron-deficient thiadiazoloquinoxaline units have furnished polymers with an extra small band gap about 0.94 eV. Bulk heterojunction solar cells fabricated with [84].PCBM as the electron acceptor, afforded a photoresponse up to 1.3 μm (Figure 77).[187]

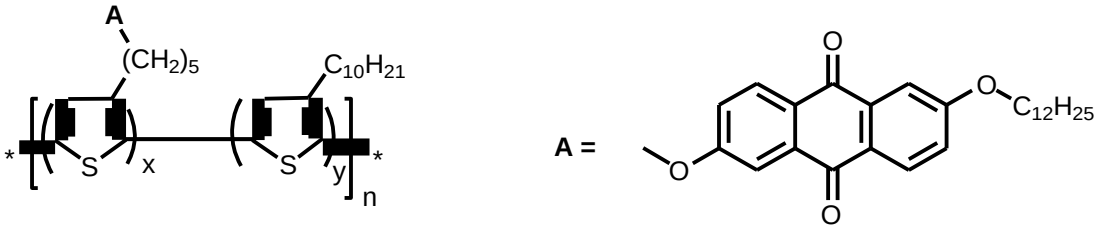

Figure 78. The structure of electron donating polythiophene covalently linked with electron accepting anthraquinone substituents.[190]

A series of electron donating polythiophene systems covalently linked with electron accepting anthraquinone substituents have been reported as photoactive materials for the fabrication of organic photoelectric conversion devices. A noteworthy feature of these materials is the good processability and the flat geometry of the acceptor to help the 3-D assembly which can be beneficial for the formation of a pathway for electron transport through the photoactive layer. This donor/acceptor polymer approach gave rise to photoinduced electron transfer from the polythiophene backbone to the anthraquinone acceptor moieties (Figure 78).[190]

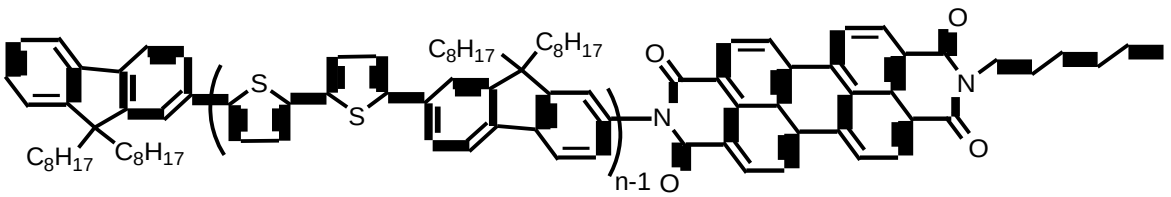

101

Figure 79. Donor - acceptor co-oligomers.[191]

The best performance for a single-molecule solar cell to date has been recorded by synthesizing donor-acceptor co-oligomers with different molecular lengths. They were designed to illustrate well-defined nanostructures with a length scale equal to or less than the exciton diffusion length of organic semiconductors. External quantum efficiency (EQE) of up to 46% at 410-500 nm and a power conversion efficiency (PCE) up to 1.50% was reported for this system (Figure 79).[191]

4.1.4. Flavins as electron acceptors

Flavins are attractive systems to incorporate into polymers as acceptor materials for organic photovoltaic cells for a number of reasons: (i) their planar structure should allow increasing of the π overlap between neighboring chains. (ii) Their well documented ability to have their redox and optical properties tuned by synthetic modification should allow convenient control of the resulting polymer properties [192]. So the incorporation of flavin into an alternating donor - acceptor copolymer should afford polymers with a tunable small band gap, leading to a range of highly efficient organic polymers suitable for use in photovoltaic cells.

4.2. The aim of the project

The main strategy of this project is to design low band gap polymers with alternating electron-rich and electron-deficient units along the conjugated polymer chain. This donor–acceptor molecular system should afford an effective way to alter the band-gap and the energy position of the valence and conductive levels, thereby extending the absorption of light towards the near-IR region (Figure 80).

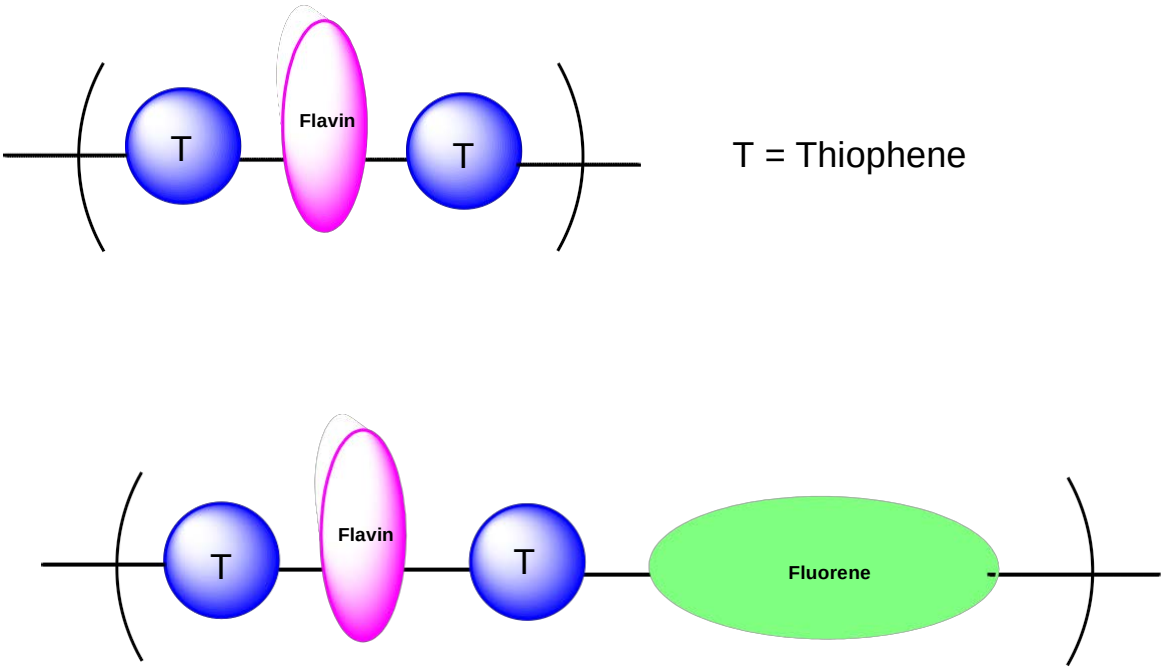

Figure 80. Sketch of the two polymers described in this chapter.

4.3. Synthesis of thiophene-flavin polymers.

The *N*-alkylated-substituted isoalloxazine monomers bearing two thiophenes (**108**) and (**110**) were targeted as potentially precursor for the formation of the new polymers (Figure 81). Scheme 26 illustrates the synthetic methodology used to furnish monomer **108** and polymer **109**.

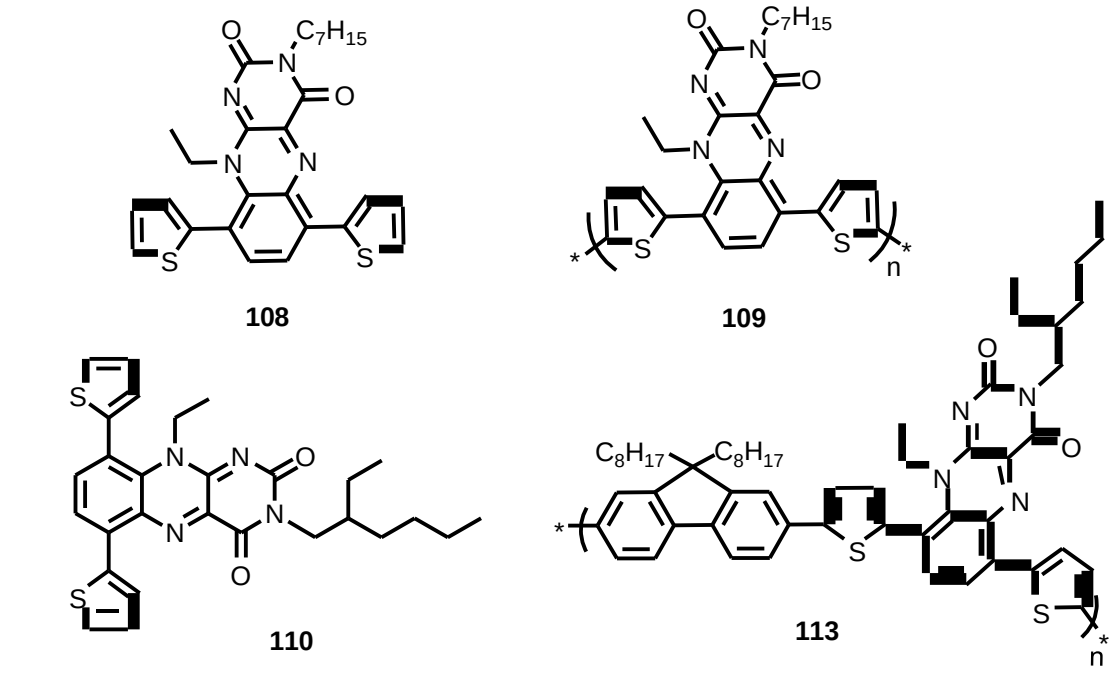

Figure 81. The structures of the monomers 108 and 110 with the two polymers 109 and 113.

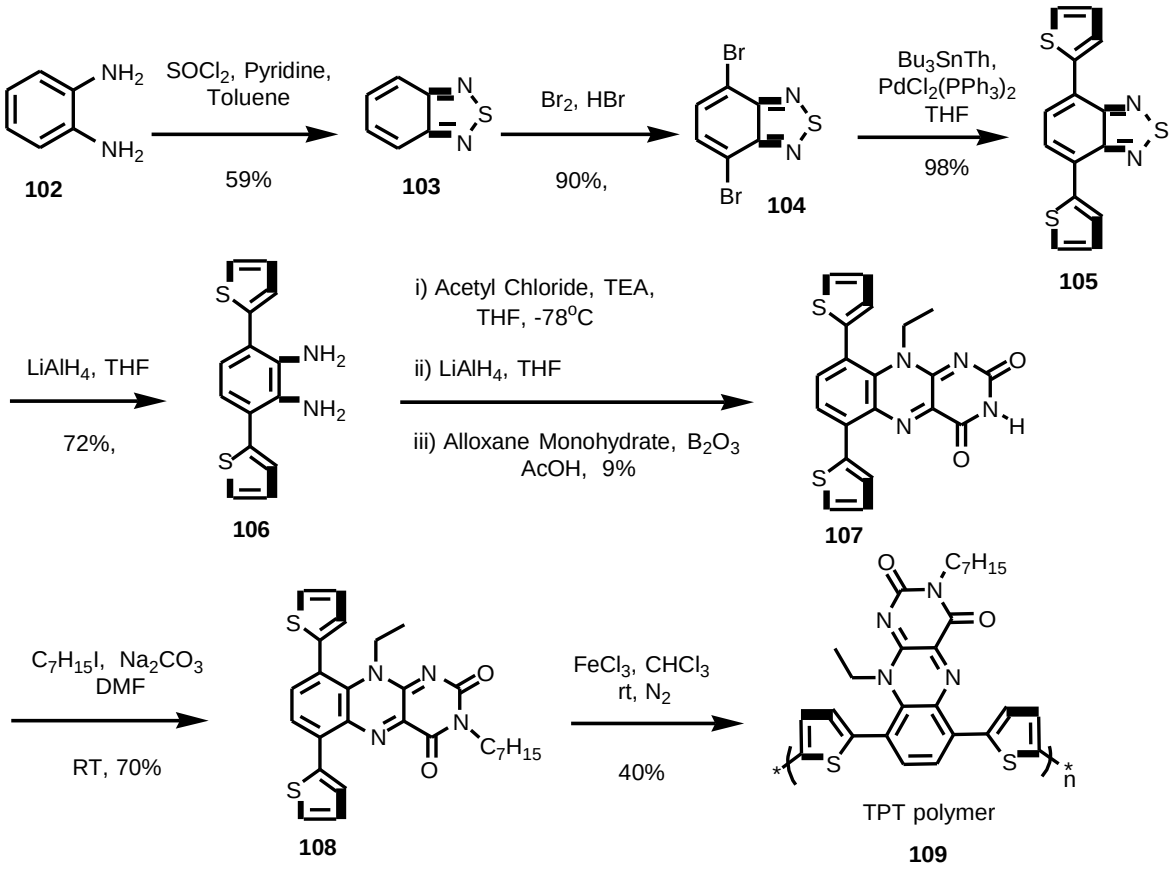

Scheme 26. Methodology of preparing the polymer 109.

1,2-Diaminobenzene (**102**) was the starting material to be converted into 2,1,3-benzothiadiazole (**103**). This was accomplished by heating 1,2-diaminobenzene under reflux in toluene with thionyl chloride and 4 eq. of pyridine. The crude product was purified *via* flash column chromatography to afford **103** in 59% yield.[193] Both amines attack the thionyl chloride in sequence to give the disulfinylamine. The addition of water would switch the molecule back to the monosulfinylamine and internal cyclisation gives the desired 2,1,3-benzothiadiazole **103** (Scheme 27).[194]

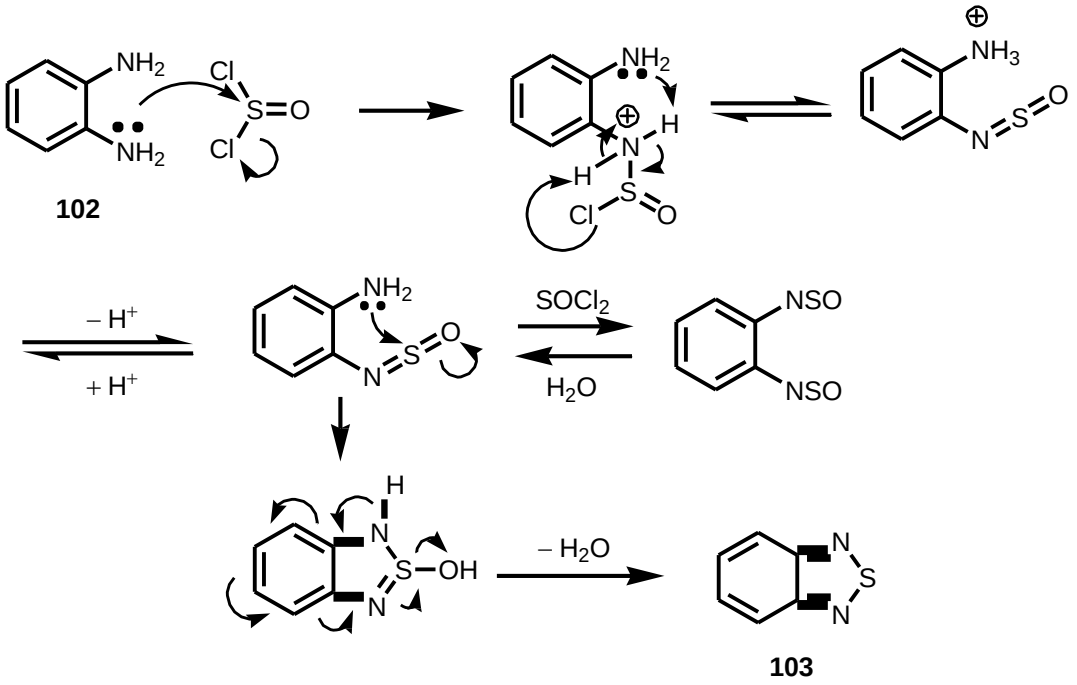

Scheme 27. Mechanism for the formation of 2,1,3-benzothiadiazole 103.[194]

Bromination was then carried out at the 4 and 7 positions to give 4,7-dibromo-2,1,3-benzothiadiazole (**104**). This was accomplished by heating 2,1,3-benzothiadiazole under reflux in excess HBr and 2 equivalents of bromine to give the crude product, which precipitated from solution and was washed with water to give **104** in 90% yield (Scheme 28).[193,195]

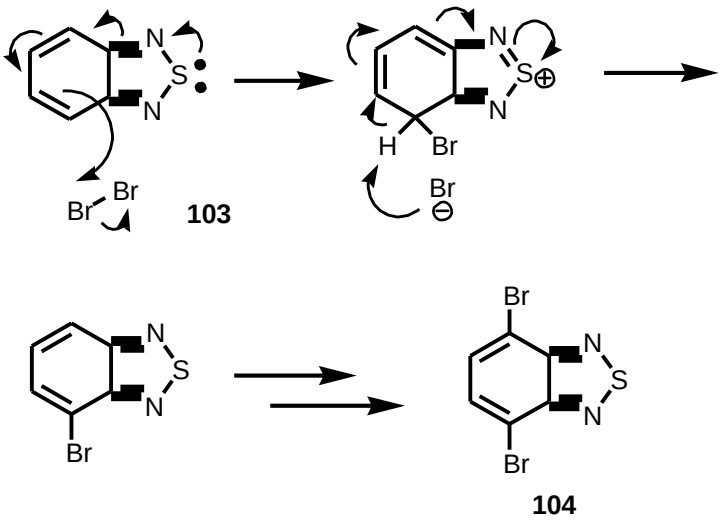

Scheme 28. Mechanism of the formation of 4,7-dibromo-2,1,3-benzothiadiazole 104.

Compound **104** was converted to 4,7-dithien-2yl benzothiadiazole **105** *via* the Stille cross-coupling reaction, by means of 2 equivalents tributyl (thien-2-yl)stannane with palladium(II)bis(triphenylphosphine) dichloride in 2 mol% giving the product, which was purified *via* flash column chromatography and recrystallised to give the product in 98% yield. Reduction of the thiadiazole ring of **105** was carried out to give the corresponding diamine using lithium aluminium hydride which after purification by flash column chromatography gave **106** in a 72% yield. The literature procedure of the reduction by using a large equivalent of zinc dust refluxing in acetic acid was also successfully undertaken.[188,196]

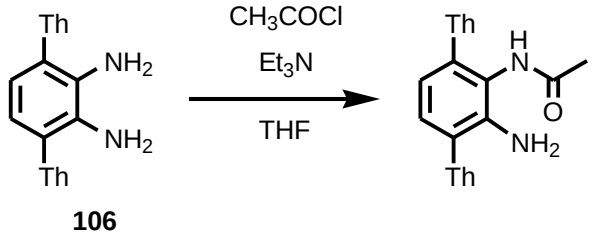

Scheme 29. Synthesis of monosubstituted 1,2-diamino-3,6-dithien-2'-ylbenzene (Th = 2-thienyl).

Mono-acylation of the diamine using acetyl chloride in the presence of triethylamine was undertaken (Scheme 29).[197] Unfortunately, the obtained product decomposed when purified using column chromatography. The reaction was carried out at –78^{o}C to decrease the opportunity of multi-acylation. The amide was then reduced to the secondary amine. The obtained product was not purified as it rapidly underwent decomposition due to the instability of the compound (Scheme 30).

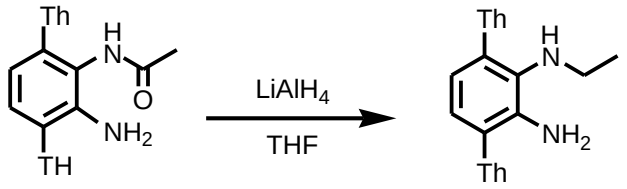

Scheme 30. Synthesis of *N*-ethyl-3,6-di(thiophen-2-yl)benzene-1,2-diamine.

This crude product was then converted to the flavin analogue by reacting with alloxan monohydrate in the presence of boric anhydride and acetic acid. Purification using flash column chromatography gave **107** in a 9 % yield (Scheme 31)[198].

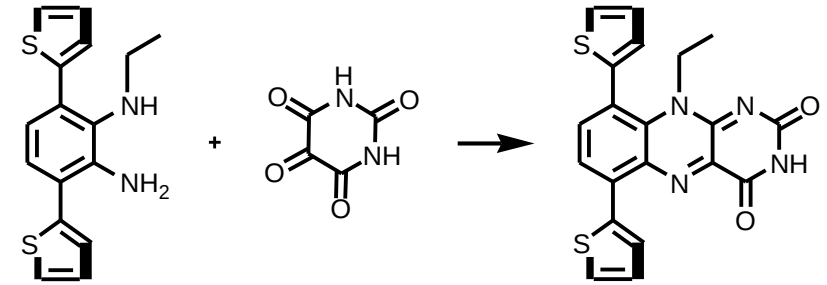

107

Scheme 31. Synthesis of the flavin 107.

The flavin was synthesized through condensation reactions occurring between the diamine and two of the carbonyls of the alloxan[199]. Boric anhydride was used to polarize the carbonyl groups on the alloxan. Furthermore, using boric anhydride can prevent unwanted side products that arise from using just alloxan in glacial acetic acid, thereby increasing flavin yields[200]. Finally, alkylation *via* alkyl halide was carried on N3 position of flavin **107** as attempt to increase the solubility. Iodoheptane was added to flavin **107** in dry DMF in the presence of sodium carbonate. The monomer **108** was obtained in 70% yield after purification using column chromatography.

Polymer **109** was synthesized by chemical oxidation of the monomer using ferric trichloride[201]. A solution of ferric trichloride (0.012 mol) in dry chloroform was mixed with a solution of a monomer (0.003 mol) in dry chloroform and stirred at room temperature for 24 hours under a gentle stream of nitrogen. The polymer was then precipitated into methanol and washed many times to remove the ferric chloride species completely from the polymer. The predicted mechanism of the chemical oxidation of the thiophenes with ferric chloride was described previously in Scheme 24.

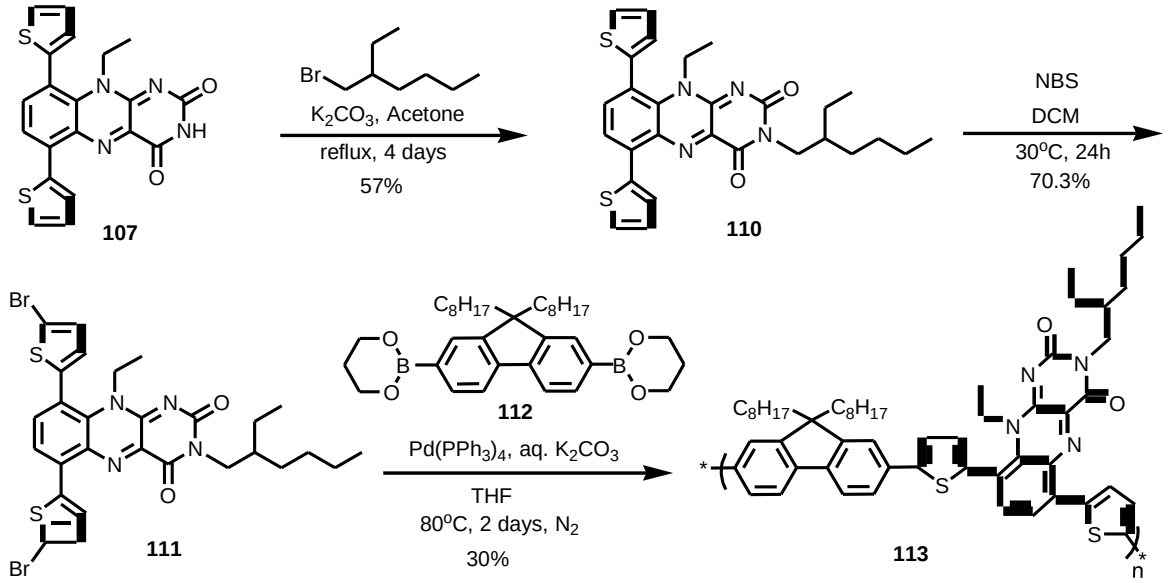

Scheme 32. Synthesis of polymer 113.

The synthesis of a novel flavin-containing conjugated alternating donor/acceptor co-polymer is summarised in Scheme 32. A novel electron poor flavin derivative bearing electron rich thiophene and fluorene units was synthesised. Firstly, the 2-ethylhexyl group was introduced to compound **107** to improve the solubility and the film-forming properties of the resulting copolymers. The resulting monomer **110** was brominated to form **111** using NBS. The addition was undertaken at 0^{o}C and in dark to avoid further bromination. The resulting yield was about 70% of compound **111**. The co-polymer **113** was synthesised *via* Suzuki cross coupling reaction of flavin dibromide **111** and the fluorine boronic ester **112**. The reaction mixture was deoxygenated by nitrogen bubbling and the reaction was carried out in the presence of palladium triphenylphosphine and aqueous potassium carbonate. The end capping of polymer bromide groups was carried out by the addition of phenyl boronic acid whereas the end capping of the boronic ester was carried out through the addition of the bromobenzene. The purification was carried out by passing it through short alumina column and then by precipitation into methanol to yield about 30% of co-polymer **113**. The mechanism for the formation of polymer **113** is illustrated in (Figure 82).

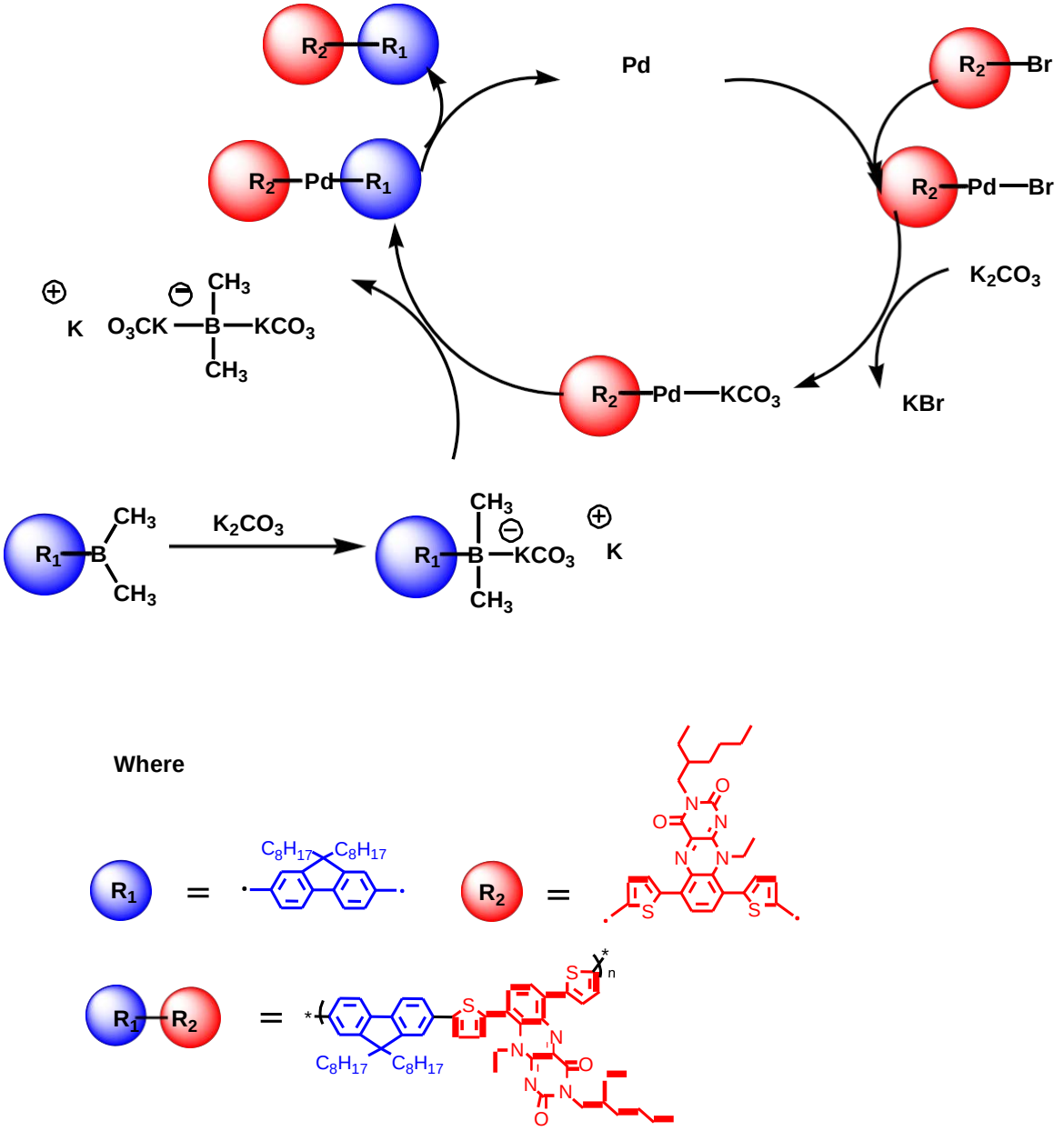

Figure 82. Mechanisim for synthesising polymer 113.

4.4. Results and Discussion

Figure 83 shows the different colours of monomer **108** compared to polymer **109**. The colour changed from red (for monomer) to green for the polymer. This reflects polymer's ability to absorb light at longer wavelength. This indicates that the electronic absorption spectrum shows a pronounced red shift by increasing the number of thiophene units in the chain.[202-204]

Figure 83. Colour of both the monomer 108 and polymer 109 in ($1x10^{-4}$ M) solution in DCM.

The X-ray crystal structure of monomer **108** is provided in Figure 84. It can be clearly seen from the crystal structure of the monomer **108** that the thiophene adjacent to the ethyl group is twisted perpendicularly in the molecule. This could be caused by the steric interaction between this thiophene and the ethyl group plus conjugation of a lone pair of electrons of the thiophene to a carbonyl of the flavin moiety (Figure 85). This torsion from the co-planarity is enough to inhibit π orbital overlap and would lead to an increase in band gap which therefore reduce the polymers ability to conduct electricity.[205]

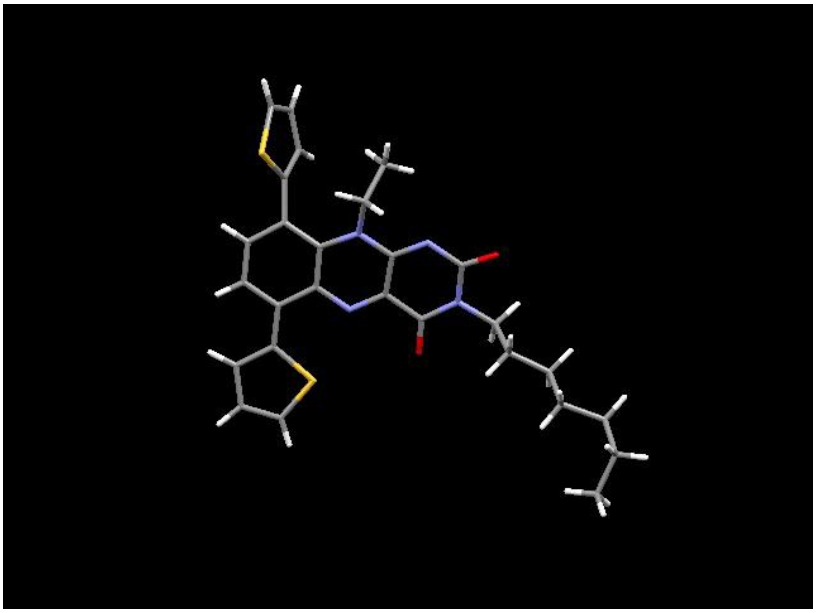

Figure 84. Crystal structure of the monomer 108.

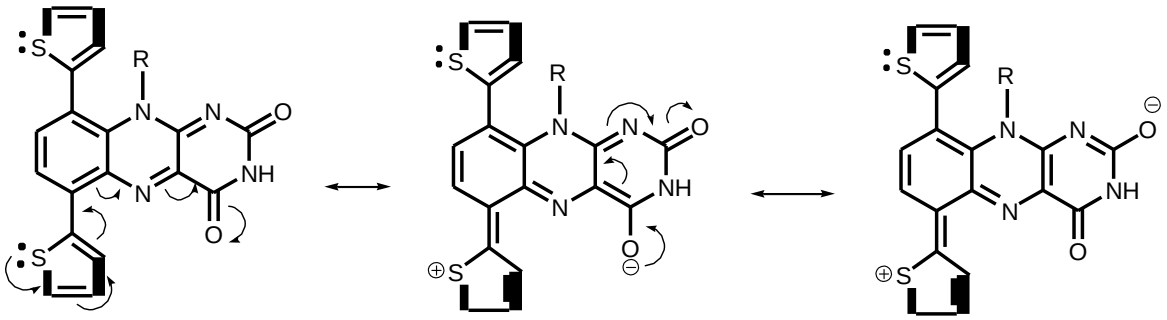

Figure 85. Conjugation of lone pair electrons of the thiophene to a carbonyl of a flavin moiety.

4.4.1. NMR Spectroscopic studies.

The spectroscopic data of all synthesized compounds are in agreement with the proposed structures. The ^{1}H NMR spectra confirmed the expected signals of the flavin's N10 methylene broad peak 4.75 ppm and 4.57 ppm for compound **107** and **108**, respectively. The ^{1}H NMR spectra was not clear for polymer **109** as it consited of very broad overlapping signals. Gel permeation chromatography (GPC) recorded in THF was used to characterize polymer **109** and provided the following data: M_n = 5237, M_w = 6709, Mp = 5443, PD = 1.28. The data are consitent with up to 10 to 13 monomer units being present in the oligomer as the molecular weight of the monomers are about 500.

4.4.2. UV-Visible Studies.

UV-Vis spectra for monomer **108** and the two polymers **109** and **113** in 1 x 10^{-5} M DCM solutions are provided in Figure 86 and Figure 87, respectively. The associated data is summarised in Table 7. Compound **108** displays the flavin's main broad peak at 440 nm, whereas polymer **109** and polymer **113** revealed a red shifted peak towards 580 nm and 560 nm, respectively. This illustrates the influence of the thiophene units on lowering band gap energies. It is known that for polythiophene derivatives the width of the gap and the position of the π-π^* absorption band, are strongly dependent on the degree of the chain regioregularity and on the molecular mass of the polymer [146-148]. However, it is clear that with increasing number of thiophene units, the band gap reduced from 2.02 eV for monomer **108** to 1.55 eV and 1.66 eV for the polymer **109** and polymer **113**, respectively.

Table 7. UV-Vis spectroscopy data of monomer 108 and the two polymers 109 and 113 in $1x10^{-5}$ M DCM.

Compounds	λ^1_{abs}	λ^1_{ons}	λ^2_{abs}	λ^2_{ons}	λ_{max}	λ_{ons}	E_{gap}
Monomer 108	285	360			440	615	2.02
Polymer 109	370	430	456	515	580	800	1.55
Polymer 113			395	455	560	750	1.66
Fluorene 112					317	330	3.77

λ_{abs} – maximum absorption wavelength of each peak (nm)

λ_{ons} – onset of each peak (nm)

E_{gap} – gap energy (ev)

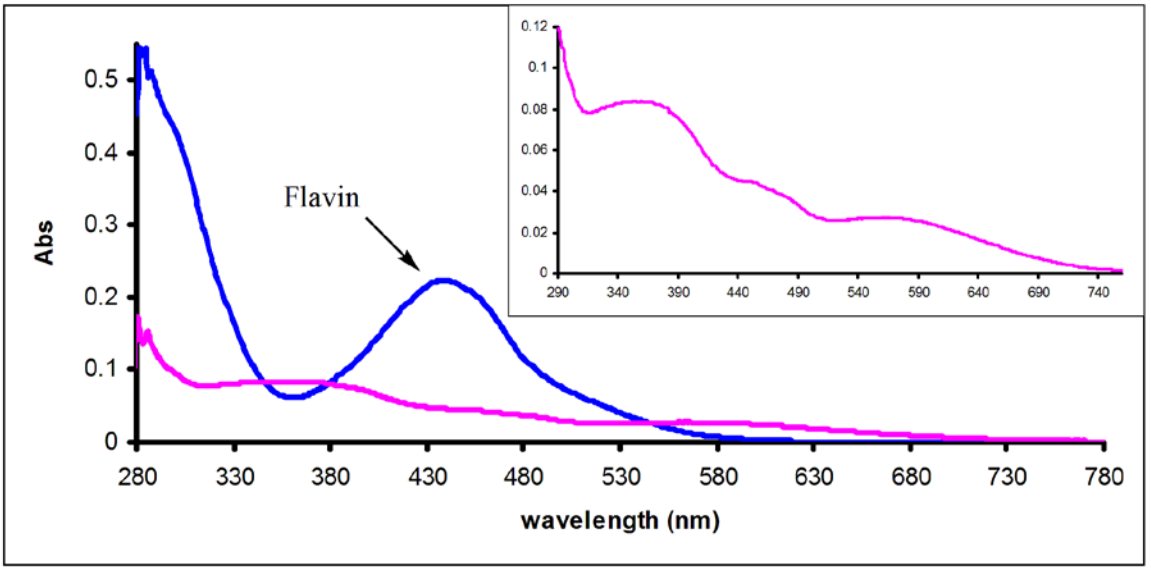

Figure 86. UV-Vis spectroscopy of monomer 108 (blue line) and polymer 109 (pink line) in $1x10^{-5}$ M DCM.

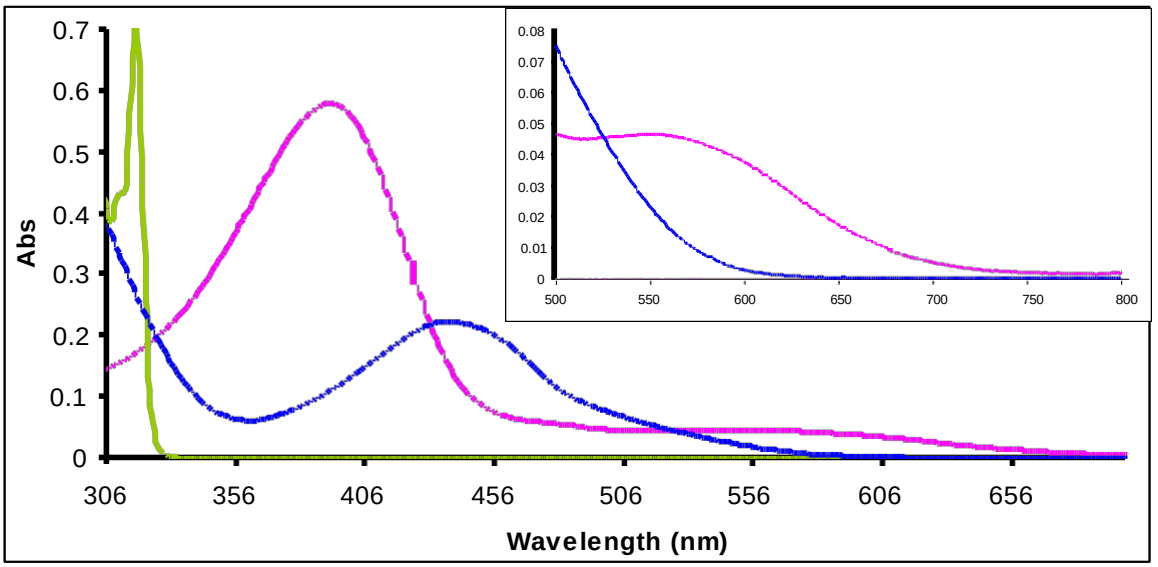

Figure 87. UV-Vis spectroscopy of monomer 108 (blue line), fluorene 112 (green line) and polymer 113 (pink line) in 1x10^{-5} M DCM.

4.4.3. Electrochemical studies

The electrochemical properties of the monomer **108** and polymers **109** and **113** were investigated by cyclic voltammetry to find out the influence of increasing the conjugation on the LUMO energy and hence the band gap. The cyclic voltammetry of monomer **108** and two polymers **109** and **113** were preformed at room temperature in a solution of (1 x 10^{-4}M) CH_2Cl_2 containing tetra-n-butyl ammonium hexafluorophosphate (Bu_4NPF_6 0.1 M) as supporting electrolyte with a platinum wire as working and counter electrodes and a silver wire as a quasi-reference electrode. E_{LUMO} values for the compounds are referred to the potential of the Fc^+/ Fc redox couple utilized as an internal standard. The scan rate was 0.1 V/s and the observed reduction potentials are collated in Table 8.

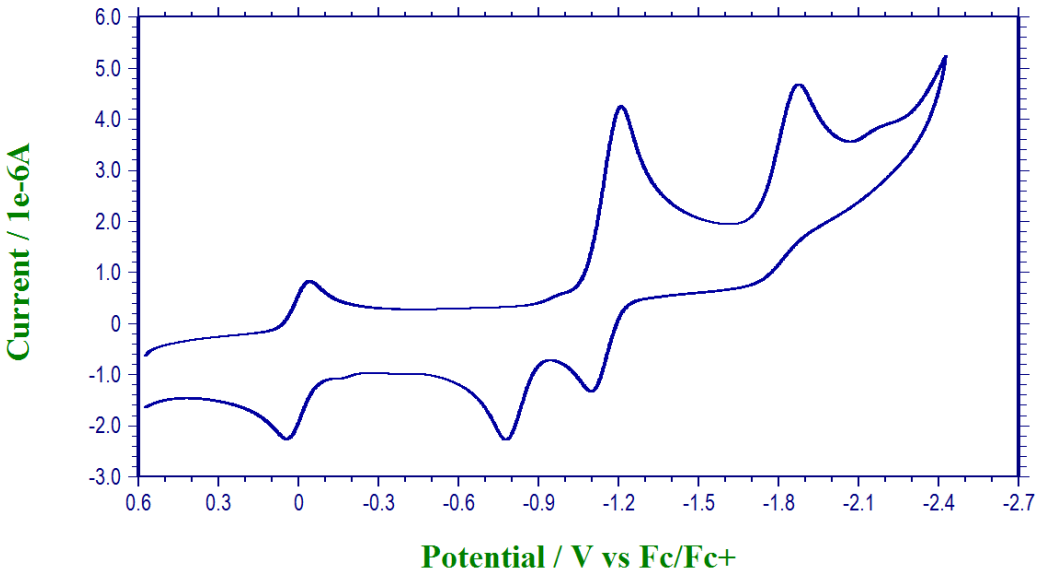

Figure 88. Cyclic voltammetry of monomer 108.

Table 8. Cyclic voltammetry Data of monomer 108 and the two polymers 109 and 113.

Compounds	E^1_{ons}	E^1_{red}	E^2_{red}	E^3_{red}	E^1_{rev}	E^2_{rev}	E^3_{rev}	ΔE	$E_{1/2}$	E_{LUMO}
108		-1.21	-1.88	-2.22	-0.78	-1.10	-1.70	-0.43	-1.00	-3.81
109	– 1.18	-1.57	-2.40		-1.29	-1.56		-0.28	-1.43	-3.37
113	– 1.03	-1.16			-1.11			-0.05	-1.14	-3.66

E^1_{ons} - Onset of first reduction potential (V)

E^1_{red} - Maximum of first reduction potential (V)

E^1_{rev} - First reversible potential (V)

ΔE - Energy differences between peak potential (forward and backward sweep) in (V)

$E_{1/2}$ - Half wave potential $E^1_{red} + E^1_{rev}/ 2$ (V)

E_{LUMO} = – 4.8 – $E_{1/2}$ (V)

The cyclic voltammogram of the monomer **108** (Figure 88) showed three reduction waves at –1.21 V, –1.88 V and at –2.22 V. Polymer **109** (Figure 90) displayed two electron reductions at –1.57 V and – 2.40 V. Whereas polymer **113** showed one reduction potential at –1.16 V (Figure 91).Obviously, the polymers revealed anodic shift which means lower reduction potential than the monomer **108**. Accordingly, the LUMO energy level of the monomer **108** and polymers **109** and **113** can be calculated from onset reduction potentials by comparing with the ferrocene value of 4.8 eV below the vacuum level. So, the calculated LUMO energy level of monomer **108** was found to be – 3.81 eV and for polymer **109** and polymer **113** are – 3.37 eV and – 3.66 eV respectively. However, the oxidation potential of ferrocene has also been reported as 4.4 eV below vacuum. The electron affinity (EA) and ionization potential (IP) of the polymers **109** and **113** can be calculated from the equations:

IP = E_{ox} **(onset)** + 4.4

EA = E_{red} **(onset)** + 4.4

Where the constant 4.4 eV in the equations between IP, EA, and redox potentials comes from the difference in gas-phase ionization potentials and electrochemical oxidation potentials of solid films and the solid-state polarization (Figure 89). The LUMO-HOMO energy gap can be calculated from the redox properties as:

E_g = IP - EA

= E_{ox} **(onset)** - E_{red} **(onset)**

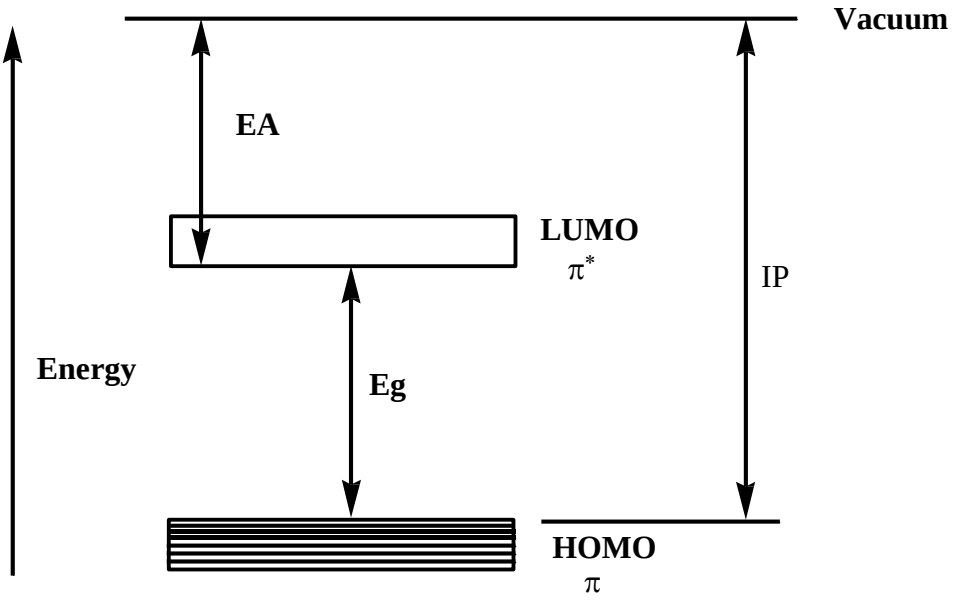

Figure 89 Schematic energy diagram of a conjugated polymer. Electron affinity (EA), ionization potential (IP), and LUMO-HOMO energy gap (E,) are defined

The electron affinity AE (LUMO level) of polymers **109** and **113** can also be calculated from the onset of the reduction waves from the equations:

Electron affinity EA of polymer **109**

EA = E_{red} (onset) + 4.4 eV[195]

= 1.18 – 4.8 eV

EA = – 3.62 eV

Electron affinity EA of polymer **113**

EA = – E_{red} (onset) – 4.8 eV

= 1.03 – 4.8 eV

EA = – 3.77 eV

Where the onset potential is in volt (V) and EA is in electronvolt (eV). The results showed the electron affinities (LUMO energies) of the two polymers are higher than the LUMO energy of the monomer **108** (– 3.81 eV). This could be caused by the influence of the regular increasing of the proportion of thiophene units on the LUMO energy levels. In addition, the LUMO energy of polymer **113** (– 3.77 eV) is lower than that of polymer **109 (**– 3.62 eV). This should be related to the stronger electron-donating ability of the fluorene unit or the delocalization of the LUMO because of better planarity between the TPT and fluorene segments. It is also worth to mention that the high LUMO energy is useful to decrease the lost energy from exiton diffusion which cannot be gained as electrical energy in heterojunction solar cells.[195]

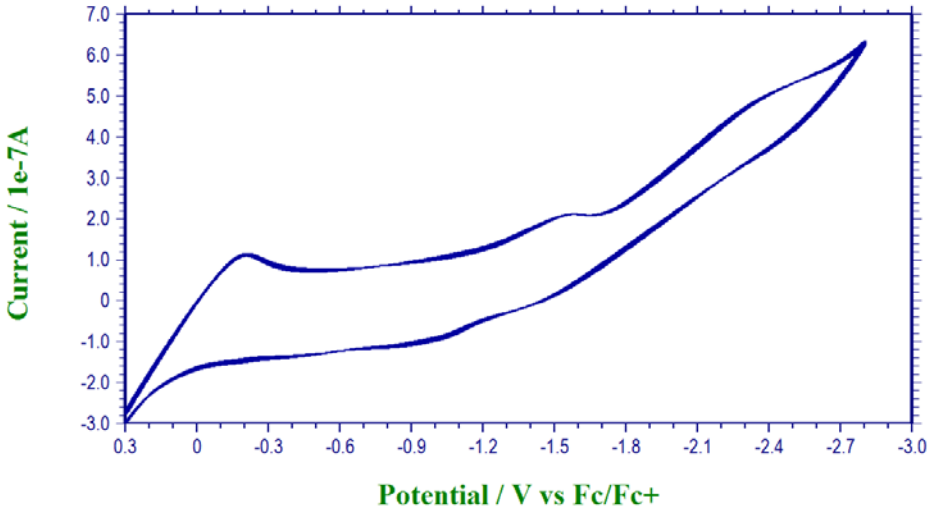

Figure 90. Cyclic voltammetry of polymer 109.

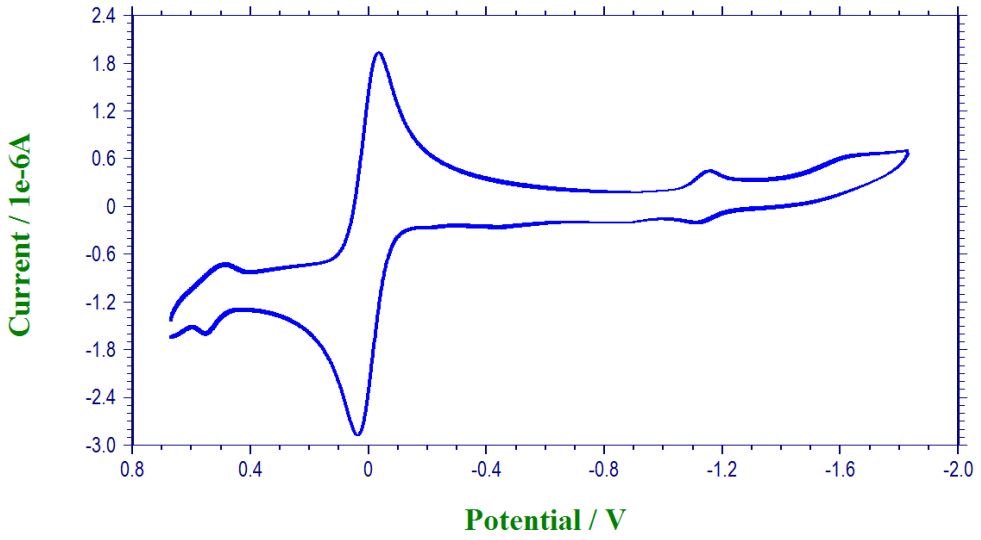

Figure 91. Cyclic voltammetry of polymer 113.

4.5. Photovoltaic devices

Photovoltaic cells were fabricated within the School of Physics and Astronomy at the University of St-Andrews using P3HT as polymer component combined with monomer **108.** Poly(3-hexylthiophene) (P3HT) is a conjugated polymer that is widely used in the ongoing researches in the field of organic photovoltaic. Therefore, monomer **108** was investigated as electron-acceptor materials in combination with P3HT which is used as the electron-donor component

4.5.1. Absorption measurements

The absorption spectrum of monomer **108** was measured on a quartz disk; the film was spin coated out of solution with 20 mg/ml in chlorobenzene. The film thickness was about 52 nm deposited using a spin speed of 1500 rpm. The results are shown in Figure 92. The material has a relatively high absorption in the green blue region.

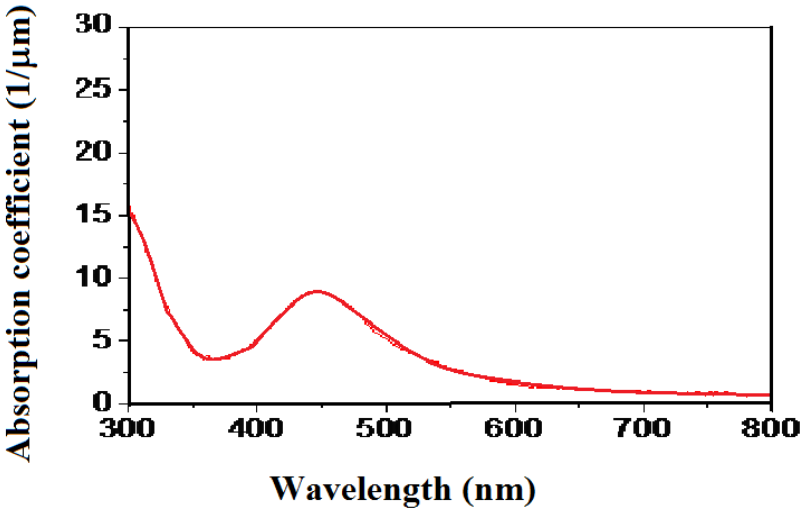

Figure 92. Absorption of monomer 108 dissolved in chlorobenzene at 20 mg/ml and spin coated on quartz disks.

4.5.2. Solubility.

Monomer **108** showed limited solubility in all tested solvents as illustrated in Figure 93, where clearly some un-dissolved particles are visible. Films were fabricated by dissolving P3HT and monomer **108** in different solvents with a concentration of 20 mg/ml or 15 mg/ml. The solution was stirred over night at 70 °C and then spin cast on cleaned quartz substrate in a nitrogen glove box. A reference made of neat P3HT is also shown in Figure 94 which reveals a good film quality.

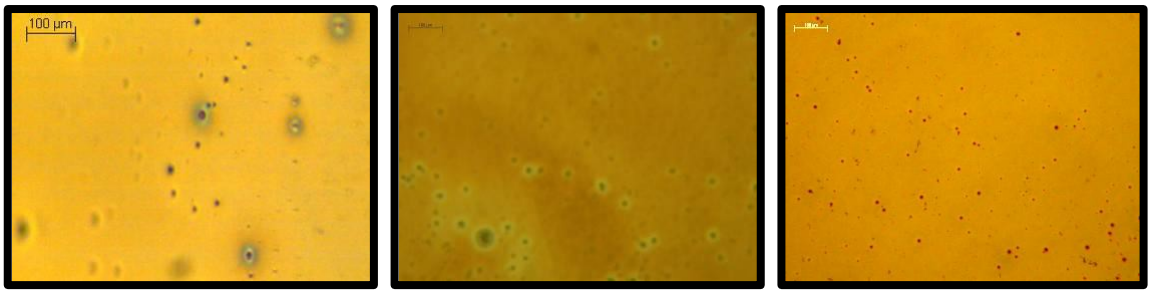

Figure 93. Microscopic images of P3HT: monomer 108 blends of different solvents spin coated on quartz disks (left - Chlorobenzene: Carbon disulfide 1:1, 20 mg/ml. middle – Chloroform 15mg/ml. right – Chlorobenzene 15 mg/ml). The colour of the images can be different to the actual film colour.

Figure 94. Microscope image of a reference of neat P3HT in 20 mg/ml chlorobenzene.

4.5.3. Fluorescence quenching

Quenching of fluorescence of P3HT indicates that charges, created by absorption of light, transfer to monomer **108** and so it is a good method to investigate charge separation. Fluorescence quantum yield was measured on P3HT: monomer 108 blends of different ratios and compared with a neat P3HT film. Films were prepared by mixing solution A made of 20 mg/ml P3HT in chlorobenzene with solution B consisting of monomer **108** dissolved in chlorobenzene by 2 mg/ml. Solution A and B were mixed by appropriate amounts to achieve a specific concentration of monomer **108** determined per total mass. Figure 95 shows the results of these measurements are shown. The curves are normalized for better comparison. Monomer **108** shows similar quenching to PCBM.

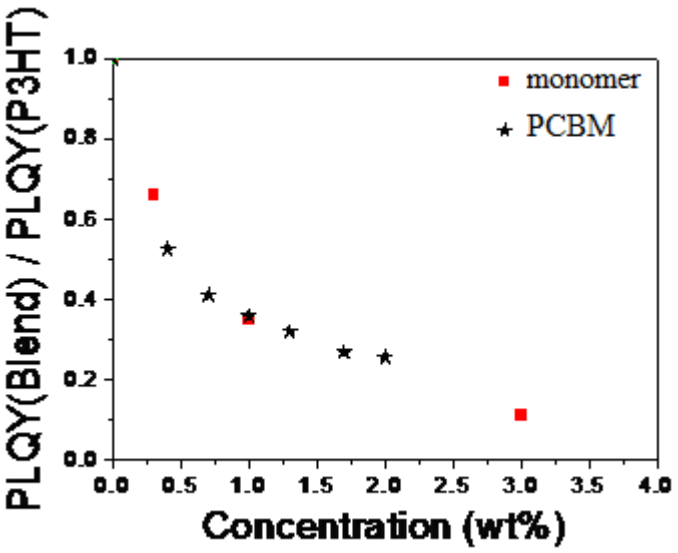

Figure 95. Fluorescence quenching of P3HT with varying amount of monomer 108. Quenching with PCBM is shown for comparison.

4.5.4. Phase aggregation

Monomer **108** forms with P3HT relatively large clusters and crystalline structures. These structures are clearly visible with an optical microscope. The films are based on 1:1 blends with a concentration of 12 mg per ml chlorobenzene. The solutions were filtered with 0.45 µm pore size before spin coating. The films dried in nitrogen atmosphere at room temperature for three days. Monomer **108** reveals large aggregates in the order of 50 to 100 µm as shown in Figure 96.

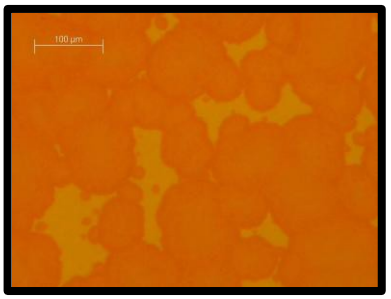

Figure 96. Microstructure of films of 108 (Scale 100 µm).

4.5.5. Solar cells

Two solar cells were prepared according to standard procedure but without PEDOT:PSS and with two different annealing temperatures 130 °C and 150 °C.

A solution of P3HT: monomer **108**, 1:1, 15 mg/ml was prepared in chlorobenzene and stirred overnight at 70 °C. The photovoltaic devices were prepared by etching the substrate with indium tin oxide (ITO) to a 4 mm wide stripe followed by plasma ashing (100 W) in O_2 for 5 minutes. Then spin coating was undertaken with P3HT: monomer **108** (filtered with 0.45 µm) with 1000 rpm, ramp 50, 90 s in a glove box and was annealled at 70 °C in a glove box for 10 minutes. The counter electrode of (Al) aluminium was deposited by vacuum evaporation and annealed at temperatures of 130 °C and 150°C in a glove box for 20 minutes.

Devices were tested with a 100 mW/cm² solar simulator from Steuernagel Lichttechnik GmbH. The current density *J* of the devices was measured by using a Keithley 2400 Sourcemeter for an applied voltage *V* form -1 to 1 V. Each device consists of four pixels with an area of 0.08 cm². Results for one selected pixel are shown in Figure 97. The spikes in the curves are mainly caused by the device itself. For both devices no diode like behaviour and no photovoltaic effect could be observed. Both currents are very low with around 1 mA/cm² in positive bias at 1 V, indicating low conductivity. The film thickness for the devices was unexpectedly high (140 nm) caused by filtering of the solutions before spin coating.

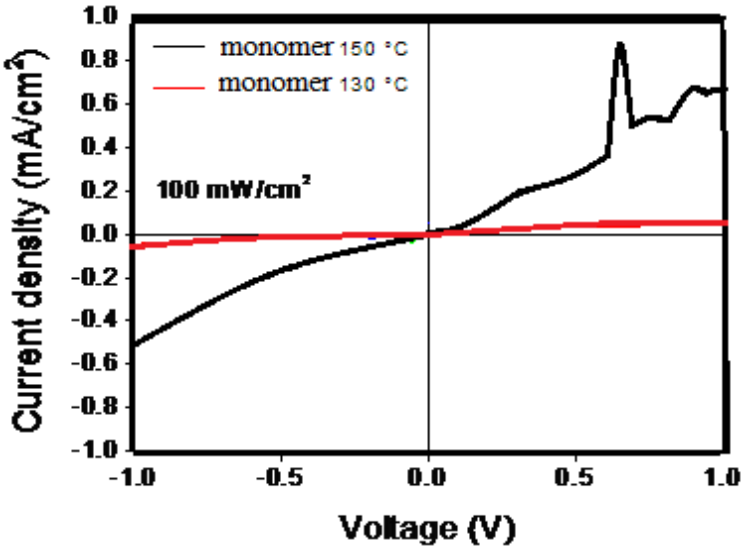

Figure 97. JV curves for devices made of P3HT: monomer 108 with a 1:1 blend.

4.6. Conclusion

A synthetic methodology has been developed to furnish flavin functionalised thiophene derivatives and their polymers to be utilized for photovoltaic cells. The UV-Vis spectroscopy showed red shift by increasing the π - conjugated thiophene units and hence showed a reduction in the band gap. Electrochemical analysis studies indicated that increasing numbers of thiophene units shifted the reduction potential negatively and as a consequence decreased negatively the LUMO energy. The fluorene functionalised co-polymer has shown to have a positively shifted reduction potential and higher LUMO energy. The X ray structure of compound 108 reveals that only one of the thiophene rings is in conjugation with the central flavin unit which would affect the conduction of any polymer produced. In addition, a film was fabricated and absorption, fluorescence quenching and film quality was investigated. The film quality was poor for all tested solvents so that filtering was necessary. Solar cells were fabricated but no diode like behaviour and no photovoltaic effect was observed and the conductivity of all devices was low. Future work will involve modifying these compounds in order to enhance solubility and potentially their photovoltaic properties. In particular, the new low band gap polymers may prove interesting candidates for the development of photovoltaic devices.

CHAPTER 5

OPTICAL PROPERTIES OF PUSH-PULL FLAVINS

5.1. Introduction

Azobenzene is an aromatic molecule consisting of two phenyl rings joined by an azo linkage (–N=N–) (Figure 98). Substituting the aromatic rings with different substituents (e.g. electron donating and electron withdrawing groups) modifies their electronic absorption properties producing a class of tunable chromophores with interesting spectroscopic and photophysical properties.[206] These derivatives were first described and synthesized in 1856.[207]

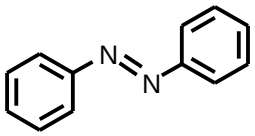

114

Figure 98. Azobenzene.

One of the most interesting properties of azobenzenes is the efficient and reversible photoisomerization, of the thermally stable *trans* to the meta-stable *cis* isomer (Figure 99). Normally, the *trans* isomer is more stable than the *cis* isomer by about 50 kJ/mol, because the *cis* isomer has a distorted configuration and is less delocalized than the *trans* isomer. Thus, azobenzene normally exists in a stable *trans* state. Under irradiation with ultraviolet light, which corresponds to the π-π* transition, photon absorption takes place and the molecule isomerizes to the meta-stable cis state. This state may in turn thermally relax back to the trans state at a wavelength in the cis absorption band or it can be induced with blue light irradiation which is equivalent to that of the n-π* transition required for *cis*-to-*trans* isomerization.[206]

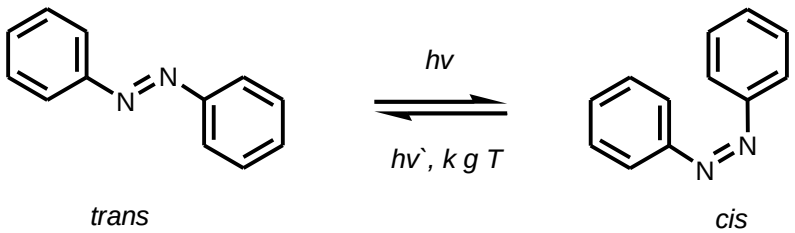

Figure 99. The thermally stable *trans* and a meta-stable *cis* isomers of azobenzene.[206]

The azo chromophores are typically grouped into three classes, based upon spectroscopic characteristics: azobenzene-type molecules, aminoazobenzene-type molecules, which are *ortho*- or *para*- substituted with an electron-donating group; and pseudo-stilbenes, which are substituted at the 4 and 4` positions with an electron donating (e.g. amino) and an electron-withdrawing group (e.g. nitro) (Figure 100).[208] This combination of electron withdrawing and electron donating groups creates a push-pull configuration leading to a highly asymmetric electron distribution within the conjugated system, and leads to a strong molecular dipole. Also noteworthy is that the absorption spectra of the *trans* and the *cis* of the pseudo-stilbenes generally have considerable overlap. Therefore, for these compounds a single wavelength of illumination light in the visible region will induce both the forward (*trans* → *cis*) and the reverse (*cis* → *trans*) photo-isomerization leading to a continuous cycling of chromophores between isomeric states. The other two classes of azo compounds required two different wavelengths of light to be used to switch between the two different states.[209]

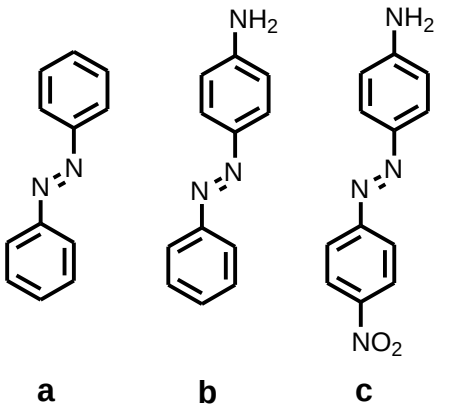

Figure 100. Example of azo chromophores of the (a) azobenzene class, (b) aminoazobenzene class, and (c) pseudo-stilbenes class.[209]

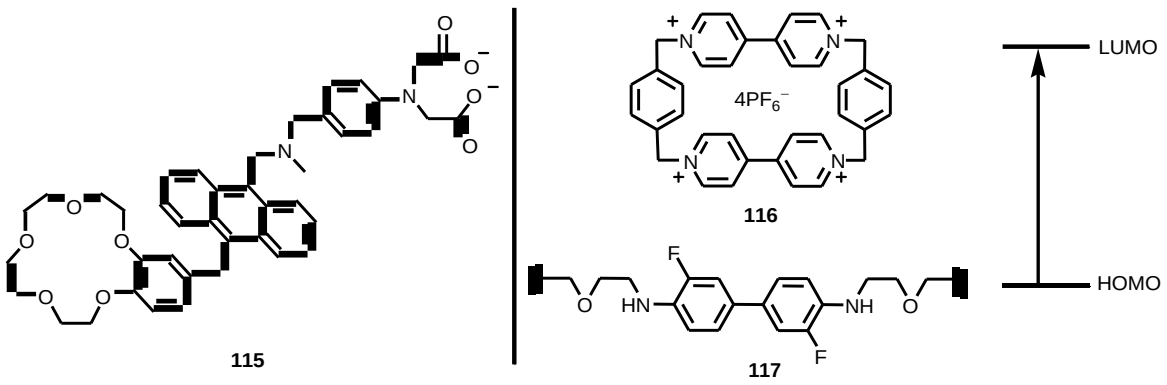

Figure 101. Potential push–pull materials for applications in optical data storage.[210,211]

The incorporation of molecular recognition groups into donor– π –acceptor (D– π –A) molecules has provided a potential method to create a push–pull system for applications in optical data storage (Figure 101) [210,211]. By tuning of bond length alteration and aromaticity, poled polymers based on push-pull conjugated or (donor– π –acceptor) systems have exhibited significant enhancements in electrooptic coefficients. This may lead to high-speed electrooptic switching elements with low drive-power requirements, suitable for telecommunications applications (Figure 102).[212]

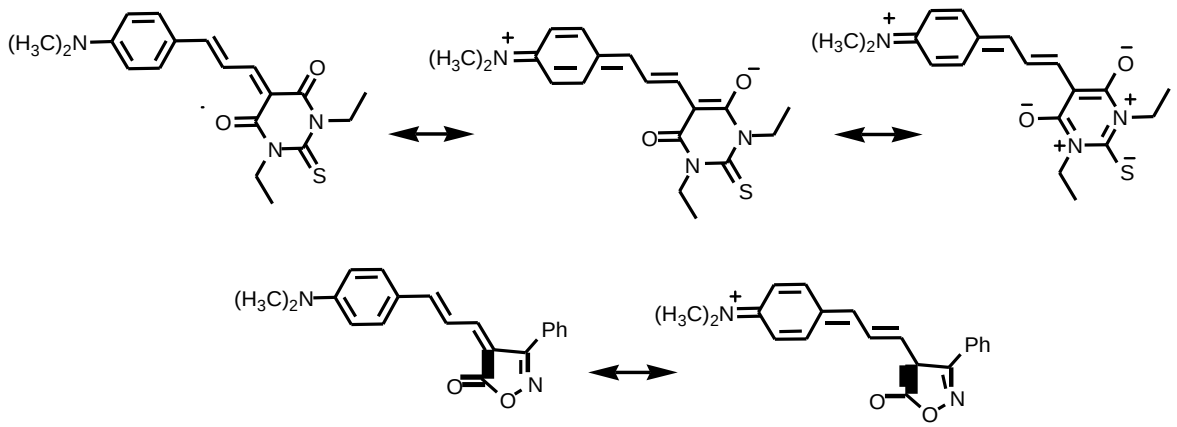

Figure 102. Neutral resonance form and a charge-separated resonance form in which the acceptor ring has aromatic character of (D– π –A) compounds.[212]

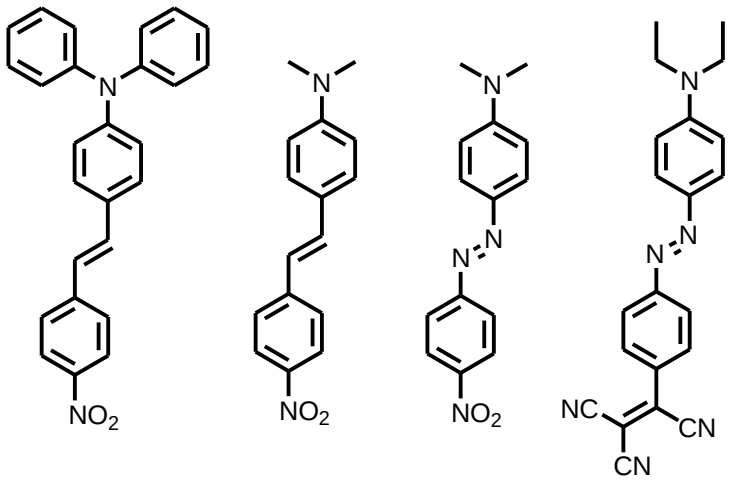

118 **119** **120** **121**

Figure 103. Structures of (D– π –A) compounds that can be used in telecommunications field. [213]

Fast progress in the telecommunications fields are pressing the necessity for enhanced photonic components. Donor-acceptor-substituted materials (Figure 103) have provided a fertile research area for optical modulation and switching. Thus, efforts were focused upon

finding stronger donor and acceptor groups. And since the hyperpolarizability could be correlated with bond length alternation, efforts were made to increase hyperpolarizability and upon increasing the length of the π-electron connective segment which would lead to a decrease of hyperpolarizability. It has been found that bond length alternation is correlated to the relative contributions of neutral and charge-separated resonance structure which is dependent upon donor-acceptor strength. Molecules with aromatic ground states tend to be more bond length alternated than a simple polyene of comparable length. This phenomena can be attributed to the high price in energy which must be paid for loss of aromaticity upon polarization.[213]

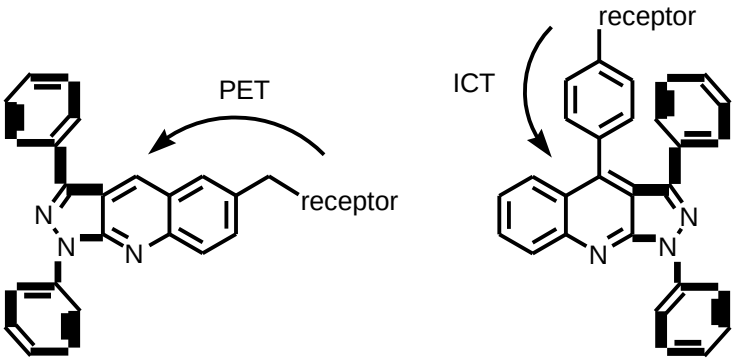

Figure 104. The molecular structures of the fluorescent molecular sensors.[214]

The chromophores of the fluorophore-spacer-receptor systems operating *via* intramolecular charge transfer (ICT) and photoinduced electron-transfer (PET) probes which possess a strong analyte-induced fluorescence improvement have been investigated as a versatile fluorescent molecular sensors (Figure 104).[214]

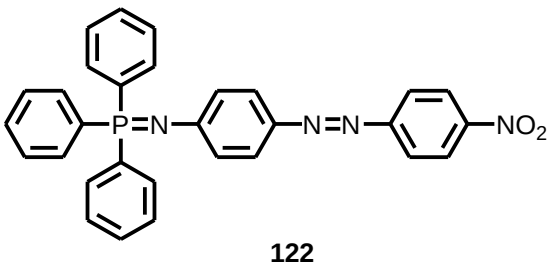

122

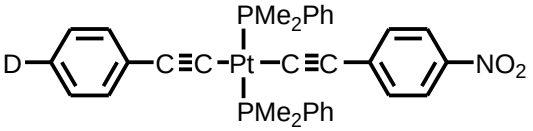

D = OMe or NMe_2

123

Figure 105. D– π –A compounds with essential properties: low-lying charge-transfer excited states, hyperpolarizability, solvatochromism, and second order optical nonlinearities.[215,216]

Combining electron donors (D) and acceptors (A) across conjugated bonds such as in (Figure 105) affords push-pull chemical structures with nonlinear optical and electro-optical effects. In push-pull nonlinear optical materials design, the donor and acceptor substituents provide the mandatory ground-state charge asymmetry, while the π-conjugation structure presents a pathway for the transfer and redistribution of electric charges under the effect of electric fields. The strengths of donor and acceptor groups and the nature and extent of π-conjugated paths determine the molecular hyperpolarizability. The active materials used in electro-optical devices involve a host polymeric backbone, functionalized with second-order nonlinear optical chromophores as guest molecules. [215,216]

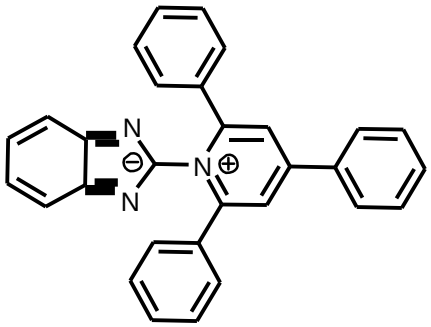

124

Figure 106. Zwitterionic benzimidazole-based pyridinium betaine dye.[217]

Zwitterionic benzimidazole-based pyridinium betaine dye (Figure 106) was shown to display a considerable charge distribution upon excitation. It has been found that both the molecular geometry and positions of the energy levels are significantly influenced by solute solvent interactions.[217] The effect of solvent polarity was also observed on *p*-(dimethylamino) benzethyne. In polar environment, the compound undertakes an intramolecular charge transfer reaction to reach a non-fluorescent intramolecular charge transfer state. This is the main nonradiative process dominating over intersystem crossing. In less polar environments, intersystem crossing is the main nonradiative channel of deactivation for the excited species.[218]

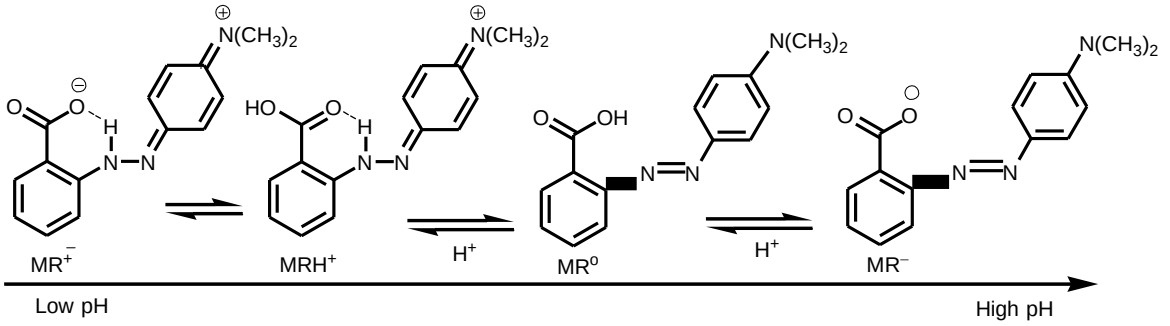

Figure 107. Methyl red identified in solution equilibria.[219]

Methyl red (MR) has complex acid - base equilibria. It has been shown to have a colorimetric response following changes in pH. Moreover, MR performs as environmental indicator due to its ability to change colour in different solvents. Because of the dipole–dipole and intermolecular solute–solvent interactions, MR appears in four different forms according to acidity of the solutions; neutral (MR°), zwitterionic ($MR^{\pm}$), protonated (MRH^{+}), and deprotonated (MR^{-}) (Figure 107).[219]

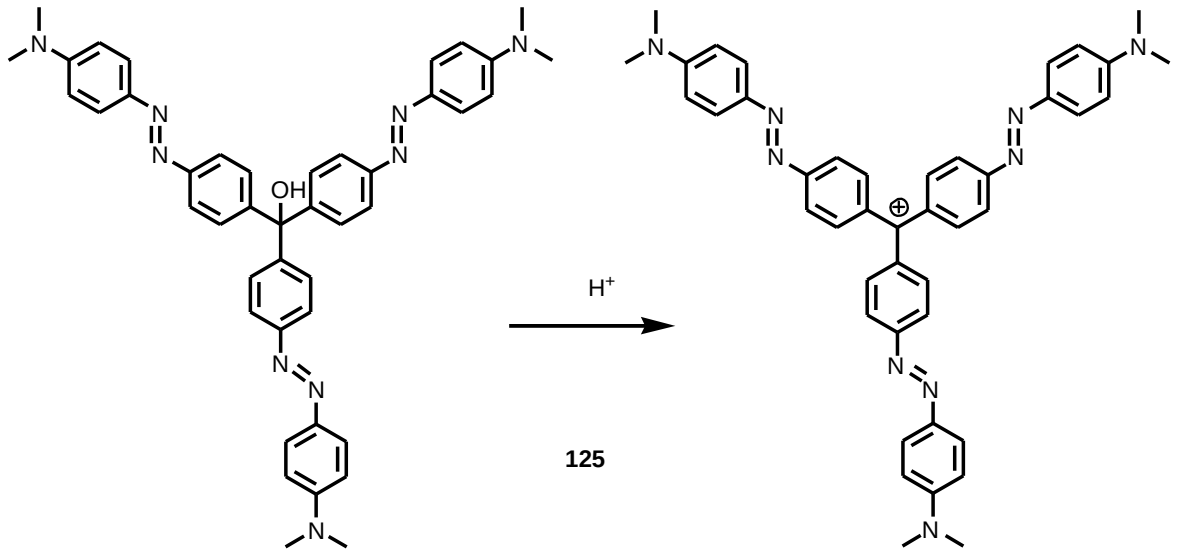

Figure 108. An octupolar dye based on an azobenzene. [220]

An interesting pH-dependent absorption behaviour for azobenzene has shown because of the conjugated spacer and the donor substituent *N*,*N*-dimethylaniline. It has been observed that the octupolar arrangement of the molecule has given rise to intramolecular electronic interactions that arise between the transition moments of the individual chromophores, while a strong acceptor center supports effective mixing of the ground state with the lowest energy excited states (Figure 108).[220]

5.2. The aim of the project

This project aims to examine how changing pH alters the absorption spectrum of push–pull system. Compound **131** was designed by blending 4-nitro-4`-(dimethyl amino)azobenzene and flavin ring. The synthetic pathway has followed a similar methodology reported in the literature[221] (Scheme 33).

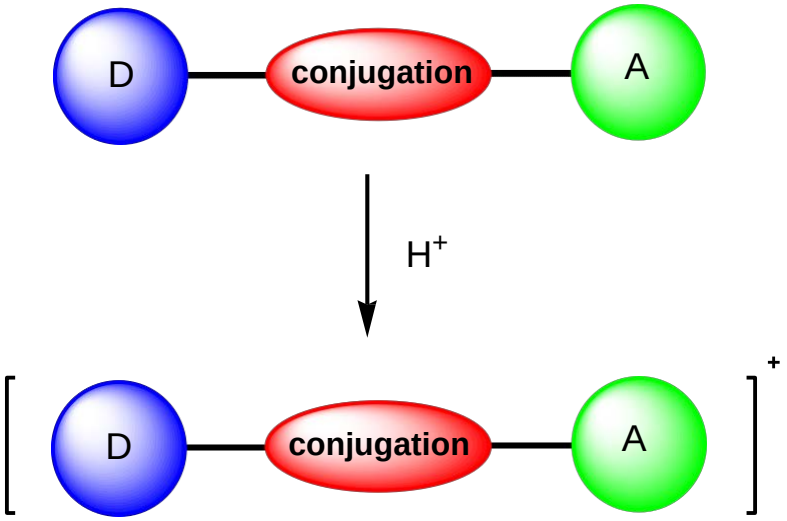

Scheme 33. Protonation of D–π–A push–pull system.

5.3. Synthesis

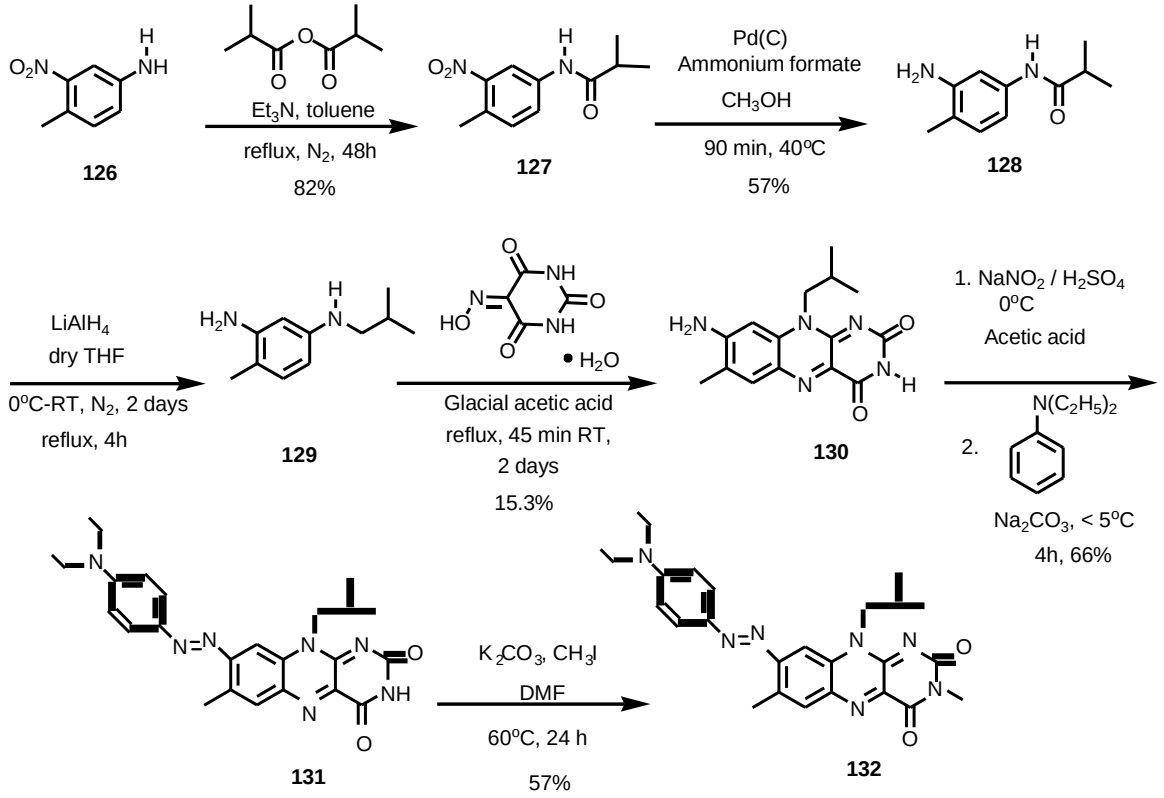

Scheme 34. Synthesis of compound 132.

N-(4-methyl-3-nitrophenyl) isobutyramide (**127**) was synthesised in 82% yield (Scheme 34) from 4-methyl-3-nitroaniline and isobutyric anhydride. The reaction was carried under reflux for two days under a nitrogen atmosphere. The crude product was purified by extraction with DCM. Then, the nitro group on the phenyl ring, was reduced to an amine using palladium on carbon in the presence of ammonium formate in methanol to afford compound **128** in 57% yield. By means of lithium aluminium hydride in dry THF, the carbonyl group was reduced to give **129**. The obtained product was not purified further as it rapidly underwent decomposition. Compound **129** was treated with violuric acid monohydrate in glacial acetic acid to produce compound **130** in 15% yield (Scheme 36).

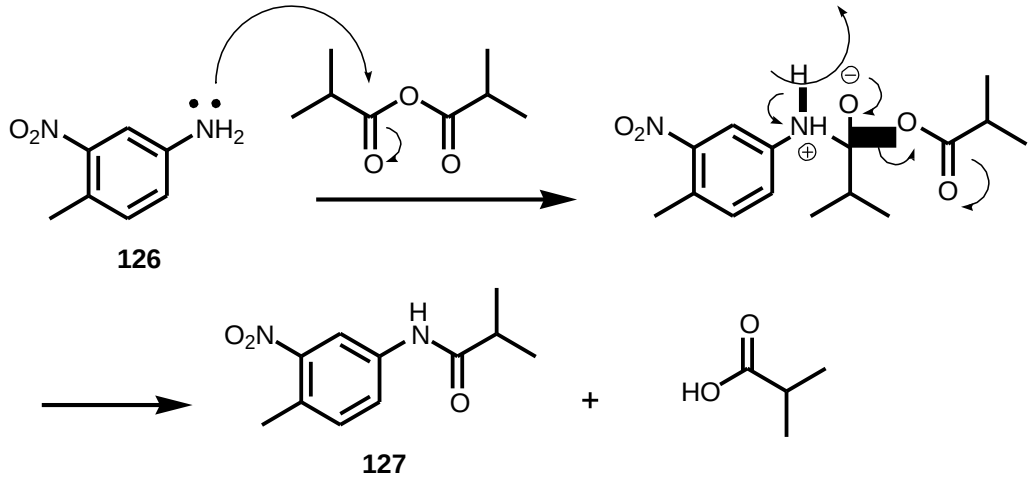

Scheme 35. Mechanism of formation of compound 127.

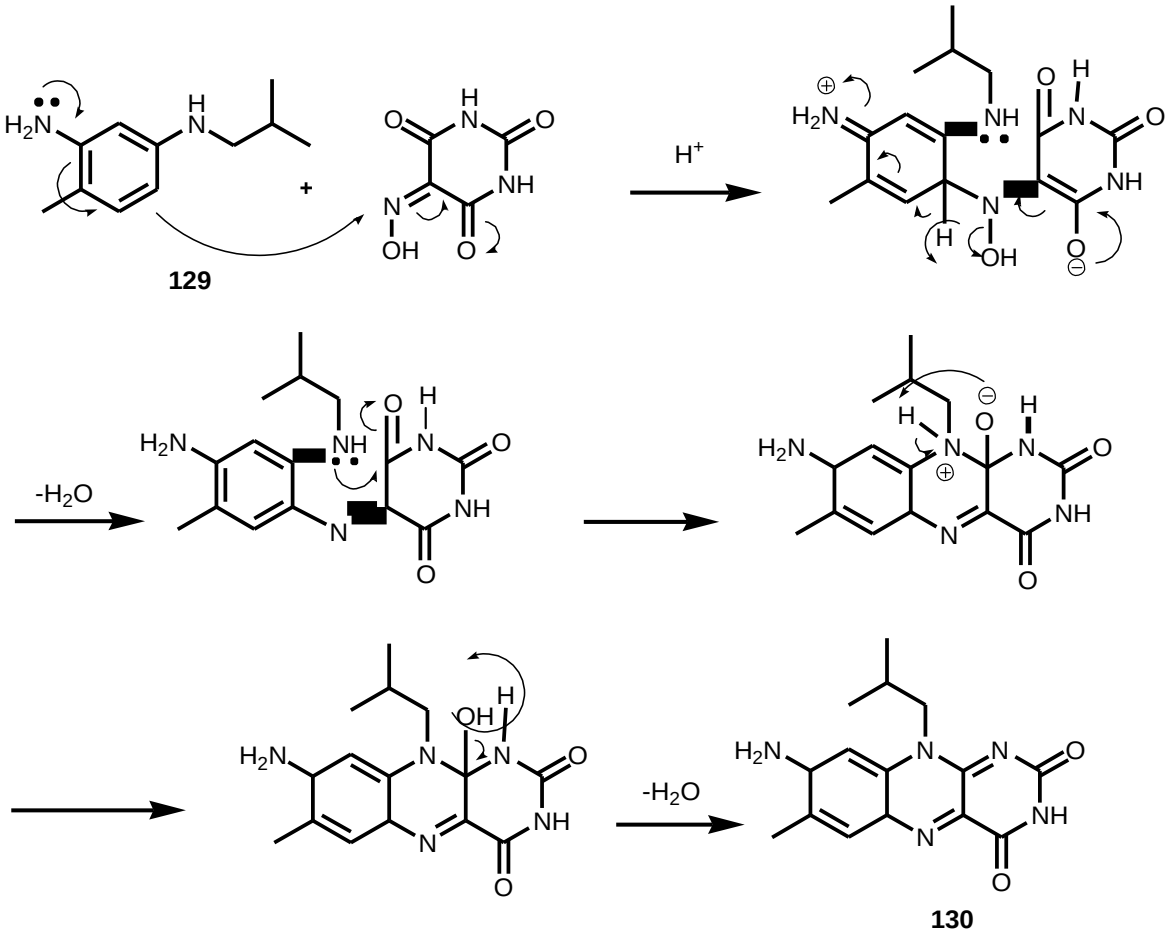

Scheme 36. Mechanism of formation of compound 130.

Compound **131** was synthesized *via* two steps starting from an aniline functionalized flavin (**130**). The first step has included preparation of diazonium salt which is generated from forming nitrous acid from sodium nitrite and conc. sulphuric acid. This was treated with the aniline functionalized flavin **130** which was dissolved in glacial acetic acid. The addition was carried out dropwise at 0^{o}C under stirring and was accompanied by a colour

change from colourless to red and finally yellow. Due to instability of diazonium salts and because of its tendency to lose the $-N^{+}\equiv N$ group as N_2 gas, the diazonium compound was not isolated and used immediately for the next step. The second step involved an azo coupling reaction. The addition of the aniline was undertaken dropwise and the colour instantly changed to blue. Purification was carried out via recrystalization to yield **131** in 66% as a blue solid (Scheme 37).

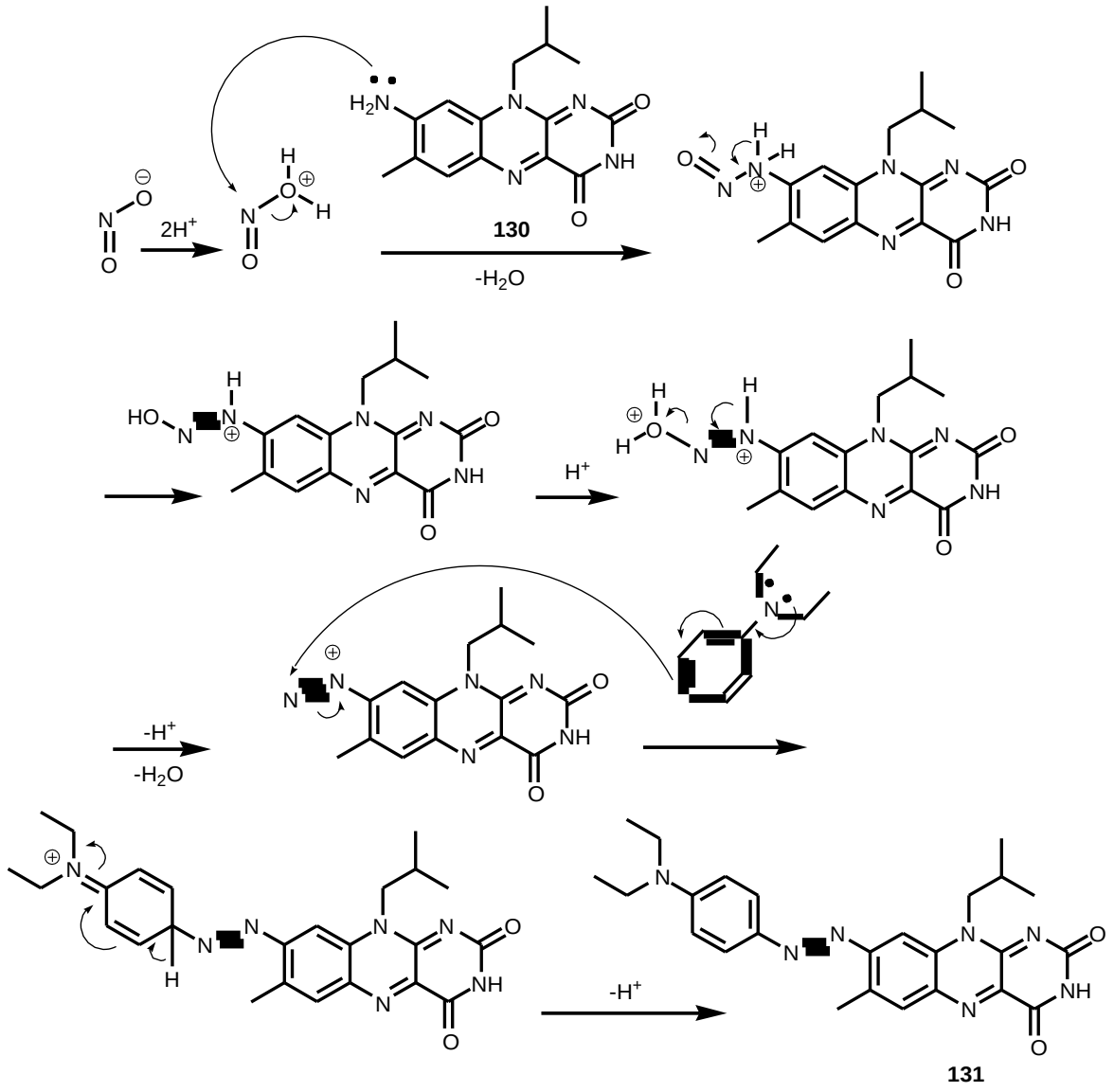

Scheme 37. Mechanism of formation of compound 131.

Finally, methylation was carried out on N3 of the flavin moiety by reacting compound **131** with methyl iodide in DMF and in the presence of potassium carbonate. The reaction was heated to 60^{o}C and left over night. The crude product was purified with flash chromatography to yield compound **132** in 57%.

5.4. Results and Discussion

5.4.1. Push–pull azobenzene

It has been reported that the incorporation of azobenzene derivative, 4-nitro-4`-(dimethyl amino)azobenzene, into a push-pull system usually furnishes systems with short fluorescent lifetimes and large solvatochromic charge transfer bands.[222,223] The straight conjugation of this derivative with flavin ring generates D–π–A push–pull system **131.**[224-226] The colorimetric response of this compound has been studied in different solvents. This solvatochromic system has the ability to act as environmental indicator as it changes colour as the solvent is changed. This mainly arises due to dipole–dipole and the intermolecular solute–solvent interactions. Also, a previous study has reported a strong absorption in the visible region at $\lambda=_{max}$ ~552 nm for compound **131** in toluene exhibiting a purple colour due to an intramolecular charge transfer (ICT).[221]

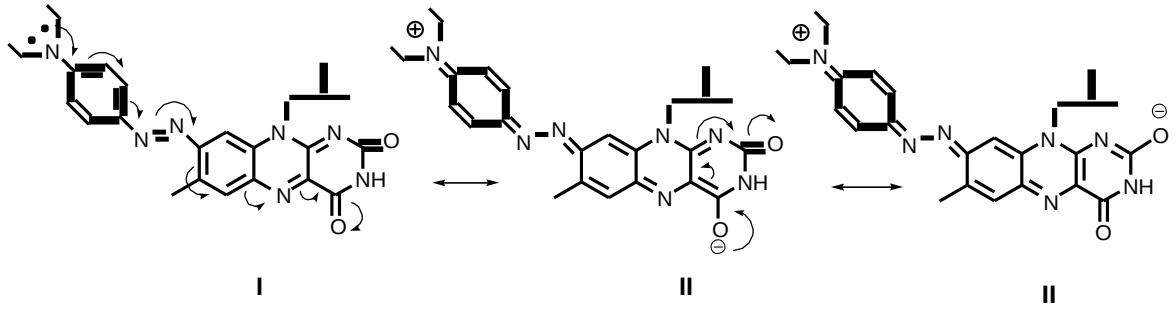

Figure 109. Resonance structures of compound 131 push-pull system: neutral (I) and zwitterionic (II) resonance form.[221]

The push–pull character of compound **131** was estimated from its solvatochromic effect. Compound **131** involves both a neutral resonance form (I) and a zwitterionic resonance form (II) which reveals a large charge separation (Figure 109). By means of combining these resonance contributions, a strong push–pull electronic character would expect for compound (**131**). On the other hand, variety solvents play a considerable role in stabilizing the disparate resonance forms. For instance, more polar solvents gave rise to a range of bathochromic shifts in intramolecular charge transition ICT and π–π* transitions, indicating that an additional solute–solvent interaction acted as a mechanism to stabilize compound **131**. Whereas, less polar solvents and hydrogen-bond accepting solvents destabilized the material by shifting the intramolecular charge transition ICT to a shorter wavelength.[221]

Both compound **131** and compound 1**32** were similarly solvatochromic and displayed similar push–pull behaviour in their UV-Vis spectra. This result signified that efficient hydrogen bonding between hydrogen-bond donating solvents and the negatively charged oxygen in the zwitterionic form was the main contribution to the stabilization of the flavin push–pull system.[221]

5.4.2. Study of the acidity effect of the medium on UV-absorption

Protonation of compound **131** with trifluoroacetic acid (TFA) was carried out in CH_2Cl_2 solution in five different concentrations of TFA. The influences of the protonation on the optical properties were determined via UV-Vis spectroscopy as shown in (Figure 110). The UV-Vis absorption results are illustrated in (Table 9). The absorption spectrum of compound **131** in CH_2Cl_2 ($1x10^{-5}$ M) without (TFA) has shown a strong peak at (λ_{max} = 600 nm) in the visible spectrum due to π–π^* transitions. The molar absorptivity of compound **131** was found to be ε = 72000 mol^{-1} cm^{-1}. As shown in Figure 111, protonation of compound **131** with trifluoroacetic acid (TFA) produces **131H$^+$** and changed the colour of the solution from blue to purple. In fact compound **131** has three possible protonation sites: the terminal NMe_2, the azo β-nitrogen and flavin's carbonyl groups. Terminal NMe_2 is the most likely position to be protonated leading to the formation of **131H$^+$**. However, the absorption maximum of **131H$^+$** (λ_{max} = 588 nm) is considerably blue shifted compared to that of compound **131** ($\Delta\lambda$ = 12 nm), suggesting that, the hypsochromic shift of compound **131H$^+$** is caused by hindering push–pull conjugated system (Me_2N donor–flavin acceptor) which greatly increased the energy of its charge transition (CT). Also, charge localization leads to a lack in contributions from the resonance or stabilized quinonoid forms to the ground state of compound **131**.

Table 9. UV-Vis spectroscopy data of the compound 131 solutions in DCM (1 x 10^{-5} M) with TFA in different concentrations.

Concentrations of the mixed TFA (X x10^{-5} M)	molar absorptivity ε x 10^{+2}	λ_{ons}	λ_{max}	E_{gap}
0	50.00	718	600	1.73
0.3	52.20	750	623	1.66
0.7	60.70	749	615	1.66
1.5	48.90	740	600	1.68
6.7	45.90	740	588	1.68
8.0	77.30	650	579	1.91

ε – (The molar absorptivity) = A(absorbance) / *c*(concentration) *l*(cell length) mol^{-1} cm^{-1}

λ_{ons} – onset of each peak (nm)

λ_{abs} – maximum absorption wavelength of each peak (nm)

E_{gap} – gap energy (ev)

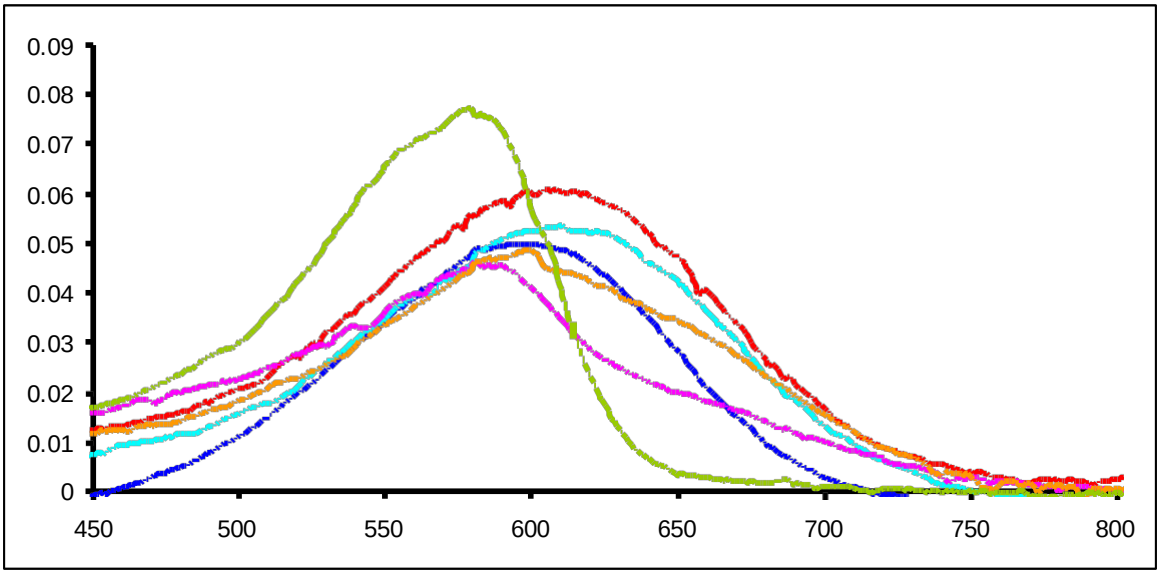

Figure 110 Absorption spectra of compound 131 (1x10^{-5} M) in DCM) mixed with various concentrations of TFA x10^{-5} M: 0% (blue line), 0.3 x10^{-5} **M (turquoise line), 0.7** x10^{-5} **M (red line), 1.5** x10^{-5} **M (orange line), 6.7** x10^{-5} **M (purple line) and 8.0** x10^{-5} **M (green line).**

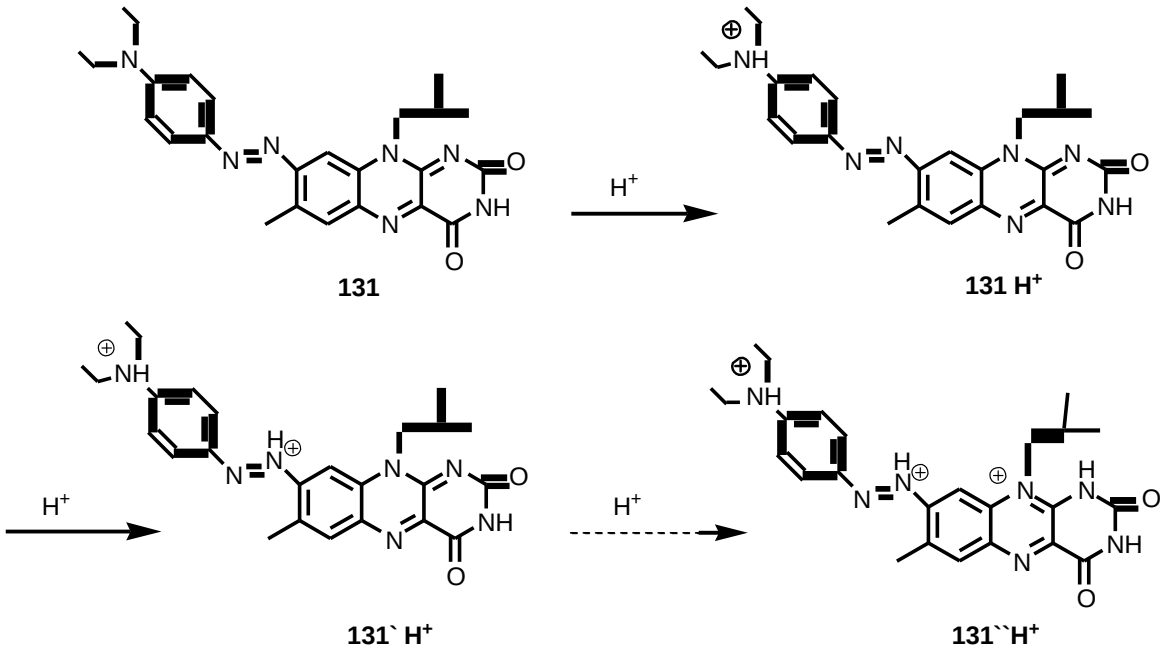

Figure 111. Protonation of compound 131.

Further addition of the TFA to the solution of compound **131H**$^+$ caused a gradual increase in intensity of the absorption band at (λ_{max} = 579 nm). This may be attributed to further protonation of **131H**$^+$ which should occur on the azo β–nitrogen to produce the tautomeric species **132`H**$^+$**,** since the NMe_2 group of **131H**$^+$ would have a lower basicity than the azo nitrogens due to the absence of its lone pair. Apparently, further protonation process would diminish the charge transfer (CT) capability leading to the observed hypsochromic shift. This fact encourages us to suggest no further protonation would take place on the flavin moiety due to the high ionization energy that accompanied with the third protonation. However, because of the close and broad absorption bands of compounds **131**, **131H**$^+$ and **131`H**$^+$**,** we could predict that they would still remain present in the medium and may be indistinguishable from each other (Figure 111).

5.5. Conclusion

In conclusion, we have described the pH dependence and the absorption properties of compound **131** which can be classified as (D–π–A) push–pull system. The results proved that increasing the acidity of the medium shifts π–π* transitions negatively about (20 nm) and changing the colour of the solution from blue to purple. This phenomenon may promote the future development of analogues of compound **131** as pH switchable probes.

CHAPTER 6

SYNTHESIS OF COLLOIDAL MACROCAPSULES

6.1. Introduction

6.1.1. Flavin and diamidopyridine DAP molecular recognition.

Molecular recognition is a term that refers to the coherence of molecules into noncovalent arrays through weak intermolecular forces such as: hydrogen bonding, hydrophobic forces, π–π interactions, metal coordination, van der Waals forces, electrostatic and electromagnetic effects. The size, shape, and chemical functionalities of the complementary units are of fundamental importance in forming host and guest complexes. Hydrogen bonding has found widespread use in host –guest complexes mainly due to their directionality, specificity, and biological relevance.[227]

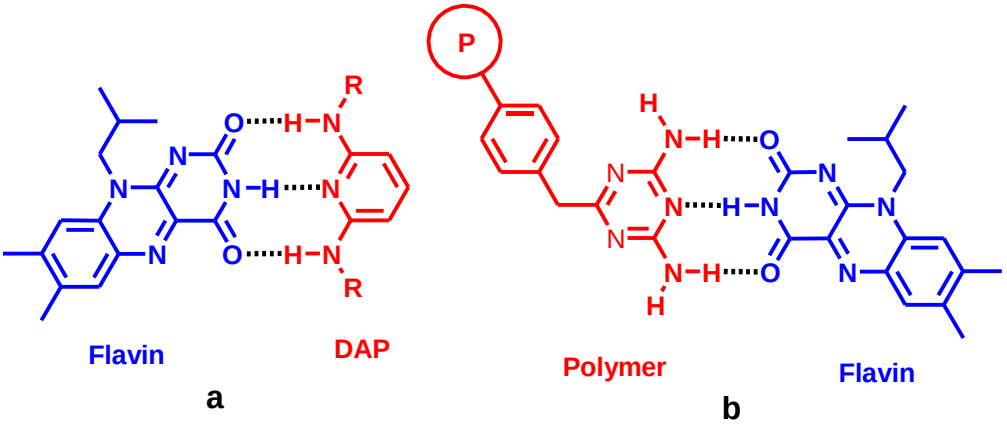

Figure 112. Molecular recognition in of flavin-DAP complexes.[228]

Model systems have been designed to stabilize the electron-rich hydrogen bond sites on the flavin, including O(2) and O(4) through specific hydrogen bond interactions (Figure 112-a). On the other hand, N(3)-methylflavin cannot efficiently create hydrogen bonded complexes with diaminopyridines DAP. [228] It has been shown that the hydrogen bonding interactions between a covalently linked flavin–diamidopyridine DAP unit (e.g. **133** and **134**) have the tendency to stabilise the flavin's radical anion state (Figure 113). [225,229]

Specific recognition can also occur between a flavin and a triazine-functionalized polymer (Figure 112-b).[230] Furthermore, flavin-functionalised self-assembled monolayers (SAMs) have been used as models for probing redox modulation through hydrogen bonding at surfaces [231]. The DAP-flavin binding affinity and the reduction potentials ($E_{1/2}$) for both the DAP-bound and unbound flavins correlates well with the nature of the substituents attached to the flavin core.[138]

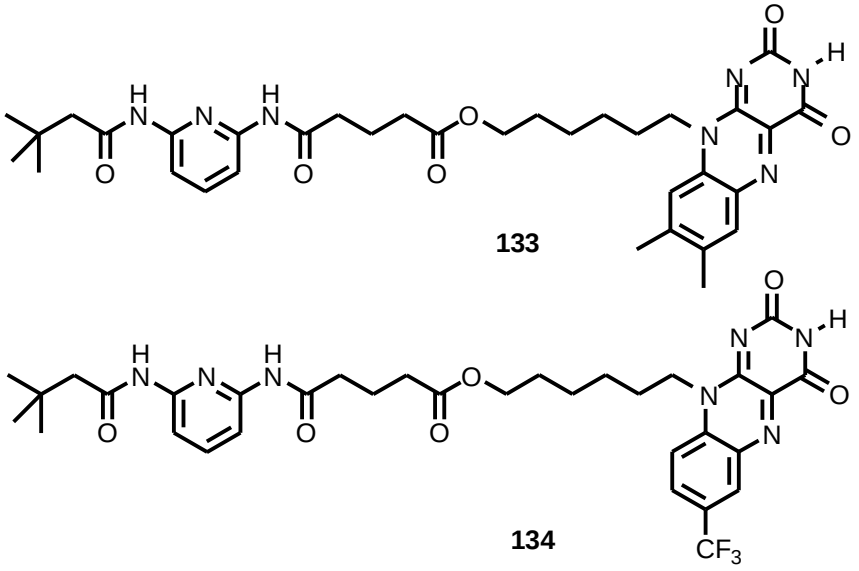

Figure 113. Flavin derivatives with the propensity to form intramolecular hydrogen bonding.[225,229]

Flavin-functionalized polystyrene copolymers (e.g. **135**) revealed reversible, redox-modulated hydrogen bonding interactions with complementary DAP units, giving unique thermal and electrochemical behaviour (Figure 114).[232] In addition, molecular recognition between flavin and diamidopyridine DAP functionalized porphyrin (**136**) systems via hydrogen bonding and π -stacking interactions has been used to modulate the electrochemical behaviour of flavin (Figure 115).[233]

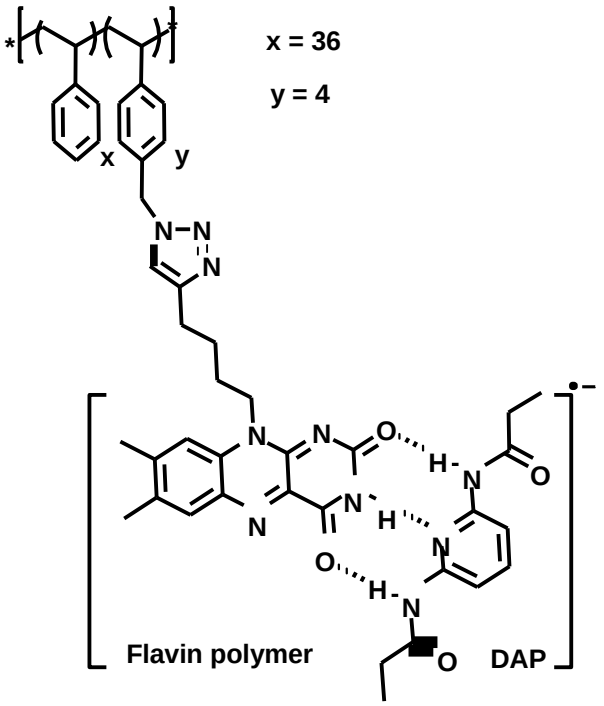

135

Figure 114. Molecular recognition between a Flavin polymer and DAP. [232]

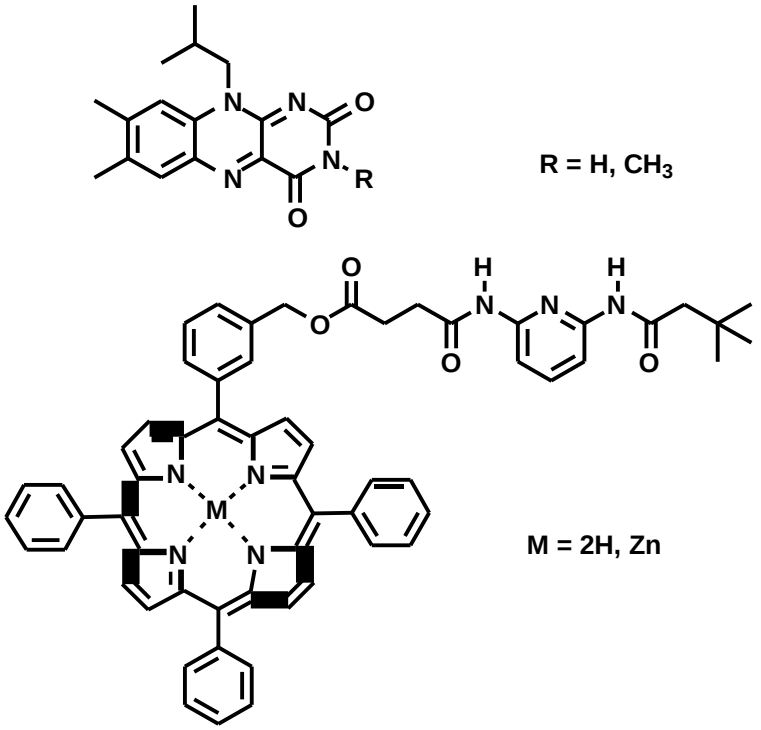

136

Figure 115. Molecular recognition between flavin and diamidopyridine DAP functionalized porphyrin systems. [233]

Hydrogen bonding is an important feature in biological molecular recognition, providing an impetus for the development of artificial recognition systems. Hydrogen bonding donating and accepting sites should be designed appropriately in order to achieve highly selective recognition within the receptor molecule. Unlike biological molecular recognition, the artificial systems are usually effective only in non-aqueous solvents. Addition of water inhibits binding efficiency between host-guest systems in nonaqueous solvents. Because most biological molecules are water-soluble and their molecular recognition is effective in aqueous solvents, molecular design of the artificial receptors requires a significant enhancement of host-guest stability (Figure 116).[234] Host–guest complexes have been modified to be effective in aqueous media by manipulation of both the location and charge of hydrogen-bonding sites to convert synthetic receptors that function only in nonpolar solvents into more polar and protic solvents (Figure 117).[235]

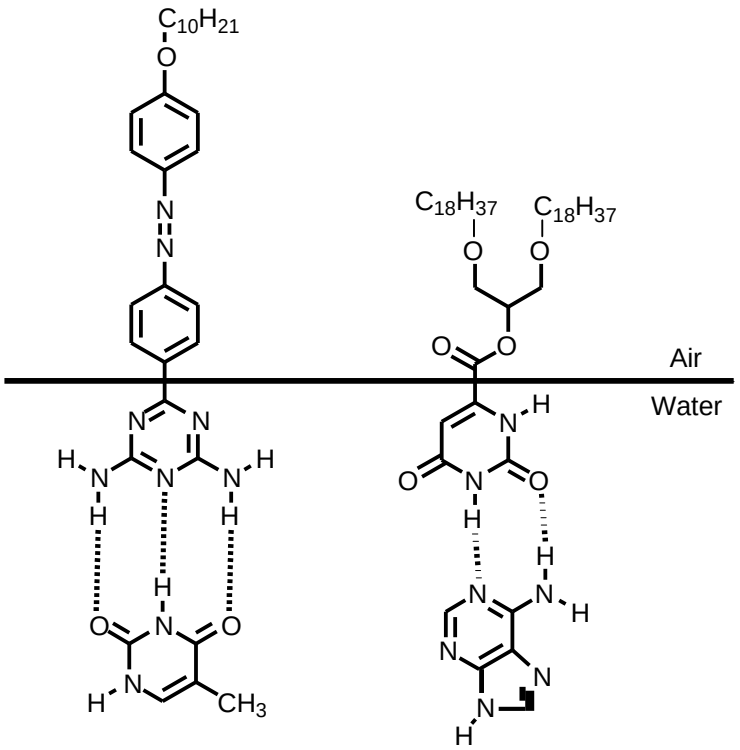

Figure 116. Recognition of Thymine and Adenine nucleic acids bases at the air-water interface.[234]

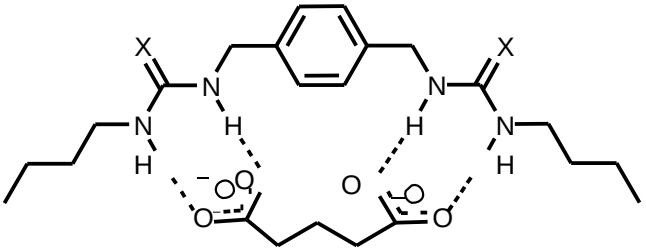

X= O or S

139

Figure 117. Hydrogen bonding receptors.[235]

6.1.2. Micelles

Micelles afford microenvironments that allow hydrogen bonding to arise between small molecules in aqueous solution (Figure 118). The pioneering work in micelles was carried out at the beginning of the twentieth century. Micelles are usually fabricated from charged particles created by an aggregate of surfactant molecules dispersed in colloidal electrolyte solutions. The typical micelle in aqueous solution forms an aggregation of the hydrophilic (head) in surrounding aqueous solvent, seizing the hydrophobic tail in the micelle centre. In polar solvents such as water, the hydrophilic heads of surfactant molecules are always surrounded by the solvent molecules that create a cage of molecules connected by hydrogen bonds. In contrast, the hydrophobic tails assemble into an oil-like core inside the micelle.

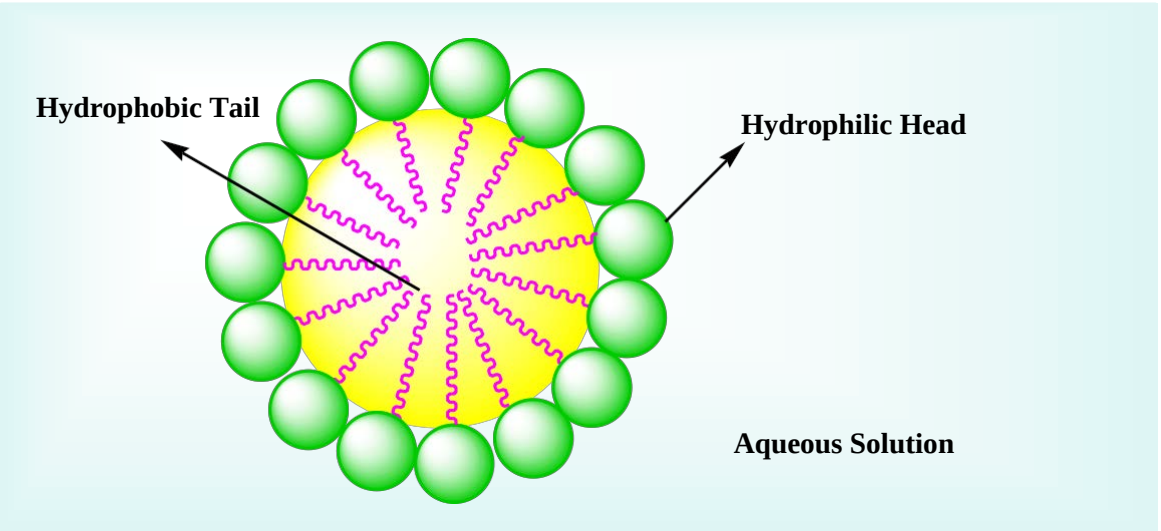

Figure 118. Structure of a typical micelle in aqueous solution

The idea of building capsules as reaction chambers has been a target for researchers over the last 50 years. They have found that simple molecules exhibit unique behaviour through molecular assemblies (Figure 119). Interactions such as van der Waals and hydrogen bonds between the exterior surface of the guest and the interior surface of the host, allow guest systems to be included into the interior of the micelle. Guests that fit the host's cavity in size and shape without leaving empty space are preferred. The presence of more than one solvent in the capsules displays special entropic effects.[236]

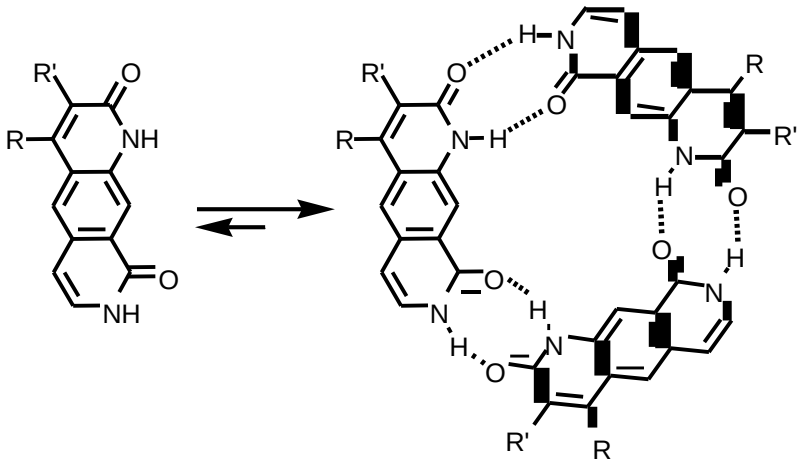

Figure 119. Self-complementary hydrogen bonding sites lead to trimers or oligomers.[236]

Aqueous host-guest systems have been designed by incorporating hydrogen-bonding groups into micelles. Host-guest systems have been fabricated within the interior of sodium dodecyl sulfate (SDS) micelles. For example, thymine and adenine functionalised ammonium amphiphiles have been shown hydrogen bond interactions within the interior of the micelle (Figure 120). [237,238]

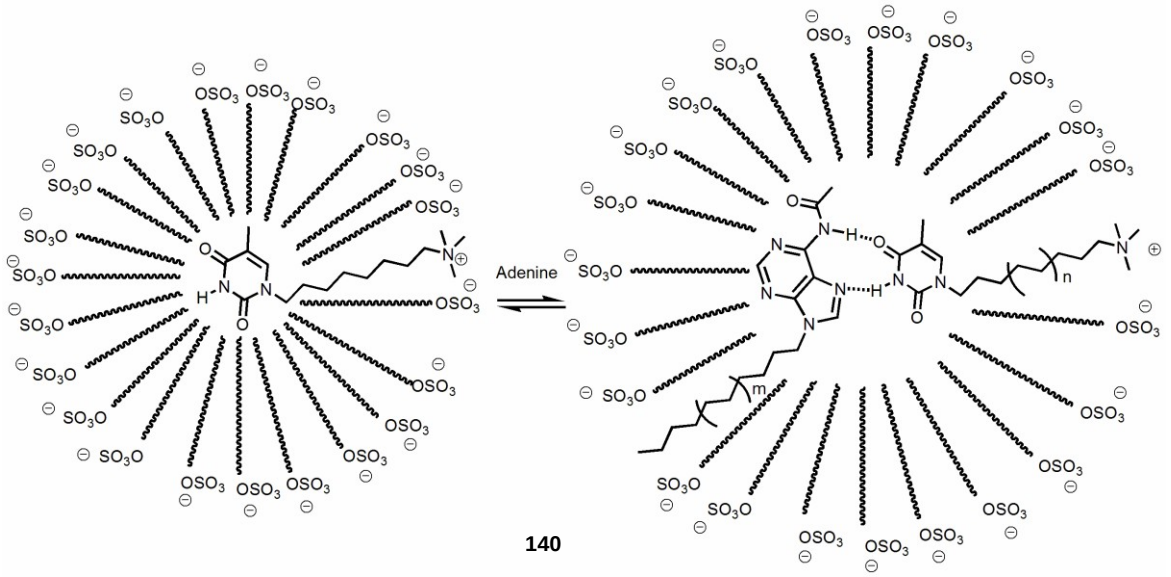

Figure 120. Hydrogen bonding within a SDS micelle. [237,238]

The effectiveness of hydrogen bonding has been improved in water to create hydrophobic environment in the surrounding area of the host–guest system. A hydrophobic porphyrin-based receptor which has a multipoint recognition in organic solvents has been customized to be soluble in water by incorporation into sodium dodecylsulphate (SDS) micelles.

Micellar recognition was shown to be effective when both hydrogen bonding and solvophobic forces act together. The addition of the organic co-solvents such as CH_2Cl_2 can tune the receptor solvation inside micelles by reducing solvophobic association and restoring some of the hydrogen bonding energy (Figure 121).[239]

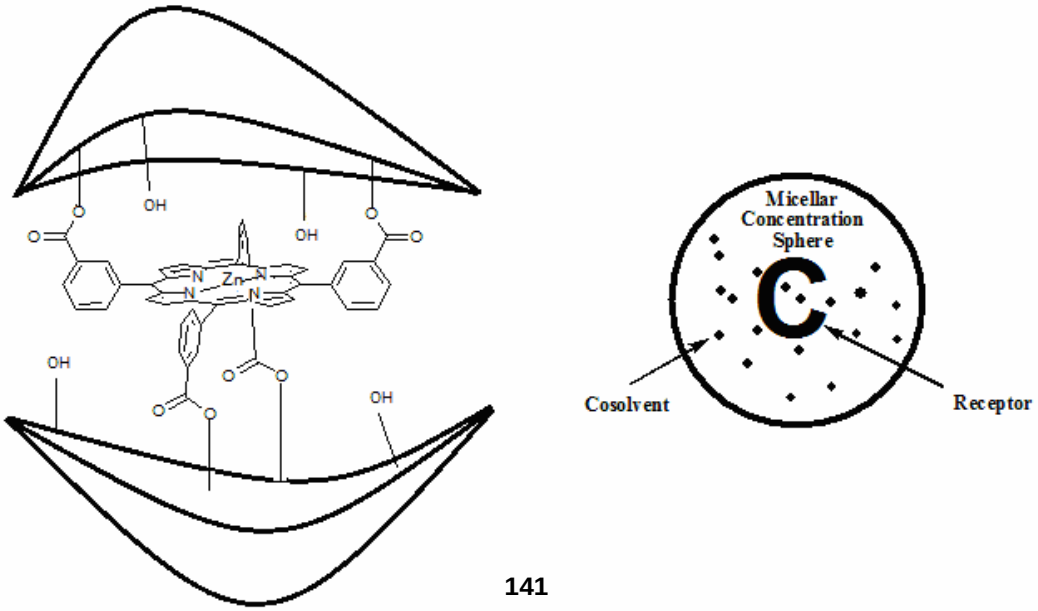

141

Figure 121. Porphyrin-based receptor in (SDS) micelles.[239]

It has been found that the oil-water emulsions present a distinctive microenvironment[240] due to the extended membrane between the two phases and can offer appropriate environment to localize the host-guest molecules. Creating a stable emulsion is essential to encapsulate the host molecule, and this can be achieved in polymeric microcapsules, vesicles and colloidal microcapsules due to their stability. Researches on polymeric microcapsules have received much attention during the last few years. Polymersomes of amphiphilic polystyrene-poly(acrylic acid) with the periphery covered with azide groups have shown the ability for further functionalization at their periphery without disrupting the aggregate morphology (Figure 122).[241] In addition, intelligent pH-switchable nanovesicles based on amphiphilic copolymer membranes[242] and a polymersome based nanoreactor for selectively fabricating enzymes have also been described.[243]

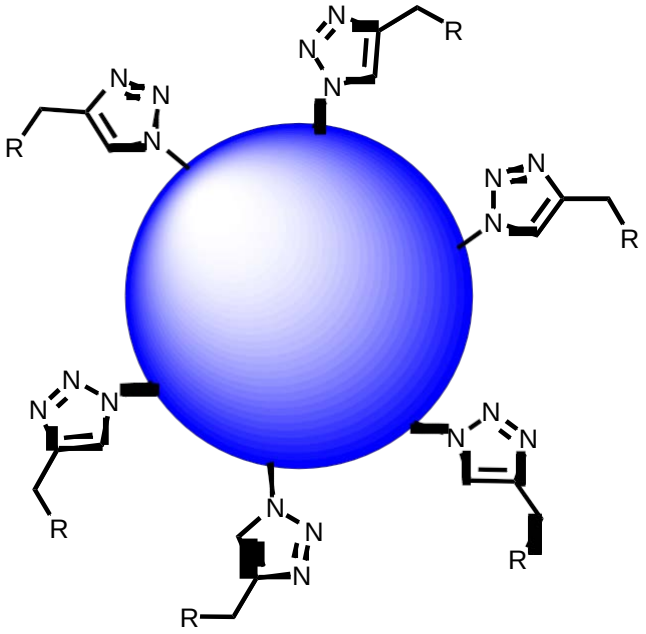

142

Figure 122. Exterior of polymersomes.[241]

The cross-linked polymerization of hydrophobic methacrylate monomers in the interior of the surfactant bilayer of dimethyldioctadecylammonium chloride vesicles have been described generating a quasi-two-dimensional polymer system.[244] Moreover, an amphiphilic triblock copolymer (poly(ethylene oxide)–poly(dimethyl siloxane)–poly(methyl oxazoline)) has been prepared to create vesicles with asymmetric membranes in aqueous solvents (Figure 123).[245]

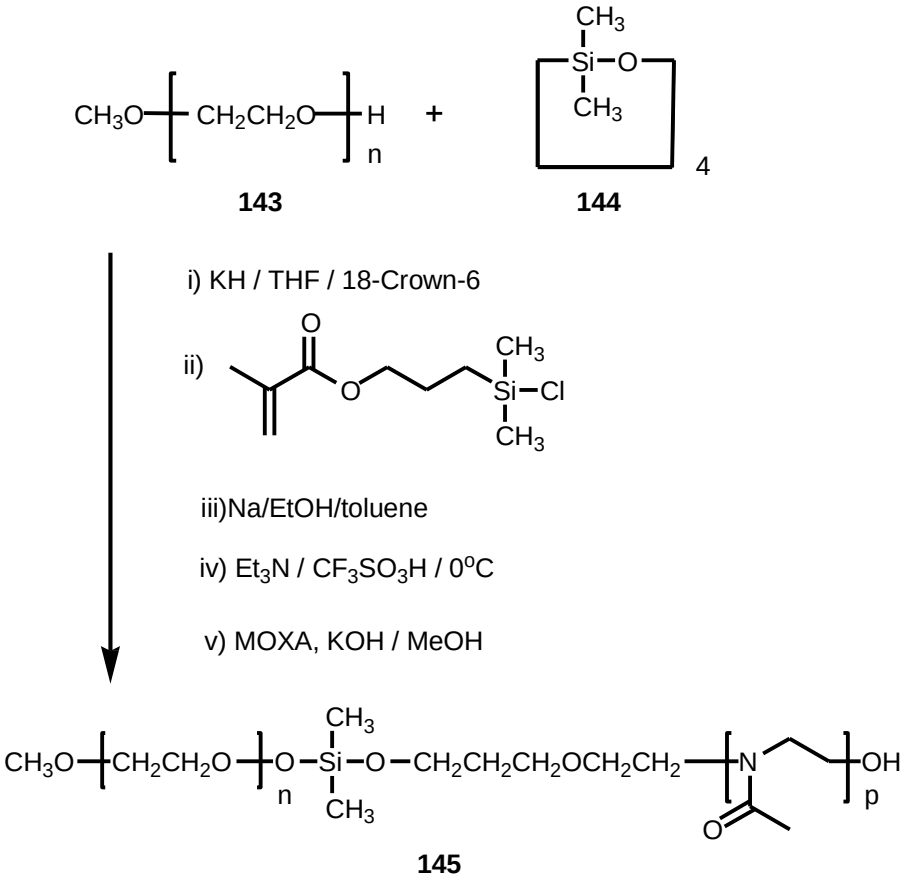

Figure 123. Synthesis of an amphiphilic triblock copolymer. [245]

The steady expansion of $BaSO_4$ crystals grown at liquid-liquid interface has been shown to be inhibited by fatty acid molecules. The crystals spontaneously organize themselves into highly linear superstructures over large length-scales.[246] The potential of engaging the water/oil interface as a platform for self-assembly of nanoparticles has been described. Capping nanoparticles with terminal ligands, determined the self-assembly of hydrophilic and hydrophobic nanoparticles of different sizes and chemical compositions at the water/oil interface, forming homogeneous and heterogeneous thin films. The interfacially active nanoparticles may be engaged to stabilize water-in-oil or oil-in-water droplets, producing the microcapsules whose shells are composed of randomly close packed nanoparticles[247]. Liquid–liquid interfacial self-assembly of nanoparticles has been also discussed and was found that the assembly can be manipulated by tuning the particle size or surface properties.[248]

Fabrication of highly stable colloidal shells and membranes by cross-linking nanoparticle self-assemblies at the liquid-liquid interface using coordination chemistry has been described. Terpyridine thiol functionalized FePt nanoparticles were self-assembled at water-toluene interfaces and cross-linked through complexation of the terpyridine with Fe(II) metal ions. These systems have the ability to be manipulated using external magnetic fields, providing a suitable means of localizing these materials (Figure 124, Figure 125).[249]

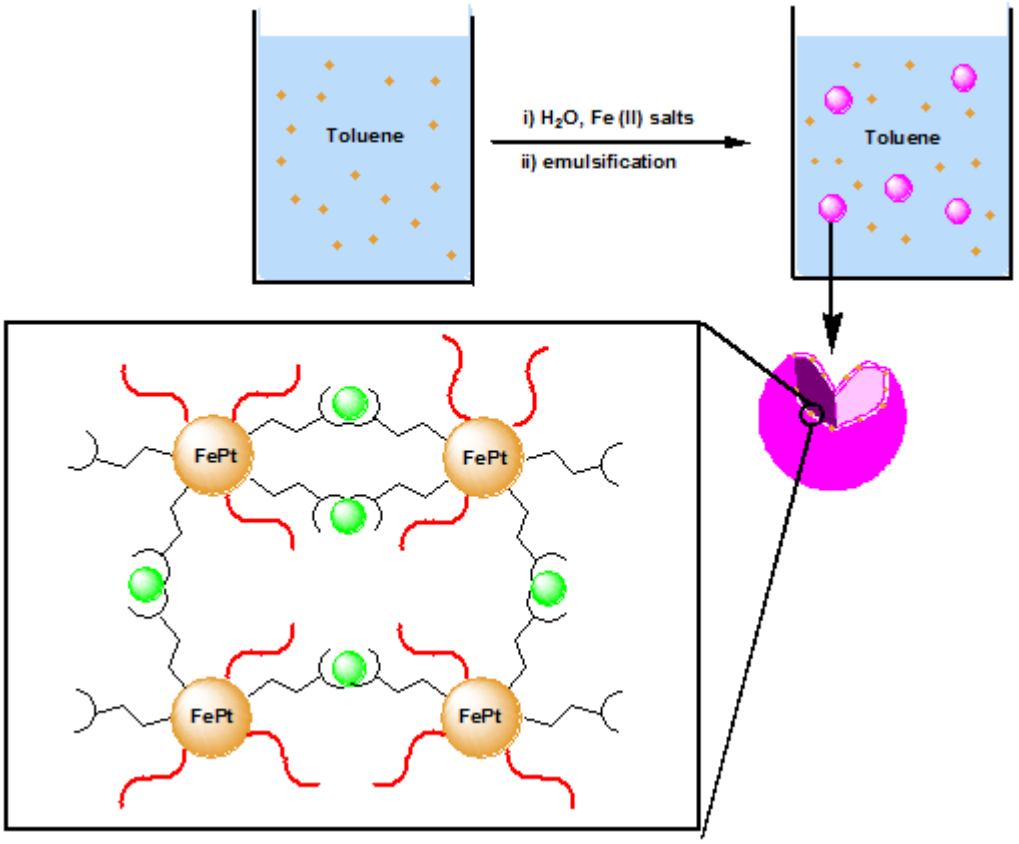

Figure 124. FePt nanoparticles colloidal shells formation at a water-toluene interface. [249]

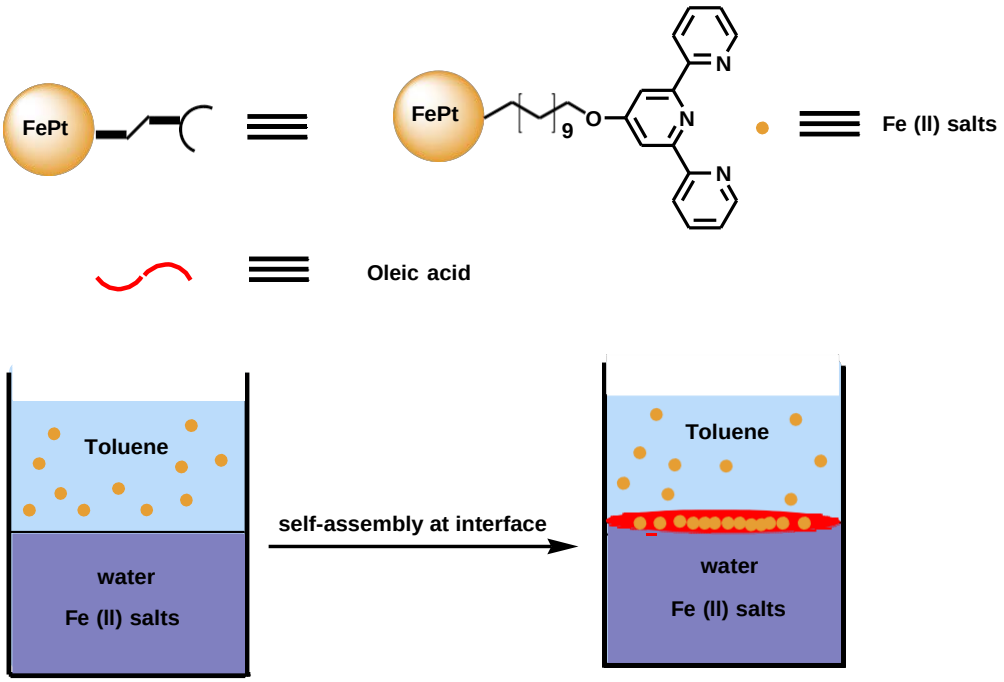

Figure 125. FePt nanoparticles membrane formation at water toluene.[249]

A pseudorotaxane fabricated from an electron rich 1,5-dialkyloxynaphthalene unit and cyclobis(paraquat-p-phenylene) ($CBPQT^{4+}$) has been shown to undergo decomplexation upon the addition of SDS. This was demonstrated by the simultaneous precipitation of ($CBPQT^{4+}$) by anion exchange reaction and the encapsulation of the naphthalene unit by incorporation into a SDS based micelle (Figure 126).[250]

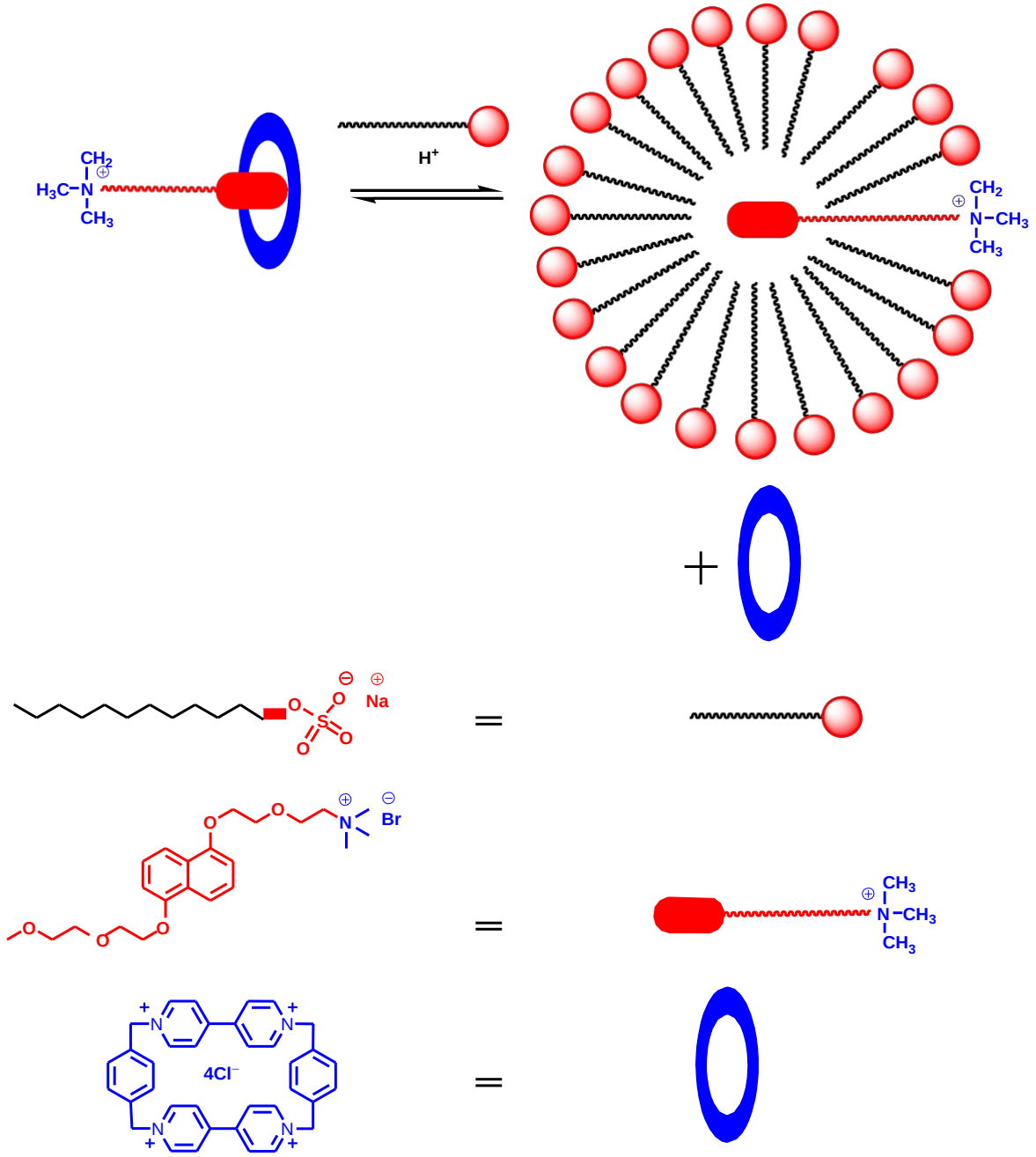

Figure 126. SDS driven decomplexation.[250]

6.2. The aim of the project

The aim of this project is to synthesise cationic alkylammonium derivatives in order to promote micelle formation with an anionic surfactant molecule such as sodium dodecyl sulfate (SDS). The attractive electrostatic interactions of cationic alkylammonium derivatives would permit the self-assembly of mixed micelles with SDS (Figure 127).[238,250,251] Through careful design of the ammonium derivative, it was hoped that molecular recognition events could occur within the interior of the micelle using DAP and flavin host-guest moieties.

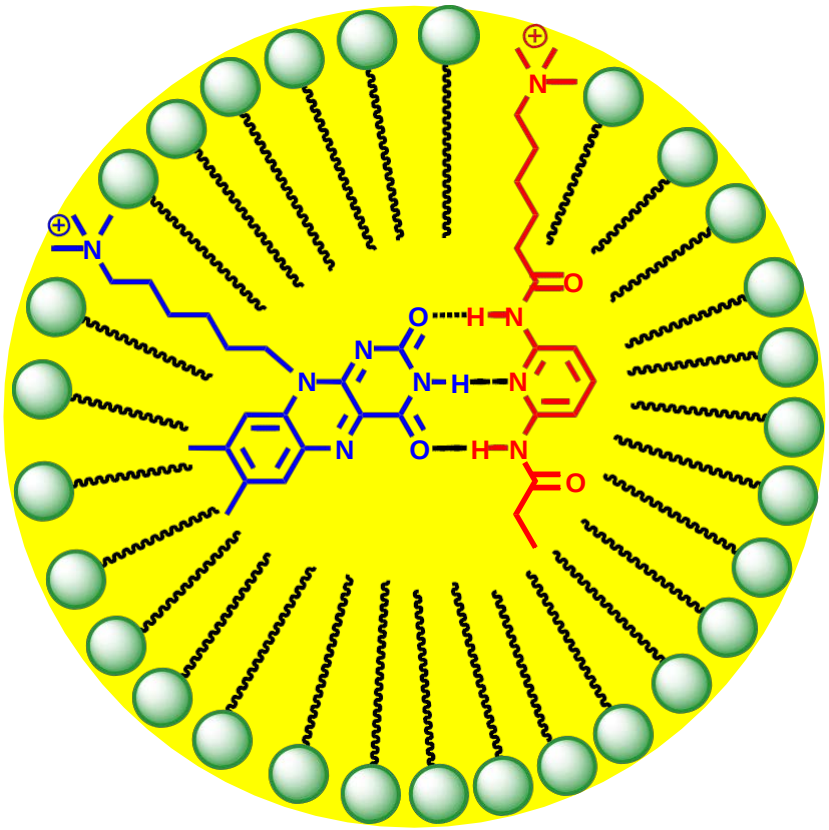

Figure 127. SDS / cationic alkylammonium derivitive based micelle.

6.3. Synthesis of the cationic ammonium derivitives

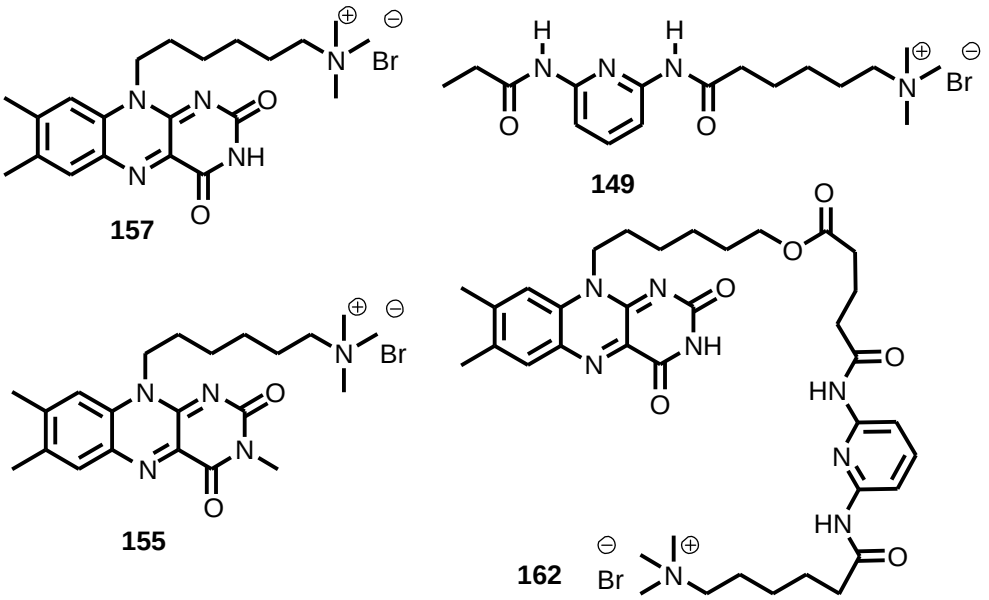

Figure 128. Cationic ammonium derivatives.

The synthetic targets for this part of my research are shown in (Figure 128). The synthesis of 6-(*N*-(6-(propionamido)pyridine-2-yl)-hexanamide) trimethyl ammonium bromide (**149**)[252] is illustrated in (Scheme 38). Firstly 2,6-diamino pyridine (**146**) was converted to *N*-(6-aminopyridin-2-yl)propionamide (**147**)[253] using a stoichiometric amount of propionyl chloride in the presence of triethylamine. Compound **147** was afforded in 26% yield. The remaining amino group in compound **147** underwent nucleophilic substitution reaction with 6-bromohexanoyl chloride[254] to produce 6-bromo-*N*-(6-(propionamido)pyridine-2-yl)hexanamide (**148**) in 61% yield. Triethylamine was used to neutralize the hydrochloric acid that is produced during the process. 6-(*N*-(6-(Propionamido)pyridine-2-yl)-hexanamide) trimethyl ammonium bromide (**149**) was synthesised from compound **148** [255]using trimethylamine in methanol to replace the terminal bromide and yield compound **149** in 83%.

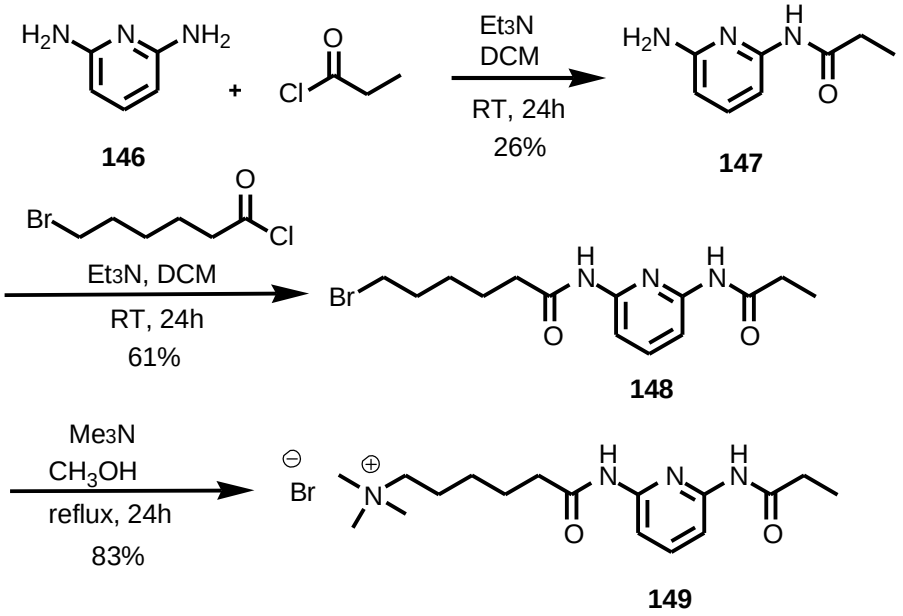

Scheme 38. Synthesis of compound 149.

Compound **155** was synthesized as illustrated in Scheme 39. Flavin **152** was a key intermediate for the syntheses of compound **155**. Several attempts have been undertaken to synthesise flavin **152** efficiently. Firstly, the literature methodology was followed[256] starting from 6-chlorouracil. However, the obtained yield was very low (1%). Thus new methods were attempted, the most successful being the one illustrated in Scheme 39. 10-(6-Hydroxy-hexyl)-7,8-dimethyl isoalloxazine (**152**) was prepared over two steps. The first step involved alkylation of 4,5-dimethylbenzene-1,2-diamine using 6-bromo-1-hexanol in THF. The reaction was catalyzed by NaI and an excess of triethylamine was used to neutralize the HCl that formed during the reaction. The second step included the reaction with alloxan monohydrate in acetic acid in presence of boric anhydride. The yield over two steps was 35%.

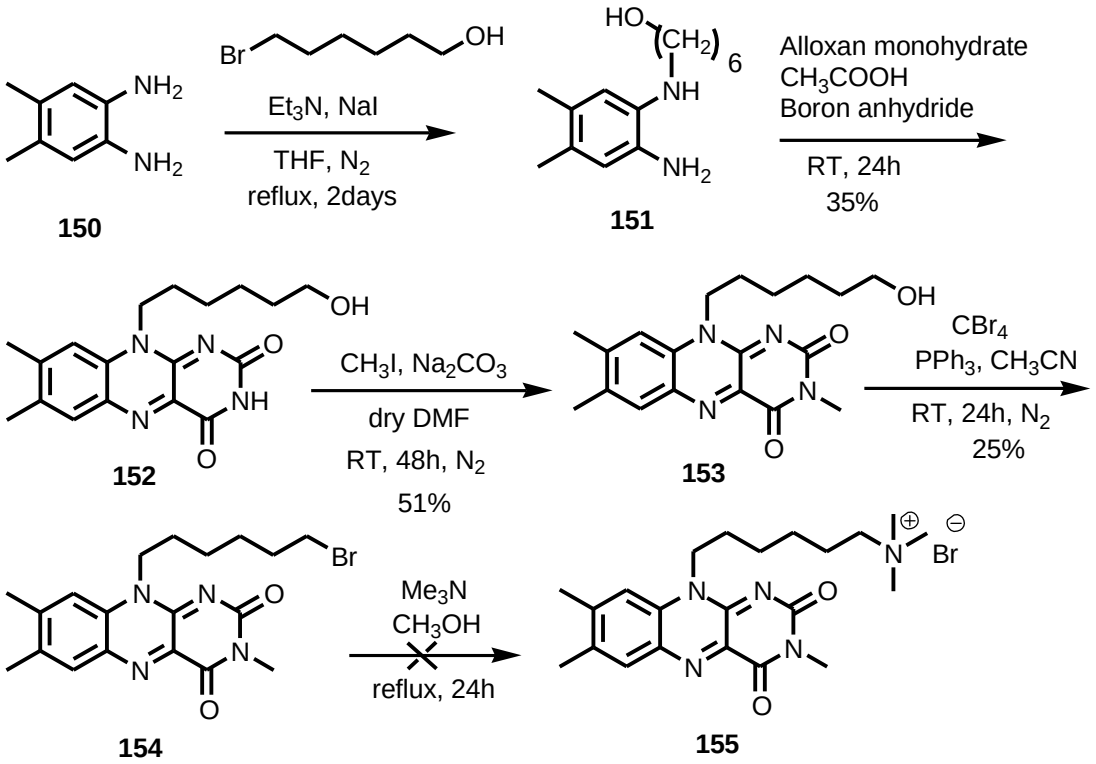

Scheme 39. Synthesis of compound 155.

Flavin **152** was then methylated on (*N*3) using methyl iodide in presence of sodium carbonate to yield **153** in 51% yield. The Appel reaction was applied to convert the alcohol to bromide. The reaction involved the addition of carbon tetrabromide and the presence of a catalytic quantity of triphenylphosphine to give **154** in 25% yield. The SN_2 mechanism is described in Scheme 40. The final step included the preparation of the ammonium salt **155** from the bromide **154**. Unfortunately, the reaction was unsuccesful.

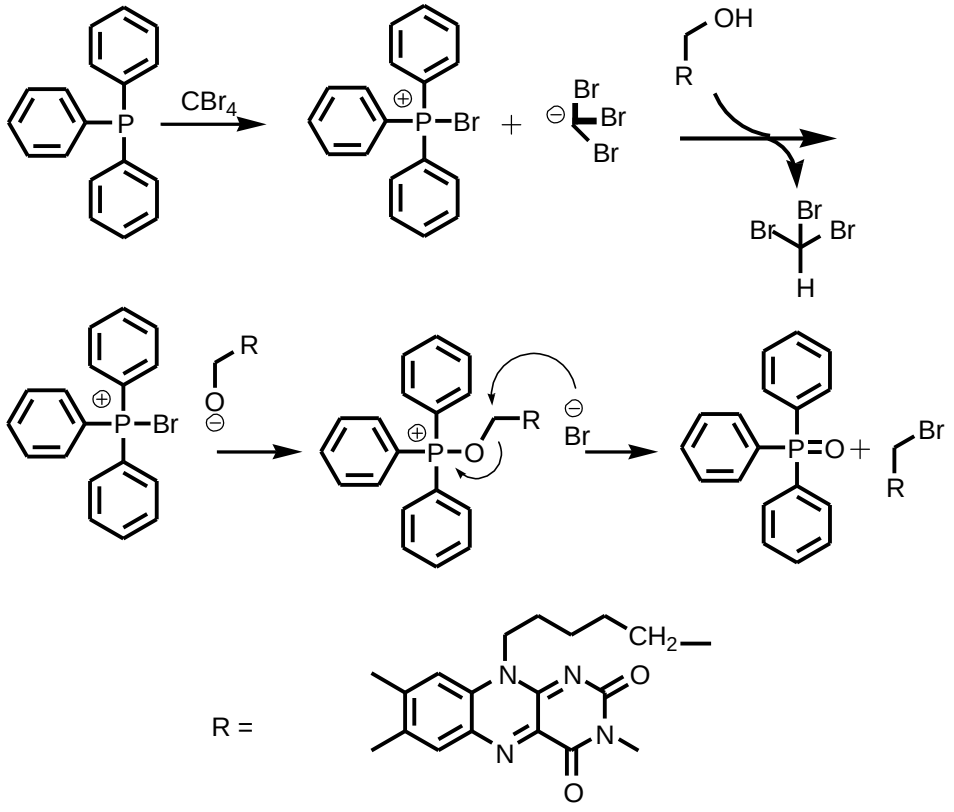

Scheme 40. The mechanisim of Appel reaction to convert the alcohol to bromide.

Consequantly, flavin **152** was then converted to the ammonium salt **157** without methylating the *N*3 position. Firstly, the Appel reaction was applied to convert the alcohol to bromide by the addition of carbon tetrabromide and the presence of a catalytic quantity of triphenylphosphine to give **156** in 60% yield. The final step for preparing the ammonium salt **157** from the bromide **156** was carried out by the addition of trimethyl amine in methanol and refluxing it for 24 hours. The purification was carried out by precipitation into ethyl acetate to yield 75% of pure ammonium salt **157** (Scheme 41).

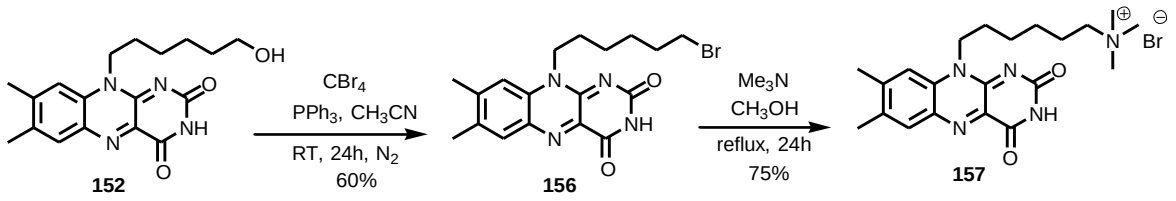

Scheme 41. Synthesis of compound 157.

Compound **162** was the last target in this project (Scheme 42). The starting material 2,6-diamino pyridine **146** was converted to *N*-(6-aminopyridin-2-yl)-6-bromohexanamide (**158**) using a stoichiometric amount of bromohexonyl chloride in the presence of triethylamine. The reaction was carried out in dichloromethane and an excess of triethylamine which was used to neutralize the hydrochloric acid that is formed during the reaction. Compound **158** was produced in 20% yield. 4-(6-(6-Bromohexanamido)pyridin-2-ylcarbamoyl)butanoic acid (**159**) was synthesized by the nucleophilic substitution reaction between the amino group of compound **158** and the acyl carbon of glutaric anhydride produced the required product (**159**). Product **159** was obtained in 53% yield.

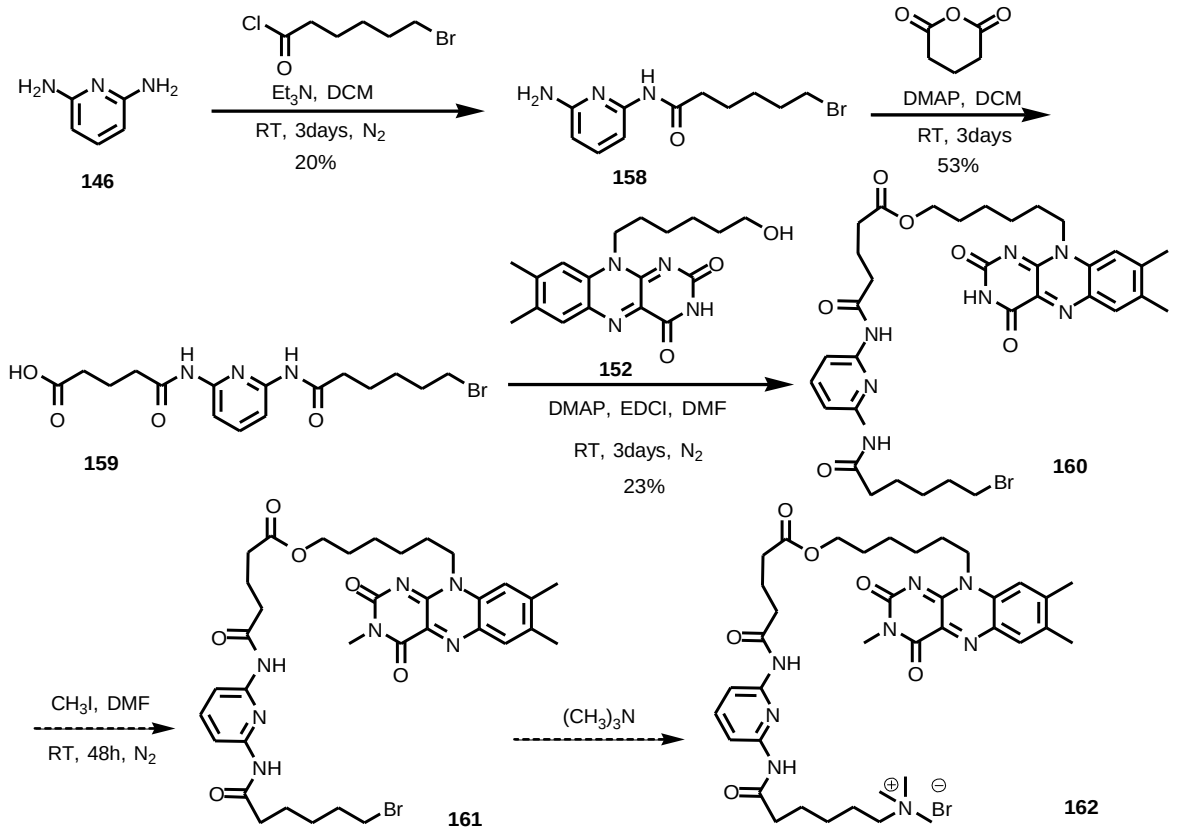

Scheme 42. Synthesis of compound 162.

The EDCI / DMAP catalyzed esterification of compound **159** and **152** yielded compound **160** in 23% yield. The proposed mechanism for EDCI promoted ester synthesis is shown in (Scheme 43). Carbodiimide group in EDCI promotes esterification by reacting with the carbonyl group of the acid and activating it towards nucleophilic substitution by the alcohol (Scheme 43). The urea that formed can be easily removed because of its water solubility. An attempt to methylate compound **160** on *N*3 was carried on by using methyl iodide but the reaction did not work. Carrying out the methylation on flavin **152** before attaching it to compound **160** would probably provide a better way of forming compound **162**.

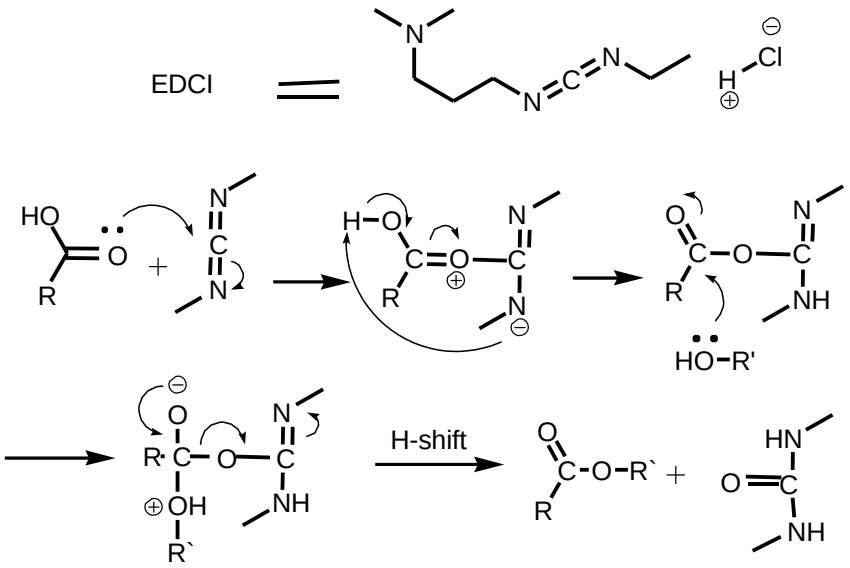

Scheme 43. Proposed mechanism for EDCI catalysed esterfication.

6.4. Results and discussion

Compound **149** was sent to the Department of Chemistry/ University of Massachusetts Amherst to examine the host–guest chemistry. A system of colloidal microcapsules was fabricated of orthogonally functionalized FePt nanoparticles (NPs) which self-assembled at the oil–water interface and crosslinked via dithiocarbamate (DTC) chemistry [257-259] then a flavin polymer (host) was encapsulated inside the microcapsules. The host–guest chemistry was performed by the introduction of the amphiphile diaminopyridine (DAP) (guest) to obtain three-point hydrogen bonding interaction at the interface.[232] Host–guest interactions at the interface were then monitored by fluorescence quenching of the flavin fluorophore.[229]

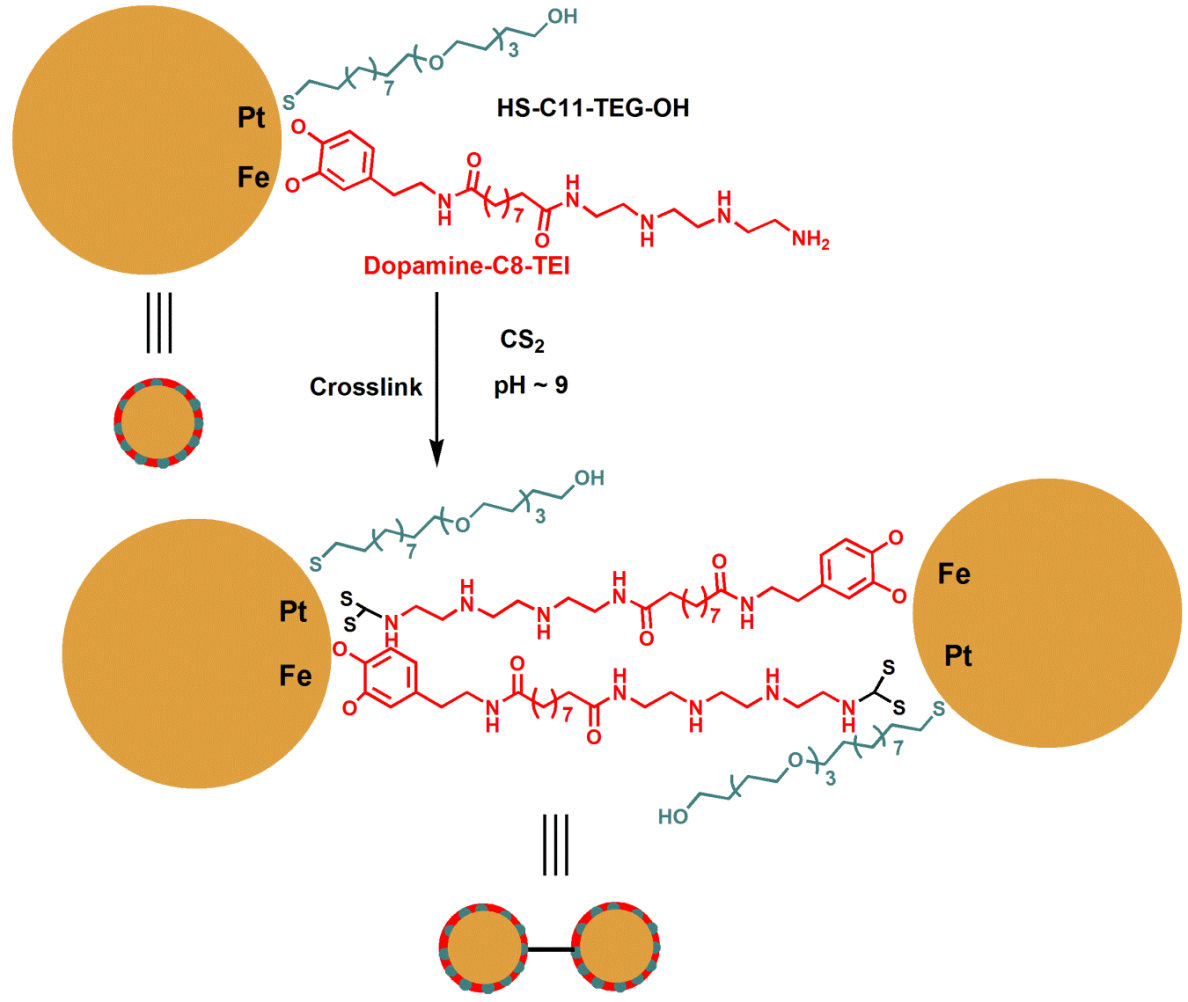

Figure 129. Orthogonal functionalization of FePt NPs. And the mechanism of cross-linking of FePt NPs via DTC chemistry to fabricate microcapsule.[252]

6.4.1. Formation of colloidal microcapsules

Colloidal microcapsules were prepared from triethyleneimine (TEI) functionalized FePt nanoparticles (NPs) (Figure 129). Firstly, NPs of oleic acid and oleyl amine coated by FePt (~7 nm) were created.[260-262] These NPs were modified by place exchange reaction with HS–C11–TEG–OH and dopamine–C8–TEI ligands, respectively. The NPs were dissolved in milliQ water and (0.1 M NaOH) solution was added to raise the pH to ~9. Afterwards, (250 ml) of this solution was transferred to an Eppendorf tube and (10 ml) of (0.5 M CS_2) in 1,2,4- trichlorobenzene (TCB) was added. The solution was shaken vigorously for (10 s) to offer a stable emulsion which was kept for 30 min before the analysis. Excess of NPs solution was added and was washed two times with milliQ water. The emulsion was then visualized by an optical microscope (OM). Using other low boiling nonpolar solvents such as dichloromethane and hexane, formed deteriorated microcapsules due to rapid evaporation of the solvent (Figure 132-a). Transmission electron microscope (TEM) analysis of microcapsules that were drop cast on carbon coated copper grid was obtained. Low magnification image of the dried capsules displayed thin film like quality, while the high-magnification image (Figure 132-b) showed that the capsule is composed of thickly crowded crosslinked FePt NPs.

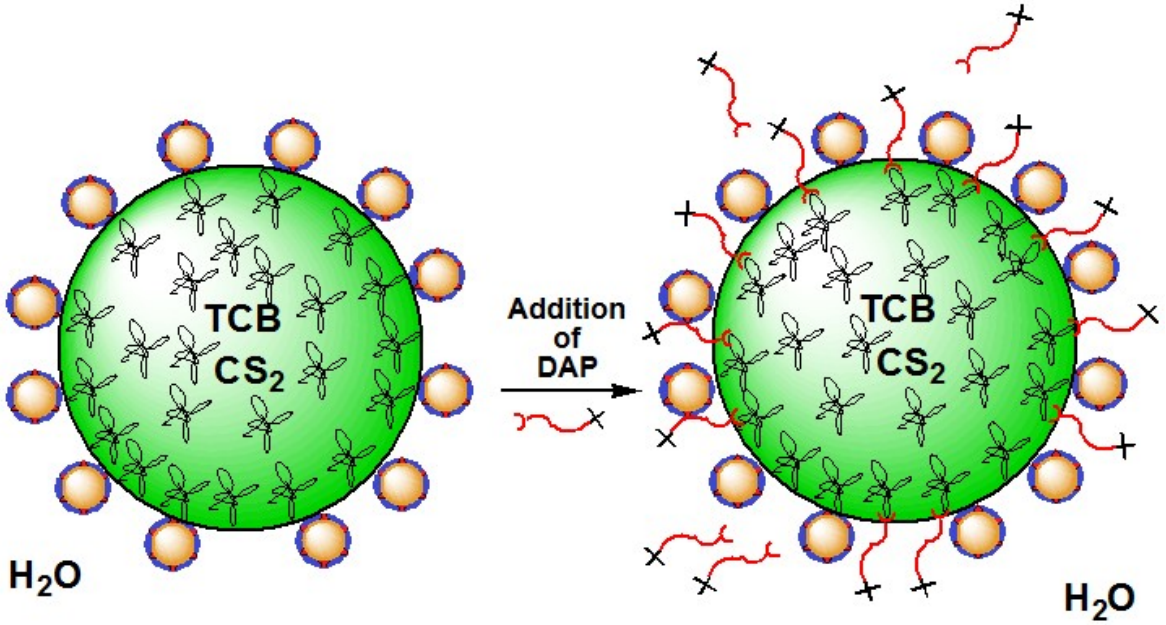

Figure 130. Flavin encapsulated microcapsule and host–guest recognition at oil–water interface.[252]

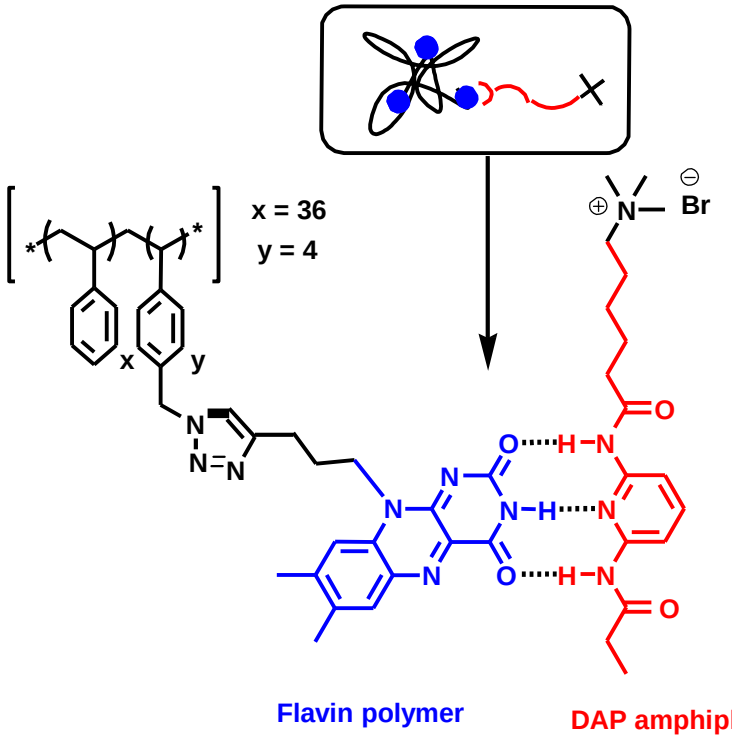

Figure 131. Three-point hydrogen bonding interaction between flavin and DAP.[252]

The fluorescence of the microcapsules in aqueous medium proved the successful encapsulation of the host flavin polymer inside the microcapsules during their formation (Figure 133-a). The recognition process inside the microcapsules was studied by adding of an excess of the guest DAP amphiphile to the aqueous solution (Figure 130 and Figure 131). The fluorescence from the microcapsule was quenched (Figure 133-b) due to three point hydrogen bonding interaction between host–guest at the oil–water interface. Observing the fluorescence intensity of a single microcapsule allowed the semiquantitative assessment of the binding constant between the flavin and the complementary DAP to be determined by fluorescence titration upon measurements performed upon the addition of equivalents of DAP. The titration resulted in a K_a ~ 250 M^{-1} (Figure 134). On the other hand, encapsulated *N*(3)-methylated polymer (Figure 133-c) was titrated with excess DAP amphiphile. Remarkably the titration failed to quench the fluorescence (Figure 133-d and Figure 134), indicating that the three point hydrogen bonding interactions were responsible for fluorescence quenching for the non-methylated flavin derivative.

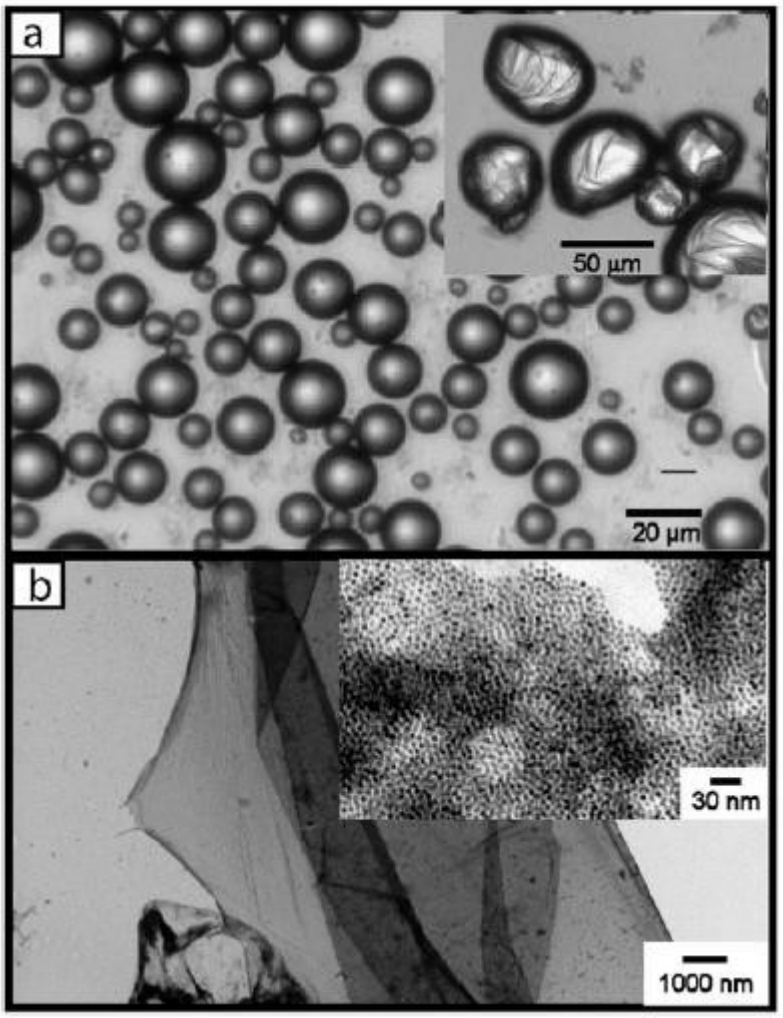

Figure 132. OM micrographs of: (a) FePt microcapsules at oil-in-water interface using DTC crosslinking strategy. Inset shows crumbled microcapsules. (b) Low-magnification TEM images of dried microcapsules showing film like texture. Inset represents higher-magnification.[252]

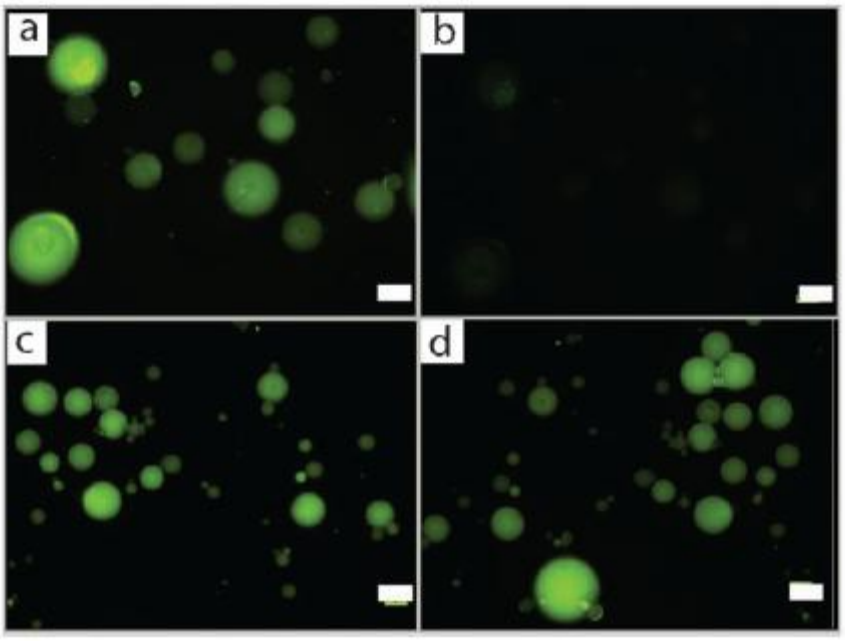

Figure 133. Fluorescence microscopy images of: (a) flavin encapsulated microcapsule; (b) after addition of excess DAP. Similarly, fluorescence images of: (c) N-methyl flavin encapsulated microcapsule and (d) after addition of excess DAP. All scale bars represent 40 nm of length.[252]

DAP–flavin recognition-mediated quenching of the latter's fluorescence prevented the straight determination of the localization of the host–guest complexes within the microsphere. Localization can be confirmed from the experiments using a planar interface. TCB was used as a solvent in this experiment to examine the fluorescence of flavin polymer, however, when excess of DAP in aqueous solution was added to the organic phase, no fluorescence quenching was demonstrated after agitation. This means that both DAP and flavin polymers are soluble only in water and oil, consequently and recognition can take place only at the interface, i.e. in the proximity of the particle shell (Figure 135).

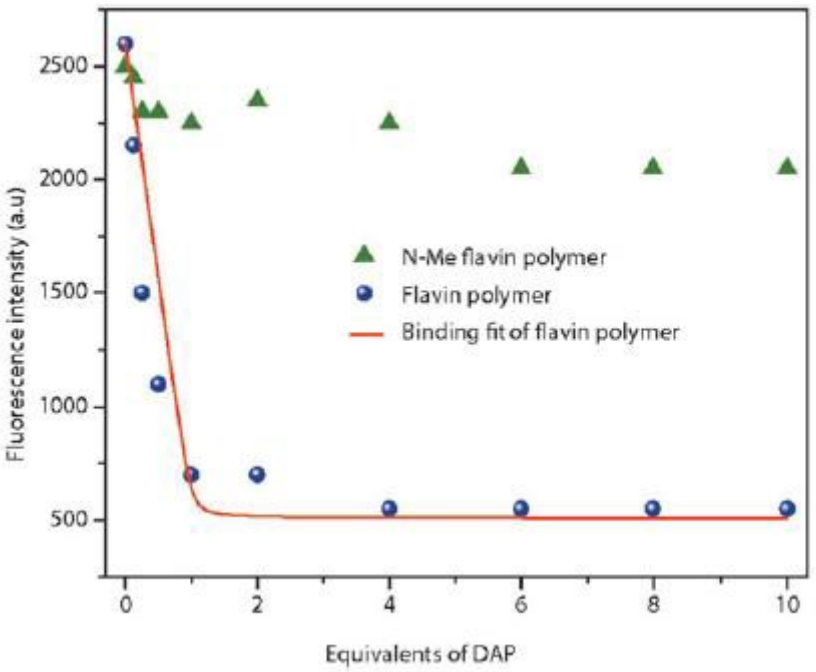

Figure 134. Binding plot shows dramatic quenching of flavin polymer fluorescence upon addition of DAP (K_a ~ 250 M^{-1}) whereas control N-methylated flavin does not show any fluorescence quenching.[252]

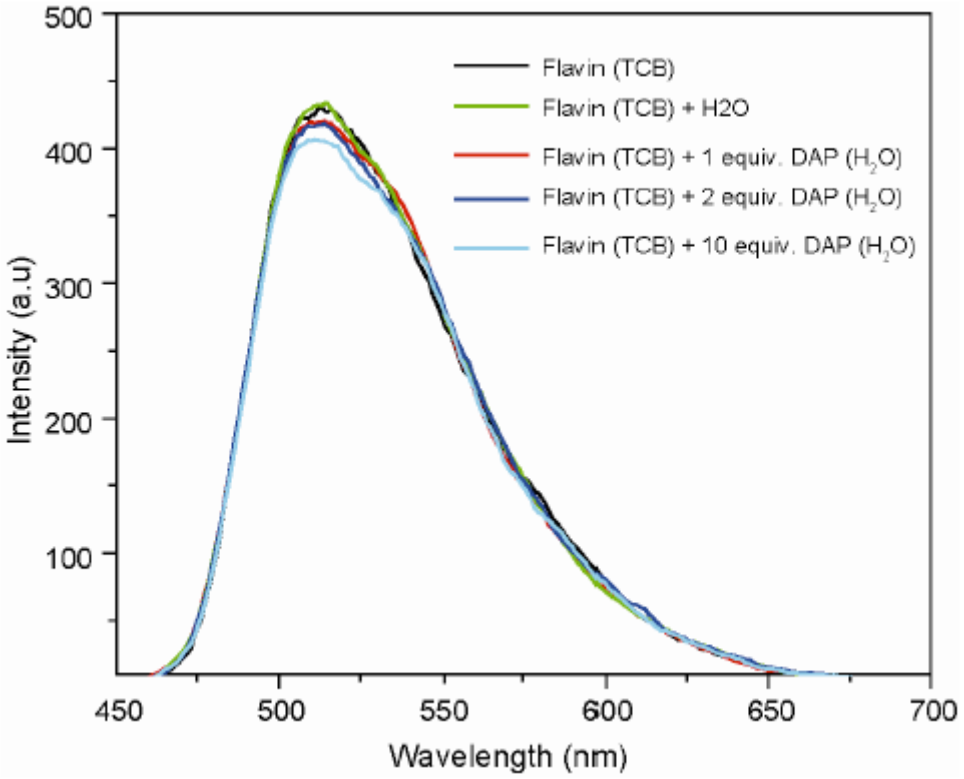

Figure 135. Fluorescence titration of flavin polymer with variable DAP equivalents.[252]

6.4.2. Formation of flavin –based micelles with SDS.

In order to determine whether flavin compound **157** could be incorporated into micelle – like structures with SDS, we have exploited the inherent fluorescence properties of the flavin nucleus to determine the critical micelle concentration (CMC) upon the addition of excess SDS. The results of these investigations are presented in Figure 136. Significant changes in the flavin's fluorescence was observed upon addition of the SDS revealing a CMC of 0.003 M/L. Interestingly the addition of the shorter chain methane sulphate failed to produce micelles under the conditions investigated.

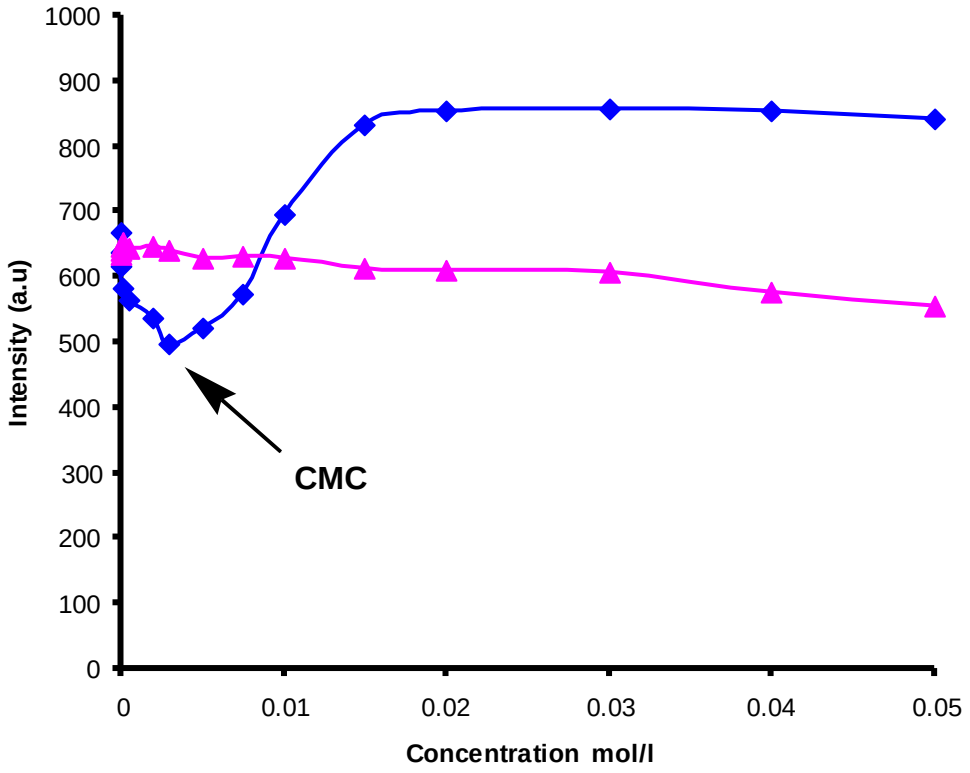

Figure 136. Fluorescence titration of flavin 157 with SDS (blue line) and methyl sulfate (purple line) recorded in water. Fluorescence emission spectra (λ_{ex}= 443 nm).

6.5. Conclusion

Ammonium functionalised DAP and flavin derivatives have been synthesised. The former has proved to be an interesting guest molecule in the formation of microcapsules. The flavin ammonium compound has been shown to form micelles upon the addition of SDS. These experiments pave the way for the formation of a flavin/DAP micelle; however, time constraints within the PhD programme prevented these experiments from being undertaken,

CHAPTER 7

EXPERIMENTAL

7.1. General.

All compounds were supplied from commercial sources and were used as received without purification unless stated. Flash column chromatography was carried out using Fisher Matrix silica 60. Macherey-Nagel aluminum backed plates pre-coated with silica gel 60 (UV_{254}) were used for thin layer chromatography and were visualized by ultra violet light.

^{1}H NMR and ^{13}C NMR spectra were recorded on Bruker Avance 400MHz spectrometers with chemical shift values in ppm. Tetramethylsilane (TMS) was used as reference for all NMR spectra ($\delta = 0.0$ ppm)

MS spectra and accurate Mass were obtained from using a JEOL JMS-700 spectrometer. They were measured under EI, CI and FAB conditions by the analytical services in the Chemistry Department of the University of Glasgow.
Transmission Infrared spectra were recorded on Perkin-Elmer RX FT-IR system.

Electrochemical experiments were carried out using dry dichloromethane with 0.1 M $TBAPF_6$ as the supporting electrolyte. Cyclic voltammograms (CV) was recorded using a CH Instrument Inc. (Austin, TX, USA.), 440 a EC Analyser.

UV - Vis absorption spectra were recorded Spectrometers using Perkin - Elmer Lambda 25 (Cambridge, U.K). All experiments were carried out at ambient temperature using $1cm^3$ quartz cuvettes. Fluorescence emission measurements were run on a Shimadzu *RF 3501PC* spectrofluorimeter (Milton Keynes, U.K.).

Gel Permeation Chromatography (GPC) analysis was used to calculate the polymer molecular weights using a Polymer Lab GPC50 instrument from Varian Inc. consisting of two 600 x 7.5 mm "PLgel 5μm MIXED-D ResiPore" columns. The recording time was set to 25 minutes under a flow rate of 1 ml/min and the oven temperature was set to 30°C.

7.2. Synthetic expermental

CHAPTER 2

1-(3-Carboxypropyl)-1-phenyl[6,6]C_{61} PCBA (35)[21]

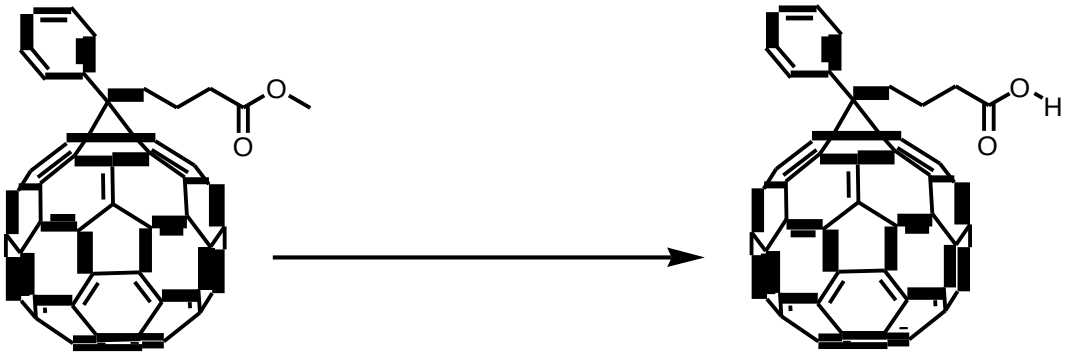

11
PCBM

35
PCBA

Acetic acid (50 ml) and hydrochloric acid (20 ml) was added to a solution of PCBM (**11**) (0.60 g, 0.66 mmol) in toluene (100 ml). The mixture was heated under reflux for 24 h. The reaction mixture was concentrated under reduced pressure and the residue was suspended in methanol, toluene and Et_2O, respectively, and each time the suspension was centrifuged and the liquid was decanted to yield **35** as a dark brown residue (0.59g, 99.8 %). Mp > 300^oC Ms (FAB / NOBA $(M + H)^+$) 898. Due to poor solubility no further charicterization has been undertaken.

2-(4-(Trifluoromethyl)-2-nitrophenylamino)ethanol (37)[263]

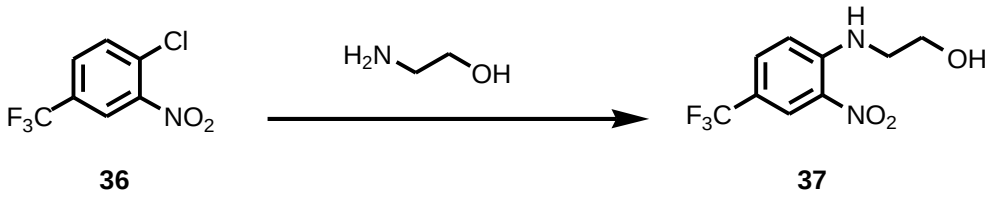

36 **37**

A solution of ethanol amine (**36**) (3.83 g, 51 mmol) triethylamine (14.14 ml, 102 mmol) and 1-chloro-2-nitro-4-(trifluoromethyl)benzene (**42**) (15.23 ml, 102 mmol) were stirred in THF (100 ml). The solution was heated under reflux for 4 h. After cooling to room temperature the solvent was evaporated under reduced pressure, and the residue was dissolved in DCM (100 ml) and washed with water (50 ml). The aqueous layer was further extracted with DCM (2 x 100 ml). The combined organic extracts were dried over $MgSO_4$, filtered and evaporated. Column chromatography (silica gel/ eluting with hexane / ethyl acetate (4:6) afforded **37** as a yellow solid (4.70 g, 37%). Mp. 73-74^{o}C. ^{1}H NMR (400MHz, $CDCl_3$) δ = 8.48 (s, 1H, C3-H_{ar}), 7.63 (dd, 1H, *J* = 2 Hz, 8.8 Hz, C5- H_{ar}), 7.00 (dd, 1H, *J* = 3.6 Hz, 8.8 Hz, C6-H_{ar}), 3.98 (dd, 2H, *J* = 5.2 Hz, 10.4 Hz, CH_2-N), 3.56 (dd, 2H, *J* = 5.2 Hz, 10.6 Hz, CH_2CH_2-N), 1.72 (t, 1H, *J* = 4.8Hz, OH). ^{13}C NMR (100MHz, $CDCl_3$) δ = 147.00 (C1), 132.14 (C5H), 131.27 (C2), 125.05 (C3H), 124.93 (CF_3), 122.24 (C4), 114.49 (C6H), 60.78 (CH_2CH_2-N), 44.95 (CH_2-N). Ms (FAB / NOBA $(M + H)^+$) 251.1. ν_{max}/cm^{-1} 3371*s* (OH), 3283*w* (NH), 3118*m* (CH_{ar}), 2952*w* (CH_{alk}), 2885*m* (CH_{alk}), 1635*s*, 1573*s* (aromatic C=C), 1532 *s*(C-NO_2), 1435*m*, 1358*s*, 1318*s* (C-NO_2), 1253*m*, 1218*s*, 1154 *s*, 1109 *s*, 1082 *s*, 1056 *s*, 913*s*, 886 *m*, 824*s* (1,2,4-trisubstituated aromatic ring), 761*s*, 687*m*. Anal. Calc. for $C_9H_9F_3N_2O_3$ (C) 43.60, (H) 3.60, (N) 11.2 found (C) 43.13, (H) 3.58, (N) 10.98.

2-(2-Amino-4-(trifluoromethyl)phenylamino)ethanol (38)[263]

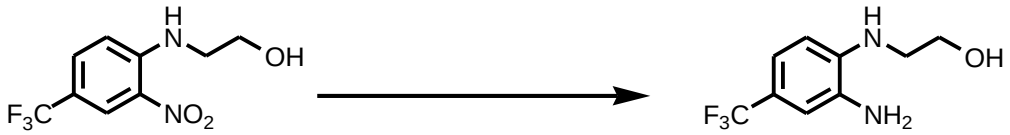

37 **38**

2-(4-(Triflouromethyl)-2-nitrophenylamino) ethanol (**37**) (4.40 g, 20 mmol) was dissolved in CH_3OH (120 ml). The solution was quickly purged with N_2, and 10% Pd/C (0.50 g) was added. Ammonium formate (7.56 g, 120 mmol) was then added to the stirred solution. The reaction mixture was stirred for 2 h. at room temperature. Then the solution was filtered and the filtrate was evaporated. The residue was dissolved in DCM (100 ml) and washed with water (50 ml). The aqueous layer was further extracted with DCM (2 x 100 ml). The combined organic extracts were dried over $MgSO_4$, filtered and evaporated to afford 2-(4-amino-4-(triflouromethyl)phenylamino)ethanol **38** as red oil (4.9 g). No further purification was attempted due to the instability of the compound.

7-(Trifluoromethyl)-10-(2-hydroxyethyl)-alloxazine (39)[263]

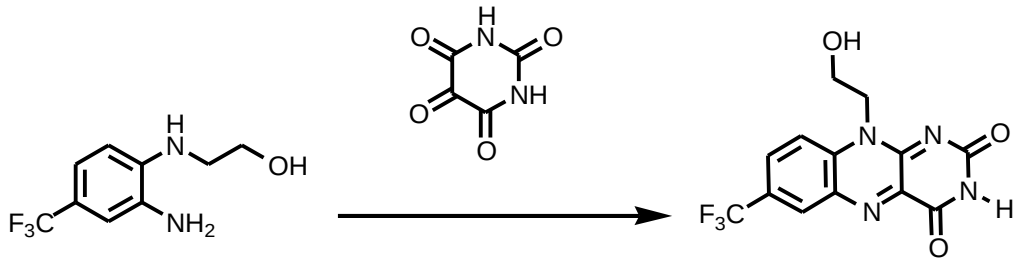

38 **39**

2-(4-Amino-4-(trifluoromethyl) phenyl amino) ethanol (**38**) (4.50 g, 20.43 mmol) was dissolved in (100 ml) acetic acid. Alloxan monohydrate (3.27 g, 20.43 mmol) and boric anhydride (2.85 g, 40.86 mmol) were added to the mixture which was heated under reflux for 2 h. The solvent was evaporated under reduced pressure. Purification by column chromatography (silica gel/ eluting with hexane/ ethyl acetate (8: 2) afforded **39** as a yellow powder (4.20 g, 63%). Mp 260-263^{o}C. ^{1}H NMR (400 MHz, DMSO) δ = 11.53 (s, 1H, NH), 8.46 (s, 1H, C6-H_{ar}), 8.24 (d, 1H, *J* = 9.2Hz, C8-H_{ar}), 8.19 (dd, 1H, *J* = 2Hz, 9.2Hz, C9-H_{ar}), 4.94 (t, 1H, *J* = 6Hz, OH), 4.70 (t, 2H, *J* = 6Hz, CH_2-N10),, 3.83 (dd, 2H, *J* = 6Hz, 11.8Hz, CH_2CH_2-N10). ^{13}C NMR (100 MHz, DMSO) δ = 177.00 (C2), 159.26 (C4), 158.00 (C), 155.43 (C), 152.00 (C), 140.29 (C), 136.00 (CF_3), 133.86 (C7), 129.73 (C8H), 128.62 (C6H), 118.87 (C9H), 57.41 (CH_2CH_2-N), 46.90 (CH_2-N).

Ms (FAB / NOBA $(M + H)^+$) 327. ν_{max}/cm^{-1} 3302*w* (OH), 3097 *s* (NH), 2999*w* (CH_{ar}), 2805*w*(CH_{alk}), 1690*m*, 1590*s* (aromatic C=C), 1557*s*, 1446*s*, 1406*s*, 1322*m*, 1293*s*, 1231*m*, 1180*s*, 1137*s*, 1050*s*, 890*s*, 836*s*, 808*s*, 766*s* 717*m*. Anal. Calc. for $C_{13}H_9F_3N_4O_3$. (C) 47.85, (H) 2.76, (N) 17.18; found (C) 47.51, (H) 2.75, (N) 16.71.

3-Dodecyl-7-(trifluoromethyl)-10-(2-hydroxyethyl)-isoalloxazine (40)

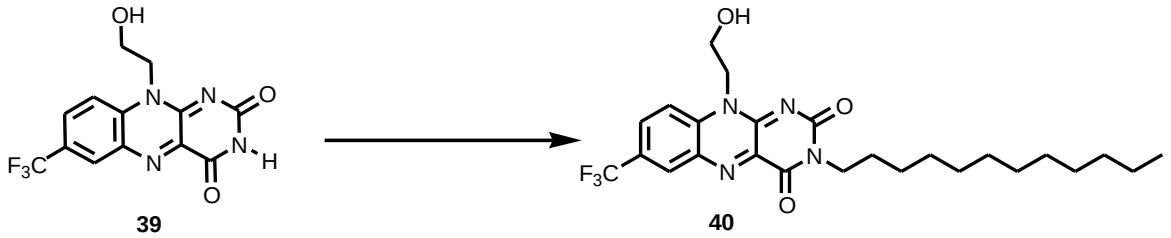

39 **40**

7-(Trifluoromethyl)-10-(2-hydroxyethyl)-alloxazine (**39**) (0.50 g, 1.53 mmol), 1-bromododecane (0.77g, 3.07 mmol) and K_2CO_3 (0.85g, 6.14 mmol) in (30 ml) dry DMF were stirred at RT for 48 h under N_2 atmosphere. The solvent was evaporated under reduced pressure. Purification by column chromatography (silica gel/ eluting with DCM/ ethyl acetate (8: 2) afforded **40** as pure yellow powder (0.74g, 97%). Mp (192-194) ^{o}C. ^{1}H NMR (400 MHz, $CDCl_3$) 8.58 (s, 1H, C6-H_{ar}), 8.04 (d, 1H, *J* = 9Hz, C8-H_{ar}), 7.99 (d, 1H, *J* = 9Hz, C9-H_{ar}), 4.92 (t, 2H, *J* = 5.2 Hz, CH_2-N10), 4.24 (q, 2H, *J* = 5.2 Hz, CH_2CH_2-N10), 4.07 (t, 2H, *J* = 7.6Hz, CH_2-N3), 2.32 (t, 1H, *J* = 5.2 Hz, OH), 1.69 (p, 2H, CH_2), 1.29 (m, 18H, CH_2), 0.88 (t, 3H, *J* = 6.8Hz, CH_3). ^{13}C NMR (100 MHz, $CDCl_3$) δ = 158.68 (C), 155.08 (C), 149.68 (C), 138.45 (C),135.46 (CF_3), 134.84 (C7), 131.06 (C8H), 130.39 (C6H), 117.26 (C9H), 60.02 (CH_2-N), 47.15 (CH_2CH_2-N), 42.37 (CH_2-N3), 31.92 (CH_2), 29.66 (CH_2), 29.63 (CH_2), 29.61(CH_2), 29.54 (CH_2), 29.35 (CH_2), 27.71 (CH_2), 26.96 (CH_2), 22.69 (CH_2), 14.13 (CH_3). Ms (FAB / NOBA $(M + H)^+$) 495.2. Accurate Mass FAB/NOBA, Theoretical ion distribution $C_{25}H_{33}N_4O_3F_3$ (*m/z*) calculated 495.2583 observed 495.2581. ν_{max}/cm^{-1} 3415*w* (OH), 3048 *s* (NH), 2920*s* (CH_{ar}), 2853*s*(CH_{alk}), 1705*s*, 1655*s* (aromatic C=C), 1589*s*, 1553*s*, 1524*s*, 1448*m*, 1358*m*, 1320*s*, 1241*m*, 1204*s*, 1241*s*, 1132*s*, 1084*s*, 1052*s*, 979*m*, 830*s*, 751*m*. Anal. Calc. for $C_{25}H_{33}F_3N_4O_3$ (C) 60.73, (H) 6.68, (N) 11.33; found (C) 60.79, (H) 6.75, (N) 11.13.

Phenyl-C61-butyric acid-{2-[3-dodecyl-7(triflouromethyl)-isoalloxazine-10-yl]ethyl} ester (44)[102]

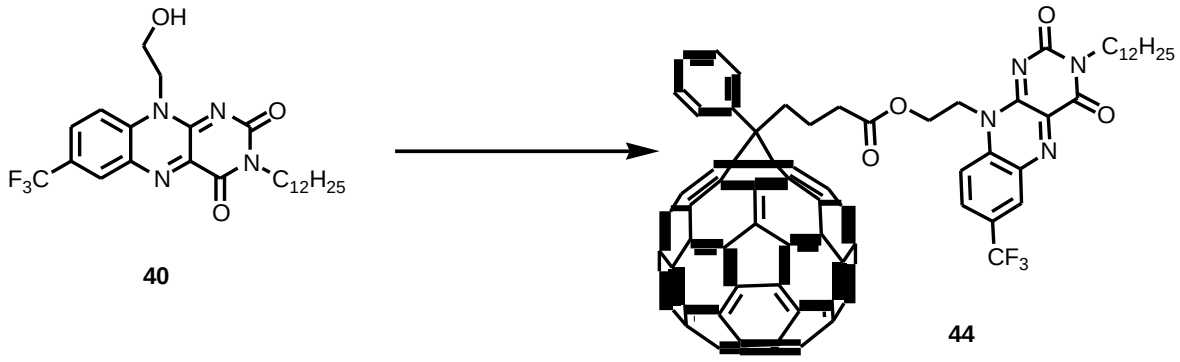

40 **44**

To a solution of PCBA (**35**) (0.54g, 0.61mmol) in CS_2 (20 ml), a solution of 3-dodecyl-7-(triflouromethyl)-10-(2-hydroxyethyl)-isoalloxazine (**40**) (0.3g, 0.61mmol) , DMAP (0.08g, 0.61mmol), DCC (0.14g, 0.67mmol) and HOBT (0.08g, 0.61mmol) in DCM (20 ml) was added at 0^oC .The reaction mixture was stirred for 48h. at RT under a N_2 atmosphere. Solvents were evaporated under reduced pressure. Purification by column chromatography (silica gel/ eluting with toluene 100% then DCM/ ethyl acetate (8: 2) afforded **44** as a brown-yellow powder (0.57g, 68.5%). Mp. 135-137^{o}C.

^{1}H NMR (400 MHz, $CDCl_3$) δ = 8.58(s, 1H, C6-H_{ar}), 8.02(dd, 1H, *J* = 1.8Hz, 9.1Hz, C8-H_{ar}), 7.92(d, 1H, *J* = 11Hz, C9-H_{ar}), 7.89(d, 2H, *J* = 6.8Hz, o-H_{ar}), 7.55(m, 2H, ,m-H_{ar}), 7.48(m, 1H, p-H_{ar}), 4.93(t , 2H, *J* = 6Hz, CH_2N10), 4.58(t, 2H, *J* = 6Hz, CH_2CH_2-N10), 4.09(t, 2H, *J* = 7.3Hz, CH_2-N3), 2.83(m, 2H, PhCCH_2), 2.45(t, 2H, *J* = 7.3Hz, CH_2CO), 2.11(m, 2H, CH_2CH_2CO), 1.71(m, 2H, CH_2), 1.35 (m, 18H, CH_2), 0.88 (t , 3H, *J* = 6.9Hz, CH_3). ^{13}C NMR (100MHz, $CDCl_3$) δ = 172.94 (COO), 171.20 (C2), 158.50 (C_f), 154.84 (C_f), 149.20 (C_f), 148.61 (C), 147.64 (C), 145.76 (C), 145.21 (C), 145.17 (C), 145.06 (C), 144.98 (C), 144.81(C), 144.65 (C), 144.62 (C), 144.52 (C), 144.43 (C), 144.03 (C), 143.76 (C), 143.72 (C), 143.14 (C), 143.06 (C), 143.02 (C), 142.96 (C), 142.88 (C), 142.17 (C), 142.13 (C), 142.08 (C), 140.98(C), 140.79 (C), 138.64 (C_f), 137.89 (C), 137.58 (C), 136.59 (CF_3), 135.09 (C), 134.74 (C7), 132.05 (CH), 131.21 (C8H), 130.74 (C6H), 130.70 (CH), 128.77 (C), 128.54(CH), 128.43 ($PhC_{2,3}$), 128.39 (CH), 128.09 ($PhC_{2,3}$), 124.30 (C), 121.60 (C), 116.40 (C9H), 79.63($C_{bridgehead}$), 60.43 (CH_2-N), 60.26 (CH_2CH_2-N), 51.54 (PhC), 43.63 (CH_2), 42.44 (CH_2-N3), 33.61 (CH_2), 33.46 ($PhCCH_2$ and CH_2COO), 31.95 (CH_2), 29.71 (CH_2), 29.68 (CH_2),

29.59 (CH_2), 29.40 (CH_2), 27.77 (CH_2), 27.00 (CH_2), 22.74 (CH_2CH_2COO), 21.99 (CH_2), 21.10 (CH), 14.23 (CH_3). Ms (FAB / NOBA $(M + H)^+$ 1373.8. ν_{max}/cm^{-1} 2918*s* (CH_{ar}), 2847*s*(CH_{alk}), 2114*m*, 1717*m*(C=O ester), 1662*s* (aromatic C=C), 1595*s*, 1558*s*, 1429*m*, 1322*s*, 1247*s*, 1214*s*, 1129*s*, 1073*m*, 988*m*, 906*m*, 817*m*, 755*m*. Anal. Calc. for $C_{96}H_{43}F_3N_4O_4$ (C) 83.91, (H) 3.13, (N) 4.08; found (C) 83.02, (H) 3.16, (N) 4.07.

Phenyl-C61-butyric acid [(6,10-dioxoanthracen-3-yl)methyl]ester (45)[102]

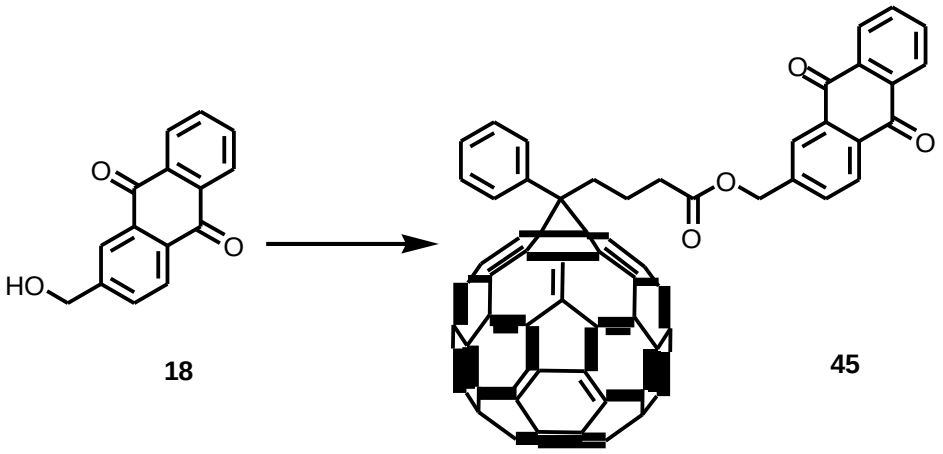

18 **45**

To a solution of PCBA (35) (0.38g, 0.42mmol) in CS_2 (15 ml), was added a solution of 2-(hydroxymethyl)-anthraquinone (**18**) (0.1 g, 0.42 mmol), DMAP (0.05 g, 0.42 mmol), DCC (0.10 g, 0.46 mmol) and HOBT (0.05 g, 0.42 mmol) in DCM (15 ml) at 0^{o}C. The reaction mixture was stirred for 48h. at RT under a N_2 atmosphere. Solvents were evaporated under reduced pressure. Purification by column chromatography (silica gel/ eluting with DCM 100%) afforded **45** as a brown powder (0.39 g, 77.5%). Mp 270-272^{o}C. ^{1}H NMR (400MHz, $CDCl_3$) δ = 8.33-8.23 (m, 4H), 7.94 (dd, 2H,*J* = 1.6Hz, 11.8Hz, CH_{ar}), 7.82 (dd, 2H, *J* = 2.6Hz, 6.5Hz, CH_{ar}), 7.75 (d, 1H, *J* = 2.3Hz, 8.1Hz, CH_{ar}), 7.55 (tt, 2H, *J* = 8.3Hz, 10Hz, CH_{ar}), 7.48 (t, 1H, *J* = 7.3Hz, 9.5Hz, CH_{ar}), 5.28 (s, 2H), 2.93 (p, 2H, $PhCCH_2$), 2.66 (t, 2H *J* = 8.1Hz, 10.5Hz, CH_2CO), 2.25 (m, 2H, CH_2CH_2CO). ^{13}C NMR (100MHz, $CDCl_3$)δ = 182.67 (C), 172.72 (COO), 148.60 (C), 147.66 (C), 145.77(C), 145.13 (C), 145.15 (C), 145.09 (C), 145.04 (C), 145.00 (C), 144.75 (C), 144.61 (C), 144.40 (C), 144.34 (C), 143.98 (C), 143.73 (C), 143.67 (C), 142.98(C), 142.95 (C) 142.87 (C), 142.82 (C), 142.61 (C), 142.13 (C), 142.11 (C), 142.05 (C), 140.92 (C), 140.70 (C), 137.94 (C), 137.53 (C), 134.30 (CH), 134.24 (CH), 133.69 (C), 133.43 (C), 133.09 (C), 133.00 (CH), 132.10 (CH), 128.47 ($PhC_{2,3}$), 128.28 ($PhC_{2,3}$), 127.79 (CH), 127.30 (CH), 126.12 (CH), 79.72 ($C_{bridgehead}$), 65.18 (CH_2), 51.70 (PhC), 33.93(CH_2), 33.56 ($PhCCH_2$ and CH_2COO), 22.31 (CH_2CH_2COO). Ms (FAB / NOBA $(M + H)^+$) 1117.8. ν_{max}/cm^{-1} 2923*w* (CH_{ar}), 2120*m*, 1735*m* (C=O ester), 1672*s*, 1591*m*, 1321*s*, 1288*s*, 1142*m*, 928*s*, 843*m*, 707*s*. Anal. Calc. for $N_{86}H_{20}O_4$ (C) 91.56, (H) 2.01; found (C) 91.15, (H) 1.89.

2-(Hydroxymethyl)-tetracyanoanthraquinon TCNAQ (41)[107]

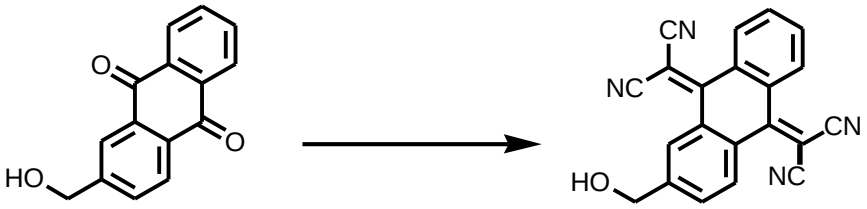

18 **41**

Under an atmosphere of N_2, two solutions were prepared. The first solution was made by the addition of $TiCl_4$ (4.13g, 22.00 mmol) and 2-(hydroxymethyl)-anthraquinone (**18**) (1.00g, 4.20 mmol) in dry $CHCl_3$ (40 ml). The second solution consisted of malononitrile (8.01g, 121 mmol) and β–alanine (2.19g, 24.60 mmol), dissolved in pyridine (3.75 ml), and dry $CHCl_3$ (50 ml). The second solution was added to the first solution. The mixture was heated under reflux for 4 h. under N_2. After being cooled the reaction mixture was poured into ice water. The aqueous phase was extracted with ethyl acetate and the organic layers were combined and dried over anhydrous $MgSO_4$, filtered and the solvent was evaporated under reduced pressure. Purification by column chromatography (silica gel/ eluting with $CHCl_3$ / ethyl acetate, 8:2) afforded **41** as a creamy white powder (0.60 g, 43%). Mp 256–257 ^oC. ^1H NMR (400MHz, $CDCl_3$) δ = 8.29 (s, 1H), 8.26 (m, 2H), 7.74 (dd, 2H, *J* = 3.3Hz, 6Hz, CH_{ar}), 7.71 (d, 1H, *J* = 7.1Hz, CH_{ar}), 4.90 (d, 2H, *J* = 5.6Hz, CH_2), 2.02 (t, 1H, *J* = 5.8Hz, OH). ^{13}C NMR (100MHz, $CDCl_3$) δ = 160.39(C), 159.98(C), 146.44(C), 132.51(CH), 132.47(CH), 130.49(C), 130.26(C), 130.18(C), 130.06(CH), 129.0 0(C), 127.78(CH), 127.62(CH), 127.59(CH), 125.29(CH), 113.11(C), 112.99(C), 82.89(C) 63.71(CH_2) Ms (FAB / NOBA $(M + H)^+$)334.1. Accurate Mass EI + ION, Theoretical ion distribution $C_{21}H_{10}N_4O$ (*m/z*) calculated 334.0855 observed 334.0859. ν_{max}/cm^{-1} 3525*s* (OH), 2923*w* (CH_{ar}), 2226*s* (C≡N), 1671*s*, 1587*m* (aromatic C=C), 1325*s*, 1295*m*, 1203*m*, 1045*s*, 932*s*, 841*m*, 771*s*, 660*s*.

Phenyl-C61-butyric acid [(9,10-tetracyanoanthraquinon-3-yl)methyl] ester TCNAQ (46)[102]

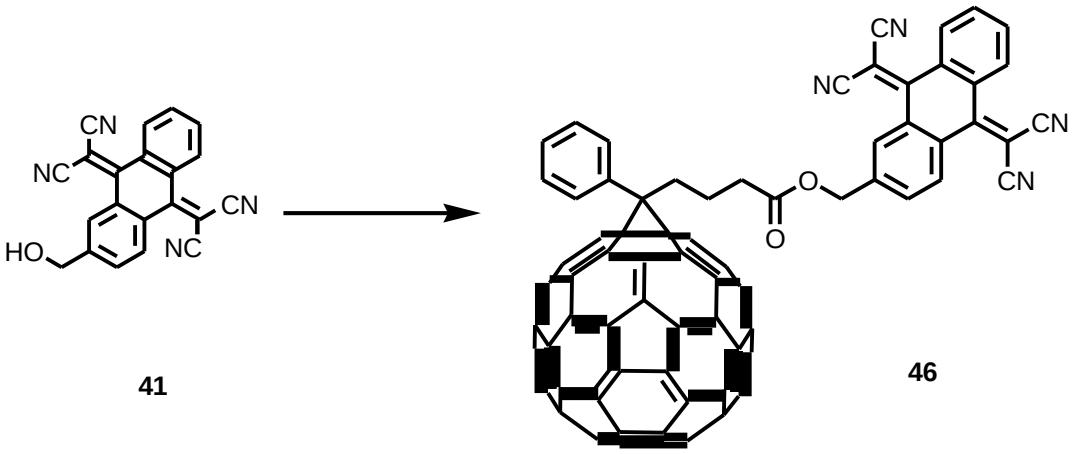

41 **46**

To a solution of PCBA (35) (0.20 g, 0.22 mmol) in CS_2 (10 ml), a solution of TCNAQ (**41**) (0.08 g, 0.22 mmol) , DMAP (0.03 g, 0.22 mmol), DCC (0.05 g, 0.25 mmol) and HOBT (0.03 g, 0.22 mmol) in 10 ml DCM was added at 0^{o}C .The reaction mixture was stirred for 48 h. at RT under N_2 atmosphere. Solvents were removed under reduced pressure. Purification by column chromatography (silica gel/ eluting with DCM 100%) and recrystallization from CH_3OH afforded **46** as a brown powder (0.15 g, 66 %). Mp 242-244 ^{o}C ^{1}H NMR (400MHz, $CDCl_3$) δ = 8.25-8.20(m, 4H, CH_{ar}), 7.93 (dd, 2H, *J* = 1.3Hz, 7.2Hz, CH_{ar}), 7.74 (dd, 2H, *J* = 3.1Hz, 6Hz, CH_{ar}), 7.66 (dd, 1H *J* = 1.5Hz, 8Hz, CH_{ar}), 7.55 (tt, 2H, *J* = 1.5Hz, 7.1Hz, 8Hz CH_{ar}), 7.48 (tt, 1H, *J* = 1.5Hz, 7.3Hz, 7.7Hz, CH_{ar}), 5.26 (s, 2H, CH_2), 2.93 (p, 2H, CH_2), 2.66 (t, 2H, *J* = 7.2Hz, 8Hz, CH_2), 2.24 (m, 2H, CH_2). ^{13}C NMR (100 MHz, $CDCl_3$) δ = 172.75 (COO), 148.75 (C), 145.81 (C), 145.21 (C),145.19 (C), 145.10 (C), 145.06 (C), 145.03 (C),144.82 (C), 144.70 (C), 144.60 (C), 144.51 (C), 144.31 (C) 144.02(C), 143.77(C), 143.65(C), 143.05 (C), 143.01(C), 142.94 (C), 142.82 (C), 142.20 (C), 142.14 (C), 142.03 (C), 141.45 (C), 140.89 (C), 140.77 (C), 137.91(C), 137.60 (C), 136.64 (C), 132.63(CH), 132.11 (CH), 131.07 (CH), 130.17 (C), 129.62 (C), 128.49 ($PhC_{2,3}$), 128.32 ($PhC_{2,3}$), 127.91 (CH), 127.70 (CH), 126.37 (CH), 112.90 (C), 1112.99 (C), 79.82 ($C_{bridgehead}$), 64.59 (CH_2), 59.30 (C), 53.42 (C), 51.71 (PhC), 33.84 (CH_2), 33.55 ($PhCCH_2$ and CH_2COO), 22.25 (CH_2CH_2COO). Ms (FAB / NOBA $(M + H)^+$) for $C_{92}H_{20}N_4O_2$ 121.8. ν_{max}/cm^{-1} 2925*w* (CH_{ar}), 2858*w* (Ch_{alk}), 2329*w*(C≡N), 2115*m*, 1734*m* (C=O ester), 1549*m*, 1425*m*, 1232*m*, 1142*s*, 1025*m*, 864*m*, 786*m*.

3-(6-Octyl-naphthalindianhydride)propan-1-ol NDI (43)[108]

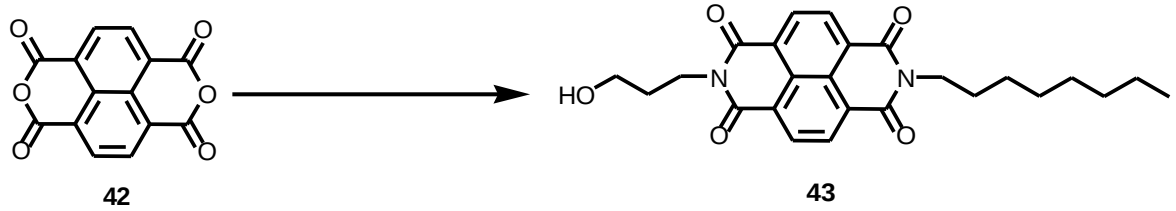

42 **43**

Naphthalene dianhydride (**42**) (5.00 g, 18.64 mmol) was dissolved in dry DMF (50 ml). The solution was heated to 140°C under N_2 atmosphere. Octylamine (2.41 g, 18.64 mmol) was added drop wise for about 10 minutes. After heating the reaction mixture under reflux for 24 h., 3-amino-1-propanol (1.40 g, 18.64 mmol) was added and was left for another 24 h. The reaction mixture was cooled down and DMF was removed under reduced pressure. Purification by column chromatography (silica gel/ eluting with DCM/acetone 9:1) afforded **43** as a purple powder (2.52g, 31%). Mp 184–186 °C. ^{1}H NMR (400 MHz, $CDCl_3$) δ = 8.74(s, 4H, $CH_{naphthalene}$), 4.38 (t, 2H, *J*= 6.3Hz, 7Hz CH_2OH), 4.19 (t, 2H, *J*= 7.5Hz, 9.5Hz CH_2), 3.64 (q, 2H), 2.67 (t, 1H, *J*= 6.3Hz, 7Hz, OH), 2.02 (q, 2H, CH_2), 1.74 (q, 2H, CH_2), 1.45-1.28 (m, 10H), 0.88 (t, 3H, *J*= 7Hz, 8Hz, CH_3). ^{13}C NMR (100MHz, $CDCl_3$)δ =163.49(C), 162.74(C), 162.53(C), 131.27(CH), 130.96(CH), 126.99(C), 126.75(C), 126.28(C), 59.26(CH_2), 41.07(CH_2), 37.59(CH_2), 36.45(CH), 31.81(CH_2), 31.44(CH), 31.02(CH_2), 29.29(CH_2), 29.19(CH_2), 28.11(CH_2), 27.10(CH_2), 22.63(CH_2), 14.07(CH_3). Ms (FAB / NOBA $(M + H)^+$) 437.2. ν_{max}/cm^{-1} 3513*s* (OH), 3079*s* (CH_{ar}), 2923*m* (CH_{alk}), 1695*s* (aromatic C=C), 1647*s*, 1580*s*, 1455*s*, 1375*s*, 1338*s*, 1243*s*, 1170*s*, 1048*m*, 895*m*, 768*s*, 711*m*.

Phenyl-C61-butyric acid [3-(6-octyl-naphthalindianhydride)propyl] ester (47)[102]

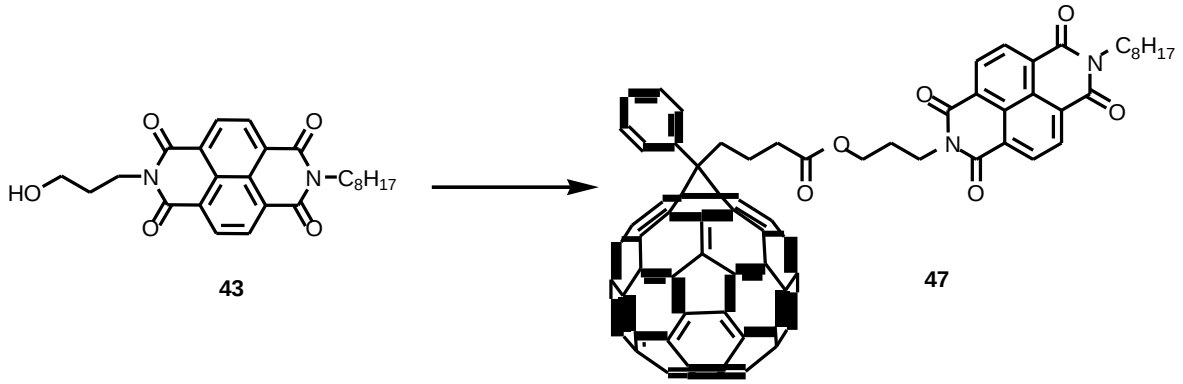

To a solution of PCBA (35) (0.20 g, 0.22 mmol) in CS_2 (10 ml), a solution of NDI (**43**) (0.10 g, 0.22 mmol), DMAP (0.03 g, 0.22 mmol), DCC (0.05 g, 0.25 mmol) and HOBT (0.03 g, 0.22 mmol) in DCM (10 ml) was added at 0^oC .The reaction mixture was stirred for 48h. at RT under N_2 atmosphere. Solvents were removed under reduced pressure. Purification by column chromatography (silica gel/ eluting with DCM 100%) followed by recrystallization from CH_3OH afforded **47** as a brown powder (0.15 g, 51%). Mp 89-91 ^oC. ^1H NMR (400MHz, $CDCl_3$) δ = 8.74(dd, 4H, *J*= 7.5Hz, 12Hz, $CH_{naphthalene}$), 7.93 (d, 2H, J= 7.5Hz, CH_{ar}), 7.54 (t, 2H, *J*= 7.5Hz, 8Hz, CH_{ar}), 7.45 (t, 1H, *J*= 7.5Hz, 8Hz, CH_{ar}), 4.30 (t, 2H, *J*= 7Hz, 8Hz, CH_2), 4.21 (m, 4H,CH_2), 2.91 (p, 2H, CH_2), 2.52 (t, 2H, *J*= 7Hz, 8Hz, CH_2), 2.10 (p, 2H, CH_2), 1.75 (p, 2H, CH_2), 1.46-1.24 (m, 12H, CH_2), 0.88 (t, 3H, *J*= 7Hz, 8Hz, CH_3). ^{13}C NMR (100MHz, $CDCl_3$) δ = 162.81 (C), 162.75 (C), 147.87 (C), 145.88 (C), 145.20 (C), 145.08 (C), 145.06 (C), 14 5.00 (C), 144.81 (C), 144.82 (C), 144.73 (C), 144.71 (C), 144.61 (C), 144.58 (C), 144.51 (C), 144.34 (C), 144.02(C), 143.78(C), 143.65 (C), 143.03 (C), 143.00 (C), 142.93 (C), 142. 87 (C), 142.21 (C), 142.15 (C), 142.04 (C), 141.01 (C), 140.93 (C), 140.75 (C), 138.03(C), 137.59(C), 136.80 (C), 132.15 (CH), 131.11 (CH), 130.99 (CH), 128.45 ($PhC_{2,3}$), 128.26 ($PhC_{2,3}$), 126.88 (C), 126.46(C), 79.93($C_{bridgehead}$), 62.19 (CH_2), 51.91 (PhC), 41.05 (CH_2), 37.88 (CH_2), 34.04 (CH_2), 33.61 ($PhCCH_2$ and CH_2COO), 31.84 (CH_2), 29.32 (CH_2), 29.21 (CH_2), 28.13 (CH_2), 27.47 (CH_2), 27.12(CH_2), 24.53 (C), 22.66 (CH_2), 22.38 (CH_2CH_2COO), 14.10 (CH_3). Ms (FAB / NOBA $(M + H)^+$) 1315.9. ν_{max}/cm^{-1} 2923*w* (CH_{ar}), 1731*s* (C=O ester), 1701*s*, 1662*s*, 1579*s*, 1452*m*, 1330*s*, 1242*s*, 1175*m*, 1070*m*,971*m*, 877*m*, 766*s*, 698*m*. Anal. Calc. for $C_{96}H_{38}N_2O_6$. (C) 87.34, (H) 2.88, (N) 2.12 found; (C) 86.00, (H) 2.80, (N) 2.20.

Phenyl-C61-butyric acid phenyl ester (48)[61,102]

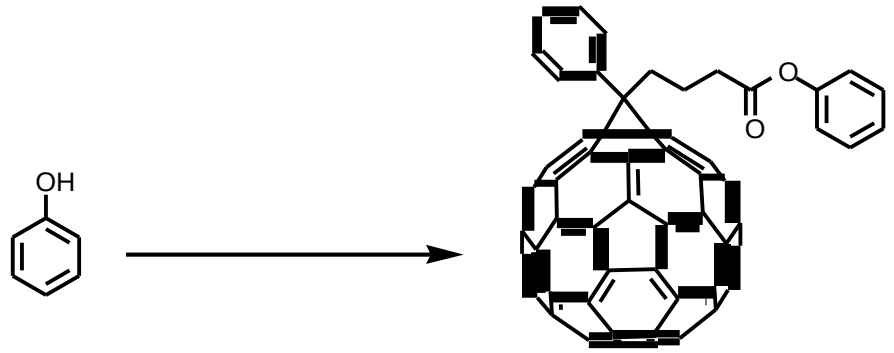

48

To a solution of PCBA (**35**) (0.50 g, 0.56 mmol) in CS_2 (20 ml) was added a solution of phenol (0.06 g, 0.61 mmol), DMAP (0.07 g, 0.61 mmol), DCC (0.13 g, 0.61 mmol) and HOBT (0.08 g, 0.56 mmol) in DCM (20 ml) at 0^{o}C. The reaction mixture was stirred for 48h at RT under N_2 atmosphere then solvents were removed in vacuum. The residue was purified by column chromatography using DCM 100% and was then recrystalized from CH_3OH to afford **48** as a brown powder (0.16 g, 29%). Mp 249-250 ^{o}C.

^{1}H NMR (400MHz, $CDCl_3$) δ = 7.96(dd, 2H, *J*= 1Hz, 7Hz, CH_{ar}), 7.56 (tt, 2H, *J*= 1.5Hz, 7.5Hz, 8Hz, CH_{ar}), 7.49 (tt, 1H, *J*= 1.5Hz, 7.5Hz, 8Hz, CH_{ar}), 7.37 (tt, 2H, , *J*= 2.5Hz, 8Hz, 8.5Hz, CH_{ar}), 7.22 (tt, 1H, *J*= 1.5Hz, 7.5Hz, 8Hz, CH_{ar}), 7.06 (dt, 2H, *J*= 1Hz, 7Hz, CH_{ar}), 3.02 (p, 2H, CH_2), 2.78 (t, 2H, *J*= 7.2Hz, 8Hz, CH_2), 2.32 (m, 2H, CH_2).

^{13}C NMR (100MHz, $CDCl_3$) δ = 171.54 (COO), 150.62 (C), 148.78, (C), 147.73 (C), 145.85 (C), 145.22 (C), 145.17 (C), 145.09 (C), 145.07 (C), 144.82 (C), 144.69 (C), 144.53 (C), 144.45 (C), 144.04 (C), 143.78 (C), 143.13 (C), 143.06 (C), 143.02 (C), 142.95 (C), 142.27 (C), 142.19 (C), 142.15 (C), 141.04 (C), 140.77 (C), 138.10 (C), 137.61 (C), 136.72 (C), 132.14 (CH), 129.45 (CH), 128.51 ($PhC_{2,3}$), 128.32 ($PhC_{2,3}$), 125.87 (CH), 121.52 (CH), 79.82 ($C_{bridgehead}$), 51.76 (PhC), 34.21 (CH_2), 33.67 ($PhCCH_2$ andCH_2COO), 22.37 (CH_2CH_2COO). Ms (FAB / NOBA $(M)^{+}$)972.5. ν_{max}/cm^{-1} 2929*w* (CH_{ar}), 2857*w* (Ch_{alk}), 1752*s* (C=O ester), 1592*m*, 1426*m*, 1227*s*, 1193*m*, 1133, 1023*m*,919*m*, 774*m*, 710*s*.

Phenyl-C_{61}-chloro butyric acid PCBCl.

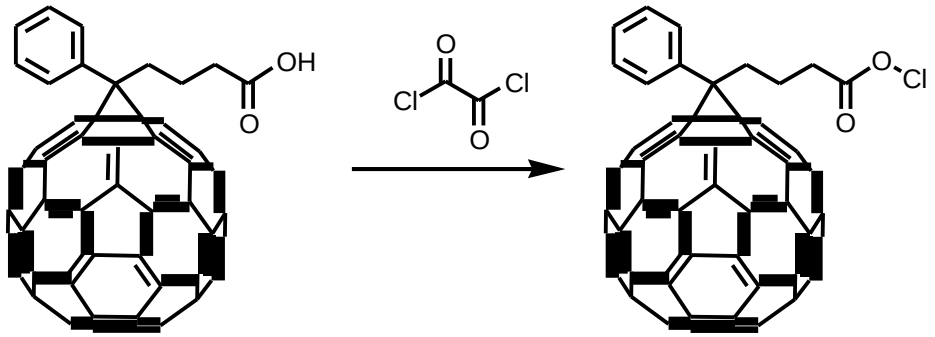

PCBA PCBCl

Oxalyl chloride (0.2 ml) was added to a suspension of PCBA (**35**) (290 mg, 0.32 mmol) in dry toluene (30 ml) and DMF (2 drops). The reaction mixture was then heated under refluxed and stirred overnight at 80^{o}C. The solvent was then evaporated under vacuum and the remaining black residue was then left without further purification.

Phenyl-C61-butyric acid benzyl ester 49 [102]

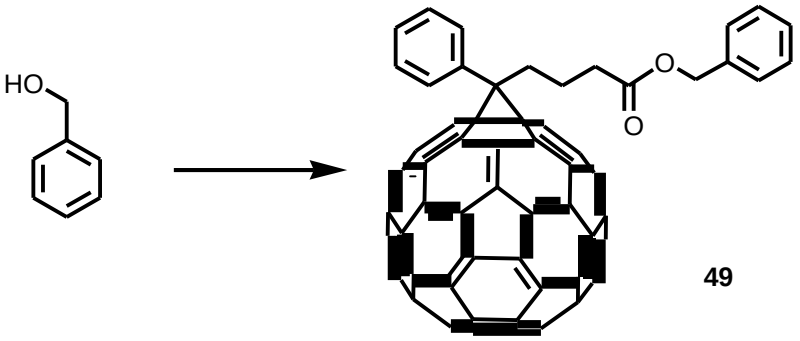

49

To a solution of PCBCl (330 mg, 0.36 mmol) in dry toluene (10 ml) was added a solution of benzyl alcohol (47 mg, 0.43 mmol), pyridine (0.01 ml, 0.72 mmol) and triethyl amine (0.1 ml, 0.72 mmol) in DCM (5 ml). A catalytic amount of DMAP (1 small crystal) was added at room temperature. The reaction mixture was heated under reflux for 24h. The reaction mixture was then cooled to room temperature to be precipitated into MeOH (200 ml). The precipitate was filtered and dried under high vacuum. The crude brown solid was purified by column chromatography (silica gel/ eluting with toluene:petroleum ether) afforded **49** as a brown powder (150 mg, 42%). ^{1}H NMR (400 MHz, $CDCl_3$) δ = 7.92(dd, 2H, *J*= 1.6 Hz, 6.8Hz, CH_{ar}), 7.54 (tt, 2H, *J*= 1.5Hz, 6.8Hz, *7*.8Hz, CH_{ar}), 7.47 (tt, 1H, *J*= 2Hz, 7.2Hz, 8Hz, CH_{ar}), 7.34 (m, 5H, CH_{ar}), 5.08 (s, 2H, CH_2), 2.91 (p, 2H, CH_2), 2.57 (t, 2H, *J*= 7.6Hz, CH_2), 2.21 (m, 2H, CH_2). ^{13}C NMR (100 MHz, $CDCl_3$) δ = 172.47 (COO), 150.62 (C), 148.71, (C), 147.72 (C), 145.87 (C), 145.27 (C), 145.10 (C) , 145.84 (C), 145.72 (C), 144.55 (C), 144.50 (C), 144.13 (C), 143.80 (C), 143.11 (C), 143.0 7 (C), 143.00 (C), 142.27 (C), 142.19 (C), 141.08 (C), 140.83 (C), 138.12 (C), 137.70 (C), 136.70 (C), 135.92 (CH), 132.14 (CH), 128.67 ($PhC_{2,3}$), 128.57 ($PhC_{2,3}$), 128.34 (CH), 79. 80 ($C_{bridgehead}$), 66.38 (PhC), 51.85 (CH_2), 34.17 (CH_2), 33.77 ($PhCCH_2$ andCH_2COO), 22.58 (CH_2CH_2COO). Ms (FAB / NOBA $(M)^+$) 986.13.

CHAPTER 3

N-(4-(trifluoromethyl)-2-nitrophenyl)benzene-1,4-diamine (80)

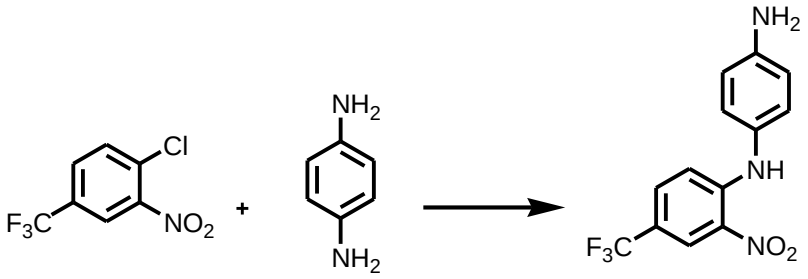

36 **79** **80**

1-Chloro-2-nitro-4-(trifluoromethyl)benzene (**36**) (5.00 g, 24.27 mmol), p-phenylenediamine (**79**) (2.40 g, 22.17 mmol) and triethylamine (3 ml, 22.17 mmol) were dissolved in THF (60 ml) and were heated under reflux for 2 days. The $N(Et)_3$.HCl salt was removed by filtration; the solvent (THF) was removed under vacuum. The residue was dissolved in DCM, washed with water (2 x 100 ml) and dried with $MgSO_4$, filtered and the solvent was removed under reduced pressure. Purification by column chromatography (silica gel/ eluting with petroleum ether/ ethyl acetate 7:3) afforded **80** as a red solid powder (3.50 g, 53%). Mp 116 ^{o}C. ^{1}H NMR (400 MHz, $CDCL_3$) δ = 9.49 (s, 1H, NH), 8.42 (s, 1H, CH), 7.40 (d, 1H, *J* = 9.2Hz, CH), 6.98 (d, 2H, *J* = 8.4Hz, CH), 6.96 (d, 1H, *J* = 8.4Hz, CH), 6.68 (d, 2H, *J* = 8.4 Hz, CH), 3.73 (s, 2H, NH) ^{13}C NMR (100 MHz, $CDCl_3$) δ = 146.79 (C), 145.79 (C), 131.61 (CH), 127.83 (C), 127.55 (CH), 124.71 (CH), 116.67 (CH), 116.04 (CH). Ms (FAB / NOBA $(M + H)^+$) 298.4ν_{max}/cm^{-1} 3414*s* (NH), 3349*s* (NH), 3221*w*(NH), 3016*m* (CH_{ar}), 2970*w* (CH_{alk}), 1738*w* (N-H), 1631*s* (aromatic C=C), 1573*s* , 1506*s*, 1357*m*, 1321*s* (C-NO_2), 1226*m*, 1091*m*, 919*s*, 827*m* (1,2,4-trisubstituated aromatic ring), 763*s*, 686*s*.

Anal Calc. for $C_{13}H_{10}F_3N_3O_2$ (C) 52.52, (H) 3.37, (N) 14.14; found (C) 52.50, (H) 3.35, (N) 14.08.

N-(2-amino-4(trifluoromethyl)phenyl)benzene-1,4-diamine (81)

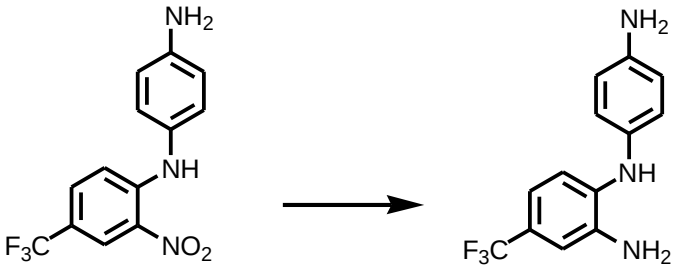

80 **81**

N-(4-(trifluoromethyl)-2-nitrophenyl)benzene-1,4-diamine (**80**) (3.50 g, 11.79 mmol), Pd(C) 10% (0.30 g) and ammonium formate (4.50 g, 71.43 mmol) were dissolved in methanol (60 ml) and were left stirring at room temperature for 1 h. The Pd(C) was removed by filtration; the solvent was removed under reduced pressure. The residue was washed with DCM to precipitate the ammonium formate, which was removed by filtration to produce a red solid (**81**) (3 g.). No further purification undergoes due to the instability of the compound.

10-(4-Aminophenyl)-7-(trifluoromethyl)-isoalloxazine (82)

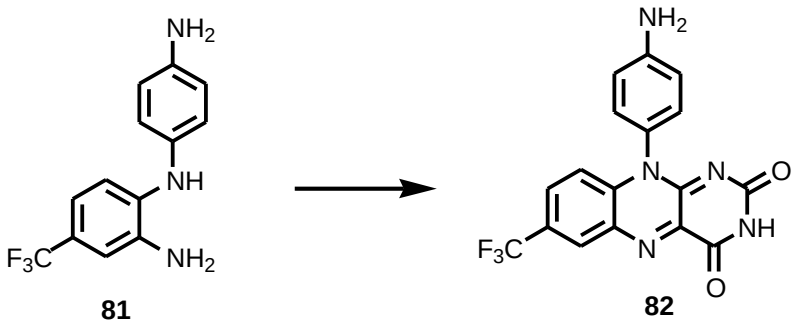

N-(2-amino-4(trifluoromethyl)phenyl)benzene-1,4-diamine (**81**) (3.00 g, 11.24 mmol), boric anhydride (0.78 g, 11.24 mmol) and alloxan monohydrate (1.6 g, 11.20 mmol) were dissolved in glacial acetic acid (50 ml) then were left stirring at room temperature for 1 h. The product was collected by adding DCM and then extracted from the reaction mixture. The mixture was dried over magnesium sulfate. The solution was filtered and the solvent was removed under reduced pressure. Purification by column chromatography (silica gel/ eluting with DCM/ petroleum ether 9:1) afforded **82** as a dark red powder (0.24 g, 55%), Mp > 300 ^{o}C. ^{1}H NMR (400 MHz, DMSO) δ = 11.52 (s, 1H, NH), 8.51 (s, 1H, CH), 8.03 (dd, 1H, *J* = 1.6Hz, 9Hz, CH), 7.09 (d, 1H, *J* = 8.8Hz, CH), 7.00 (d, 2H, *J* = 8.4Hz, CH), 6.78 (d, 2H, *J* = 8.4Hz, CH), 5.63 (s, 2H, NH_2). ^{13}C NMR (100 MHz, DMSO) δ = 159.28(C), 155.60(C), 152.70(C), 150.07(C), 141.16(C), 137.47(C), 133.84(C), 129.91(CH), 128.45(CH), 127.95(C), 125.80(C), 125.47(C), 124.90(CH), 123.14(CH), 122.20(CH), 118.68(CH), 114.34(CH). Ms (FAB / NOBA $(M + H)^{+}$)373.8. ν_{max}/cm^{-1} 3470*w*(NH), 3347(NH)*s*, 3016*m*(NH), 2970*s*(CH_{ar}), 2948*w*(CH_{alk}), 1737*w*(C=O amide) 1653*m*, 1538*m*, 1505*m*, 1446*m*, 1345w, 1293*s*, 1229*w*,1110*s*, 1065*s*, 903*s*, 841*s*, 765*s*. Anal Calc. for $C_{17}H_{10}F_3N_5O_2$ (C) 54.69, (H) 2.68, (N) 18.76 found (C) 53.42, (H) 2.68, (N) 17.67.

10-(4-(6-Octyl-naphthalindianhydride)phenyl)-7-(trifluoromethyl)-isoalloxazine (83)

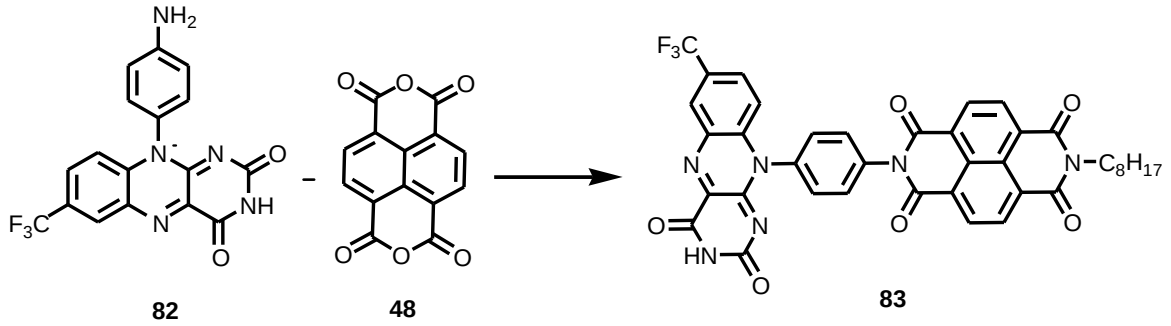

82 **48** **83**

A solution of naphthalene dianhydride (**48**) (0.30 g, 1.34 mmol) in dry DMF (50 ml) was heated to 140^{o}C under N_2 atmosphere then octylamine (0.19 g, 1.34 mmol) was added drop wise. The reaction mixture was heated under reflux for 24 h. before 10-(4-aminophenyl)-7-(triflouromethyl)-isoalloxazine (**82**) (0.50 g, 1.34 mmol) was added. After 5 days heating under reflux, the reaction mixture was cooled down. DMF was removed under reduced pressure. Purification by column chromatography (silica gel/ eluting with DCM/ acetone 9:1) and followed by recrystallization from diethyl ether afforded **83** as a yellowish brown powder (0.10 g, 10 %). Mp 190-192^{o}C. ^{1}H NMR (400 MHz, $CDCl_3$) δ = 11.65 (s, 1H, NH), 8.75 (s, 4H, CH_{NDI}), 8.61 (s, 1H, CH_{ar}), 8.12 (dd, 1H, *J* = 2.1Hz, 9.2Hz, CH_{ar}), 7.82 (d, 2H, *J* = 8.6Hz, CH_{ar}), 7.63 (d, 2H, *J* = 8.6Hz, CH_{ar}), 6.98 (d, 1H, *J* = 9.2Hz, CH_{ar}), 4.09 (t, 1H, *J* = 7.4Hz, 9.5Hz CH_2). 1.69 (br, 2H, CH_2), 1.23-135 (br, 10H, CH_2), 0.87 (t, 3H, *J* = 5.2Hz, 7Hz, CH_3). ^{13}C NMR (100 MHz, $CDCl_3$) δ = 162.85(C), 162.65(C), 159.09(C), 131.31(CH), 130.49(CH),128.47(CH), 126.86(C), 126.49(CH), 117.84(CH), 40.19(CH_2), 31.22(CH_2), 28.68(CH_2), 28.55(CH_2), 27.35(CH_2), 26.51(CH_2), 22.07(CH_2), 13.94(CH_3). Ms (FAB / NOBA $(M + H)^+$)735.8. Accurate Mass FAB/NOBA, Theoretical ion distribution $C_{39}H_{29}N_6O_6F_3$ (*m/z*) calculated 735.2179 observed 735.2173. ν_{max}/cm^{-1} 3357*w*(NH), 3082*m*(CH_{ar}), 2923*m*, 2855*w*(CH_{alk}), 1791*w*($C{=}O_{anhydride}$) 1716*m*(N-H) 1659*s*, 1595*s*, 1549*m*, 1333s, 1305*m*, 1248*m*, 1202*s*, 1166*s*, 1129*m*, 1068*s*, 841*m*, 767*s*.

4-(Trifluoromethyl)-N-isobutyl-2-nitrobenzenamine (84) [198]

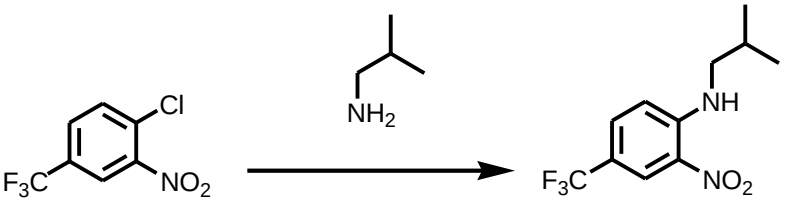

36 **84**

A solution of 1-chloro-2-nitro-4-(trifluoromethyl)benzene (**36**) (18.5 g, 81.85 mmol), isobutyl amine (18.4 g, 251 mmol) and triethylamine (18 mL) in THF (180 ml) was heated under reflux overnight. The ammonium salt was removed by filtration and the solvent (THF) was removed under vacuum. The residue was dissolved in DCM (100 ml), washed with water (100 ml x 3). The organic layer was dried over $MgSO_4$, filtered and the filtrate was evaporated under reduced pressure. The resultant product **84** was a yellow solid (18.2 g, 85%). $C_{11}H_{13}N_2O_2F_3$ (262.1). Mp 52°C (lit = 52-54°C[198]). Ms (FAB / NOBA $(M + H)^+$) 263. ^{1}H NMR (400 MHz, $CDCl_3$) δ = 8.53 (1H, d, *J* = 2Hz); 8.46 (1H, br s); 7.64 (1H, dd, *J* = 9Hz, 2Hz); 6.98 (1H, d, *J* = 9Hz); 3.25 (2H, m); 2.10 (1H, m); 1.12 (6H, d, *J* = 6Hz).

4-(Trifluoromethyl)-N-isobutylbenzene-1,2-diamine (85) [198]

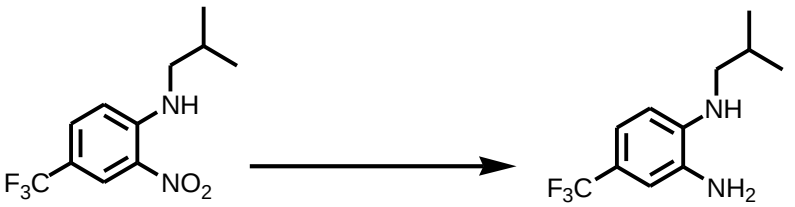

84 **85**

4-(Trifluoromethyl)-*N*-isobutyl-2-nitrobenzenamine (**84**) (18.1 g, 69.3 mmol) was dissolved in CH_3OH (300 ml). The solution was purged with N_2 and 10% Pd/C (1.4 g) was added. Ammonium formate (22.0g, 0.34moles) was then added to the vigorously stirred solution. The reaction mixture was left stirring under nitrogen atmosphere at room temperature for 2 h. The solution was then filtered and solvent was removed under reduced pressure. The residue was dissolved in DCM (150 ml), filtered to separate the ammonium formate and washed with distilled water (100 ml x3), dried under $MgSO_4$ and filtered. The filtrate was evaporated to afford **85** as yellow oil 15.7g (98%). No further purification was attempted due to the instability of the compound. $C_{11}H_{15}N_2F_3$ (232.1). ^{1}H NMR (400 MHz, $CDCl_3$) δ = 7.08 (1H, dd *J* = 9Hz and 1.5Hz, ArH), 6.74 (1H, d *J* = 1.5Hz, ArH), 6.53 (1H, d, *J* = 9Hz, ArH), 3.90 (2H, br s, NH_2), 2.89 (2H, d, *J* = 8Hz, CH_2CH), 2.18 (1H, br s, NH), 1.87 (1H, m, CH), 0.96 (6H, d, *J* = 8Hz, $2CH_3$).

7-(Triflouromethyl)-10-(isobutyl)-isoalloxazine (86) [198]

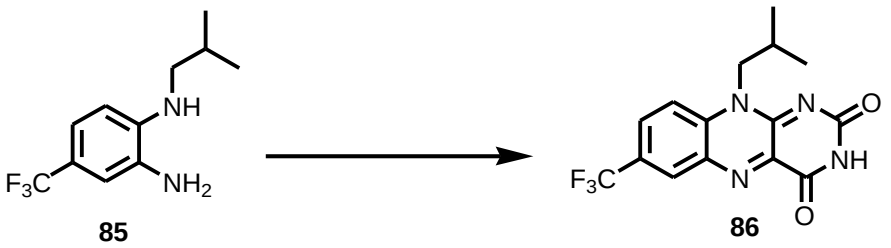

85 **86**

4-(Trifluoromethyl)-N-isobutylbenzene-1,2-diamine (**85**) (15.5g, 67.1 mmol) was dissolved in (350 ml) glacial acetic acid. Alloxan monohydrate (11.5 g, 80.5 mmol) and boric anhydride (9.4 g, 135.0 mmol) were then added. The mixture was left stirring at r.t. After 2 h., solvent was removed under reduced pressure. The residue was then diluted with distilled water (300 ml) and extracted with DCM (300 ml x3). The organic layers and solid material were separated from the aqueous layer and the dull yellow solid was isolated by filtration. The resultant product was filtered and washed with water and recrystalized from ethanol (300 ml) to afforded compound **86** (12.4 g, 47%). $C_{15}H_{13}N_4O_2F_3$ (338.3). Mp >220^{o}C as published [198]. Ms (FAB / NOBA $(M + H)^+$) 339. ^{1}H NMR (400 MHz, $CDCl_3$) δ 8.98 (1H, s, NH), 8.61 (1H, d, *J* =2Hz, ArH), 8.07 (1H, dd, *J* =9Hz and 2Hz, ArH), 7.78 (1H, d, *J*=9Hz, ArH), 4.46 (2H, br s, NCH_2), 2.27 (1H, m, CH-isobutyl), 1.08 (6H, d, *J* =7Hz, $2CH_3$).

3-(4-Nitrobenzyl)-7-(triflouromethyl)-10-(isobutyl)-isoalloxazine (87) [198]

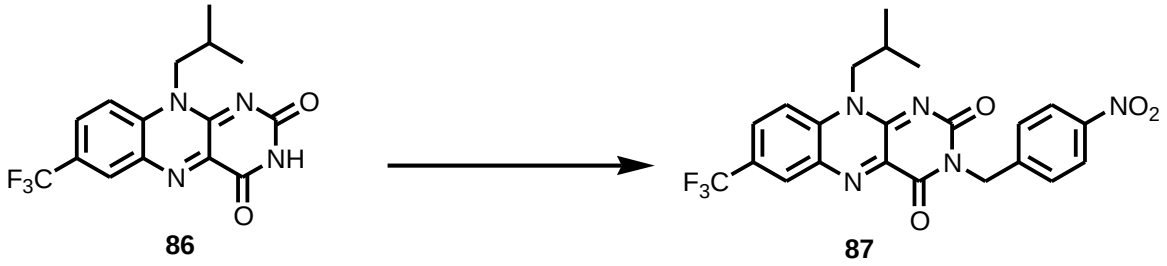

7-(Triflouromethyl)-10-(isobutyl)-isoalloxazine (**86**) (2.8g, 8.3mmol) was dissolved in DMF (45 ml). 4-nitrobenzyl chloride (2.1g, 12.4mmol) and K_2CO_3 (4.0g, 28.9mmol) in (200 ml) acetone were then added and stirred at RT protected from light for 2 days. The reaction mixture was filtered to remove K_2CO_3 and solvent was removed by reduced pressure. The residue was rinsed with a 1:1 mixture of diethyl ether/hexane (50mL) to remove DMF residue. Purification by column chromatography (silica gel/ eluting with DCM followed by DCM/acetone (90:10) afforded **87** as a yellow solid (3.79g, 96%). $C_{22}H_{18}N_5O_4F_3$ (473.13). Mp.= 184°C (lit = 184-186°C[198]). ^{1}H NMR (400 MHz, $CDCl_3$) δ 8.59 (1H, d, *J* = 2Hz, ArH_{alox}), 8.16 (2H, d, *J* = 8.5, 2ArH), 8.06 (1H, dd, *J* = 8Hz, 2Hz, ArH_{alox}), 7.76 (3H, m, 2ArH + ArH_{alox}), 5.31 (2H, s, $ArCH_2$), 4.55 (2H, br s, NCH_2), 2.44 (1H, sept, *J* = 7Hz, CH), 1.06 (6H, d, *J* = 6.5Hz, $2CH_3$).

3-(4-Aminobenzyl)-7-(triflouromethyl)-10-(isobutyl)-isoalloxazine (88) [198]

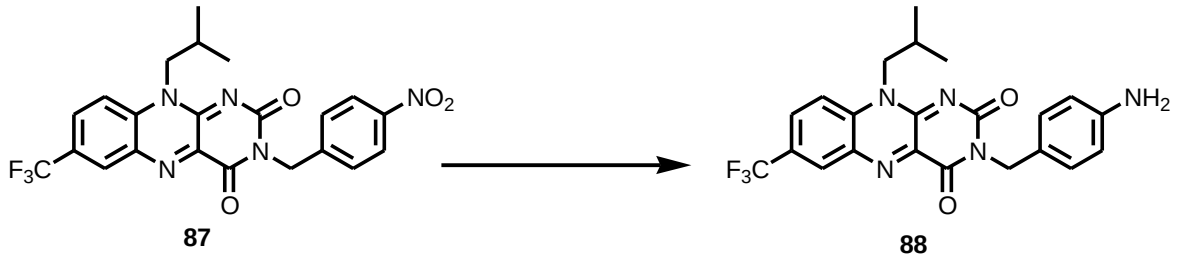

To a solution of 3-(4-nitrobenzyl)-7-(triflouromethyl)-10-(isobutyl)-isoalloxazine (**87**) (2.65 g, 5.6 mmol) in a mixture of methanol- THF (200 ml, 3:1), 5% Pd/C (400 mg), ammonium formate (1.07g, 17 mmol), and 5 drops of glacial acetic acid were added and left stirring at room temperature for 1h under nitrogen environment. The reaction mixture was filtered to remove Pd(C) and the filtrate was concentrated under reduced pressure. The remaining residue was dissolved in THF (150 mL), stirred to precipitate ammonium formate and filtered then the filtrate was concentrated under reduced pressure. Purification using column chromatography (silica gel/ eluting with DCM followed by DCM/acetone (80:20)) afforded **88** as a yellow solid (2.42g, 97%). $C_{22}H_{20}N_5O_2F_3$ (443.16). Mp > 230^oC as published[198]. ^1H NMR (400 MHz, $CDCl_3$) δ 8.52 (1H, d *J*=2Hz, ArH_{alox}), 7.99 (1H, dd, *J*=9Hz, 2Hz, ArH_{alox}), 7.71 (1H, d, *J*=9Hz, ArH_{alox}), 7.50 (2H, d, *J*=8.3, ArH), 6.56 (2H, d, *J*=8.3, 2ArH), 5.12 (2H, s, $ArCH_2$), 4.57 (2H, br s, NCH_2), 3.63 (2H, s, NH_2), 2.40 (1H, sept, *J*=7Hz, CH), 1.01 (6H, d, *J*=6.6Hz, $2CH_3$).

3-(4-(6-Octyl-naphthalindianhydride)benzyl)-7-(triflouromethyl)-10-(isobutyl)-isoalloxazine (89)

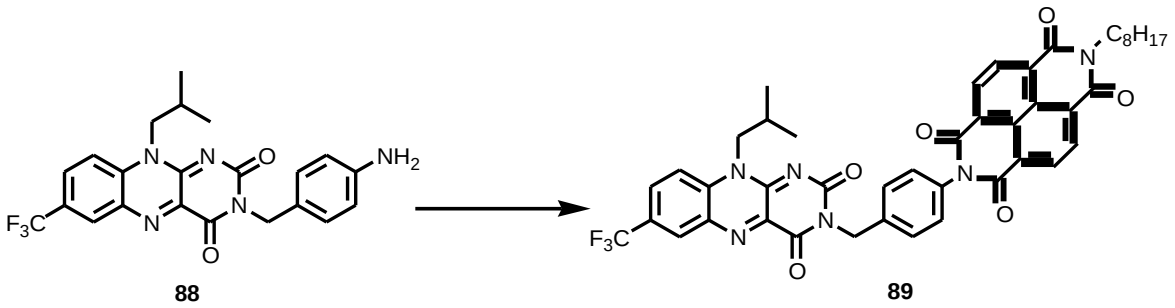

88 **89**

Naphthalene dianhydride (**48**) (0.36 g, 1.35 mmol) was dissolved in dry DMF (30 ml). The solution was heated to about 140^{o}C under N_2 atmosphere. To this, octylamine (0.18 g, 1.35 mmol) was added drop wise for about 10 minutes and the reaction mixture was heated under reflux for 24 h. 3-(4-Aminobenzyl)-7-(triflouromethyl)-10-(isobutyl)-isoalloxazine (**88**) (0.3 g, 0.68 mmol) was added and the mixture was left for another 4 days. The reaction mixture was cooled down and the DMF was removed under reduced pressure. Purification by column chromatography (silica gel/ eluting with 100% DCM) followed by recrystallization from diethyl ether afforded **89** as a brown yellowish product (0.06 g, 11 %). Mp 190-192^{o}C (dec). ^{1}H NMR (400 MHz, $CDCl_3$) δ = 8.78 (s, 4H, CH_{NDI}), 8.59 (d, 1H, *J* = 1.2Hz, CH_{ar}), 8.04 (dd, 1H, *J* = 2Hz, 9Hz, CH_{ar}), 7.89 (d, 2H, *J* = 8.4Hz, CH_{ar}), 7.76 (d, 1H, *J* = 8.8Hz, CH_{ar}), 7.28 (d, 2H, *J* = 8.4Hz, CH_{ar}), 4.62 (br, 2H, CH_2). 4.21 (t, 2H, *J* = 7.6Hz, 9.3Hz, CH_2), 2.48 (m, 1H, CH), 1.76 (m, 2H, CH_2), 1.44-1.22 (m, 12H, CH_2), 1.08 (d, 6H, *J* = 6.8Hz, CH_3), 0.88 (t, 3H, *J* = 6.6Hz, 75Hz, CH_3). ^{13}C NMR (100 MHz, $CDCl_3$) δ = 162.99(C), 162.77(C), 131.62(CH), 131.39(CH), 130.99(CH), 130.80(CH), 128.46(CH), 127.00(C),126.64(C), 116.72(CH), 44.75(CH_2), 41.09(CH_2), 31. 80(CH_2), 29.28(CH_2), 29.19(CH_2), 28.09(CH_2), 27.48(CH), 27.10(CH_2), 22.29(CH_2), 20.1 1 (CH_3), 14.09(CH_3). Ms (FAB / NOBA $(M + H)^+$) 804.6. Accurate Mass FAB/NOBA, Theoretical ion distribution $C_{44}H_{39}N_6O_6F_3$ (*m/z*) calculated 805.2961 observed 805.2971. ν_{max}/cm^{-1} 3062*w*(CH_{ar}), 2925*m*, 2855*w*(CH_{alk}), 1707*s*($C{=}O_{anhydride}$), 1660*s*(C=O amide), 1594*m*, 1558*s*, 1450*s*, 1340*m*, 1222*m*, 1170*m*, 1124*m*, 1002*m*, 820*m*, 767*s*, 717*m*. Anal Calc. for $C_{44}H_{39}F_3N_6O_6$ (C) 65.66, (H) 4.88, (N) 10.44 found (C) 65.16, (H) 5.01, (N) 9.99.

CHAPTER 4

2,1,3-Benzothiadiazole (103)[264]

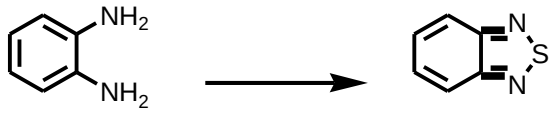

102 **103**

Thionyl chloride (14.82 g, 120 mmol) was added dropwise to a solution of 1,2-phenylenediamine (**102**) (10.81 g, 100 mmol) in toluene (80 mL) and pyridine (35 ml). The reaction mixture was heated under reflux at 90 °C for 2 h. After cooling, the mixture was filtered. Solvents were removed under reduced pressure. Purification by column chromatography (silica gel/ eluting with ethyl acetate in petroleum ether 2:8) afforded 103 as white crystals (8.05 g, 59%). Mp: 44-45 °C HRMS EI (m/z) $C_6H_4N_2S$ [M^+] 136.04.
^{1}H NMR (400 MHz, $CDCl_3$) δ 8.04 (dd, 2H, *J*= 3.4Hz, 7.2Hz) 7.63 (dd, 2H, *J*= 3.4Hz, 7.2Hz);

4,7-Dibromo-2,1,3-benzothiadiazole (104)[187,193,265]

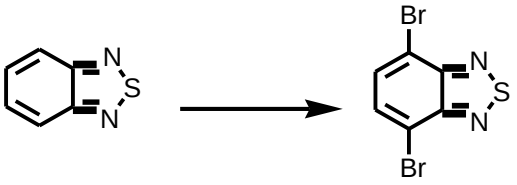

103 **104**

2,1,3-Benzothiadiazole (**103**) (6.80 g, 50 mmol) was added to HBr (70 mL). Bromine (7.74 mL, 150 mmol) in HBr (50 mL) was added slowly *via* a dropping funnel to the refluxing mixture. After six hours the solid was filtered off and washed exhaustively with water. The solid was then washed once with diethyl ether and dried under vacuum for eight h. to give the desired product **104** as cream needles (13.28 g, 90%). Mp:187-188°C. HRMS EI (m/z) $C_6H_2Br_2N_2S$ [M^+] 291.9/ 293.9. ^{1}H NMR (400 MHz, $CDCl_3$) δ 7.76 (s, 2H).

4,7-Di(thiophen-2-yl)benzo-[2,1,3]-benzothiadiazole. (105)[188,265]

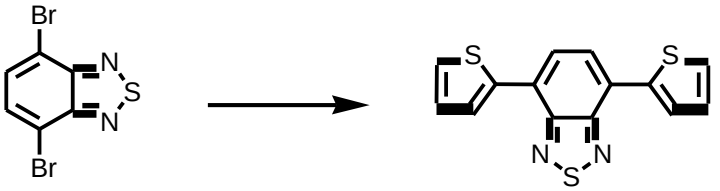

104 **105**

4,7-Dibromo-2,1,3-benzothiadiazole (**104**) (12.82 g, 43.6 mmol) and tributyl(thien-2-yl)stannane (30.50 mL. 95.9 mmol) were added to THF (300 mL). To this, $PdCl_2(PPh_3)_2$ (0.61 g, 0.9 mmol) was added. The mixture was heated under reflux for three h. The solvent was removed under reduced pressure. Purification by column chromatography (silica gel/ eluting with petroleum ether 100%) afforded **105** as red needles (12.69 g, 98.6%). Mp 120-121°C. HRMS EI (m/z) $C_{14}H_8N_2S_3$ [M^+] 300.0. ^{1}H NMR (400 MHz, $CDCl_3$) δ 8.06 (d, 2H, *J* = 3.6 Hz) 7.82 (s, 2H), 7.40 (d, 2H, *J*= 4.8Hz), 7.15 (t, 2H, *J* = 3.6Hz, 4.4Hz);

3,6-Di(thiophen-2-yl)benzene-1,2-diamine).(106)

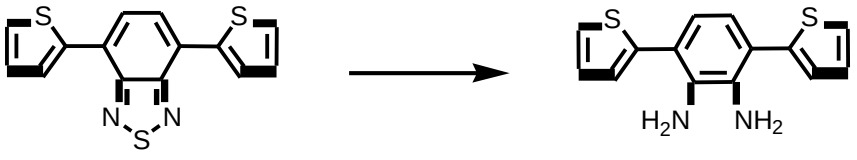

105 **106**

4,7-Dithien-2'-yl-2,1,3-benzothiadiazole (**105**) (5.86 g, 21.5 mmol) was added to THF (150 mL) and cooled to 0 °C. Lithium aluminium hydride (3.04 g, 80.0 mmol) was added portionwise. When the addition of lithium aluminium hydride was complete, the reaction mixture was left stirring for 1 h. at room temperature and then heated under reflux for 24 h. The mixture was then cooled to 0°C and water (10 mL) was added slowly. The product was extracted with diethyl ether (3 x 20 mL) and the organic extracts were washed with brine (3 x 20 mL) and dried over magnesium sulphate and filtered and then concentrated under reduced pressure. Purification by column chromatography (silica gel/ eluting with 100% DCM) gave (**106**) as a pink solid (4.20 g, 72%). Mp 108-109°C. ^{1}H NMR (400 MHz, $CDCl_3$) δ 7.41 (d, 2H, *J*= 5.2), 7.23 (d, 2H, J= 2.4Hz), 7.18 (t, 2H, J= 4Hz, 4.4Hz), 6.92 (s, 2H), 3.89 (br, 4H, NH). HRMS EI (*m/z*) $C_{14}H_{13}N_2S_2$ [M^+] 272.1 ν_{max}/cm^{-1} 3396*s* (NH), 3363*s* (NH), 3327*s*(NH), 3258*w* (NH), 2209*w* (CH_{ar}), 1735*w* (N-H), 1647*w* (aromatic C=C), 1608*s* , 1442*s* (N-H), 1240*s*, 1132*s*, 1065*s*, 868*s*, 763*w*, 722*m* (1,2,4-trisubstituated aromatic ring), 668*w*.

6,9-Dithien-2-yl-10-ethyl-isoalloxazine (107)

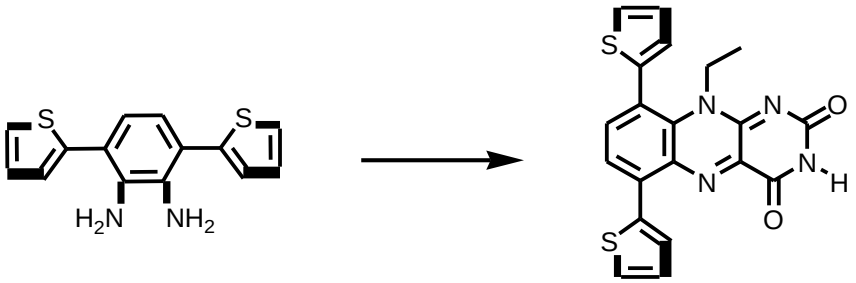

106 **107**

1,2-Diamino-3,6-dithien-2'-ylbenzene (**106**) (4.34 g, 15.96 mmol) and triethylamine (3.29 mL, 23.94 mmol) were dissolved in THF (150 ml). At –78 ˚C, acetyl chloride (1.14 mL, 15.96 mmol) was added drop wise and the mixture was allowed to stir for 24 h. at room temperature. The reaction mixture was concentrated under reduced pressure to give orange crystals. The crude product (5.03 g) was dissolved in THF (125 ml) and cooled to 0 ˚C. Lithium aluminium hydride (3.63 g, 95.4 mmol) was then added portion wise and was left stirring for 24 h. Water (10 mL) followed by 10% sodium hydroxide solution (10 mL) was added dropwise. The precipitate was then filtered and the filtrate was then extracted with diethyl ether (3 x 20 mL). The extracts were washed with brine (3x2 ml) and dried over magnesium sulphate. The mixture was filtered and concentrated under reduced pressure to give red oil. The crude product (3.47 g) was then dissolved in acetic acid (150 mL). Alloxan monohydrate (1.85 g, 11.57 mmol) and boric anhydride (1.6 g, 23 mmol) were added to the mixture and was allowed to stir overnight. The mixture was concentrated under reduced pressure. Purification by column chromatography (silica gel/ eluting with 15-25% acetone in DCM) followed by recrystallisation from ethanol gave the desired product **107** as dark red crystals (0.56g, 9%). Mp 280 ˚C. ^{1}H NMR (400 MHz, $CDCl_3$) δ 8.41 (br, 1H, s), 7.94 (d, 1H, *J* = 4Hz), 7.93 (dd, 1H, *J* = 1.2Hz, 4Hz), 7.78 (d, 1H, *J* = 8Hz), 7.66 (dd, 1H, *J* = 0.8Hz, 5.2Hz), 7.52 (dd, 1H, *J* = 1.2Hz, 5.2Hz), 7.21 (dd, 1H, *J* = 4Hz, 5.2Hz), 7.15 (dd, 1H, *J* = 3.2Hz, 4.8Hz), 7.12 (dd, 1H, *J* = 1.2Hz, 3.2Hz), 4.57(br, 2H, CH_2), 1.09(t, 3H, *J* = 7.2Hz). ^{13}C NMR (100 MHz, $CDCl_3$) δ 159.65 (C),155.81 (C), 152.03 (C), 139.89 (C), 141.30 (CH), 137.48 (C), 135.77 (C), 132.68 (C), 132.84 (CH), 132.21 (C), 132.48 (CH), 129.07 (C), 129.74 (CH), 128.21 (CH), 127.69 (CH), 127.40 (CH), 123.61 (CH), 121.47 (C), 43.84 (CH_2), 13.97 (CH_3). Ms (FAB / NOBA $(M + H)^+$) 406.1 ν_{max}/cm^{-1} 3162*w*(NH), 3099*m*, 3040*m*, 2997*m*(CH_{ar}), 2821*s*(CH_{alk}), 1716*s*(C=O amide) 1654*s*, 1591*s*, 1572*s*, 1539*s*, 1505*s*, 1462*s*, 1418*m*, 1349*m*,1253*s*, 1229*s*, 1049*m*, 807*m*.

6,9-Dithien-2-yl-10-ethyl-3-heptyl-isoalloxazine (108)

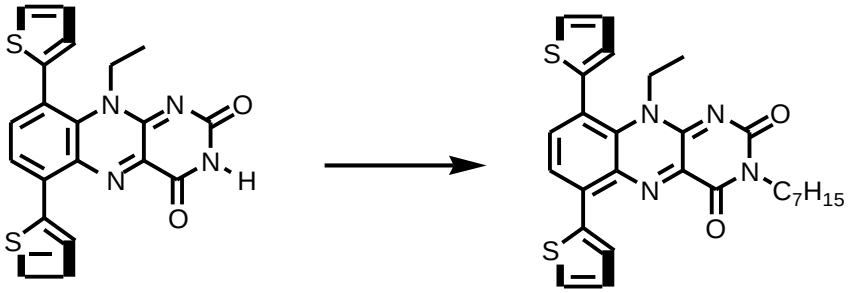

107 **108**

To a solution of 6,9-dithien-2-yl-10-ethyl-isoalloxazine (**107**) (0.23 g, 0.57 mmol) in dry DMF (13 ml), iodoheptane (0.19 ml, 1.13 mmol) and sodium carbonate (0.31 g, 2.27 mmol) were added. The reaction mixture was allowed to stir for 48 h. at room temperature. DMF was removed under reduced pressure. Purification by column chromatography (silica gel/ eluting with ethyl acetate in DCM 1:9) followed by recrystallisation from ethanol gave the desired product (**108**) as a red crystals (0.2g, 70%). Mp 183-184^{o}C. ^{1}H NMR (400 MHz, $CDCl_3$) δ 7.97 (dd, 1H, *J* = 1.2Hz, 4Hz), 7.95 (d, 1H, *J* = 8.4Hz), 7.78 (d, 1H, *J* = 8Hz), 7.68 (dd, 1H, *J* = 1.2Hz, 8.4Hz), 7.54 (dd, 1H, *J* = 1.2Hz, 5.2Hz), 7.23 (dd, 1H, *J* = 4Hz, 5.2Hz), 7.18 (dd, 1H, *J* = 4Hz, 5.2Hz), 7.14 (dd, 1H, *J* = 1.2Hz, 3.6Hz), 4.57(br, 2H, CH_2), 4.13 (t, 2H, *J*= 7.6Hz, CH_2), 1.78 (m, 2H, CH_2), 1.46-1.26 (m, 10H,CH_2), 1.10 (t, 3H, *J* = 6.8Hz, CH_3), 0.91 (t, 3H, *J*= 6.8Hz, CH_3). ^{13}C NMR (100 MHz, $CDCl_3$) δ 159.39 (C),155.84 (C), 150.29 (C), 140.77 (CH), 139.95 (C), 138.00 (C), 137.31 (C), 135.39 (C), 132.75 (C), 132.75 (C), 132.40 (CH), 129.46 (CH), 128.09 (CH), 127.63 (CH), 127.56 (CH), 127.23 (CH), 123.18 (CH), 121.29 (C), 43.08 (CH_2), 42.27 (CH_2), 31.80 (CH_2), 29.08 (CH_2), 27.83 (CH_2), 27.07 (CH_2), 22.61 (CH_2), 14.10 (CH_3), 14.05 (CH_3). MS (FAB / NOBA $(M + H)^+$) 505.0. ν_{max}/cm^{-1} 3080*w*(CH_{ar}), 2924*m*, 2853*s*(CH_{alk}), 1703*s*(C=O amide), 1645*s*, 1596*s*, 1575*s*, 1539*s*, 1512*s*, 1470*s*, 1435*s*, 1342*m*,1266*s*, 1217*m*, 1046*m*, 842*m*, 674*m*. Anal Calc. for $C_{27}H_{28}N_4O_2S_2$. (C) 64.26, (H) 5.59, (N) 11.10 found (C) 63.59, (H) 5.69, (N) 10.51.

Poly(6,9-Dithien-2-yl-10-ethyl-3-heptyl-isoalloxazine) (109)[201]

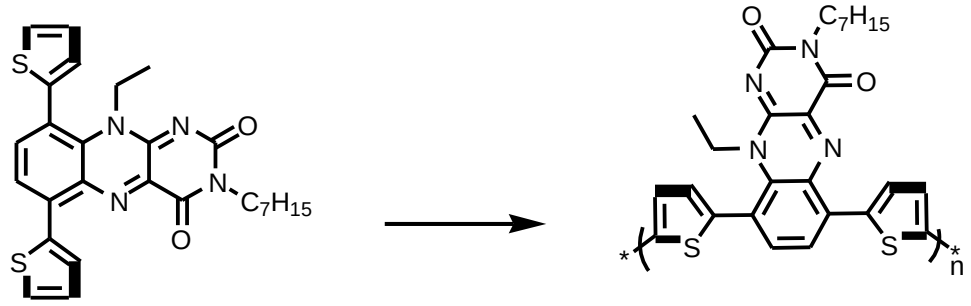

108 **109**

Chemical oxidation of the monomer 6,9-dithien-2-yl-10-ethyl-3-heptyl-isoalloxazine (**108**) was carried in a three necked flask, iron trichloride (0.19 g, 1.19 mmol) was dissolved in dry chloroform (10 ml) under N_2 to which a solution of monomer 38 (0.15g, 0.30mmol) in chloroform (5ml) was added dropwise. The mixture was stirred for 24 h. at room temperature under a gentle N_2 stream. Then the solution was precipitated into methanol (1 L), the black precipitate was collected via suction filtration and washed with methanol many times to afford a dark greenish powder of polymer **109**. The polymer was characterized by gel permeation chromatography GPC in THF which gave: Mn = 5237, Mw = 6709, Mp = 5443, PD = 1.28 Area % = 100.000

6,9-Dithien-2-yl-10-ethyl-3-(2-ethyl-hexyl)-isoalloxazine (110)

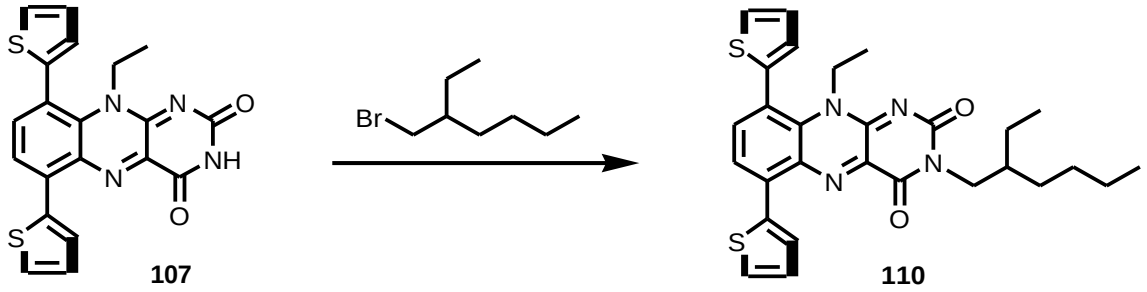

107 **110**

To a solution of 6,9-dithien-2-yl-10-ethyl-isoalloxazine (**107**) (1.1g, 2.7 mmol) in acetone (50 ml), 1-bromo-2-ethyl-hexane (4g, 22.6 mmol) and potassium carbonate (750 mg, 5.4 mmol) were added and left stirring under reflux for 4 days. The reaction mixture was then allowed to cool to room temperature and solids were removed by filtration. Solvent was removed under reduced pressure. Purification by column chromatography (silica gel/ eluting with DCM then DCM / MeOH (98:02) gave the desired product **110** as a red crystals (0.8g, 57%).. ^{1}H NMR ($CDCl_3$, 400 MHz) δ 7.93 (dd, 1H, *J* = 1.2Hz, 3.6Hz), 7.91 (d, 1H, *J* = 8Hz), 7.74 (d, 1H, *J* = 8Hz), 7.64 (dd, 1H, *J* = 0.8Hz, 5.2Hz), 7.50 (dd, 1H, *J* = 1.2Hz, 5.2Hz), 7.19 (dd, 1H, *J* = 4Hz, 5.2Hz), 7.15 (dd, 1H, *J* = 3.6Hz, 5.2Hz), 7.12 (dd, 1H, *J* = 1.2Hz, 3.2Hz), 4.05(br, 2H, CH_2), 4.13 (t, 2H, *J*= 6.5Hz, CH_2), 2.00 (m, 1H, CH_2), 1.38 - 1.29 (m, 8H,CH_2), 1.06 (t, 3H, *J* = 7Hz, CH_3), 0.92 (t, 3H, *J*= 7.6Hz, CH_3), 0.88 (t, 3H, *J*= 7Hz, CH_3). ^{13}C NMR ($CDCl_3$, 100 MHz) δ 159.71 (C),156.17 (C), 150.29 (C), 140.67 (CH), 139.96 (C), 137.94 (C), 137.34 (C), 135.42 (C), 133.42 (C), 132.76 (C), 132.35 (CH), 129.46 (CH), 128.10 (CH), 127.61 (CH), 127.51 (CH), 127.24 (CH), 123.16 (CH), 121.28 (C), 45.94 (CH_2), 43.06 (CH_2), 37.51 (CH), 30.59 (CH_2), 28.64 (CH_2), 23.89 (CH_2), 23.13 (CH_2), 14.13 (CH_3), 14.03 (CH_3), 10.58 (CH_3).

6,9-Bis-(5-bromo-thiophen-2-yl)-10-ethyl-3-(2-ethyl-hexyl)-isoalloxazine (111)

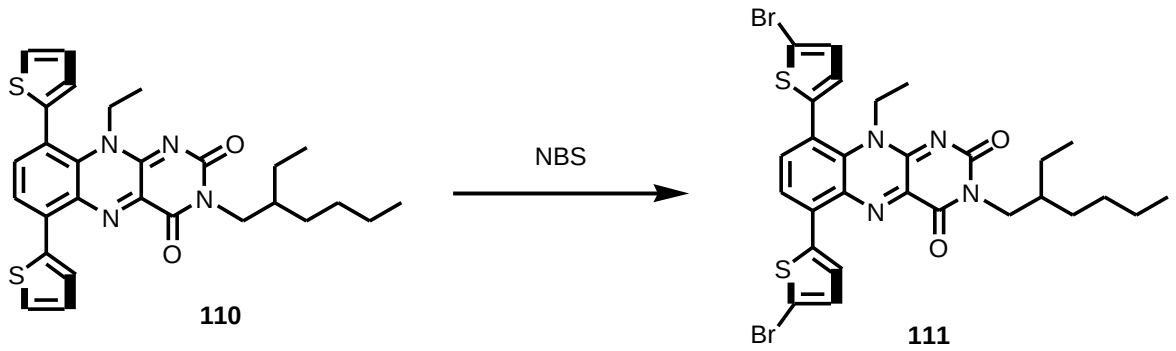

110 **111**

A solution of 6,9-dithien-2-yl-10-ethyl-3-(2-ethyl-hexyl)-isoalloxazine (**110**) (2.5 g, 4.8 mmol) in DCM (100 ml) was prepared and protected from light. After cooling to 0^{o}C, N-bromosuccinimide (3.4 g, 12.3 mmol) was added in one portion. After 24 h. of stirring at 30 ^{o}C the reaction was cooled to room temperature then was diluted with DCM (100 ml) and was washed with water (150 ml x 3). The extracted organic layer was then dried over anhydrous $MgSO_4$ and filtered then concentrated under reduced pressure. The desired product was purified by column chromatography using CH_2Cl_2 / petroleum ether 50:50 to yield **111** as a red brown solid (2.27 g, 70%) ^{1}H NMR ($CDCl_3$, 400 MHz) δ 7.83 (dd, 1H, *J* = 2.8Hz, 8Hz), 7.70 (t, 1H, *J* = 8Hz), 7.62 (d, 1H, *J* = 9.2Hz), 7.13 (d, 1H, *J* = 4Hz), 7.11 (dd, 1H, *J* = 2.4Hz, 3.6Hz), 6.89 (t, 1H, *J* = 4Hz), 4.60(br, 2H, CH_2), 4.05 (q, 2H, *J*= 5.2Hz, 8 Hz CH_2), 1.98 (m, 1H, CH_2), 1.38 - 1.29 (m, 8H,CH_2), 1.12 (m, 3H, CH_3), 0.92 (t, 3H, *J*= 7Hz, CH_3), 0.89 (t, 3H, *J*= 6.8Hz, CH_3). ^{13}C NMR ($CDCl_3$, 100 MHz) δ 159.41 (C),155.99 (C), 150.29 (C), 141.35 (CH), 138.26 (C), 137.98 (C), 137.98 (C), 135.62 (C), 132.86 (C), 130.43 (CH), 129.96 (CH), 128.99 (CH), 128.56 (CH), 121.97 (CH), 121.56 (CH), 45.96 (CH_2), 43.29 (CH_2), 37.52 (CH), 30.58 (CH_2), 28.61 (CH_2), 23.91 (CH_2), 23.16 (CH_2), 14.18 (CH_3), 13.95 (CH_3), 10.64 (CH_3). Ms (FAB / NOBA $(M+H)^+$) $C_{28}H_{28}Br_2N_4O_2S_2$ 674.0 /676.49.

Synthesis of polymer 113

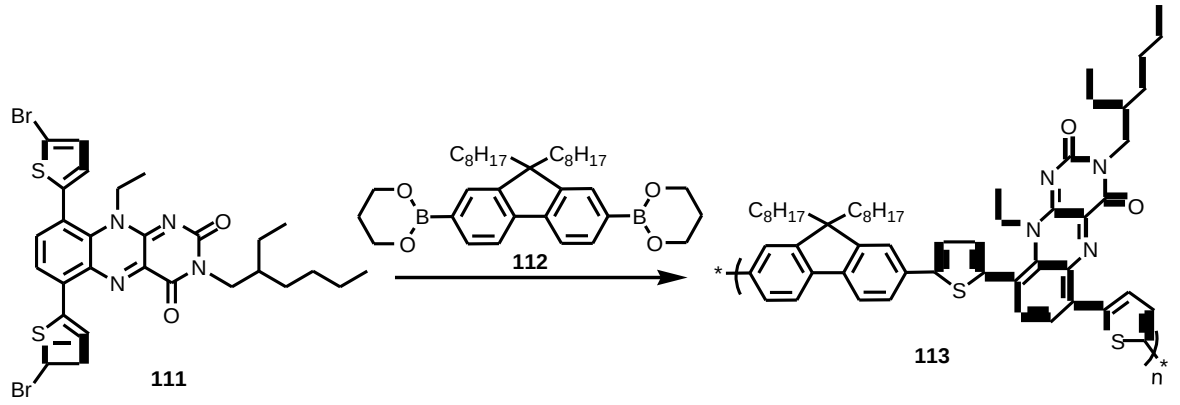

9,9-Dioctyl fluorine-2,7-bis(trimethyl borate) (**112**) (335 mg, 0.60 mmol) and 5,5-dibromo-2,2-bithiophene flavin (**111**) (370 mg, 0.55 mmol) were dissolved in THF (15 ml) to which 10% aq K_2CO_3 (2 ml) was added together with $Pd(PPh_3)_4$ (20 mg, 0.017 mmol). The mixture was deoxygenated by N_2 bubbling for 15 min. The flask was sealed under N_2 and heated for 2 days at 80^{o}C protected from light. End capping of the polymer was carried out by addition of phenyl boronic acid (4 mg) then left to stir for a further 12 h. at 80^{o}C before adding bromobenzene (10 mg) to end cap the boronic ester group of the polymer. The mixture was stirred a further 12 h. at 80^{o}C. The mixture was diluted with chloroform (100 ml) and washed with distilled water (100 ml x 3). The organic layer was dried over $MgSO_4$, filtered and evaporated. The product was passed through a short column of alumina to remove catalyst. The polymer was dissolved in $CHCl_3$ (25 ml) and precipitated into MeOH to yield a greenish polymer **113**. Yield (150 mg, 30.2%) $(C_{57}H_{68}N_4O_2S_2)_n$

The polymer was characterized by gel permeation chromatography GPC in THF. The result was Mp = 17134, Mn = 11632, Mw = 20268, PD = 1.74243 Area % = 100.000

CHAPTER 5

N-(4-methyl-3-nitrophenyl) isobutyramide (127) [221]

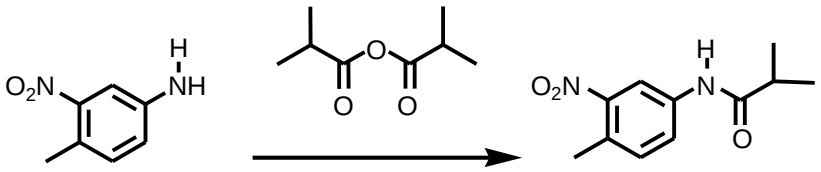

126 **127**

A solution of 4-methyl-3-nitroaniline (**126**) (10 g, 65.70 mmol), triethylamine (66.60 ml, 0.48 mol) and isobutyric anhydride (47.3 ml, 0.29 mol) in toluene (112 ml) was stirred with heating to reflux under nitrogen. After 48 h. the reaction was stopped and solvent was evaporated under reduced pressure to give a dark-brown liquid residue which was dissolved in CH_2Cl_2 (150 ml), and washed with saturated aqueous sodium bicarbonate solution (2 x 100 ml) and once with water (100 ml). The organic layer was dried with anhydrous magnesium sulphate, filtered and the solvent was removed under reduced pressure and the residue was recrystallized from methanol. The pale yellow crystals were collected by filtration to afford **127** (12 g, 82%). Mp=113^{o}C. ^{1}H NMR (400 MHz, $CDCl_3$)/ppm 8.32 (bs, 1H, NH), 8.19 (d, 1H, *J* = 2.2Hz, CH_2), 7.77 (dd, 1H, *J* = 2.3Hz, 8.3Hz, CH), 7.24(d, 1H, *J* = 8.3Hz, CH), 2.58(sept, 1H, CH), 2.52(s, 3H, CH_3), 1.19(d, 6H, *J* = 7Hz, CH_3).

N-(3-amino-4-methylphenyl) isobutyramide (128) [221]

127 **128**

Pd on carbon (100.4 mg) was added to a solution of ammonium formate (9.06 g, 0.14 mol) in methanol (190 ml). The reaction flask was flushed with nitrogen before the addition of *N*-(4-methyl-3-nitrophenyl)isobutyramide (**127**) (3.06 g, 13.77 mmol). The reaction mixture was stirred for 90 minutes at 40 ^{o}C before the mixture was filtered to remove the Pd catalyst. The solvent was removed under reduced pressure to give a white solid residue. The residue was then suspended with DCM (190 ml) and heated to up to 40 ^{o}C for 30 minutes to separate the soluble material from the insoluble ammonium formate, which was separated by filtration. The solvent was removed by reduced pressure to give pure product of **128** (1.5g, 57%). Mp 160^{o}C. ^{1}H NMR (400 MHz, $CDCl_3$) δ = 7.25 (s, 1H, CH_{ar}), 7.03 (br, 1H, NH), 6.98 (d, 1H, *J* = 8Hz, CH_{ar}), 6.62 (d, 1H, *J* = 8Hz, CH_{ar}), 3.65 (br, 2H, NH_2), 2.49 (m, 1H, CH), 2.15 (s, 3H, CH_3), 1.27 (d, 6H, *J* = 6Hz, CH_3).

N1 –isobutyl-4-methylbenzene-1, 3-diamine (129) [221]

128 **129**

In an ice bath, $LiAlH_4$ (3.01 g, 79.30 mmol) was added with stirring to dry THF (200 ml) under a N_2 atmosphere. To this stirred suspension *N*-(3-amino-4-methylphenyl) isobutyramide (**128**) (3.51g, 18.27mmol) was added. The ice bath was removed and the stirred reaction mixture was left at room temperature overnight. The reaction was heated under reflux for 4 h and the reaction mixture was left again stirring at room temperature overnight. The remaining $LiAlH_4$ was deactivated by drop-wise addition of water (7 ml), aqueous sodium hydroxide (15 wt%, 7 ml) and another amount of water (14 ml). The white precipitate was removed by filtration and washed with diethyl ether (150 ml). The solution was dried over magnesium sulphate, and the solvent was evaporated under reduced pressure to give the dark brown liquid as crude **129** (3.11g). No further purification and no further analysis were done due to instability of the product.

8-Amino-10-isobutyl-7-methyl-isoalloxazine (130) [221]

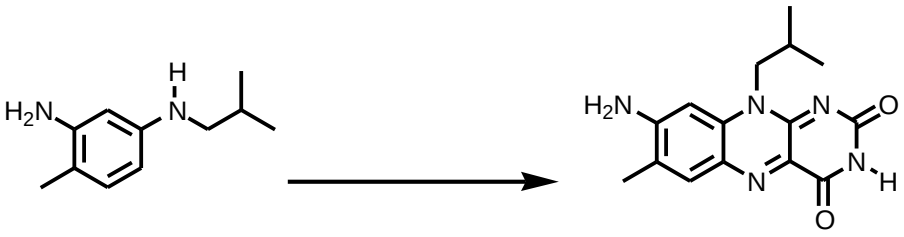

129 **130**

N[1] –isobutyl-4-methylbenzene-1,3-diamine (**129**) (3.11g) and violuric acid monohydrate (3.06g, 17.48 mmol) were dissolved in glacial acetic acid (150 ml). The stirred reaction mixture was heated under reflux for 45 minutes and then was left stirring at room temperature for two days. The orange precipitate was collected by filtration and washed with water (60 ml) and diethyl ether (20 ml). The orange product **130** (0.8g, 15.3%) was obtained. Mp > 300. ^{1}H NMR (400 MHz, DMSO) δ = 10.94 (s, 1H, NH), 7.67 (s, 1H, CH_{ar}), 7.22 (br, 2H, NH_2), 6.79 (s, 1H, CH), 4.33 (bs, 2H, CH_2), 2.35 (m, 1H, CH), 2.24 (s, 3H, CH_3), 0.96 (d, 6H, *J* = 6.8Hz, CH_3).

10-Isobutyl-7-methyl-8-{(4-diethylamino)-phenylazo}-isoalloxazine (131)[221]

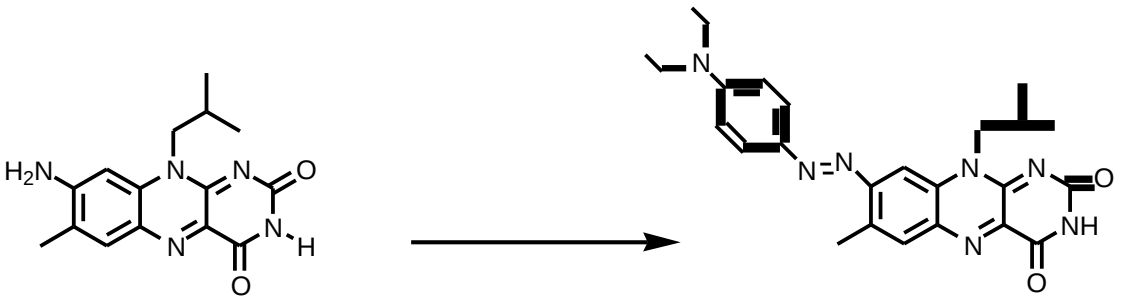

130 **131**

8-Amino-10-isobutyl-7-methyl-isoalloxazine (**130**) (0.30 mg, 0.99 mmol) was dissolved in glacial acetic acid (35 ml) under heating and then this solution was allowed to cool down to room temperature. On drop-wise addition of the flavin solution to a stirred mixture of sodium nitrate (0.08 mg, 1.09 mmol) and conc. sulphuric acid (1.5 ml), prepared at 0^{o}C, a colour change from colourless over red to yellow occurred. The temperature was maintained below 5^{o}C. Water was added to prevent the mixture from freezing. The diazonium salt solution was stirred for another 30 minutes at 0^{o}C. The flask was charged with N-diethyl aniline and aqueous sulphuric acid (18wt%, 5 ml) and cooled down to 0^{o}C. The diazonium salt solution was afterwards added drop wise to the acidic aniline mixture. Instantly a colour change to blue-took place. Subsequently the pH of the reaction mixture was raised to 4.2 by careful addition of solid sodium carbonate. Water was added to prevent high viscosity of the mixture. On raising the pH a bluish-green precipitate formed. This was collected by filtration after another 4 h. of stirring at 0^{o}C. The solid was washed intensively with water to remove sodium carbonate. The crude product (0.34 g) was collected and recrystalysed from ethanol and acetone (5:1), yield **131** as a blue solid (0.3g, 66%). ^{1}H NMR (400 MHz, $CDCl_3$) δ = 8.31 (s, 1H, NH), 8.11 (s, 1H, CH_{ar}), 7.88 (d, 2H, *J* = 8.4Hz, CH_{ar}), 7.70 (s, 1H, CH_{ar}), 6.71 (d, 2H, J = 8.8Hz, CH_{ar}), 4.61 (br, 2H, CH_2), 3.46 (q, 4H, CH_2), 2.41 (m, 1H, CH), 1.22 (t, 6H, *J* = 7.2Hz, CH_3), 0.99 (d, 6H, *J* = 6.8Hz, CH_3).

10-Isobutyl-7-methyl-8-{(4-diethylamino)-phenylazo}-3-methyl-isoalloxazine (132) [221]

131 **132**

To a solution of 10-isobutyl-7-methyl-8-{(4-diethylamino)-phenylazo}-isoalloxazine (**131**) (0.17 g, 0.37 mmol) and K_2CO_3 (0.21 g, 1.48 mmol) in DMF (15 ml) at 60 ^oC, CH_3I (0.11 g, 0.74 mmol) was added. The reaction was allowed to proceed overnight. Upon cooling, the solvent was reduced under reduced pressure. The reaction was quenched with water and extracted with chloroform. The organic layers were combined, washed extensively with water and then washed with brine, dried over anhydrous $MgSO_4$, filtered, and reduced under reduced pressure onto silica gel. The crude product was then purified using flash column chromatography (1:1) Hexane/ Ethyl Acetate followed by recrystalization from methanol yielding **132** as a blue solid (0.10 g, 57%). ^1H NMR (400 MHz, $CDCl_3$) δ = 8.13 (s, 1H, CH_{ar}), 7.88 (d, 2H, *J* = 8.8Hz, CH_{ar}), 7.68 (s, 1H, CH_{ar}), 6.71 (d, 2H, *J* = 10Hz, CH_{ar}), 4.62 (br, 2H, CH_2), 3.47 (s, 3H, CH_3), 3.45 (q, 4H, CH_2), 2.39 (m, 1H, CH), 1.21 (t, 6H, *J* = 6.4Hz, CH_3), 0.98 (d, 6H, *J* = 6.4Hz, CH_3).

CHAPTER 6

N-(6-aminopyridin-2-yl)propionamide (147)[253]

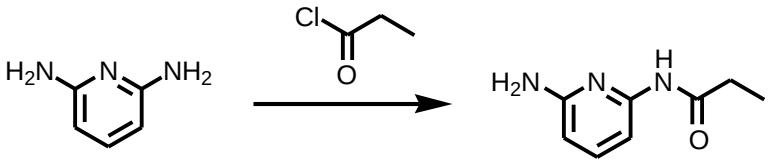

146 **147**

2,6-Diamino pyridine (**146**) (10 g, 91.74 mmol) was dissolved in a mixture of CH_2Cl_2 (500 ml) and triethylamine (13 ml, 91.74 mmol). To this propionyl chloride (8 ml, 91.74 mmol) was added drop wise for 1 h and left stirring at room temperature for 24 h. The ammonium salt was removed by filtration. The solvent was removed under reduced pressure. Purification by column chromatography (silica gel/ eluting with DCM/ethyl acetate 4:1) yielded (**147**) as a creamy solid (4.00 g, 26%), Mp 142-143^oC. ^1H NMR (400 MHz, $CDCl_3$) δ 7.61 (s, 1H, NH), 7.47 (d, 1H, *J* = 7.6Hz), 7.38 (t, 1H, *J* = 8Hz), (d, 1H, *J* = 8Hz), 4.24 (s, 2H, NH_2), 2.31 (dd, 2H, *J* = 7.6Hz, 14Hz, CH_2), 1.15 (t, 3H, *J* = 7.6Hz, CH_3). Ms (FAB / NOBA $(M + H)^+$) 166.1.

6-Bromo-N-(6-(propionamido)pyridine-2-yl)hexanamide (148)[252,254]

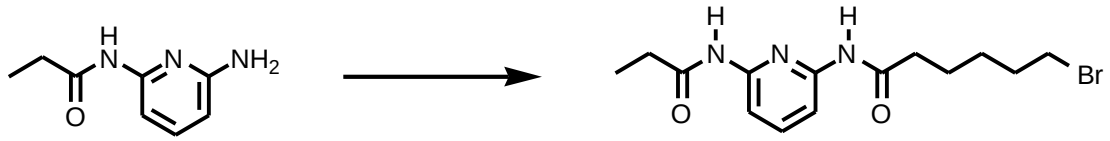

147 **148**

To a stirred solution of 2-ethylamido-6-aminopyridine (**147**) (0.4g, 2.4 mmol) in CH_2Cl_2 (200 ml) was added 6-bromohexanoyl chloride (0.57 g. 2.7 mmol) and triethylamine (0.35 ml). The reaction mixture was stirred for 24 h. at room temperature and then water (100 ml) was cautiously added. The organic layer was separated and the aqueous layer was further extracted with CH_2Cl_2 (2 x 100 ml). The organic extracts were combined, dried over $MgSO_4$, filtered and concentrated under reduced pressure. Purification by column chromatography (silica gel/ eluting with CH_2Cl_2/ethyl acetate, 80/20) afforded **148** as a white solid (0.5 g, 61 %). Mp. 93-95 ^oC. ^1H NMR (400 MHz, $CDCl_3$): 7.90 (t, 2H, J = 7.6Hz, CH_{ar}), 7.71 (t, 1H, J = 8Hz, CH_{ar}), 3.40 (t, 2H, J = 2.8Hz, CH_2), 2.41 (m, 4H, CH_2), 1.91 (m, 2H, CH_2), 1.76 (m , 2H, CH_2), 1.54 (m, 2H, CH_2), 1.21 (m, 3H, CH_3). ^{13}C NMR (100 MHz, $CDCl_3$): 173.03(C); 171.98(C); 149.78(C); 149.76(C); 140.41(CH); 109.44(CH); 50.08(C); 44.78(C); 36.97(CH_2); 33.63(CH_2); 32.28(CH_2); 30.40(CH_2); 27.57(CH_2); 24.44(CH_2); 9.38(CH_3). Ms (m/z, CI) 342/344 (100%) (M+H). Anal. Calc. for $C_{14}H_{20}N_3O_2Br$ (C) 49.13, (H) 5.89; (N) 12.28; found (C) 49.46, (H) 5.78, (N) 12.11.

6-(N-(6-(Propionamido)pyridine-2-yl)-hexanamide) trimethyl ammonium bromide (149) [252,255]

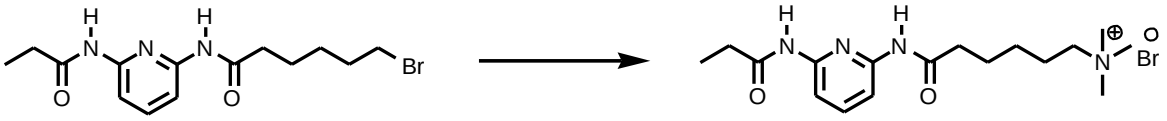

148 **149**

To a stirred solution of 2-ethylamido-6-(6-bromohexylamido) pyridine (**148**) (0.5 g, 1.5 mmol) in methanol (10 ml) was added trimethylamine (2 ml, 30 % solution in methanol). The reaction was heated under reflux for 24 h. The solution was concentrated under reduced pressure and precipitated into a vigorously stirred solution of diethyl ether (100 ml). The precipitate was filtered and washed with ice-cold diethyl ether. The product was dried under high-vacuum for 24 h to afford product **149** as a white solid (0.5 g. 83%). Mp. 87-92 ^{o}C. ^{1}H NMR _ (400 MHz, D_2O): 7.70 (t, 1H , *J* = 8Hz , CH), 7.45 (d, 2H, *J* = 8Hz, CH), 3.20 (m, 2H, CH_2), 3.00 (s, 9H, CH_3), 2.40 (m, 4H, CH_2), 1.75 (m, 2H, CH_2), 1.65 (m, 2H, CH_2), 1.35 (m, 2H, CH_2), 1.10 (t, 3H, *J* = 8Hz, CH_3). ^{13}C NMR (100 MHz, D_2O): 176.77(C), 175.40(C), 149.27(C), 149.10(C), 141.23(CH); 111.17(CH); 111.03(CH); 66.37(CH_2); 52.80(CH_3); 52.76(CH_3); 52.72(CH_3); 36.30(CH_2); 30.02(CH_2); 24.97(CH_2); 24.39(CH_2); 22.07(CH_2); 8.96(CH_3). Ms (m/z, FAB) 322 (40 %) (M^+ (-Br)). Anal. Calc. for $C_{17}H_{29}N_4O_2Br$ (C) 50.87, (H) 7.28; (N) 13.96; found (C) 50.66, (H) 7.20, (N) 13.69.

10-(6-Hydroxy-hexyl)-7,8-dimethyl isoalloxazine (152) [256]

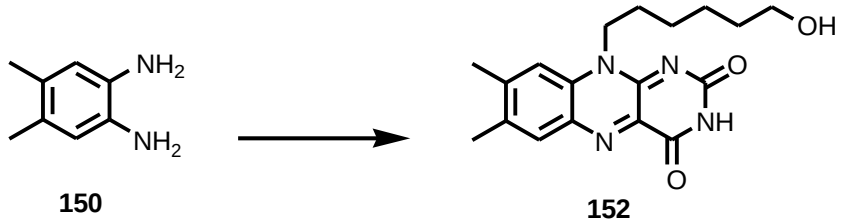

150 **152**

To a solution of 4,5-dimethylbenzene-1,2-diamine (**150**) (1g, 7.35 mmol), sodium iodide (2.2g, 14.5 mmol) and triethyl amine (5.2 ml, 36.5 mmol) in dry THF (50 ml), 6-bromo-1-hexanol (1 ml, 7.35 mmol) was added drop wise. The reaction mixture was heated under refluxed under N_2 for two days. The solvent was removed by vacuum. Without further treatment, the residue was dissolved in acetic acid (50 ml) then alloxan monohydrate (1.20 g, 7.35mmol) and boric anhydride (0.51 g, 7.35mmol) was added. The reaction mixture was then left stirring at room temperature over night. The solvent was then removed by vacuum and the resultant compound was purified by column chromatography (silica gel eluted by DCM/ acetone 5:5) afforded **152** as a yellow powder (0.88 g, 35%). Mp = 270^{o}C) lit = 270^{o}C [256]). ^{1}H NMR (400 MHz, DMSO) δ = 11.31 (1H, s, NH), 7.91 (1H, s, ArH), 7.80 (1H, s, ArH), 4.58 (2H, t, *J* = 7.6Hz, OCH_2), 3.49 (1H, t, *J* = 5.2Hz, OH), 3.42 (2H, q, NCH_2), 2.53 (3H, s, CH_3), 2.42 (3H, s, CH_3), 1.72 (2H, m, CH_2), 1.50-1.38 (6H, m, $3CH_2$). ^{13}C NMR (400 MHz, DMSO) δ = 159.98 (C), 155.71 (C), 149.99 (C), 146.57 (C), 137.15 (C), 135.74 (C), 133.77(C), 130.99 (CH), 130.69 (C), 116.01 (CH), 60.54 (CH_2), 44.10(CH_2), 32.41(CH_2), 26.51 (CH_2), 26.02 (CH_2), 25.26 (CH_2), 20.59 (CH_3), 18.77 (CH_3). Ms FAB / NOBA $(M + H)^+$) 343.3. Accurate Mass FAB/NOBA, Theoretical ion distribution $C_{18}H_{22}N_4O_3$ (*m/z*) calculated 343.1770 observed 343.1767. ν_{max}/cm^{-1} 3415*w* (OH), 3097*w* (NH), 2050*s* (CH_{ar}), 2956*s* (CH_{alk}), 2841*w* ,1699*m*, 1539*m* (aromatic C=C), 1338*s*, 1260*m*, 1215*m*, 1143*m*, 1023*w*, 868*m*.

10-(6-Hydroxyhexyl)-3,7,8-trimethyl-alloxazine (153)[231]

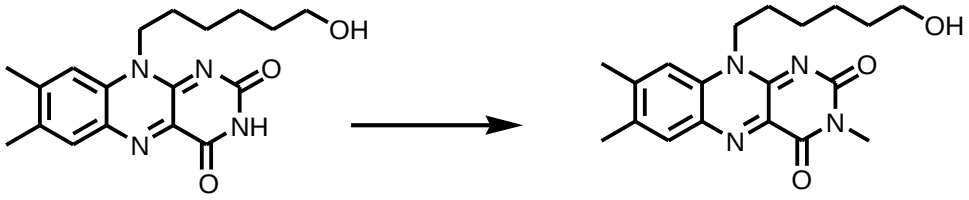

A solution of 10-(6-hydroxy-hexyl)-7,8-dimethyl isoalloxazine (**152**) (0.39 g, 1.14 mmol), methyl iodide (0.35 ml, 2.28 mmol) and sodium carbonate (0.36 g, 3.42 mmol) in dry DMF (50 ml) was stirred at room temperature under nitrogen. After two days, the reaction was stopped and the solvent was removed under vacuum. The resultant product was then purified by column chromatography (silica gel eluted by ethyl acetate followed by ethyl acetate/ methanol 9:1) afforded **153** as a yellow/ orange solid (0.21 g, 51%). Mp = 236-238^{o}C (lit = 235-238^{o}C [231]). ^{1}H NMR (400 MHz, DMSO) δ = 7.95 (1H, s, ArH), 7.85 (1H, s, ArH), 4.61 (2H, t, *J* = 7.6Hz, OCH_2), 3.39 (1H, t, *J* = 5.2Hz, OH), 3.40 (2H, m, NCH_2), 3.28 (3H, s, NCH_3), 2.54 (3H, s, CH_3), 2.42 (3H, s, CH_3), 1.73 (2H, m, CH_2), 1.52-1.33 (6H, m, $3CH_2$). ^{13}C NMR (100 MHz, DMSO) δ = 159.76 (C), 155.21 (C), 148.47 (C), 146.80 (C), 136.15 (C), 135.89 (C), 134.03 (C), 131.01 (CH), 130.65 (C), 116.01 (CH), 60.54 (CH_2), 43.99 (CH_2), 32.36 (CH_2), 27.95 (CH_3), 26.61 (CH_2), 25.99 (CH_2), 25.25 (CH_2), 20.61 (CH_3), 18.79 (CH_3). Ms (FAB / NOBA $(M + H)^+$) 357.0

10-(6-Bromohexyl)-3,7,8-trimethyl-alloxazine (154)

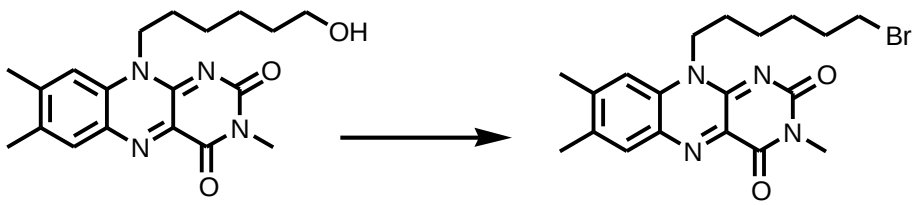

153 **154**

Triphenylphosphene (0.44 g, 1.67 mmol) was added to a solution of carbon tetrabromide (0.55 g, 1.67 mmol) and 10-(6-Hydroxyhexyl)-3,7,8-trimethyl-alloxazine (**153**) (0.30 g, 0.84 mmol) in degassed dry acetonitrile (50 ml) in 0^{o}C. The mixture was stirred at room temperature under nitrogen overnight. The solvent was evaporated and the crude product was purified by column chromatography (silica gel: DCM/ Ethyl acetate, 3:1) and recrystallized from methanol to give **154** as a yellow powder (0.10 g, 25%). ^{1}H NMR (400 MHz, $CDCl_3$) δ = 8.09 (1H, s, ArH), 7.38 (1H, s, ArH), 4.71 (2H, br, $BrCH_2$), 3.53 (3H, s, NCH_3), 3.43 (2H, t, *J* = 6.8Hz, NCH_2), 2.57 (3H, s, CH_3), 2.45 (3H, s, CH_3), 1.90 (4H, m, $2CH_2$), 1.56 (4H, m, $2CH_2$). ^{13}C NMR (100 MHz, $CDCl_3$): δ = 160.16 (C), 156.10 (C), 147.70 (C), 136.60 (C), 135.69 (C), 135.00 (C), 132.90 (CH), 130.92(C), 115.03 (CH), 44.50 (CH_2), 33.67 (CH_2), 32.43 (CH_2), 28.79 (CH_3), 27.81 (CH_2), 27.01 (CH_2), 25.98 (CH_2), 21.68 (CH_3), 19.50 (CH_3). Ms (FAB / NOBA $(M + H)^+$) for $C_{19}H_{23}BrN_4O_2$ 419/420. ν_{max}/cm^{-1} 2037*w* (CH_{ar}), 2853*s* (CH_{alk}), 1700*s* ,1654*s* (C=O ester), 1581*s*, 1541*s*, 1518*m*, 1410*m*, 1280*m*, 1050*w*, 950s, 766*s*, 600*m*.

6-[(3,7,8-Trimethyl-alloxazine)-10yl]-hexyl ammonium bromide (155)

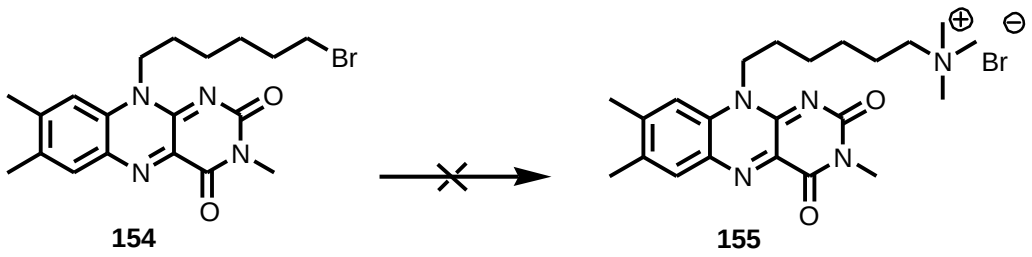

154 **155**

To a solution of 10-(6-bromohexyl)-3,7,8-trimethyl-alloxazine (**154**) (0.09 g) in methanol (50 ml) was added trimethylamine (31-35% in ethanol) (4 ml) drop wise . The mixture was stirred at reflux overnight. The mixture was concentrated to minimum and was added to diethyl ether (100 ml) slowly. The precipitate was filtered and washed with diethyl ether. The spectroscopy of the product was not consistent with the proposed structure of **155**.

10-(6-Bromohexyl)-7,8-dimethyl-alloxazine (156)

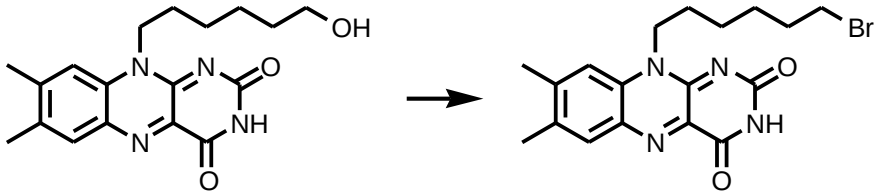

152 **156**

Triphenylphosphine (0.613 g, 2.34 mmol) was added to a solution of carbon tetrabromide (0.78 g, 2,34 mmol) and 10-(6-hydroxy-hexyl)-7,8-dimethyl isoalloxazine (**152**) (0.40 g, 1.17 mmol) in degassed dry acetonitrile (50 ml) in 0^{o}C. The mixture was stirred at room temperature, under nitrogen, overnight. The solvent was evaporated and the crude product was purified by flash column chromatography (silica gel: acetone / Ethyl acetate, 3:7) to afford **156** as an orange solid (284 mg, 60 %). ^{1}H NMR (400 MHz, DMSO) δ 11.31 (s, 1H), 7.91 (s, 1H), 7.81 (s, 1H), 4.58 (t, 2H), 3.56 (t, *J* = 6.8 Hz, 2H), 2.53 (s, 3H), 2.41 (s, 3H), 1.84 (q, 2H), 1.74 (q, 2H), 1.49 (s, 4H).

6-[(7,8-Dimethyl-alloxazine)-10yl]-hexyl ammonium bromide (157)

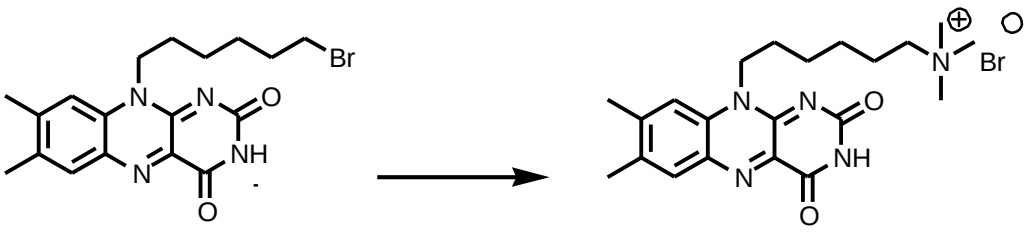

156 **157**

To a solution of 10-(6-bromohexyl)-7,8-dimethyl-alloxazine (**156)** (0.21 g, 0.56 mmol) in methanol (90 ml), trimethylamine (2 ml, 8,40 mmol) was added dropwise. The mixture was stirred at reflux overnight. The mixture was concentrated under reduce pressure to a volume of 10 ml and ethyl acetate (150 ml) was slowly added. The resulting yellow suspension was removed by filtration and precipitate washed with ethyl acetate to yield compound **157** as a yellow powder (151 mg, 75 %). ^{1}H NMR (400 MHz, MeOD) δ 7.85 (d, *J* = 8.4 Hz, 1H), 7.78 (d, *J* = 8.4 Hz, 1H), 7.35 (t, *J* = 7.4 Hz, 2H), 6.96 (d, *J* = 7.6 Hz, 1H), 6.95 (d, J = 7.6 Hz, 1H), 4.36-4.29 (m, 4H), 4.09-3.98 (m, 6H), 3.71 (s, 4H), 3.62 (t, *J* = 4.6 Hz, 2H), 3.16 (s, 9H).

N-(6-aminopyridin-2-yl)-6-bromohexanamide (158)

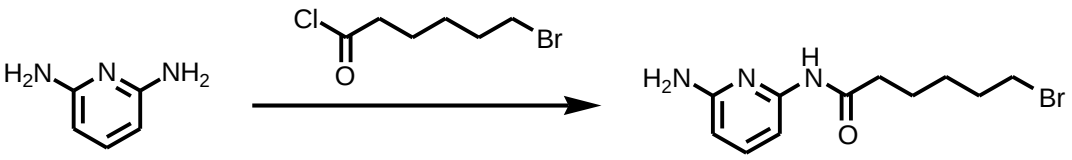

146 **158**

2,6-Diaminopyridine (**146**) (5 g, 45.87mmol) was dissolved in a mixture of CH_2Cl_2 (200 ml) and triethylamine (6.5 ml). To this bromohexonyl chloride (9.78 ml, 45.87 mmol) was added dropwise over 1 h. and left stirring under N_2 at room temperature for 3 days. The ammonium salt was removed by filtration. The solvent was removed under reduced pressure, then THF (100 ml) was added to precipitate the ammonium salt, filtered and the filtrate was concentrated under reduced pressure. Purification by column chromatography (silica gel/ eluting with DCM/ethyl acetate 8:2) afforded **158** as a creamy solid (4.27 gram, 20%), ^{1}H NMR (400 MHz, DMSO) δ 10.03 (s, 1H, NH), 9.12 (s, 2H, NH_2), 8.62 (t, 1H, *J* = 7.6Hz), 8.18 (t, 2H, *J* = 5Hz), 4.63 (t, 2H, *J* = 6.8Hz), 2.42 (d, 2H, *J* = 7Hz), 1.96 (m, 2H), 1.63 (m, 2H), 1.31 (m, 2H). Ms (FAB / NOBA $(M + H)^+$) 286.1.

4-(6-(6-bromohexanamido)pyridin-2-ylcarbamoyl)butanoic acid (159)

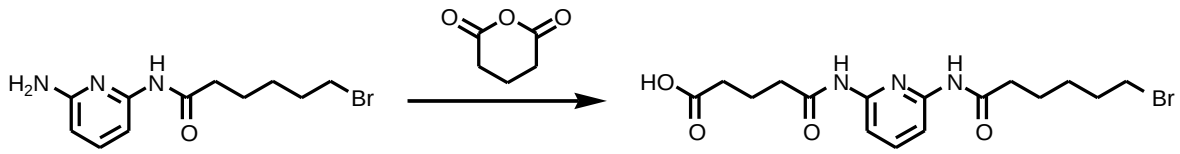

158 **159**

To a stirred solution of N-(6-aminopyridin-2-yl)-6-bromohexanamide (**158**) (2 g, 7.02 mmol) and DMAP (0.86 g, 7.02 mmol) in DCM (150 ml), glutaric anhydride (0.88 g. 7.72 mmol) was added. After stirring for 3 days, the reaction mixture was filtered and the filtrate was concentrated under reduced pressure. The remaining white solid was dissolved in $CHCl_3$ and allowed to crystallize at 0^oC for 24 h. The precipitate was filtered off and left to dry to yield **159** as a white solid (1.5 g, 53 %). ^1H NMR (DMSO, 400 MHz) δ 10.64 (s, 1H, NH), 8.12 (d, 1H, J = 8Hz, CH), 7.89 (t, 1H, *J* = 8Hz, CH), 6.99 (d, 1H, *J* = 8Hz, CH), 3.63 (t, 1H, *J* = 6.8Hz, CH of CH_2Br), 3.53 (t, 1H, *J* = 6.8Hz, CH of CH_2Br), 2.73 (t, 4H, *J* = 6.4Hz), 2.37 (t, 2H, *J* = 7.2Hz, CH_2), 1.97 (br, 2H, CH2), 1.81 (sept, 1H, CH of CH_2), 1.73 (sept, 1H, CH of CH_2), 1.60 (sept, 2H, CH_2), 1.39 (sept, 2H, CH_2).

^{13}C NMR (100 MHz, DMSO): 151.91(C); 147.91(C); 140.32(CH); 118.83(CH); 112.99(CH); 45.22(CH_2); 35.76(CH_2); 34.96(CH_2); 32.09(C); 31.94(C), 31.75(C), 27.10(CH_2); 25.83(CH_2); 24.16(CH_2), 24.03(CH_2), 16.76(CH_2). Ms (m/z, CI) 399/400 (100%) (M+H). ν_{max}/cm^{-1} 3320*w*(NH), 3225*w*(NH), 2939*w*(COOH), 2701*w*(CH_{ar}), 1688*m*(C=O amide), 1617*s*, 1587*s*, 1538*s*, 1436*m*, 1284*s*, 1213*m*, 1145*s*, 915*w*,807*m*, 731*m*. Anal. Calc. for $C_{16}H_{22}N_3O_4Br$ (C) 48.01, (H) 5.54; (N) 10.50; found (C) 47.71, (H) 5.88, (N) 6.29.

6-(7,8-Dimethyl isoalloxazine-10-yl)hexyl 4-(6-(6-bromohexanamido)pyridin-2-ylcarbamoyl)butanoate (160)

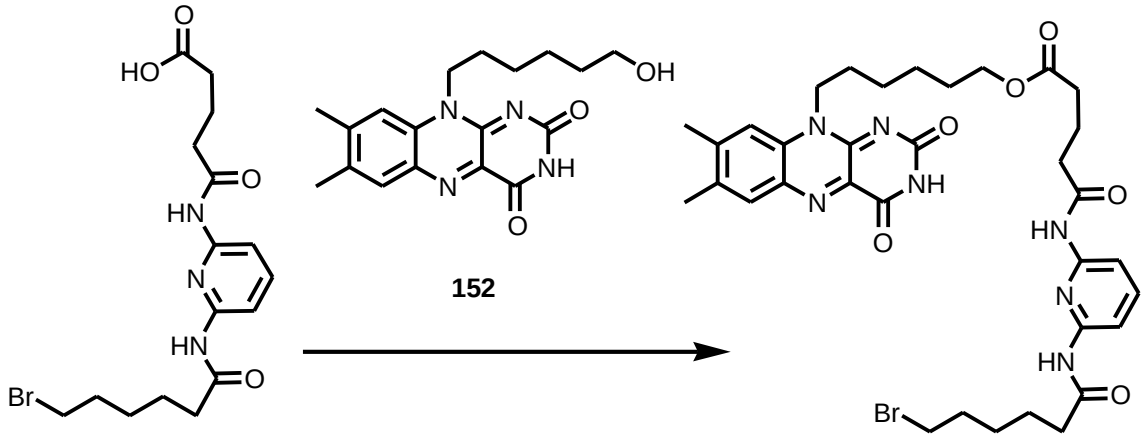

159 **152** **160**

10-(6-Hydroxy-hexyl)-7,8-dimethyl isoalloxazine (**152**) (0.2 g, 0.58 mmol), DMAP (0.07 g, 0.58 mmol) and EDCI (0.11g, 0.58 mmol) were dissolved in dry DMF (20 ml). 4-(6-(6-bromohexanamido)pyridin-2-ylcarbamoyl)butanoic acid (**159**) (0.23 g, 0.58 mmol) was then added to the reaction mixture and stirred under N_2 for 3 days at room temperature. The reaction mixture was concentrated to minimum and purified by column chromatography silica gel eluting with DCM/ acetone (9:1) and crystallized from ether to afford **160** as a yellow solid (0.095 g, 23%). ^{1}H NMR (DMSO, 400 MHz) δ = 11.30 (s, 1H, NH), 10.01 (s, 1H, NH), 9.99 (s, 1H, NH), 7.81 (s, 1H, CH), 7.77 (s, 1H, CH), 7.68 (br, 3H, CH), 4.55 (t, 2H, *J* = 7.2Hz, CH_2), 4.02 (t, 2H, *J* = 6.4Hz, CH_2), 3.63 (t, 1H, *J* = 6.8Hz, CH of CH_2Br), 3.53 (t, 1H, *J* = 6.8Hz, CH of CH_2Br), 2.50 (s, 3H, CH_3), 2.39 (s, 3H, CH_3), 2.39 (s, 3H, CH_3), 2.39 (m, 4H, $2CH_2$), 1.81 (sept, 2H, CH_2), 1.71 (sept, 2H, CH_2), 1.73 (m, 6H, $3CH_2$), 1.49-1.38 (m, 8H, $4CH_2$). ^{13}C NMR (100 MHz, DMSO) δ = 159(C),155.65 (C), 150.23 (C), 150.00(C), 146.55(C), 139.82 (CH), 137.12 (C), 135.72 (C), 133.79 (C), 131.02 (C), 130.68 (C), 151.99 (CH), 108.92 (CH), 63.73 (CH_2), 45.27 (CH_2), 35.87 (CH_2), 35.02 (CH_2), 32.83 (CH_2), 32.09 (CH_2), 31.78 (CH_2), 28.02 (CH_2), 27.13 (CH_2), 26.34 (CH_2), 25.87 (CH_2), 25.15 (CH_2), 24.20 (CH_2), 20.57 (CH_2), 20.24 (CH_3), 18.74 (CH_3). Ms (FAB / NOBA $(M+H)^+$) 723.9. ν_{max}/cm^{-1} 3268*w*(NH), 3207*w*(NH), 3055*w*(NH), 2941*w*, 2860*w*(CH_{ar}), 1691*w*(C=O amide), 1667*w*(C=O amide), 1580*s*, 1540*s*, 1444*s*, 1274*w*, 1243*w*, 11251*s*, 1005*w*, 802*m*, 735*m*.

6-(3,7,8-Trimethyl isoalloxazine-10-yl)hexyl 4-(6-(6-bromohexanamido)pyridin -2-ylcarbamoyl)butanoate (161)

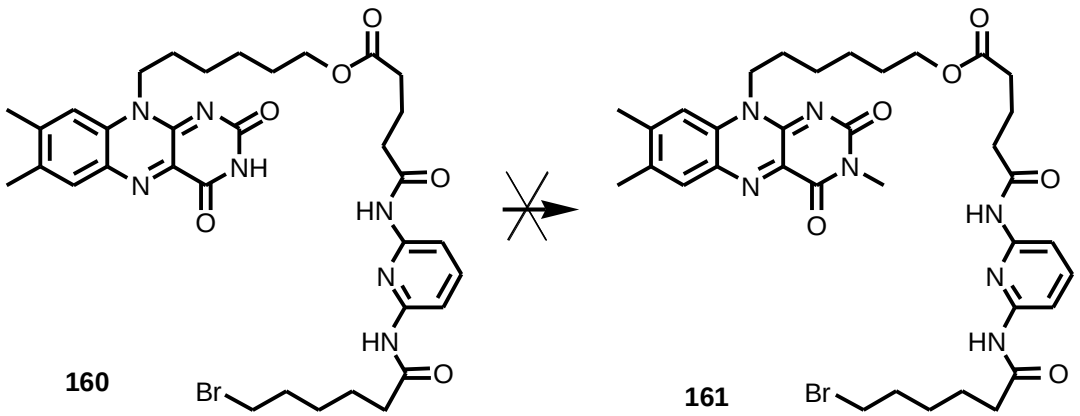

To a solution of 6-(7,8-dimethyl isoalloxazine-10-yl)hexyl 4-(6-(6-bromohexanamido) pyridin-2-ylcarbamoyl)butanoate (**160**) (0.1 g, 0.14 mmol) in dry DMF (10 ml), iodomethane (0.022 ml, 0.14 mmol) and sodium carbonate (0.015 g, 0.14mmol) were added. The reaction mixture was allowed to stir under N_2 for 48 h. at room temperature. DMF was removed under reduced pressure. Purification by column chromatography (silica gel/ eluting with $CHCl_3$/ acetone, 9:1) followed by recrystallisation from diethyl ether gave the desired product **161** as a yellow crystals (0.06g, 58%). ν_{max}/cm^{-1} 3400*w*(NH), 3072*w*(NH), 2936*w*, 2860*w*(CH_{ar}), 1708*s*, 1647*w*(C=O amide), 1576*s*, 1535*s*, 1351*s*, 1274*w*, 1173*s*, 1014*w*, 859*m*, 773*m*, 736*m*

APPENDICES

Table 10. Crystal data and structure refinement for 110.

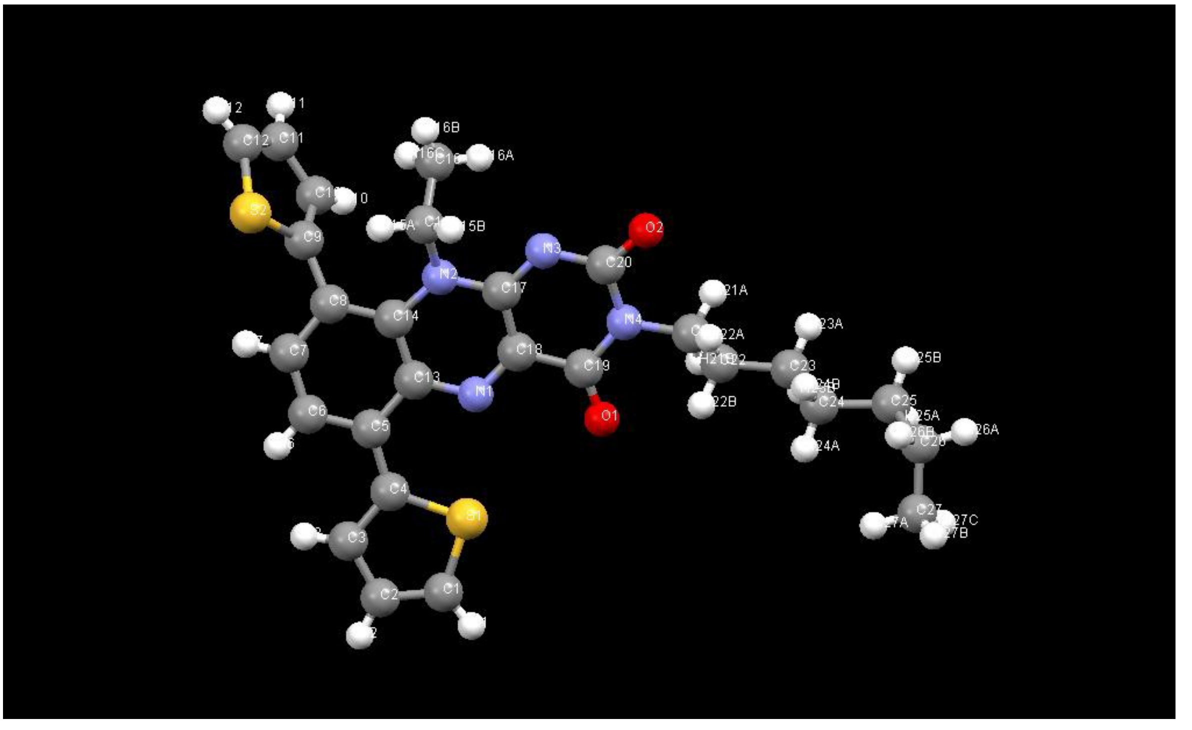

Identification code   n_y92

Empirical formula   C27 H28 N4 O2 S2

Formula weight   504.65

Temperature   150(2) K

Wavelength   0.71073 A

Crystal system, space group   Monoclinic, P2(1)/c

Unit cell dimensions   a = 9.1270(7) A   alpha = 90 deg.
b = 18.9897(16) A   beta = 105.388(7) deg.
c = 29.174(3) A   gamma = 90 deg.

Volume   4875.2(7) A^3

Z, Calculated density   8, 1.375 Mg/m^3

Absorption coefficient   0.252 mm^-1

F(000)   2128

Crystal size	0.50 x 0.20 x 0.03 mm
Theta range for data collection	2.14 to 25.37 deg.
Limiting indices	-11<=h<=10, -22<=k<=22, -35<=l<=35
Reflections collected / unique	34446 / 8847 [R(int) = 0.1019]
Completeness to theta = 25.37	99.1 %
Absorption correction	Empirical
Max. and min. transmission	0.9925 and 0.8844
Refinement method	Full-matrix least-squares on F^2
Data / restraints / parameters	8847 / 26 / 655
Goodness-of-fit on F^2	1.006
Final R indices [I>2sigma(I)]	R1 = 0.0841, wR2 = 0.2080
R indices (all data)	R1 = 0.1686, wR2 = 0.2664
Extinction coefficient	none
Largest diff. peak and hole	0.90 and -0.45 e.A^-3

Table 2. Atomic coordinates (x 10^4) and equivalent isotropic displacement parameters (A^2 x 10^3) for n_y92.
U(eq) is defined as one third of the trace of the orthogonalized Uij tensor.

	x	y	z	U(eq)
C(1)	-6659(7)	4620(3)	1356(3)	50(2)
C(2)	-7346(7)	5039(3)	1614(3)	43(2)
C(3)	-6950(6)	4874(3)	2103(3)	38(2)
C(4)	-5949(6)	4291(3)	2206(2)	29(1)
C(5)	-5406(6)	3969(3)	2670(2)	26(1)
C(6)	-5910(6)	4220(3)	3050(2)	36(2)
C(7)	-5289(7)	3964(3)	3504(2)	35(2)
C(8)	-4245(6)	3422(3)	3613(2)	29(1)
C(9)	-3489(7)	3288(3)	4118(2)	35(2)
C(10)	-1923(8)	3445(4)	4348(2)	43(2)
C(11)	-1647(8)	3295(4)	4840(3)	59(2)
C(12)	-2842(8)	3063(4)	4982(3)	52(2)
C(13)	-4357(6)	3405(3)	2766(2)	23(1)
C(14)	-3865(6)	3089(3)	3226(2)	25(1)
C(15)	-3018(8)	1935(3)	3641(2)	46(2)
C(16)	-1537(9)	1811(4)	3978(3)	61(2)
C(17)	-2474(6)	2243(3)	2895(2)	20(1)
C(18)	-2899(5)	2647(3)	2460(2)	20(1)
C(19)	-2340(5)	2410(3)	2054(2)	20(1)
C(20)	-1193(6)	1408(3)	2569(2)	23(1)
C(21)	-824(6)	1541(3)	1766(2)	23(1)
C(22)	-1872(6)	1012(3)	1442(2)	25(1)
C(23)	-1140(6)	689(3)	1084(2)	26(1)
C(24)	-2207(6)	224(3)	720(2)	31(1)
C(25)	-1389(7)	-165(3)	396(2)	39(2)
C(26)	-2476(8)	-581(3)	6(2)	45(2)
C(27)	-3415(8)	-143(4)	-396(2)	54(2)
C(28)	-1620(7)	-2014(3)	1222(2)	42(2)
C(29)	-2248(7)	-2493(3)	1459(3)	41(2)
C(30)	-1904(6)	-2376(3)	1955(2)	28(1)
C(31)	-976(6)	-1765(3)	2076(2)	26(1)
C(32)	-466(6)	-1477(3)	2557(2)	24(1)
C(33)	-1017(6)	-1743(3)	2921(2)	29(1)

C(34)	-446(6)	-1515(3)	3384(2)	31(1)
C(35)	625(6)	-981(3)	3512(2)	27(1)
C(36)	1354(7)	-892(3)	4035(2)	33(1)
C(37)	2760(20)	-1163(12)	4298(4)	58(6)
C(37')	1040(70)	-550(40)	4424(6)	100(40)
C(38)	3066(10)	-1043(4)	4785(2)	70(2)
C(39)	1940(10)	-699(4)	4884(2)	63(2)
C(40)	583(6)	-904(3)	2677(2)	21(1)
C(41)	1053(6)	-621(3)	3147(2)	21(1)
C(42)	1989(7)	480(3)	3609(2)	32(1)
C(43)	3538(8)	528(4)	3970(2)	51(2)
C(44)	2469(6)	256(3)	2853(2)	20(1)
C(45)	2071(5)	-120(3)	2408(2)	19(1)
C(46)	2678(5)	152(3)	2012(2)	19(1)
C(47)	3760(6)	1121(3)	2563(2)	24(1)
C(48)	4188(6)	1058(3)	1761(2)	26(1)
C(49)	3140(6)	1597(3)	1457(2)	31(1)
C(50)	3836(6)	1925(3)	1092(2)	29(1)
C(51)	2760(7)	2415(3)	747(2)	43(2)
C(52)	3385(11)	2645(6)	343(3)	52(3)
C(53)	2364(16)	3045(7)	-63(5)	93(4)
C(54)	2230(20)	3759(9)	102(8)	96(7)
C(52')	3750(50)	2990(20)	516(16)	103(17)
C(53')	2890(30)	3513(19)	158(12)	68(10)
C(54')	1330(30)	3273(17)	-119(11)	59(8)
C(54")	2050(50)	3580(20)	-282(14)	83(11)
N(1)	-3838(5)	3174(2)	2396(2)	21(1)
N(2)	-3003(5)	2477(2)	3261(2)	25(1)
N(3)	-1711(5)	1649(2)	2942(2)	24(1)
N(4)	-1452(4)	1815(2)	2143(2)	20(1)
N(5)	1133(4)	-647(2)	2321(2)	20(1)
N(6)	1920(5)	-9(2)	3207(2)	22(1)
N(7)	3253(5)	848(2)	2927(2)	23(1)
N(8)	3548(5)	751(2)	2128(2)	24(1)
O(1)	-2652(4)	2706(2)	1669(1)	24(1)
O(2)	-507(4)	858(2)	2587(1)	32(1)
O(3)	2401(4)	-124(2)	1625(1)	27(1)
O(4)	4428(4)	1684(2)	2604(1)	36(1)
S(1)	-5526(2)	3996(1)	1688(1)	42(1)
S(2)	-4439(2)	3003(1)	4518(1)	52(1)
S(3)	-575(2)	-1402(1)	1578(1)	38(1)
S(4)	473(5)	-521(2)	4420(1)	61(1)
S(4')	3030(20)	-1318(14)	4245(5)	43(4)

Table 3. Bond lengths [A] and angles [deg] for n_y92.

C(1)-C(2)	1.360(10)
C(1)-S(1)	1.698(6)
C(2)-C(3)	1.410(9)
C(3)-C(4)	1.417(8)
C(4)-C(5)	1.448(8)
C(4)-S(1)	1.749(6)
C(5)-C(6)	1.391(8)
C(5)-C(13)	1.415(7)
C(6)-C(7)	1.384(9)
C(7)-C(8)	1.382(8)
C(8)-C(14)	1.413(7)
C(8)-C(9)	1.474(9)
C(9)-C(10)	1.440(9)
C(9)-S(2)	1.717(6)
C(10)-C(11)	1.418(10)
C(11)-C(12)	1.340(10)
C(12)-S(2)	1.708(7)
C(13)-N(1)	1.362(7)
C(13)-C(14)	1.429(8)
C(14)-N(2)	1.393(7)
C(15)-C(16)	1.465(10)
C(15)-N(2)	1.514(7)
C(17)-N(3)	1.313(6)
C(17)-N(2)	1.359(6)
C(17)-C(18)	1.445(7)
C(18)-N(1)	1.298(6)
C(18)-C(19)	1.479(7)
C(19)-O(1)	1.221(6)
C(19)-N(4)	1.374(6)
C(20)-O(2)	1.212(6)
C(20)-N(3)	1.374(7)
C(20)-N(4)	1.430(7)
C(21)-N(4)	1.463(6)
C(21)-C(22)	1.530(7)
C(22)-C(23)	1.510(7)
C(23)-C(24)	1.520(7)
C(24)-C(25)	1.539(7)
C(25)-C(26)	1.518(8)
C(26)-C(27)	1.507(9)
C(28)-C(29)	1.357(9)

C(28)-S(3)	1.679(6)
C(29)-C(30)	1.416(9)
C(30)-C(31)	1.424(7)
C(31)-C(32)	1.461(8)
C(31)-S(3)	1.733(6)
C(32)-C(33)	1.387(7)
C(32)-C(40)	1.430(7)
C(33)-C(34)	1.381(8)
C(34)-C(35)	1.388(8)
C(35)-C(41)	1.406(7)
C(35)-C(36)	1.505(8)
C(36)-C(37)	1.408(12)
C(36)-S(4)	1.698(6)
C(37)-C(38)	1.391(12)
C(38)-C(39)	1.313(11)
C(39)-S(4)	1.666(8)
C(40)-N(5)	1.359(6)
C(40)-C(41)	1.429(7)
C(41)-N(6)	1.392(6)
C(42)-N(6)	1.484(7)
C(42)-C(43)	1.526(8)
C(44)-N(7)	1.319(6)
C(44)-N(6)	1.358(6)
C(44)-C(45)	1.441(7)
C(45)-N(5)	1.297(6)
C(45)-C(46)	1.500(7)
C(46)-O(3)	1.210(6)
C(46)-N(8)	1.377(7)
C(47)-O(4)	1.222(6)
C(47)-N(7)	1.369(7)
C(47)-N(8)	1.416(7)
C(48)-N(8)	1.471(6)
C(48)-C(49)	1.516(7)
C(49)-C(50)	1.511(7)
C(50)-C(51)	1.523(7)
C(51)-C(52)	1.504(10)
C(52)-C(53)	1.505(12)
C(53)-C(54)	1.456(15)
C(52')-C(53')	1.50(2)
C(53')-C(54')	1.511(19)

C(2)-C(1)-S(1)	113.1(6)
C(1)-C(2)-C(3)	113.5(6)

C(2)-C(3)-C(4)	111.6(6)
C(3)-C(4)-C(5)	124.8(6)
C(3)-C(4)-S(1)	110.1(5)
C(5)-C(4)-S(1)	125.0(4)
C(6)-C(5)-C(13)	116.8(6)
C(6)-C(5)-C(4)	119.8(5)
C(13)-C(5)-C(4)	123.4(5)
C(7)-C(6)-C(5)	120.3(5)
C(8)-C(7)-C(6)	124.2(6)
C(7)-C(8)-C(14)	116.8(6)
C(7)-C(8)-C(9)	118.0(5)
C(14)-C(8)-C(9)	124.8(5)
C(10)-C(9)-C(8)	125.0(5)
C(10)-C(9)-S(2)	111.4(5)
C(8)-C(9)-S(2)	123.2(4)
C(11)-C(10)-C(9)	108.5(6)
C(12)-C(11)-C(10)	116.0(7)
C(11)-C(12)-S(2)	111.7(6)
N(1)-C(13)-C(5)	116.5(5)
N(1)-C(13)-C(14)	121.4(5)
C(5)-C(13)-C(14)	122.0(5)
N(2)-C(14)-C(8)	124.6(5)
N(2)-C(14)-C(13)	116.7(5)
C(8)-C(14)-C(13)	118.7(5)
C(16)-C(15)-N(2)	114.5(6)
N(3)-C(17)-N(2)	119.2(5)
N(3)-C(17)-C(18)	124.0(5)
N(2)-C(17)-C(18)	116.6(4)
N(1)-C(18)-C(17)	123.4(5)
N(1)-C(18)-C(19)	118.3(5)
C(17)-C(18)-C(19)	118.1(4)
O(1)-C(19)-N(4)	122.3(5)
O(1)-C(19)-C(18)	123.4(5)
N(4)-C(19)-C(18)	114.3(5)
O(2)-C(20)-N(3)	122.3(5)
O(2)-C(20)-N(4)	117.9(5)
N(3)-C(20)-N(4)	119.7(4)
N(4)-C(21)-C(22)	113.1(4)
C(23)-C(22)-C(21)	112.1(4)
C(22)-C(23)-C(24)	113.6(4)
C(23)-C(24)-C(25)	112.6(5)
C(26)-C(25)-C(24)	112.5(5)
C(27)-C(26)-C(25)	114.8(5)

C(29)-C(28)-S(3)	113.3(5)
C(28)-C(29)-C(30)	114.0(6)
C(29)-C(30)-C(31)	109.8(5)
C(30)-C(31)-C(32)	124.1(5)
C(30)-C(31)-S(3)	111.1(4)
C(32)-C(31)-S(3)	124.8(4)
C(33)-C(32)-C(40)	116.4(5)
C(33)-C(32)-C(31)	120.7(5)
C(40)-C(32)-C(31)	122.8(5)
C(34)-C(33)-C(32)	121.0(5)
C(33)-C(34)-C(35)	123.2(5)
C(34)-C(35)-C(41)	118.0(5)
C(34)-C(35)-C(36)	116.5(5)
C(41)-C(35)-C(36)	125.2(5)
C(37)-C(36)-C(35)	127.3(7)
C(37)-C(36)-S(4)	108.3(7)
C(35)-C(36)-S(4)	124.0(4)
C(38)-C(37)-C(36)	113.8(11)
C(39)-C(38)-C(37)	110.4(9)
C(38)-C(39)-S(4)	115.5(6)
N(5)-C(40)-C(41)	121.4(5)
N(5)-C(40)-C(32)	116.5(5)
C(41)-C(40)-C(32)	122.2(5)
N(6)-C(41)-C(35)	125.1(5)
N(6)-C(41)-C(40)	116.8(5)
C(35)-C(41)-C(40)	118.1(5)
N(6)-C(42)-C(43)	114.9(5)
N(7)-C(44)-N(6)	119.0(5)
N(7)-C(44)-C(45)	124.4(5)
N(6)-C(44)-C(45)	116.5(5)
N(5)-C(45)-C(44)	123.7(5)
N(5)-C(45)-C(46)	118.2(5)
C(44)-C(45)-C(46)	117.9(4)
O(3)-C(46)-N(8)	123.5(5)
O(3)-C(46)-C(45)	122.9(5)
N(8)-C(46)-C(45)	113.6(5)
O(4)-C(47)-N(7)	121.2(5)
O(4)-C(47)-N(8)	117.9(5)
N(7)-C(47)-N(8)	120.9(5)
N(8)-C(48)-C(49)	112.5(4)
C(50)-C(49)-C(48)	111.8(4)
C(49)-C(50)-C(51)	113.5(5)
C(52)-C(51)-C(50)	112.5(6)

C(51)-C(52)-C(53)	118.7(9)
C(54)-C(53)-C(52)	107.3(14)
C(52')-C(53')-C(54')	115(3)
C(18)-N(1)-C(13)	119.2(5)
C(17)-N(2)-C(14)	121.8(5)
C(17)-N(2)-C(15)	115.3(4)
C(14)-N(2)-C(15)	120.4(5)
C(17)-N(3)-C(20)	119.2(4)
C(19)-N(4)-C(20)	124.1(4)
C(19)-N(4)-C(21)	118.7(4)
C(20)-N(4)-C(21)	117.0(4)
C(45)-N(5)-C(40)	119.0(4)
C(44)-N(6)-C(41)	121.7(4)
C(44)-N(6)-C(42)	115.0(4)
C(41)-N(6)-C(42)	121.7(4)
C(44)-N(7)-C(47)	118.5(4)
C(46)-N(8)-C(47)	124.3(4)
C(46)-N(8)-C(48)	117.5(4)
C(47)-N(8)-C(48)	118.0(4)
C(1)-S(1)-C(4)	91.7(3)
C(12)-S(2)-C(9)	92.2(3)
C(28)-S(3)-C(31)	91.8(3)
C(39)-S(4)-C(36)	91.9(4)

Symmetry transformations used to generate equivalent atoms:

Table 4. Anisotropic displacement parameters (A^2 x 10^3) for n_y92. The anisotropic displacement factor exponent takes the form: -2 pi^2 [h^2 a*^2 U11 + ... + 2 h k a* b* U12]

	U11	U22	U33	U23	U13	U12
C(1)	40(4)	40(4)	65(5)	26(4)	7(4)	2(3)
C(2)	26(3)	20(3)	79(5)	9(3)	8(3)	-1(3)
C(3)	21(3)	24(3)	66(5)	0(3)	7(3)	-9(3)
C(4)	16(3)	22(3)	53(4)	-3(3)	14(3)	-1(2)
C(5)	16(3)	15(3)	51(4)	-9(3)	17(3)	-5(2)
C(6)	27(3)	22(3)	64(5)	-13(3)	22(3)	-5(3)
C(7)	41(4)	23(3)	48(4)	-18(3)	23(3)	-3(3)
C(8)	34(3)	21(3)	41(4)	-9(3)	27(3)	-10(2)
C(9)	35(4)	32(3)	46(4)	-14(3)	27(3)	-4(3)
C(10)	51(4)	52(4)	36(4)	-14(3)	27(3)	3(3)
C(11)	42(4)	59(5)	76(6)	-30(4)	13(4)	0(4)
C(12)	64(5)	54(5)	37(4)	-16(3)	12(4)	0(4)
C(13)	19(3)	15(3)	38(3)	-3(2)	11(3)	-6(2)
C(14)	29(3)	17(3)	35(3)	-7(2)	21(3)	-9(2)
C(15)	79(5)	32(4)	35(4)	7(3)	28(4)	11(3)
C(16)	86(6)	52(5)	46(5)	-9(4)	21(4)	-8(4)
C(17)	23(3)	16(3)	25(3)	-5(2)	13(2)	-2(2)
C(18)	15(3)	14(3)	32(3)	-1(2)	10(2)	-7(2)
C(19)	16(3)	21(3)	28(3)	-4(2)	12(2)	-5(2)
C(20)	17(3)	26(3)	26(3)	3(2)	7(2)	1(2)
C(21)	19(3)	27(3)	25(3)	-5(2)	12(2)	0(2)
C(22)	19(3)	31(3)	30(3)	2(3)	14(2)	-1(2)
C(23)	22(3)	32(3)	25(3)	-4(3)	9(2)	3(2)
C(24)	36(3)	28(3)	28(3)	-6(3)	10(3)	-4(3)
C(25)	52(4)	38(4)	30(3)	-11(3)	16(3)	5(3)
C(26)	65(5)	27(3)	47(4)	-20(3)	19(4)	2(3)
C(27)	58(5)	51(5)	52(5)	-17(4)	14(4)	-9(4)
C(28)	33(4)	46(4)	45(4)	-20(3)	7(3)	-2(3)
C(29)	29(3)	29(3)	61(5)	-6(3)	5(3)	-3(3)
C(30)	23(3)	20(3)	38(4)	-8(3)	2(3)	6(2)
C(31)	23(3)	21(3)	38(3)	-1(3)	16(3)	3(2)
C(32)	20(3)	15(3)	38(3)	4(2)	12(3)	8(2)

C(33)	28(3)	18(3)	49(4)	7(3)	25(3)	4(2)
C(34)	31(3)	34(3)	37(4)	7(3)	22(3)	7(3)
C(35)	32(3)	27(3)	29(3)	12(3)	19(3)	11(3)
C(36)	45(4)	32(3)	27(3)	7(3)	18(3)	3(3)
C(37)	90(12)	66(13)	32(7)	-6(6)	42(7)	27(7)
C(38)	87(6)	75(6)	39(5)	13(4)	2(4)	22(5)
C(39)	103(7)	63(5)	27(4)	9(4)	27(4)	2(5)
C(40)	21(3)	19(3)	24(3)	1(2)	10(2)	6(2)
C(41)	19(3)	18(3)	29(3)	5(2)	12(2)	9(2)
C(42)	44(4)	29(3)	29(3)	-6(3)	18(3)	-1(3)
C(43)	53(4)	69(5)	27(4)	-3(3)	2(3)	-7(4)
C(44)	19(3)	20(3)	21(3)	6(2)	4(2)	10(2)
C(45)	15(3)	18(3)	26(3)	3(2)	9(2)	5(2)
C(46)	15(3)	18(3)	26(3)	7(2)	9(2)	4(2)
C(47)	17(3)	25(3)	31(3)	1(2)	9(2)	-1(2)
C(48)	23(3)	32(3)	27(3)	7(3)	12(2)	1(2)
C(49)	25(3)	40(4)	32(3)	7(3)	15(3)	1(3)
C(50)	28(3)	31(3)	29(3)	4(3)	9(3)	-5(3)
C(51)	37(4)	49(4)	40(4)	-1(3)	8(3)	14(3)
C(52)	69(7)	48(6)	30(5)	25(5)	-4(5)	-19(5)
N(1)	19(2)	14(2)	33(3)	-1(2)	12(2)	-4(2)
N(2)	34(3)	17(2)	29(3)	-4(2)	16(2)	0(2)
N(3)	24(2)	23(2)	26(3)	0(2)	11(2)	2(2)
N(4)	19(2)	17(2)	25(2)	-3(2)	10(2)	1(2)
N(5)	16(2)	19(2)	27(3)	4(2)	10(2)	6(2)
N(6)	26(2)	21(2)	22(2)	-1(2)	12(2)	4(2)
N(7)	21(2)	24(2)	25(3)	-2(2)	6(2)	-2(2)
N(8)	18(2)	28(3)	29(3)	3(2)	10(2)	-2(2)
O(1)	27(2)	25(2)	21(2)	3(2)	9(2)	-2(2)
O(2)	36(2)	29(2)	37(2)	4(2)	18(2)	13(2)
O(3)	27(2)	33(2)	24(2)	-1(2)	14(2)	1(2)
O(4)	31(2)	35(2)	42(3)	-5(2)	13(2)	-14(2)
S(1)	39(1)	39(1)	50(1)	12(1)	14(1)	9(1)
S(2)	57(1)	64(1)	41(1)	-6(1)	23(1)	-12(1)
S(3)	40(1)	40(1)	37(1)	-10(1)	16(1)	-9(1)
S(4)	77(3)	81(2)	37(2)	-3(1)	33(1)	12(2)
S(4')	51(7)	56(10)	24(6)	-13(5)	15(6)	27(6)

REFERENCES

(1) Kuhn, R.; Rudy, H.; Wagner-Jauregg, T. *Berichte der deutschen chemischen Gesellschaft (A and B Series)* **1933**, *66*, 1950-1956.

(2) Niemz, A.; Rotello, V. M. *Acc. Chem. Res.*, **1998**, *32*, 44-52.

(3) Miura, R. *Chem. Rec.*, **2001**, *1*, 183-194.

(4) Mueller, F. *ChemInform* **1992**, *23*.

(5) Mizutani, H.; Miyahara, I.; Hirotsu, K.; Nishina, Y.; Shiga, K.; Setoyama, C.; Miura, R., *J. Biochem.*, **1996**, *120*, 14-17.

(6) Goetzberger, A.; Hebling, C.; Schock, H.-W. *Mater. Sci. and Eng.: R: Reports*, **2003**, *40*, 1-46.

(7) G.A, C. *Solar Cells* **1983**, *8*, 47-83.

(8) Wöhrle, D.; Meissner, D. *Adv. Mater.*, **1991**, *3*, 129-138.

(9) Brabec, C. J.; Sariciftci, N. S.; Hummelen, J. C., *Adv. Functional Mater.*, **2001**, *11*, 15-26.

(10) Dimitrakopoulos, C. D.; Mascaro, D. J., *IBM J. Res. Dev.*, **2001**, *45*, 11-27.

(11) Sumio, I., *J. Cryst Growth*, **1980**, *50*, 675-683.

(12) Ghosh, A. K.; Feng, T., *J. App. Phys.*, **1978**, *49*, 5982-5989.

(13) Morel, D. L.; Ghosh, A. K.; Feng, T.; Stogryn, E. L.; Purwin, P. E.; Shaw, R. F.; Fishman, C., *App. Phys. Lett.*, **1978**, *32*, 495-497.

(14) Tang, C. W., *App. Phys. Lett.*, **1986**, *48*, 183-185.

(15) Hiramoto, M.; Suezaki, M.; Yokoyama, M., *Chem. Lett.*, **1990**, *19*, 327-330.

(16) Hiramoto, M.; Fujiwara, H.; Yokoyama, M., *App. Phys. Lett.*, **1991**, *58*, 1062-1064.

(17) Hiramoto, M.; Fujiwara, H.; Yokoyama, M., *J. Appl. Phys.*, **1992**, *72*, 3781-3787.

(18) Karg, S.; Riess, W.; Dyakonov, V.; Schwoerer, M., *Synth. Met.*, **1993**, *54*, 427-433.

(19) Antoniadis, H.; Hsieh, B. R.; Abkowitz, M. A.; Jenekhe, S. A.; Stolka, M., *Synth. Met.*, **1994**, *62*, 265-271.

(20) Sariciftci, N. S.; Braun, D.; Zhang, C.; Srdanov, V. I.; Heeger, A. J.; Stucky, G.; Wudl, F., *App. Phys. Lett.*, **1993**, *62*, 585-587.

(21) Hummelen, J. C.; Knight, B. W.; Lepeq, F.; Wudl, F.; Yao, J.; Wilkins, C. L., *J. Org. Chem.*, **1995**, *60*, 532-538.

(22) Sariciftci, N. S.; Smilowitz, L.; Heeger, A. J.; Wudl, F., *Science*, **1992**, *258*, 1474-1476.

(23) Hoppe, H.; Sariciftci, N. S., *J. Mater. Res.*, **2004**, *19*, 1924-1945.

(24) Tada, K.; Hosoda, K.; Hirohata, M.; Hidayat, R.; Kawai, T.; Onoda, M.; Teraguchi, M.; Masuda, T.; Zakhidov, A. A.; Yoshino, K., *Synth. Met.*, **1997**, *85*, 1305-1306.

(25) Halls, J. J. M.; Walsh, C. A.; Greenham, N. C.; Marseglia, E. A.; Friend, R. H.; Moratti, S. C.; Holmes, A. B., *Nature*, **1995**, *376*, 498-500.

(26) Granstrom, M.; Petritsch, K.; Arias, A. C.; Lux, A.; Andersson, M. R.; Friend, R. H., *Nature,* **1998**, *395*, 257-260.

(27) Peumans, P.; Forrest, S. R. *App. Phys. Lett.,* **2001**, *79*, 126-128.

(28) Kroon, J. M.; Wienk, M. M.; Verhees, W. J. H.; Hummelen, J. C., *Thin Solid Films,* **2002**, *404*, 223-228.

(29) Munters, T.; Martens, T.; Goris, L.; Vrindts, V.; Manca, J.; Lutsen, L.; De Ceuninck, W.; Vanderzande, D.; De Schepper, L.; Gelan, J.; Sariciftci, N. S.; Brabec, C. J., *Thin Solid Films,* **2002**, *404*, 247-251.

(30) Geens, W.; Aernouts, T.; Poortmans, J.; Hadziioannou, G., *Thin Solid Films,* **2002**, *404*, 438-443.

(31) Gebeyehu, D.; Pfeiffer, M.; Maennig, B.; Drechsel, J.; Werner, A.; Leo, K., *Thin Solid Films,* **2004**, *452*, 29-32.

(32) Huynh, W. U.; Dittmer, J. J.; Alivisatos, A. P., *Science,* **2002**, *295*, 2425-2427.

(33) Savenije, T. J.; Warman, J. M.; Goossens, A., *Chem. Phys. Lett.,* **1998**, *287*, 148-153.

(34) Saito, Y.; Kitamura, T.; Wada, Y.; Yanagida, S., *Synth. Met.,* **2002**, *131*, 185-187.

(35) Arici, E.; Hoppe, H.; Schaffler, F.; Meissner, D.; Malik, M. A.; Sariciftci, N. S., *Thin Solid Films,* **2004**, *452*, 612-618.

(36) Hiramoto, M.; Kishigami, Y.; Yokoyama, M., *Chem. Lett.,* **1990**, *19*, 119-122.

(37) Lane, P. A.; Rostalski, J.; Giebeler, C.; Martin, S. J.; Bradley, D. D. C.; Meissner, D., *Sol. Energy Mater. Sol. Cells,* **2000**, *63*, 3-13.

(38) Rostalski, J. r.; Meissner, D., *Sol. Energy Mater. Sol. Cells,* **2000**, *63*, 37-47.

(39) Pfeiffer, M.; Beyer, A.; Plannigs, B.; Nollau, A.; Fritz, T.; Leo, K.; Schlettwein, D.; Hiller, S.; Wahrle, D. , *Sol. Energy Mater. Sol. Cells,* **2000**, *63*, 83-99.

(40) Gebeyehu, D.; Maennig, B.; Drechsel, J.; Leo, K.; Pfeiffer, M., *Sol. Energy Mater. Sol. Cells*, **2003**, *79*, 81-92.

(41) Drechsel, J.; Mannig, B.; Kozlowski, F.; Gebeyehu, D.; Werner, A.; Koch, M.; Leo, K.; Pfeiffer, M., *Thin Solid Films,* **2004**, *452*, 515-517.

(42) Maennig, B.; Drechsel, J.; Gebeyehu, D.; Simon, P.; Kozlowski, F.; Werner, A.; Li, F.; Grundmann, S.; Sonntag, S.; Koch, M.; Leo, K.; Pfeiffer, M.; Hoppe, H.; Meissner, D.; Sariciftci, N. S.; Riedel, I.; Dyakonov, V.; Parisi, J., *App. Phys. A: Mate. Sci. & Proc,*. **2004**, *79*, 1-14.

(43) Dresselhaus, M. S.; Dresselhaus, G.; Eklund, P. C. In *Science of Fullerenes and Carbon Nanotubes*; Academic Press: San Diego, **1996.**

(44) Lee, C. H.; Yu, G.; Moses, D.; Pakbaz, K.; Zhang, C.; Sariciftci, N. S.; Heeger, A. J.; Wudl, F. *Phys. Rev. B,* **1993**, *48*, 15425-15433.

(45) Morita, S.; Zakhidov, A. A.; Yoshino, K. *Solid State Commun.*, **1992**, *82*, 249-252.

(46) Burroughes, J. H.; Bradley, D. D. C.; Brown, A. R.; Marks, R. N.; Mackay, K.; Friend, R. H.; Burns, P. L.; Holmes, A. B., *Nature*, **1990**, *347*, 539-541.

(47) Braun, D.; Heeger, A. J., *App. Phys. Lett.*, **1991**, *58*, 1982-1984.

(48) Adam, D.; Schuhmacher, P.; Simmerer, J.; Haussling, L.; Siemensmeyer, K.; Etzbachi, K. H.; Ringsdorf, H.; Haarer, D., *Nature*, **1994**, *371*, 141-143.

(49) Funahashi, M.; Hanna, J.-i., *Phys. Rev. Lett.*, **1997**, *78*, 2184-2187.

(50) Sirringhaus, H.; Brown, P. J.; Friend, R. H.; Nielsen, M. M.; Bechgaard, K.; Langeveld-Voss, B. M. W.; Spiering, A. J. H.; Janssen, R. A. J.; Meijer, E. W.; Herwig, P.; de Leeuw, D. M., *Nature*, **1999**, *401*, 685-688.

(51) Sirringhaus, H.; Wilson, R. J.; Friend, R. H.; Inbasekaran, M.; Wu, W.; Woo, E. P.; Grell, M.; Bradley, D. D. C., *App. Phys. Lett.*, **2000**, *77*, 406-408.

(52) Aasmundtveit, K. E.; Samuelsen, E. J.; Guldstein, M.; Steinsland, C.; Flornes, O.; Fagermo, C.; Seeberg, T. M.; Pettersson, L. A. A.; Inganas, O.; Feidenhans'l, R.; Ferrer, S., *Macromolecules*, **2000**, *33*, 3120-3127.

(53) Pacios, R.; Nelson, J.; Bradley, D. D. C.; Brabec, C. J., *App. Phys. Lett.*, **2003**, *83*, 4764-4766.

(54) Choulis, S. A.; Nelson, J.; Kim, Y.; Poplavskyy, D.; Kreouzis, T.; Durrant, J. R.; Bradley, D. D. C., *App. Phys. Lett.*, **2003**, *83*, 3812-3814.

(55) Veenstra, S. C.; Malliaras, G. G.; Brouwer, H. J.; Esselink, F. J.; Krasnikov, V. V.; van Hutten, P. F.; Wildeman, J.; Jonkman, H. T.; Sawatzky, G. A.; Hadziioannou, G., *Synth. Met.*, **1997**, *84*, 971-972.

(56) Tsuzuki, T.; Shirota, Y.; Rostalski, J. r.; Meissner, D., *Sol. Energy Mater. Sol. Cells*, **2000**, *61*, 1-8.

(57) Shaheen, S. E.; Radspinner, R.; Peyghambarian, N.; Jabbour, G. E., *App. Phys. Lett.* **2001**, *79*, 2996-2998.

(58) Gregg, B. A., *J. Phys. Chem. B*, **2003**, *107*, 4688-4698.

(59) Al-Ibrahim, M.; Roth, H. K.; Zhokhavets, U.; Gobsch, G.; Sensfuss, S., *Sol. Energy Mater. Sol. Cells*, **2005**, *85*, 13-20.

(60) Tu, G.; Bilge, A.; Adamczyk, S.; Forster, M.; Heiderhoff, R.; Balk, L. J.; Mühlbacher, D.; Morana, M.; Koppe, M.; Scharber, M. C.; Choulis, S. A.; Brabec, C. J.; Scherf, U. *Macromolecular Rapid Commun.*, **2007**, *28*, 1781-1785.

(61) Troshin, P. A.; Hoppe, H.; Renz, J.; Egginger, M.; Mayorova, J. Y.; Goryachev, A. E.; Peregudov, A. S.; Lyubovskaya, R. N.; Gobsch, G.; Sariciftci, N. S.; Razumov, V. F., *Adv. Func. Mater.*, **2009**, *19*, 779-788.

(62) Chang, L.; Lademann, H. W. A.; Bonekamp, J.-B.; Meerholz, K.; Moulé, A. J., *Adv. Func. Mater.*, **2011**, *21*, 1779-1787.

(63) Savenije, T. J.; Kroeze, J. E.; Yang, X.; Loos, J., *Thin Solid Films*, **2006**, *512*, 2-6.

(64) Brabec, C. J.; Cravino, A.; Meissner, D.; Sariciftci, N. S.; Fromherz, T.; Rispens, M. T.; Sanchez, L.; Hummelen, J. C., *Adv. Func. Mater.*, **2001**, *11*, 374-380.

(65) Kroto, H. W.; Heath, J. R.; O'Brien, S. C.; Curl, R. F.; Smalley, R. E., *Nature*, **1985**, *318*, 162-163.

(66) Zhang, Q. L.; O'Brien, S. C.; Heath, J. R.; Liu, Y.; Curl, R. F.; Kroto, H. W.; Smalley, R. E., *J. Phys. Chem.*, **1986**, *90*, 525-528.

(67) Imahori, H.; Fukuzumi, S., *Adv. Func. Mater.*, **2004**, *14*, 525-536.

(68) Kratschmer, W.; Lamb, L. D.; Fostiropoulos, K.; Huffman, D. R., *Nature*, **1990**, *347*, 354-358.

(69) Taylor, R.; Walton, D. R. M., *Nature*, **1993**, *363*, 685-693.

(70) Olah, G. A.; Bucsi, I.; Aniszfeld, R.; Surya Prakash, G. K., *Carbon*, **1992**, *30*, 1203-1211.

(71) Xie, Q.; Perez-Cordero, E.; Echegoyen, L., *J. Am. Chem. Soc.*, **1992**, *114*, 3978-3980.

(72) Tycko, R.; Dabbagh, G.; Rosseinsky, M. J.; Murphy, D. W.; Fleming, R. M.; Ramirez, A. P.; Tully, J. C., *Science*, **1991**, *253*, 884-886.

(73) Allemand, P. M.; Koch, A.; Wudl, F.; Rubin, Y.; Diederich, F.; Alvarez, M. M.; Anz, S. J.; Whetten, R. L., *J. Am. Chem. Soc.*, **1991**, *113*, 1050-1051.

(74) Guo, T.; Scuseria, G. E., *Chem. Phys. Lett.*, **1992**, *191*, 527-532.

(75) Dubois, D.; Kadish, K. M.; Flanagan, S.; Haufler, R. E.; Chibante, L. P. F.; Wilson, L. J., *J. Am. Chem. Soc.*, **1991**, *113*, 4364-4366.

(76) Dubois, D.; Kadish, K. M.; Flanagan, S.; Wilson, L. J., *J. Am. Chem. Soc.*, **1991**, *113*, 7773-7774.

(77) Bosi, S.; Da Ros, T.; Spalluto, G.; Prato, M., *Eur. J. Medicinal Chem.*, **2011**, *38*, 913-923.

(78) Diederich, F.; Gomez-Lopez, M., *Chem. Soc. Rev.*, **1999**, *28*, 263-277.

(79) Carroll, J. B.; Cooke, G.; Garety, J. F.; Jordan, B. J.; Mabruk, S.; Rotello, V. M., *Chem Commun* **2005**, 3838-3840.

(80) Guldi, D. M.; Martin, N., *J. Mater. Chem.*, **2002**, *12*, 1978-1992.

(81) Chuard, T.; Deschenaux, R., *J. Mater. Chem.*, **2002**, *12*, 1944-1951.

(82) Brusatin, G.; Signorini, R., *J. Mater. Chem.*, **2002**, *12*, 1964-1977.

(83) Wudl, F., *J. Mater. Chem.* **2002**, *12*, 1959-1963.

(84) Maggini, M.; Scorrano, G.; Prato, M., *J. Am. Chem. Soc.*, **1993**, *115*, 9798-9799.

(85) Echegoyen, L.; Echegoyen, L. E., *Acc. Chem. Res.*, **1998**, *31*, 593-601.

(86) Illescas, B.; Martan, N.; Seoane, C., *Tetrahedron Lett.*, **1997**, *38*, 2015-2018.

(87) Saito, G.; Teramoto, T.; Otsuka, A.; Sugita, Y.; Ban, T.; Kusunoki, M.; Sakaguchi, K., *Synth. Metals*, **1994**, *64*, 359-368.

(88) Crane, J. D.; Hitchcock, P. B.; Kroto, H. W.; Taylor, R.; Walton, D. R. M., *J. Chem. Soc., Chem. Commun.*, **1992**, 1764-1765.

(89) Suzuki, T.; Maruyama, Y.; Akasaka, T.; Ando, W.; Kobayashi, K.; Nagase, S., *J. Am. Chem. Soc.*, **1994**, *116*, 1359-1363.

(90) Illescas, B. M.; Martin, N., *J. Org. Chem.*, **2000**, *65*, 5986-5995.

(91) Illescas, B.; Martin, N.; Pacz, I.; Seoane, C., *Synth. Met.*, **1999**, *103*, 2344-2347.

(92) Herranz, M. A.,Illescas, B.; Marta, N.; Luo, C.; Guldi, D. M., *J. Org. Chem.* **2000**, *65*, 5728-5738.

(93) Chamberlain, T. W.; Davies, E. S.; Khlobystov, A. N.; Champness, N. R., *Chem – Eur. J.*, **2011**, *17*, 3759-3767.

(94) Yu, G.; Gao, J.; Hummelen, J. C.; Wudl, F.; Heeger, A. J., *Science*, **1995**, *270*, 1789-1791.

(95) Coakley, K. M.; McGehee, M. D., *Chem. Mater.*, **2004**, *16*, 4533-4542.

(96) Thompson, B. C.; Kim, Y.-G.; Reynolds, J. R., *Macromolecules*, **2005**, *38*, 5359-5362.

(97) Meijer, E. J.; de Leeuw, D. M.; Setayesh, S.; van Veenendaal, E.; Huisman, B. H.; Blom, P. W. M.; Hummelen, J. C.; Scherf, U.; Klapwijk, T. M., *Nat Mater*, **2003**, *2*, 678-682.

(98) Rauch, T.; Henseler, D.; Schilinsky, P.; Waldauf, C.; Hauch, J.; Brabec, C., J., *Nanotechnology*, **2004**. 4th IEEE Conference on, 2004; p 632-634.

(99) Shaheen, S. E.; Brabec, C. J.; Sariciftci, N. S.; Padinger, F.; Fromherz, T.; Hummelen, J. C., *App. Phys. Lett.*, **2001**, *78*, 841-843.

(100) Li, G.; Shrotriya, V.; Huang, J.; Yao, Y.; Moriarty, T.; Emery, K.; Yang, Y., *Nat Mater*, **2005**, *4*, 864-868.

(101) Kim, K.; Liu, J.; Namboothiry, M. A. G.; Carroll, D. L., *App. Phys., Lett.*, **2007**, *90*, 3.

(102) Baffreau, J. r. m.; Dumur, F. d. r.; Hudhomme, P. t., *Org. Lett.*, **2006**, *8*, 1307-1310.

(103) Sheehan, J. C.; Hess, G. P., *J. Am. Chem. Soc.*, **1955**, *77*, 1067-1068.

(104) Neises, B.; Steglich, W. *Angew. Chem. Int. Ed. in English*, **1978**, *17*, 522-524.

(105) König, W.; Geiger, R. *Chemische Berichte*, **1970**, *103*, 788-798.

(106) Dutra, J. K.; Cuello, A. O.; Rotello, V. M., *Tetrahedron Lett.*, **1997**, *38*, 4003-4004.

(107) Torres, E.; Panetta, C. A.; Metzger, R. M., *J. Org. Chem.*, **1987**, *52*, 2944-2945.

(108) Sandanaraj, B. S.; Demont, R.; Thayumanavan, S., *J. Am. Chem. Soc.*, **2007**, *129*, 3506-3507.

(109) Balch, A. L.; Catalano, V. J.; Lee, J. W.; Olmstead, M. M., *J. Am. Chem. Soc.*, **1992**, *114*, 5455-5457.

(110) Mukhopadhyay, P.; Iwashita, Y.; Shirakawa, M.; Kawano, S.-i.; Fujita, N.; Shinkai, S., *Angew. Chem. Int.Ed.*, **2006**, *45*, 1592-1595.

(111) Vollmann, H.; Becker, H.; Corell, M.; Streeck, H., *Justus Liebigs Annalen der Chem.*, **1937**, *531*, 1-159.

(112) Hünig, S.; Groβ, J.; Lier, E. F.; Quast, H., *Justus Liebigs Annalen der Chem.*, **1973**, *1973*, 339-358.

(113) Sotiriou-Leventis, C.; Mao, Z.; Rawashdeh, A.-M. M., *J. Org. Chem.*, **2000**, *65*, 6017-6023.

(114) R. Ashton, P.; E. Boyd, S.; Brindle, A.; J. Langford, S.; Menzer, S.; Perez-Garcia, L.; A. Preece, J.; M. Raymo, i.; Spencer, N.; Fraser Stoddart, J.; J. P. White, A.; J. Williams, D., *New J. Chem.*, **1999**, *23*, 587-602.

(115) Katz, H. E.; Lovinger, A. J.; Johnson, J.; Kloc, C.; Siegrist, T.; Li, W.; Lin, Y. Y.; Dodabalapur, A., *Nature*, **2000**, *404*, 478-481.

(116) Bhosale, S. V.; Jani, C. H.; Langford, S. J., *Chem. Soc. Rev.*, **2008**, *37*, 331-342.

(117) Amabilino, D. B.; Stoddart, J. F., *Chem. Rev.*, **1995**, *95*, 2725-2828.

(118) Irwin, R. S., *J. Polym. Sci. Part C: Polym. Lett.*, **1988**, *26*, 159-163.

(119) Vicic, D. A.; Odom, D. T.; Naaez, M. E.; Gianolio, D. A.; McLaughlin, L. W.; Barton, J. K., *J. Am. Chem. Soc.*, **2000**, *122*, 8603-8611.

(120) Lee, H. N.; Xu, Z.; Kim, S. K.; Swamy, K. M. K.; Kim, Y.; Kim, S.-J.; Yoon, J., *J. Am. Chem. Soc.*, **2007**, *129*, 3828-3829.

(121) Pengo, P.; Panto, G. D.; Otto, S.; Sanders, J. K. M., *J. Org. Chem.*, **2006**, *71*, 7063-7066.

(122) Würthner, F.; Ahmed, S.; Thalacker, C.; Debaerdemaeker, T., *Chem. – Eur. J.*, **2002**, *8*, 4742-4750.

(123) Rager, C.; Waarthner, F., *J. Org. Chem.*, **2007**, *72*, 8070-8075.

(124) Horne, W. S.; Ashkenasy, N.; Ghadiri, M. R., *Chem. –Eur. J.*, **2005**, *11*, 1137-1144.

(125) Andric, G.; Boas, J. F.; Bond, A. M.; Fallon, G. D.; Ghiggino, K. P.; Hogan, C. F.; Hutchison, J. A.; Lee, M. A.; Langford, S. J.; Pilbrow, J. R.; Troup, G. J.; Woodward, C. P., *Aust. J. Chem.*, **2004**, *57*, 1011-1019.

(126) Miller, L. L.; Duan, R. G.; Hong, Y.; Tabakovic, I., *Chem.Mater.*,**1995**, *7*, 1552-1557.

(127) Bauscher, M.; Maentele, W., *J. Phys. Chem.*, **1992**, *96*, 11101-11108.

(128) Erten, A.; Posokhov, Y.; Alp, S.; Aasli, S. d. k., *Dyes and Pigments*, **2005**, *64*, 171-178.

(129) Zhong, C. J.; Kwan, W. S. V.; Miller, L. L., *Chem. Mater.*, **1992**, *4*, 1423-1428.

(130) Tomasulo, M.; Naistat, D. M.; White, A. J. P.; Williams, D. J.; Raymo, F. i. M., *Tetrahedron Lett.*, **2005**, *46*, 5695-5698.

(131) Brochsztain, S.; Rodrigues, M. A.; Demets, G. J. F.; Politi, M. J., *J. Mater. Chem.*, **2002**, *12*, 1250-1255.

(132) -Khouly, M., Kim, J., Kay, K.-Y., Choi, C., Ito, O. and Fukuzumi, S., *chem. Eur. J.*, **2009**, *15*, 5301-5310.

(133) Hansen, J. G.; Feeder, N.; Hamilton, D. G.; Gunter, M. J.; Becher, J.; Sanders, J. K. M., *Org. Lett.*, **2000**, *2*, 449-452.

(134) Fallon, G. D.; Lee, M. A. P.; Langford, S. J.; Nichols, P. J., *Org. Lett.*, **2004**, *6*, 655-658.

(135) Le Pleux, L.; Smeigh, A. L.; Gibson, E.; Pellegrin, Y.; Blart, E.; Boschloo, G.; Hagfeldt, A.; Hammarstrom, L.; Odobel, F., *Energy & Environmental Science*, **2011**, *4*, 2075-2084.

(136) Susarova, D. K.; Troshin, P. A.; Haglinger, D.; Koeppe, R.; Babenko, S. D.; Lyubovskaya, R. N.; Razumov, V. F.; Serdar Sariciftci, N., *Sol. Energy Mater. Sol. Cells*, **2011**, *94*, 803-811.

(137) Durban, M. M.; Kazarinoff, P. D.; Luscombe, C. K., *Macromolecules*, **2011**, *43*, 6348-6352.

(138) Legrand, Y.-M.; Gray, M.; Cooke, G.; Rotello, V. M., *J. Am. Chem. Soc.*, **2003**, *125*, 15789-15795.

(139) Shinohara, H.; Gratzel, M.; Vlachopoulos, N.; Aizawa, M., *J. Electroanalytical Chem. and Interfacial Electrochemistry*, **1991**, *321*, 307-320.

(140) Anandan, S.; Latha, S.; Maruthamuthu, P., *J. Photochemistry and Photobiology A: Chem.*, **2002**, *150*, 167-175.

(141) Losi, A. *Photochemistry and Photobiology*, **2007**, *83*, 1283-1300.

(142) Shirakawa, H.; Louis, E. J.; MacDiarmid, A. G.; Chiang, C. K.; Heeger, A. J., *J. Chem. Soc., Chem. Commun.*, **1977**, 578-580.

(143) Mastragostino, M.; Soddu, L., *Electrochimica Acta*, **1990**, *35*, 463-466.

(144) Gaanes, S.; Neugebauer, H.; Sariciftci, N. S., *Chem. Rev.*, **2007**, *107*, 1324-1338.

(145) Colvin, V. L.; Schlamp, M. C.; Alivisatos, A. P., *Nature*, **1994**, *370*, 354-357.

(146) Lee, S. A.; Hotta, S.; Nakanishi, F., *J. Phys. Chem. A.*, **2000**, *104*, 1827-1833.

(147) Roncali, J., *Chem. Rev.*, **1992**, *92*, 711-738.

(148) Bair, J. S.; Harrison, R. G., *J. Org. Chem.*, **2007**, *72*, 6653-6661.

(149) Bao, Z.; Dodabalapur, A.; Lovinger, A. J., *App. Phys. Lett.*, **1996**, *69*, 4108-4110.

(150) Martina, V.; Ionescu, K.; Pigani, L.; Terzi, F.; Ulrici, A.; Zanardi, C.; Seeber, R., *Analytical and Bioanalytical Chemistry*, **2007**, *387*, 2101-2110.

(151) Yamamoto, T.; Sanechika, K.; Yamamoto, A., *J. Polym. Sci: Polym. Lett. Ed.*, **1980**, *18*, 9-12.

(152) Lin, J. W. P.; Dudek, L. P., *J. Polym. Sci.: Polym. Chem. Ed.*, **1980**, *18*, 2869-2873.

(153) McCullough, R. D.; Lowe, R. D., *J. Chem. Soc., Chem. Commun.*, **1992**, 70-72.

(154) Andersson, M. R.; Selse, D.; Berggren, M.; Jaervinen, H.; Hjertberg, T.; Inganaes, O.; Wennerstroem, O.; Oesterholm, J. E., *Macromolecules*, **1994**, *27*, 6503-6506.

(155) Chen, T. A.; O'Brien, R. A.; Rieke, R. D., *Macromolecules*, **1993**, *26*, 3462-3463.

(156) Chen, T. A.; Rieke, R. D., *J. Am. Chem. Soc.*, **1992**, *114*, 10087-10088.

(157) Costa Bizzarri, P.; Andreani, F.; Della Casa, C.; Lanzi, M.; Salatelli, E., *Synth. Metals*, **1995**, *75*, 141-147.

(158) Fraleoni-Morgera, A.; Della-Casa, C.; Lanzi, M.; Costa-Bizzarri, P., *Macromolecules*, **2003**, *36*, 8617-8620.

(159) Pomerantz, M.; Tseng, J. J.; Zhu, H.; Sproull, S. J.; Reynolds, J. R.; Uitz, R.; Arnott, H. J.; Haider, M. I., *Synth. Metal.*, **1991**, *41*, 825-830.

(160) Barbarella, G.; Bongini, A.; Zambianchi, M., *Macromolecules*, **1994**, *27*, 3039-3045.

(161) Qiao, X.; Wang, X.; Zhao, X.; Liu, J.; Mo, Z., *Synth. Metal.*, **2000**, *114*, 261-265.

(162) Andreani, F.; Salatelli, E.; Lanzi, M., *Polymer*, **1996**, *37*, 661-665.

(163) Laakso, J.; JÃ¤rvinen, H.; Skagerberg, B., *Synth. Metal.*, **1993**, *55*, 1204-1208.

(164) Lukkari, J.; Kankare, J.; Visy, C., *Synth. Metal.*, **1992**, *48*, 181-192.

(165) McFarlane, S. L.; Deore, B. A.; Svenda, N.; Freund, M. S., *Macromolecules*, **2011,** *43*, 10241-10245.

(166) Groenendaal, L.; Jonas, F.; Freitag, D.; Pielartzik, H.; Reynolds, J. R., *Adv. Mater.*, **2000**, *12*, 481-494.

(167) Heywang, G.; Jonas, F., *Adv. Mater.*, **1992**, *4*, 116-118.

(168) Carter, S. A.; Angelopoulos, M.; Karg, S.; Brock, P. J.; Scott, J. C., *App. Phys. Lett.*, **1997**, *70*, 2067-2069.

(169) Frederik C, K., *Sol. Energy Mater. Sol. Cells*, **2008**, *92*, 715-726.

(170) Jonas, F.; Morrison, J. T., *Synth. Met.*, **1997**, *85*, 1397-1398.

(171) Andersson, P.; Forchheimer, R.; Tehrani, P.; Berggren, M., *Adv. Func. Mater.*, **2007**, *17*, 3074-3082.

(172) Chen, L.; Yuan, C.; Dou, H.; Gao, B.; Chen, S.; Zhang, X., *Electrochimica Acta*, **2009**, *54*, 2335-2341.

(173) Michalska, A.; Maksymiuk, K., *Analytica Chimica Acta*, **2004**, *523*, 97-105.

(174) Setti, L.; Fraleoni-Morgera, A.; Ballarin, B.; Filippini, A.; Frascaro, D.; Piana, C. *Biosensors and Bioelectronics*, **2005**, *20*, 2019-2026.

(175) Lefebvre, M. C.; Qi, Z.; Pickup, P. G., *J. Electrochemical Soc.*, **1999**, *146*, 2054-2058.

(176) Loewe, R. S.; Khersonsky, S. M.; McCullough, R. D., *Adv. Mater.*, **1999**, *11*, 250-253.

(177) Winder, C.; Sariciftci, N. S., *J. Mater. Chem.*, **2004**, *14*, 1077-1086.

(178) Cravino, A.; Sariciftci, N. S., *J. Mater. Chem.*, **2002**, *12*, 1931-1943.

(179) Leclerc, M., *J. Polym. Sci. Part A: Polym. Chem.*, **2001**, *39*, 2867-2873.

(180) Bundgaard, E.; Krebs, F. C., *Sol. Energy Mater. Sol. Cells*, **2007**, *91*, 954-985.

(181) Hughes, E. D.; Le Fevre, C. G.; Le Fevre, R. J. W., *J. Chem. Soc., (Resumed)* **1937**, 202-207.

(182) Burns, D. M.; Iball, J., *Nature*, **1954**, *173*, 635-635.

(183) Pavlačková, P.; Cimrová, V.; Výprachtický, D.; Kmínek, I., *Macromolecular Symposia*, **2008**, *268*, 105-109.

(184) Dennler, G.; Scharber, M. C.; Brabec, C. J., *Adv. Mater.*, **2009**, *21*, 1323-1338.

(185) Huang, F.; Chen, K.-S.; Yip, H.-L.; Hau, S. K.; Acton, O.; Zhang, Y.; Luo, J.; Jen, A. K. Y., *J. Am. Chem. Soc.*, **2009**, *131*, 13886-13887.

(186) Brabec, C. J.; Gowrisanker, S.; Halls, J. J. M.; Laird, D.; Jia, S.; Williams, S. P., *Adv. Mater.*, **2011**, *22*, 3839-3856.

(187) Zoombelt, A. P.; Fonrodona, M.; Wienk, M. M.; Sieval, A. B.; Hummelen, J. C.; Janssen, R. A. J., *Org. Lett.*,**2009**, *11*, 903-906.

(188) Kitamura, C.; Tanaka, S.; Yamashita, Y., *Chem. Mater.*, **1996**, *8*, 570-578.

(189) Wudl, F.; Kobayashi, M.; Heeger, A. J., *J. Org. Chem.*, **1984**, *49*, 3382-3384.

(190) Luzzati, S.; Scharber, M.; Catellani, M.; Lupsac, N.-O.; Giacalone, F.; Segura, J. L.; Martin, N.; Neugebauer, H.; Sariciftci, N. S. *Synth. Met.s* **2003**, *139*, 731-733.

(191) Bu, L.; Guo, X.; Yu, B.; Qu, Y.; Xie, Z.; Yan, D.; Geng, Y.; Wang, F., *J. Am. Chem. Soc.*, **2009**, *131*, 13242-13243.

(192) Edwards, A. M. In *Flavins Photochemistry and Photobiology*; *Roy. Soc. Chem.*, **2006**; Vol. 6.

(193) Pilgram, K.; Zupan, M.; Skiles, R., *J. Heterocyclic Chem.*, **1970**, *7*, 629-633.

(194) Beecken, H., *Chemische Berichte*, **1967**, *100*, 2170-2177.

(195) DaSilveira Neto, B. A.; Lopes, A. S. A.; Ebeling, G.; Gonasalves, R. S.; Costa, V. E. U.; Quina, F. H.; Dupont, J., *Tetrahedron*, **2005**, *61*, 10975-10982.

(196) Prashad, M.; Liu, Y.; Repic, O. *ChemInform* **2001**, *32*, no-no.

(197) Katritzky, A. R.; Witek, R. M.; Rodriguez-Garcia, V.; Mohapatra, P. P.; Rogers, J. W.; Cusido, J.; Abdel-Fattah, A. A. A.; Steel, P. J., *J. Org. Chem.*, **2005**, *70*, 7866-7881.

(198) Cooke, G.; Garety, J. F.; Jordan, B.; Kryvokhyzha, N.; Parkin, A.; Rabani, G.; Rotello, V. M., *Org. Lett.*, **2006**, *8*, 2297-2300.

(199) Kumar, V.; Woode, K. A.; Bryan, R. F.; Averill, B. A., *J. Am. Chem. Soc.*, **1986**, *108*, 490-496.

(200) Kuhn, R.; Weygand, F. *Berichte der deutschen chemischen Gesellschaft (A and B Series)* **1935**, *68*, 1282-1288.

(201) Leclerc, M.; Diaz, F. M.; Wegner, G. *Die, Makromolekulare Chemie*, **1989**, *190*, 3105-3116.

(202) Berggren, M.; Inganas, O.; Gustafsson, G.; Rasmusson, J.; Andersson, M. R.; Hjertberg, T.; Wennerstrom, O., *Nature*, **1994**, *372*, 444-446.

(203) Berggren, M.; Inganas, O.; Gustafsson, G. r.; Andersson, M. R.; Hjertberg, T.; Wennerstram, O., *Synth. Metals*, **1995**, *71*, 2185-2186.

(204) Meng, H.; Huang, W., *J. Org. Chem.*, **2000**, *65*, 3894-3901.

(205) McCullough, R. D.; Lowe, R. D.; Jayaraman, M.; Anderson, D. L., *J. Org. Chem.*, **1993**, *58*, 904-912.

(206) Barrett, C. J.; Mamiya, J.-i.; Yager, K. G.; Ikeda, T., *Soft Matter*, **2007**, *3*, 1249-1261.

(207) Noble, A. *Justus Liebigs Annalen der Chemie* **1856**, *98*, 253-256.

(208) Rou, H. *CRC Press, Boca Raton FL* **1990**.

(209) Yager, K. G.; Barrett, C. J. In *Intelli. Mater.*; *Roy. Soc. Chem.*, **2008**.

(210) Magri, D. C.; Brown, G. J.; McClean, G. D.; de Silva, A. P., *J. Am. Chem. Soc.*, **2006**, *128*, 4950-4951.

(211) Ikeda, T.; Aprahamian, I.; Stoddart, J. F., *Org. Lett.*, **2007**, *9*, 1481-1484.

(212) Marder, S. R.; Cheng, L.-T.; Tiemann, B. G.; Friedli, A. C.; Blanchard-Desce, M.; Perry, J. W.; Skindha¸j, J. r., *Science*, **1994**, *263*, 511-514.

(213) Dalton, L. R.; Harper, A. W.; Ghosn, R.; Steier, W. H.; Ziari, M.; Fetterman, H.; Shi, Y.; Mustacich, R. V.; Jen, A. K. Y.; Shea, K. J., *Chem. Mater.*, **1995**, *7*, 1060-1081.

(214) Rurack, K.; Danel, A.; Rotkiewicz, K.; Grabka, D.; Spieles, M.; Rettig, W., *Org. Lett.*, **2002**, *4*, 4647-4650.

(215) Nguyen, P.; Lesley, G.; Marder, T. B.; Ledoux, I.; Zyss, J., *Chem. Mater.*, **1997**, *9*, 406-408.

(216) Katti, K. V.; Raghuraman, K.; Pillarsetty, N.; Karra, S. R.; Gulotty, R. J.; Chartier, M. A.; Langhoff, C. A., *Chem. Mater.*, **2002**, *14*, 2436-2438.

(217) Sworakowski, J.; Lipiaski, J. Ziaaek, A. u.; Palewska, K.; Neaipaarek, S., *J. Phys. Chem.*, **1996**, *100*, 12288-12294.

(218) Chattopadhyay, N.; Serpa, C.; Pereira, M. M.; Seixas de Melo, J.; Arnaut, L. G.; Formosinho, S. o. J., *J. Phys. Chem. A.*, **2001**, *105*, 10025-10030.

(219) Benedict, J. B.; Cohen, D. E.; Lovell, S.; Rohl, A. L.; Kahr, B., *J. Am. Chem. Soc.*, **2006**, *128*, 5548-5559.

(220) Sengupta, S.; Sadhukhan, S. K., *Bull. Chem. Soc. Jap.*, **2003**, *76*, 1223-1226.

(221) Jordan, B. J.; Pollier, M. A.; Ofir, Y.; Joubanian, S.; Mehtala, J. G.; Sinkel, C.; Caldwell, S. T.; Kennedy, A.; Rabani, G.; Cooke, G.; Rotello, V. M., *Chem. Commun.*, **2008**, 1653-1655.

(222) Schmidt, B.; Sobotta, C.; Malkmus, S.; Laimgruber, S.; Braun, M.; Zinth, W.; Gilch, P., *J. Phys. Chem. A*, **2004**, *108*, 4399-4404.

(223) Tirelli, N.; Suter, U. W.; Altomare, A.; Solaro, R.; Ciardelli, F.; Follonier, S.; Bosshard, C.; Gaanter, P. *Macromolecules* **1998**, *31*, 2152-2159.

(224) Bayir, A.; Jordan, B. J.; Verma, A.; Pollier, M. A.; Cooke, G.; Rotello, V. M., *Chem. Commun.*, **2006**, 4033-4035.

(225) Boyd, A. S. F.; Carroll, J. B.; Cooke, G.; Garety, J. F.; Jordan, B. J.; Mabruk, S.; Rosair, G.; Rotello, V. M., *Chem. Commun.*, **2005**, 2468-2470.

(226) Cooke, G.; Rotello, V. M., *Chem. Soc. Rev.*, **2002**, *31*, 275-286.

(227) Conn, M. M.; Rebek, J., *Chem. Rev.*, **1997**, *97*, 1647-1668.

(228) Breinlinger, E.; Niemz, A.; Rotello, V. M., *J. Am. Chem. Soc.*, **1995**, *117*, 5379-5380.

(229) Caldwell, S. T.; Cooke, G.; Hewage, S. G.; Mabruk, S.; Rabani, G.; Rotello, V.; Smith, B. O.; Subramani, C.; Woisel, P., *Chem. Commun.*, **2008**, 4126-4128.

(230) Deans, R.; Rotello, V. M., *J. Org. Chem.*, **1997**, *62*, 4528-4529.

(231) Cooke, G.; Duclairoir, F. M. A.; John, P.; Polwart, N.; Rotello, V. M., *Chem. Commun.*, **2003**, 2468-2469.

(232) Carroll, J. B.; Jordan, B. J.; Xu, H.; Erdogan, B.; Lee, L.; Cheng, L.; Tiernan, C.; Cooke, G.; Rotello, V. M., *Org. Lett.*, **2005**, *7*, 2551-2554.

(233) McDonald, N. A.; Subramani, C.; Caldwell, S. T.; Zainalabdeen, N. Y.; Cooke, G.; Rotello, V. M., *Tetrahedron Lett.*, **2011**, *52*, 2107-2110.

(234) Ariga, K.; Kunitake, T., *Acc. Chem. Res.*, **1998**, *31*, 371-378.

(235) Fan, E.; Van Arman, S. A.; Kincaid, S.; Hamilton, A. D., *J. Am. Chem. Soc.*, **1993**, *115*, 369-370.

(236) Rebek, J., *Chem. Soc. Rev.*, **1996**, *25*, 255-264.

(237) Nowick, J. S.; Chen, J. S., *J. Am. Chem. Soc.*, **1992**, *114*, 1107-1108.

(238) Nowick, J. S.; Chen, J. S.; Noronha, G., *J. Am. Chem. Soc.*, **1993**, *115*, 7636-7644.

(239) Bonar-Law, R. P., *J. Am. Chem. Soc.*, **1995**, *117*, 12397-12407.

(240) Ishikita, H.; Knapp, E.-W., *J. Bio. Chem.*, **2003**, *278*, 52002-52011.

(241) Opsteen, J. A.; Brinkhuis, R. P.; Teeuwen, R. L. M.; Lowik, D. W. P. M.; van Hest, J. C. M., *Chem. Commun.*, **2007**.

(242) Broz, P.; Driamov, S.; Ziegler, J.; Ben-Haim, N.; Marsch, S.; Meier, W.; Hunziker, P., *Nano Lett.*, **2006**, *6*, 2349-2353.

(243) Vriezema, D. M.; Garcia, P. M. L.; Sancho Oltra, N.; Hatzakis, N. S.; Kuiper, S. M.; Nolte, R. J. M.; Rowan, A. E.; van Hest, J. C. M., *Angew. Chem. Int. Ed.*, **2007**, *46*, 7378-7382.

(244) Hotz, J.; Meier, W., *Langmuir*, **1998**, *14*, 1031-1036.

(245) Stoenescu, R.; Meier, W., *Chem. Commun.*, **2002**.

(246) Rautaray, D.; Banpurkar, A.; Sainkar, S. R.; Limaye, A. V.; Ogale, S.; Sastry, M., *Cryst. Growth & Design*, **2003**, *3*, 449-452.

(247) Wang, D.; Duan, H.; Mohwald, H., *Soft Matter*, **2005**, *1*.

(248) Boker, A.; He, J.; Emrick, T.; Russell, T. P., *Soft Matter*, **2007**, *3*.

(249) Arumugam, P.; Patra, D.; Samanta, B.; Agasti, S. S.; Subramani, C.; Rotello, V. M., *J. Am. Chem. Soc.*, **2008**, *130*, 10046-10047.

(250) Louisy, J.; Delattre, F.; Lyskawa, J.; Malfait, A.; Maclean, C. E.; Sambe, L.; Zhu, N.; Cooke, G.; Woisel, P., **2011**, *Chem. Commun.*, *47*, 6819-6821.

(251) Malliaris, A.; Binana-Limbele, W.; Zana, R., *J. Colloid Interface Sci.*, **1986**, *110*, 114-120.

(252) Patra, D.; Pagliuca, C.; Subramani, C.; Samanta, B.; Agasti, S. S.; Zainalabdeen, N.; Caldwell, S. T.; Cooke, G.; Rotello, V. M., *Chem. Commun.*, **2009**, 4248-4250.

(253) Berl, V.; Schmutz, M.; Krische, M. J.; Khoury, R. G.; Lehn, J.-M., *Chem. – A Eur. J.*, **2002**, *8*, 1227-1244.

(254) Hirst, S. C.; Hamilton, A. D., *Tetrahedron Lett.*, **1990**, *31*, 2401-2404.

(255) Chevalier, Y.; Le Perchec, P., *J. Phys. Chem.*, **1990**, *94*, 1768-1774.

(256) Frier, C.; Daccout, J.-L.; Fontecave, M., *J. Org. Chem.*, **1997**, *62*, 3520-3528.

(257) Sharma, J.; Chhabra, R.; Yan, H.; Liu, Y., *Chem. Commun.*, **2008**.

(258) Dubois, F.; Mahler, B. t.; Dubertret, B. t.; Doris, E.; Mioskowski, C., *J. Am. Chem. Soc.*, **2006**, *129*, 482-483.

(259) Park, M.-H.; Ofir, Y.; Samanta, B.; Arumugam, P.; Miranda, O. R.; Rotello, V. M., *Adv. Mater.*, **2008**, *20*, 4185-4188.

(260) Srivastava, S.; Samanta, B.; Jordan, B. J.; Hong, R.; Xiao, Q.; Tuominen, M. T.; Rotello, V. M., *J. Am. Chem. Soc.*, **2007**, *129*, 11776-11780.

(261) Ofir, Y.; Samanta, B.; Arumugam, P.; Rotello, V. M., *Adv. Mater.*, **2007**, *19*, 4075-4079.

(262) Chen, M.; Liu, J. P.; Sun, S., *J. Am. Chem. Soc*., **2004**, 126, 8394-8395.

(263) Vavilov, G. A.; Pushkareva, Z. V.; Mokrushin, V. S., *Chem. Heterocyclic Comp.*, **1970**, 6, 111-113.

(264) Nunn, A. J.; Ralph, J. T., *J. Chem. Soc. C: Org*., **1966**, 1568-1570.

(265) Huang, F.; Hou, L.; Shen, H.; Jiang, J.; Wang, F.; Zhen, H.; Cao, Y., *J. Mater. Chem*., **2005**, 15, 2499-2507.